Volume 68
Number 7 / Numéro 7
July / Juillet
2011

An NRC Research Press Journal
Un journal de NRC Research Press

Canadian Journal of Fisheries and Aquatic Sciences

Journal canadien des sciences halieutiques et aquatiques

www.nrcresearchpress.com

NRC Research Press

ISSN 0706-652X / CJFSDX 68(7) 1157–1306 (2011)

The *Canadian Journal of Fisheries and Aquatic Sciences*, previously published as *Contributions to Canadian Biology* 1901–1925, *Contributions to Canadian Biology and Fisheries* 1926–1934, *Journal of the Biological Board of Canada* 1934–1937, and *Journal of the Fisheries Research Board of Canada* 1938–1979, is issued monthly to form annual volumes of 12 numbers plus supplements.

Editorial policy. The Journal publishes original research articles, perspectives (syntheses, critiques, reevaluations), discussions (comment and reply), and rapid communications. Manuscripts may concern cells, organisms, populations, communities, ecosystems, or processes that affect aquatic systems. They may cover a range of disciplines including biology and ecology of marine and freshwater organisms, limnology, oceanography, physiology, toxicology, genetics, economics, disease, and management. Preference will be given to manuscripts that emphasize understanding of observed phenomena and interpretation of experimental results. The Journal encourages papers that lead from clearly stated purpose or rationale and from testable hypotheses, concepts, or questions to identifiable conclusions or syntheses. Such papers may amplify, modify, question, or redirect accumulated knowledge embodied in contemporary perceptions of a particular state of aquatic sciences. The Journal discourages papers that are essentially descriptive, except in emerging disciplines; have only site-specific or local applications (a certain year, place, taxon, chemical compound, etc.); only confirm previously established principles; or apply standard techniques without breaking new methodological ground.

Manuscripts for publication should be submitted to the Editorial Office via NRC Research Press' online submission and peer review system (**ScholarOne**) at mc.manuscriptcentral.com/cjfas-pubs.

Submissions in either English or French are acceptable. The information must be original, that is, not copyrighted, published, or submitted elsewhere except in abstract form or unless by written consent of the Editors.

Correspondence concerning accepted manuscripts and corrected proofs should be sent to NRC Research Press, Ottawa, ON K1A 0R6, Canada (fax: 613-952-7656; e-mail: pubs@nrcresearchpress.com).

Instructions to Authors are published at nrcresearchpress.com/page/cjfas/authors. The **Publishing Policy** of NRC Research Press is available at nrcresearchpress.com/page/about/policies/pub.

Publié sans interruption depuis 1901, le *Journal canadien des sciences halieutiques et aquatiques* a paru sous plusieurs titres : *Contributions to Canadian Biology* 1901–1925, *Contributions to Canadian Biology and Fisheries* 1926–1934, *Journal of the Biological Board of Canada* 1934–1937, et *Journal of the Fisheries Research Board of Canada* 1938–1979. Le Journal paraît tous les mois, formant ainsi un volume de 12 numéros, et offre en plus jusqu'à deux suppléments par année.

Politique éditoriale. On publie, dans le Journal, des articles rendant compte de recherche originale, des perspectives (synthèses, critiques et réévaluations), des discussions (commentaires et réponses) et des communications rapides. Les documents peuvent porter sur les cellules, organismes, populations, communautés, écosystèmes ou processus qui affectent les systèmes aquatiques. Ils peuvent relever de divers domaines y compris la biologie et l'écologie des organismes marins et d'eau douce, la limnologie, l'océanographie, la physiologie, la toxicologie, la génétique, l'économie, la pathologie et la gestion. On accorde la préséance aux articles qui contribuent à la compréhension de phénomènes observés et à l'interprétation de résultats expérimentaux. On invite les auteurs à soumettre des articles ayant des objectifs précis ou relevant d'hypothèses, de concepts ou de questions vérifiables et se terminant par de solides conclusions ou d'utiles synthèses. Ces articles enrichissent, changent, mettent en question ou réorientent les connaissances acquises sur divers aspects des sciences aquatiques. On décourage toutefois la soumission d'articles simplement descriptifs (à moins qu'il ne s'agisse de nouvelles disciplines), d'application très limitée (applicables à une seule année, une seule région ou un seul taxon, portant sur un unique composé chimique, etc.); d'articles qui ne font que reprendre les principes énoncés dans des articles précédents; et d'articles rendant compte de l'application de normes sans gain de méthodologie.

Les auteurs sont invités à soumettre leur **manuscrit** au Bureau de la rédaction par le truchement du Système de soumission et d'examen en direct des articles (**ScholarOne**) de NRC Research Press au mc.manuscriptcentral.com/cjfas-pubs.

Les contributions peuvent être en anglais ou en français. Elles doivent être originales, c.-à.-d. qu'elles ne doivent pas avoir fait l'objet d'un copyright, avoir été publiées ou soumises ailleurs, sauf sous forme abrégée ou avec le consentement des rédacteurs en chef.

La correspondance ayant trait aux manuscrits acceptés et les épreuves corrigés doivent être envoyées à NRC Research Press, Ottawa, ON K1A 0R6, Canada (télécopieur : 613-952-7656; courriel : pubs@nrcresearchpress.com).

Les **Recommandations aux auteurs** sont publiées au nrcresearchpress.com/page/cjfas/authors. La **Politique éditoriale** est disponible auprès de NRC Research Press au nrcresearchpress.com/page/about/policies/pub.

The ***Canadian Journal of Fisheries and Aquatic Sciences*, ISSN 0706-652X**, is published **Monthly, 12 times per year**, by **NRC Research Press, c/o USACAN Media Dist. Srv. Corp.** at 26 Power Dam Way, Suite S1-S3, Plattsburgh, NY 12901, USA. Periodicals postage paid at Plattsburgh, NY. POSTMASTER: Send address changes to ***Canadian Journal of Fisheries and Aquatic Sciences***, c/o NRC Research Press, P.O. Box 2888, Plattsburgh, NY 12901, USA.

This Journal is indexed or abstracted in / Cette revue est signalée ou résumée dans
Aqualine; Aquatic Sciences and Fisheries Abstracts; BIOBASE; Biological and Agricultural Index; BIOSIS; CAB Abstracts; Canadian Fisheries Abstracts; Chemical Abstracts; Current Awareness in Biological Sciences; Current Abstracts; Current Contents; General Science Index; GeoRef; Oceanic Abstracts; PASCAL; Pollution Abstracts; Referativnyi Zhurnal; Science Citation Index; Water Resources Abstracts

Volume 68, Number 7, July 2011

Canadian Journal of Fisheries and Aquatic Sciences

Published by the NRC Research Press

Volume 68, numéro 7, juillet 2011

Journal canadien des sciences halieutiques et aquatiques

Publié par NRC Research Press

Editors / Rédacteurs en chef Don Jackson and Rolf Vinebrooke

Assistant to the Editors / Adjointe au rédacteur en chef **Holly Foster**

Associate Editors / Comité de rédaction

M.J. Bradford, *Simon Fraser University*
D. Brickman, *Fisheries and Oceans Canada, Dartmouth*
S.E. Campana, *Fisheries and Oceans Canada, Dartmouth*
Y. Chen, *University of Maine*
I. Fleming, *Memorial University of Newfoundland*
D. Fraser, *Concordia University*
B.M. Gillanders, *University of Adelaide*
J.W.A. Grant, *Concordia University*
M.M. Hansen, *Aarhus University*
R. Hilborn, *University of Washington*
J.M. Jech, *National Marine Fisheries Service, NOAA, Woods Hole, Mass.*
B. Jonsson, *Norwegian Institute for Nature Research*
J. Karlsson, *Umeå University*
K.A. Kidd, *University of New Brunswick*
C.E. Kraft, *Cornell University*
D.L. MacLatchy, *Wilfrid Laurier University*
P. Magnan, *Université du Québec à Trois Rivières*
C.T. Marshall, *University of Aberdeen*
P. Moran, *Universidad de Vigo*
J. Post, *University of Calgary*
Y.T. Prairie, *Université du Québec à Montréal*
T.J. Quinn II, *University of Alaska – Fairbanks*
C.W. Ramcharan, *Laurentian University*
J.S. Richardson, *The University of British Columbia*
M.-J. Rochet, *French Research Instritute for Exploitation of the Sea, Nantes*
K. Rose, *Louisiana State University*
J. Rosenfeld, *British Columbia Ministry of Fisheries*
B. Sainte-Marie, *Fisheries and Oceans Canada, Mont-Joli*
R.E.H. Smith, *University of Waterloo*
S.J. Smith, *Fisheries and Oceans Canada, Dartmouth*
W.G. Sprules, *University of Toronto*
E.B. Taylor, *University of British Columbia*
W. Tonn, *University of Alberta*
M. Trudel, *Fisheries and Oceans Canada, Nanaimo*
A. Vasemägi, *University of Turku*
C.J. Walters, *University of British Columbia*
G. Weyhenmeyer, *Uppsala University*

NRC Research Press / NRC Research Press

Fax / télécopieur : 613-952-7656; e-mail / courriel : pubs@nrcresearchpress.com; URL / URL : nrcresearchpress.com

Editor-in-Chief / Directeur de la publication **Bruce P. Dancik**
Deputy Editor-in-Chief / Sous-directrice de la publication **Cindy E. Prescott**
Executive Director / Directeur général **Cameron D. Macdonald**

Director, Business Strategy and Development / Directeur, Stratégie et développement des affaires **Mike Boroczki**
Manager, Business Development / Gestionnaire du développement **Peter D'Amico**
Marketing and Sales Coordinator / Coordonnatrice des ventes et du marketing **Judy Letourneau** (613-993-0151)
Client Services Representative / Représentante des services à la clientèle **Eileen Evans-Nantais** (613-990-7873)

Director, Publishing Operations / Directrice, Services d'édition **Suzanne Kettley**
Managing Editor / Directrice de la rédaction **Cecily M. Pearson** (613-993-9099)
Scientific Publishing Editors / Réviseurs de publications scientifiques **Thad Costigan**
Publishing Assistant / Adjointe à l'édition **Diana Leck**

Production Manager / Gestionnaire de la production **Judy Hum**
e-Publishing Technician / Technicien à l'édition électronique **Jeffrey Wisking**
Graphics Technician / Technicien en graphisme **Leslie Cameron**
Web Technician / Technicien Web **Dennis Cafferty**

NRC Research Press accepts no responsibility for statements or opinions expressed by a contributor. Acceptance of an advertisement, announcement, or other material does not imply endorsement by either the Journal's Editors or NRC Research Press.

© 2011 Canadian Science Publishing or its licensors

As of 2009, copyright in all articles in NRC Research Press journals remains with the authors. All articles published previously are copyright Canadian Science Publishing (which operates as NRC Research Press) or its licensors.

No part of the NRC Research Press journals may be reproduced, stored, or transmitted in any form or by any means, without the written permission of the publisher, except as stated below.

Under the Canadian *Copyright Act*, individuals may download or print single copies of articles for personal research or study. Any person may reproduce short excerpts from articles in the journals for any purpose that respects the moral rights of authors, provided that the source is fully acknowledged. As a courtesy, the consent of authors of such material should be obtained directly from the author.

Authorization to reproduce items for other than personal research or study, as stated above, may be obtained by clicking on the "Reprints and Permissions" link in the table of contents of the electronic article in question or via Access Copyright (www.accesscopyright.ca).

NRC Research Press also extends certain additional rights to authors.

The above rights do not extend to copying or reproduction for general distribution, for advertising or promotional purposes, for creating new collective works, or for resale. For such copying or reproduction, arrangements must be made with NRC Research Press, Ottawa, ON K1A 0R6, Canada.

Subscription information

The *Canadian Journal of Fisheries and Aquatic Sciences* (ISSN 0706-652X) is published monthly by NRC Research Press. The 2011 subscription rates are as follows. Institutional: electronic $1240; print, $1490; electronic + print, $1865. Personal: electronic, $320, print + electronic, $430. For all orders outside Canada, rates are in U.S. dollars. Print subscriptions include second class postage. For air mail add US$204 to the foreign rate. Canadian customers please include GST (business no. 81942 4656 RT0001). Subscriptions are entered for the calendar year. Remittances should be made payable to Canadian Science Publishing. Price for regular single issues: institutional, $150.00; personal, $50.00. Supplements will be priced separately. Special rates apply to members of Canadian scientific and engineering societies if they subscribe through their respective societies.

Issues of the *Canadian Journal of Fisheries and Aquatic Sciences* are available on the Web. Pricing information can be found at nrcresearchpress.com/page/librarians/subscriptions/pricing.

There are no refunds on cancelled subscriptions once delivery has begun. All claims must be submitted within 12 months of the publication date. The publisher expects to supply missing issues only when losses have occurred in transit and when the reserve stock will permit. Subscriptions, renewals, requests for single or back issues, and all remittances should be sent to Canadian Science Publishing, NRC Research Press, Subscription Office, P.O. Box 830399, Birmingham, AL 35283-0399, USA (telephone: 1-800-633-4931 in North America or 1-800-852-7404 outside North America; fax: 205-995-1588).

Microform backfiles are available from NA Publishing Inc., P.O. Box 998, Ann Arbor, MI 48106-0998, U.S.A., (734) 302-6500. www.napublishing.com.

NRC Research Press ne se tient en aucune façon responsable des opinions exprimées par un collaborateur ou des déclarations que pourrait faire ce dernier. La publication d'annonces publicitaires, d'avis et autres n'implique pas l'endossement de leur contenu par les rédacteurs en chef de la Revue ou NRC Research Press.

© 2011 Éditions Sciences Canada ou ses concédants de licence

Depuis 2009, les auteurs conservent le droit d'auteur de tout article qu'ils publient dans les revues de NRC Research Press. Éditions Sciences Canada (qui œuvre sous la dénomination commerciale NRC Research Press) ou leurs concédants de licence, quant à eux, se réservent les droits d'auteur sur tous les articles précédemment publiés à NRC Research Press.

Il est interdit de reproduire, de sauvegarder ou de transmettre toute partie des revues de NRC Research Press dans quelque format ou de quelque façon que ce soit sans le consentement écrit de l'éditeur, sauf dans les cas énoncés ci-après.

Aux termes de la *Loi sur le droit d'auteur* du Canada, les particuliers peuvent télécharger ou imprimer des copies individuelles d'articles pour leurs études ou leurs recherches personnelles. Toute personne peut reproduire de courts extraits des articles d'une revue pourvu que les droits moraux de l'auteur soient respectés et que la source soit clairement indiquée. Il convient de demander directement à l'auteur son consentement.

On peut obtenir l'autorisation de reproduire du contenu à d'autres fins que l'usage personnel (tel que décrit ci-dessus), en cliquant sur le lien « Réimpressions et autorisations » dans la table des matières de l'article électronique en question ou par l'intermédiaire d'Access Copyright (www.accesscopyright.ca).

NRC Research Press accorde aussi des privilèges supplémentaires aux auteurs.

Les droits ci-dessus ne s'appliquent pas à la reproduction à grande échelle aux fins de distribution générale, de publicité ou de promotion, de compilation de nouveaux ouvrages collectifs ou de revente, par exemple. Les droits de reproduction de ce genre doivent faire l'objet d'une entente particulière avec NRC Research Press, Ottawa, ON K1A 0R6, Canada.

Renseignements sur l'abonnement

Journal canadien des sciences halieutiques et aquatiques (ISSN 0706-652X) est une publication mensuelle de NRC Research Press. En 2011, les tarifs d'abonnement pour les organismes sont les suivants : 1240 $ pour la version électronique; 1490 $ pour l'imprimé; 1865 $ pour les deux versions. Pour leur part, les particuliers paient les tarifs suivants : 320 $ pour la version électronique; 430 $ pour la version électronique et l'imprimé. Les tarifs des commandes provenant de l'extérieur du Canada sont en dollars des États-Unis. L'abonnement à l'imprimé comprend le tarif du courrier de deuxième classe. L'expédition par avion exige des frais de 204 $US en sus du prix d'abonnement à l'étranger. Les clients du Canada doivent ajouter la TPS (numéro d'entreprise 81942 4656 RT0001). Les abonnements sont pour l'année civile. Tout paiement doit être adressé aux Éditions sciences Canada. Le prix par numéro régulier est de 150,00 $ pour les organismes et de 50,00 $ pour les particuliers. Le prix des hors-série varie. Les membres des sociétés canadiennes de sciences et de génie bénéficient de taux préférentiels en s'abonnant via leurs sociétés respectives.

Tous les numéros de Journal canadien des sciences halieutiques et aquatiques sont accessibles sur le Web. On trouvera des renseignements sur les tarifs au nrcresearchpress.com/page/librarians/subscriptions/pricing.

Aucun remboursement ne sera accordé, ni aucune annulation acceptée, une fois que les livraisons auront commencé. Toute réclamation doit être présentée dans les 12 mois suivant la date de publication. L'éditeur ne fournira de numéros manquants que si le document a été perdu pendant l'expédition et que si les réserves le permettent. Pour un abonnement ou un renouvellement, pour une demande de numéro (actuel ou ancien), ainsi que pour une réclamation, adressez-vous au Bureau des abonnements, Éditions Sciences Canada, NRC Research Press, P.O. Box 830399, Birmingham, AL 35283-0399, É.-U. (téléphone : 1-800-633-4931, en Amérique du Nord, ou 1-800-852-7404, ailleurs; télécopieur : 205-995-1588).

On peut obtenir les archives sur microforme auprès de NA Publishing, Inc., P.O. Box 998, Ann Arbor, MI 48106-0998, U.S.A., (734) 302-6500, www.napublishing.com.

RAPID COMMUNICATION / COMMUNICATION RAPIDE

A deathly odor suggests a new sustainable tool for controlling a costly invasive species

C. Michael Wagner, Eric M. Stroud, and Trevor D. Meckley

Abstract: Here we confirm a long-standing anecdotal observation; the sea lamprey (*Petromyzon marinus*) actively avoids the odor emitted by decaying conspecifics. We extracted the semiochemical mixture produced by the putrefying carcasses of sea lampreys via Soxhlet extraction in ethanol and exposed groups of 10 migratory-phase lampreys to either the putrefaction extract ($N = 8$) or an ethanol control ($N = 8$) in a laboratory raceway. Sea lampreys rapidly avoided the putrefaction odor while exhibiting no response to the ethanol control. This response was elicited with a diluted mixture (1:373 000) and was maintained for 40 min (the duration of exposure), after which the lampreys quickly returned to their nominal distribution. The ease with which this odor is obtained, and the rapid and consistent behavioral response, suggests the substance will prove useful as a repellent in the sea lamprey control program carried out in the Laurentian Great Lakes.

Résumé : Nous confirmons ici une observation anecdotique de longue date, voulant que la grande lamproie marine (*Petromyzon marinus*) évite de manière active l'odeur émise par les cadavres en décomposition des lamproies de même espèce. Nous avons extrait le mélange sémiochimique produit par des carcasses en putréfaction de grandes lamproies marines par extraction Soxhlet en éthanol; nous avons ensuite exposé des groupes de 10 lamproies en phase migratrice à soit l'extrait de putréfaction ($N = 8$), soit à un témoin d'éthanol ($N = 8$) dans un canal de nage en laboratoire. Les grandes lamproies marines évitent rapidement l'odeur de putréfaction, alors qu'elles n'ont aucune réaction au témoin d'éthanol. Cette réaction est provoquée par un mélange dilué (1:373 000) et se maintient pendant 40 min (durée de l'exposition), après quoi les lamproies retrouvent rapidement leur répartition normale. La facilité avec laquelle on peut obtenir cette odeur et la réaction comportementale constante qu'elle provoque font croire que cette substance s'avérera utile comme répulsif dans le programme de lutte contre la grande lamproie marine en cours dans les Grands Lacs laurentiens.

[Traduit par la Rédaction]

Introduction

When an organism's lifetime fitness is bound to a single reproductive episode, the ability to locate a habitat that is favorable for the acquisition of mates and subsequent deposition of offspring becomes a vital enterprise. The sea lamprey, *Petromyzon marinus*, a devastating invasive species in the Laurentian Great Lakes, relies on the odor emitted by overlapping generations of larvae to navigate into streams with suitable spawning and rearing habitat (Sorensen and Hoye 2007). Upon arrival, another odor emitted by mature males lures females onto nests to complete spawning (Johnson et al. 2009). These pheromones have proven to be powerful attractants when applied to stream water, and considerable effort has been expended to identify novel ways to exploit this communication system to achieve pest management purposes (Johnson et al. 2009; Wagner et al. 2009). To date, those efforts have been fully focused on the manipulation of attraction.

The sea lamprey reproductive migration is also notable in that it is nocturnal. This tendency is consistent with the avoidance of risk and reasonable given that a migrant is required to enter increasingly narrow and shallow waterways. Rich arrays of olfactory alarm cues are used by aquatic organism to assess risk (Ferrari et al. 2010). Among these are odors emitted by dead and decaying conspecifics (so-called necromones; Yao et al. 2009). Recognition and avoidance of the death odor may commonly serve to reduce risks associated with predators or sources of contagion in aquatic environments (Brown 2003). For a migrating sea lamprey, this odor may also indicate the cessation of spawning, particularly in the absence of the reproductive pheromone.

Based largely on anecdotal information, the existence of a novel alarm cue, possibly a necromone, has recently been speculated for the sea lamprey (Imre et al. 2010). If elucidated, a lamprey alarm cue could prove useful in pest management that employs behavioral manipulation via chemical stimuli. Here, we report a laboratory experiment that demonstrates the sea lamprey is chemically aware of, and actively

Received 25 January 2011. Accepted 22 April 2011. Published at www.nrcresearchpress.com/cjfas on 8 July 2011.
J2011-0010

Paper handled by Associate Editor Cliff Kraft.

C.M. Wagner and T.D. Meckley. Michigan State University, 13 Natural Resources Building, East Lansing, MI 48823, USA.
E.M. Stroud. Shark Defense Technologies, LLC, P.O. Box 2593, Oak Ridge, NJ 07438, USA.

Corresponding author: C. Michael Wagner (e-mail: mwagner@msu.edu).

Can. J. Fish. Aquat. Sci. **68**: 1157–1160 (2011) doi:10.1139/F2011-072 Published by NRC Research Press

avoids, the odor emitted by decaying conspecifics. We discuss the implications of this finding for the rapid development of novel pest management practices based on the simultaneous use of attractants and repellents.

Materials and methods

Experimental subjects

We obtained adult migratory-phase sea lampreys from the US Fish and Wildlife Service, who trapped the animals as part of the their annual control program. All subjects came from two tributaries to Lake Huron, the Ocqueoc and Cheboygan rivers in northern Michigan, and were captured during May 2010. After capture, we placed the lampreys into flow-through tanks receiving Lake Huron water (5–10 °C depending on date with 100% exchange every 2 h) at the nearby US Geological Survey Hammond Bay Biological Station (Millersburg, Michigan). Prior to use, we selected lampreys in visibly good condition and moved them into pretrial holding tanks receiving the same Lake Huron water as the experimental raceway. Use of sea lampreys was approved by the Michigan State University Institutional Animal Care & Use Committee (AUF No. 02/10-020-00).

Collection of the semiochemical mixture

We extracted the putative alarm odor from individual lamprey carcasses at four time points postmortem (0, 24, 48, and 120 h) using a 1 L 71/60 Soxhlet apparatus with a six-bulb, water-cooled Allihn condenser and a 3 L solvent reservoir heated with a hemispherical mantle. Aerobic decay of each carcass took place under laboratory conditions in a 1 L high-density polyethylene bottle at room temperature. Prior to extraction we washed the carcasses with 100 mL of solvent (50% *w/w* solution of 190 proof ethyl alcohol and deionized water) and set aside the rinsate. We then mounted a single decayed carcass onto a glass extraction thimble and added 800 mL of the solvent solution. We maintained the solvent temperature in the reservoir at 65–80 °C and cycled the extractor three times per carcass. At the conclusion of the extraction we allowed the solvent to cool to room temperature before combining it with the rinsate to form the time-specific putrefaction extract. Because we did not know when during aerobic decay the compound(s) responsible for the behavioral response are produced or released, we formed the final test mixture by combining 500 mL from each of the four time-specific extracts (0, 24, 48, and 120 h), hereafter referred to as the putrefaction extract.

Behavioral assay

To determine whether exposure to the putrefaction extract repels sea lampreys, we examined space use by 16 groups of 10 migratory-phase adult sea lampreys (160 individuals total, each used once) in a 5.00 m × 1.85 m section of laboratory raceway receiving a continuous discharge of 680 L·min^{-1} at a depth of 20 cm (Fig. 1). We examined the lampreys' movements in response to two treatments: (*i*) the composited mixture of time-specific putrefaction extracts (described above) and (*ii*) an ethanol control. We completed eight replicates of each treatment. All trials took place 1 h after sunset.

Four hours prior to the start of a trial, we placed a new group of 10 migratory-phase adult sea lampreys (five male, five female) into a holding cage in the downstream portion of the raceway to allow for acclimation to test conditions. Each trial was 100 min in duration and comprised three periods: (*i*) a 20 min pretrial observation period, where lampreys were released from the cage and allowed to swim freely; (*ii*) a 40 min stimulus period, where an odor was pumped into one side of the channel; and (*iii*) a 40 min post-trial observation period that began after stimulus introduction was ceased. We mixed 40 mL of a stimulus (ethanol or putrefaction extract) with 400 mL of raceway water and pumped the mixture at a rate of 10 mL·min^{-1} into one side of the channel using a laboratory peristaltic pump. We alternated the side of the channel receiving the stimulus across replicates within each treatment (four left-side trials and four right-side trials for each treatment).

Data collection and analysis

We illuminated the raceway with infrared lights and recorded lamprey movements with an overhead night-vision video camera. At the conclusion of the experiment we reviewed the video from each trial and assigned each lamprey a position on a six-square grid every 30 s based on the location of the animal's head (Fig. 1). From these data we calculated the proportion of lampreys on the stimulus and nonstimulus side of the raceway during each period (prestimulus, stimulus, and poststimulus). We used a general linear model (GLM; SYSTAT v.12, Systat Software Inc., Chicago, Illinois) to ascertain whether differences in the proportion of lampreys on the scented side of the channel (dependent variable) vs. the unscented side were a function of treatment (ethanol or putrefaction extract), time period (prestimulus, stimulus, or poststimulus), or the side of the channel receiving the scent (right or left). All two-way interactions were included. Because we predicted (*i*) strong avoidance of the putrefaction extract during the stimulus period, (*ii*) no change in distribution in response to exposure to the ethanol control, and (*iii*) no effect of the side of the channel receiving the scent, we expected significant main effects of treatment and time period and a significant interaction between the two. To ascertain whether the differences detected in the GLM were due to avoidance during the stimulus period, we performed an individual analysis of variance (ANOVA) for each treatment, testing for differences between time periods with Tukey's honestly significant difference test (HSD, $\alpha = 0.05$).

Results

As predicted, there were significant treatment ($F_{[1,38]} = 53.8$, $P < 0.001$) and time period main effects ($F_{[2,38]} = 53.0$, $P < 0.001$) and a treatment × time period interaction ($F_{[2,38]} = 46.5$, $P < 0.001$) in the GLM. The side of the tank that received the stimulus (main effect, $F_{[1,38]} = 1.1$, $P = 0.29$) and all other two-way interactions were not significant (treatment × side, $F_{[1,38]} = 3.7$, $P = 0.06$; time period × side, $F_{[2,38]} = 0.937$, $P = 0.40$). The behavioral responses of migratory phase sea lampreys in the raceway were consistent with a strong avoidance of the putrefaction extract (Fig. 2). During the ethanol control trials, the proportion of lampreys that chose the scented side of the raceway varied between 45% and 55%, with no significant preference for either side (ANOVA, $F_{[2,21]} = 0.54$, $P = 0.59$; Fig. 2*a*). Conversely, ad-

Fig. 1. Overhead view of the raceway setup for behavioral avoidance testing. Water flowed from left to right (arrow), and odors were introduced from peristaltic pumps (solid circles) on the right (R) or left (L) side of the channel placed upstream of a block net (thick vertical line). The bottom of the raceway was lined with white plexiglass and marked into six equal-sized grid squares to ascertain space use (dotted lines and numbers). At the start of a trial, subjects were released from the holding cage (HC) and recorded with an overhead video camera.

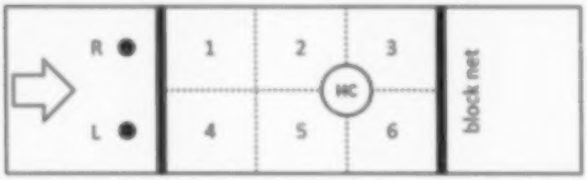

dition of the putrefaction extract quickly induced strong avoidance of the scented side during the 40 min stimulus period (ANOVA, $F_{[2,21]} = 29.6$, $P < 0.001$; Tukey's HSD, prestimulus vs. stimulus, $P < 0.001$, poststimulus vs. stimulus, $P < 0.001$; Fig. 2*b*). On average, lampreys spent 12%–15% of the time on the scented side during the stimulus period, often darting back to the unscented side and quickly swimming downstream. Lampreys exposed to the putrefaction extract returned to the nominal prestimulus distribution 6–8 min after odor introduction ceased (Tukey's HSD, prestimulus vs. poststimulus, $P = 0.99$).

Fig. 2. Mean (± 1 SE) proportion of lampreys on the scented side of the channel for ethanol control (*a*) and putrefaction extract (*b*) trials ($N = 8$). Sea lampreys actively avoided the putrefaction extract but exhibited no response to the ethanol control.

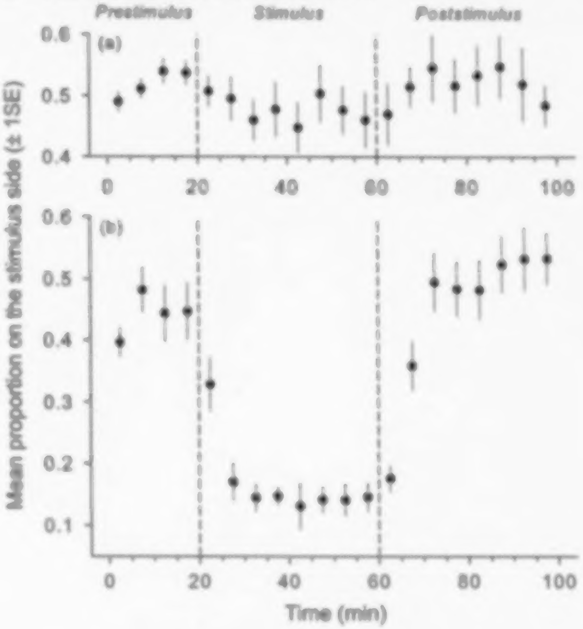

Discussion

There is considerable evidence that risk-indicating olfactory cues are used by many aquatic species to assess potential fitness costs associated with space and resource use (Lima and Dill 1990; Brown 2003). Laframboise et al. (2007) recently described three distinct olfactory sensory neuron morphotypes intermingled in the sea lamprey olfactory organ. This arrangement closely parallels that of teleost fishes (Hamdani and Doving 2007), where the axons of each morphotype converge to a separate and specific region of the olfactory bulb, and three distinct connections to the brain arise, thereby mediating three fundamental behavioral processes. One pathway is tuned to reproductive pheromones, another to food odors, and the third to social cues and alarm substances. The similarities revealed in the sea lamprey olfactory architecture imply a reliance on odors for fundamental processes beyond reproduction, and the behavioral evidence reported here suggests the avoidance of harm is also mediated by olfaction in the sea lamprey.

We observed sea lampreys actively avoiding a dilute odor of decaying conspecifics (≈ 1:373 000, assuming full mixing into one half of the channel). By avoiding the odor of decaying conspecifics during the annual spawning migration, we hypothesize that sea lampreys may be alleviating one or more of three circumstances that potentially have strong negative effects on reproductive success: (*i*) entering streams where spawning has already ceased (if combined with the absence of reproductive pheromones), (*ii*) movement through areas of the watershed where terrestrial and (or) aquatic predators are killing migrating lampreys, and (*iii*) deposition of offspring in streams where high larval mortality is occurring. Regardless of the ultimate function, the confluence between reliance on innately acquired responses to olfactory stimuli and a geographic feature of the sea lamprey migration reveals a unique opportunity to achieve sea lamprey control with a natural repellent. This rationale was first proposed by James Miller (Michigan State University, East Lansing, Michigan) and is also mentioned in Imre et al. (2010).

The push–pull approach (Miller and Cowles 1990) involves the use of behavior-modifying chemical stimuli to manipulate the distribution of herbivorous insects and thereby reduce crop damage. Repellents "push" pests away from sites needing protection and attractants "pull" them into areas where they become vulnerable to pesticide application. As sea lampreys migrate, they transition from unconstrained movements in a three-dimensional environment (lake or ocean) to constrained movements in a network of stream channels. As noted previously, migrating sea lampreys appear to choose a river based on the emission of larval odor (Sorensen and Hoye 2007; Wagner et al. 2009) and are not preconditioned to enter the natal stream (Waldman et al. 2008). Because migrants attempting to move into spawning grounds located high in the watershed must first pass through the lower river channels, they sequentially pass bifurcations in the network. Thus, we may divert migrating lampreys away from a repellent-treated tributary and into the adjacent fork if activated with the migratory pheromone. Because successful blockage at any point low in the network protects all areas upstream of the node, a large fraction of the watershed may be blocked off with applications at a few sites, greatly limiting the amount of spawning area available and thereby the area in need of subsequent pesticide treatment. The success of the push–pull manipulation, whether perpetrated at the river mouth or at a branch higher in the watershed, will likely rely on providing the lampreys with a simultaneous and simple choice between two options, one noxious and one attractive.

Existence of the sea lamprey alarm substance presents two substantial opportunities. Scientifically, it may represent a habitat-quality cue that mediates reproductive decision making by an ancient migratory species: a potentially novel use of a substance typically viewed as an indirect predator cue. Second, because it can be cheaply and rapidly collected, its utility in pest management may be verified prior to undertaking the costly and time-intensive process of isolation and full chemical elucidation.

Acknowledgements

Michael Siefkes, three anonymous reviewers, and the journal editorial staff made several useful suggestions that substantially improved the final manuscript. We are grateful to the Great Lakes Fishery Commission for encouraging our public–private partnership and for providing travel funds and access to the Hammond Bay Biological Station. Additional funding for this work was provided by the Michigan State University Center for Water Sciences Venture Grant program. Daniel Hayes generously provided statistical consultations. Brett Diffin and Anne Scott provided valuable assistance in the laboratory.

References

Brown, G.E. 2003. Learning about danger: chemical alarm cues and local risk assessment in prey fishes. Fish Fish. **4**: 227–234. doi:10.1046/j.1467-2979.2003.00132.x.

Ferrari, M.O., Wisenden, B.D., and Chivers, D.P. 2010. Chemical ecology of predator–prey interactions in aquatic ecosystems: a review and prospectus. Can. J. Zool. **88**(7): 698–724. doi:10.1139/Z10-029.

Hamdani, E.H., and Doving, K.B. 2007. The functional organization of the fish olfactory system. Prog. Neurobiol. **82**(2): 80–86. doi:10.1016/j.pneurobio.2007.02.007. PMID:17433527.

Imre, I., Brown, G.E., Bergstedt, R.A., and McDonald, R. 2010. Use of chemosensory cues as repellents for sea lamprey: potential directions for population management. J. Great Lakes Res. **36**(4): 790–793. doi:10.1016/j.jglr.2010.07.004.

Johnson, N.S., Yun, S.S., Thompson, H.T., Brant, C.O., and Li, W. 2009. A synthesized pheromone induces upstream movement in female sea lamprey and summons them into traps. Proc. Natl. Assoc. Sci. U.S.A. **106**(4): 1021–1026. doi:10.1073/pnas.0808530106. PMID:19164592.

Laframboise, A.J., Ren, X., Chang, S., Dubuc, R., and Zielinski, B.S. 2007. Olfactory sensory neurons in the sea lamprey display polymorphisms. Neurosci. Lett. **414**(3): 277–281. doi:10.1016/j.neulet.2006.12.037. PMID:17254708.

Lima, S.L., and Dill, L.M. 1990. Behavioural decisions made under the risk of predation: a review and prospectus. Can. J. Zool. **68**(4): 619–640. doi:10.1139/z90-092.

Miller, J.R., and Cowles, R.S. 1990. Stimulo-deterrent diversion: a concept and its possible application to onion maggot control. J. Chem. Ecol. **16**(11): 3197–3212. doi:10.1007/BF00979619.

Sorensen, P.W., and Hoye, T.R. 2007. A critical review of the discovery and application of a migratory pheromone in an invasive fish, the sea lamprey *Petromyzon marinus* L. J. Fish Biol. **71**: 100–114. doi:10.1111/j.1095-8649.2007.01681.x.

Wagner, C.M., Twohey, M.B., and Fine, J.M. 2009. Conspecific cueing in the sea lamprey: Do reproductive migrations consistently follow the most intense larval odor? Anim. Behav. **78**(3): 593–599. doi:10.1016/j.anbehav.2009.04.027.

Waldman, J., Grunwald, C., and Wirgin, I. 2008. Sea lamprey *Petromyzon marinus*: an exception to the rule of homing in anadromous fishes. Biol. Lett. **4**(6): 659–662. doi:10.1098/rsbl.2008.0341. PMID:18713713.

Yao, M., Rosenfeld, J., Attridge, S., Sidhu, S., Aksenov, V., and Rollo, C.D. 2009. The ancient chemistry of avoiding risks of predation and disease. Evol. Biol. **36**(3): 267–281. doi:10.1007/s11692-009-9069-4.

Nutrient fluxes and the recent collapse of coastal California salmon populations

Jonathan W. Moore, Sean A. Hayes, Walter Duffy, Sean Gallagher, Cyril J. Michel, and David Wright

Abstract: Migratory salmon move nutrients both in and out of fresh waters during the different parts of their life cycle. We used a mass-balance approach to quantify recent changes in phosphorus (P) fluxes in six coastal California, USA, watersheds that have recently experienced dramatic decreases in salmon populations. As adults, semelparous Chinook (*Oncorhynchus tshawytscha*) and coho (*Oncorhynchus kisutch*) salmon imported 8.3 and 10.4 times more P from the ocean, respectively, than they exported as smolts, while iteroparous steelhead (i.e., sea-run rainbow trout, *Oncorhynchus mykiss*) imported only 1.6 times more than they exported as kelts and smolts. Semelparous species whose life histories led them to import more nutrients were also the species whose populations decreased the most dramatically in California in recent years. In addition, the relationship between import and export was nonlinear, with export being proportionally more important at lower levels of import. This pattern was driven by two density-dependent processes — smolts were larger and disproportionately more abundant at lower spawner abundances. In fact, in four of our six streams we found evidence that salmon can drive net export of P at low abundance, evidence for the reversal of the "conveyor belt" of nutrients.

Résumé : Les saumons migrateurs déplacent des nutriments tant vers les eaux douces qu'hors des eaux douces durant les différentes étapes de leur cycle biologique. Nous utilisons une méthode de bilan massique pour mesurer les changements récents dans les flux de phosphore (P) dans six bassins versants côtiers de Californie, É.-U., qui ont connu des déclins spectaculaires de leurs populations de saumons. Au stade adulte, les saumons chinook (*Oncorhynchus tshawytscha* et coho (*Oncorhynchus kisutch*) sémelpares importent respectivement 8,3 et 10,4 fois plus de P de l'océan qu'ils n'en exportent au stade saumoneau; en revanche, les truites arc-en-ciel anadromes (*Oncorhynchus mykiss*) itéropares importent seulement 1,6 fois plus qu'ils en exportent comme bécards et saumoneaux. Les espèces sémelpares dont le cycle biologique les amène à importer plus de nutriments sont aussi les espèces dont les populations ont décru de façon la plus spectaculaire en Californie ces dernières années. De plus, la relation entre l'importation et l'exportation n'est pas linéaire et l'exportation est proportionnellement plus importante aux faibles niveaux d'importation. Ce patron s'explique par deux processus dépendants de la densité — les saumoneaux sont de plus grande taille et de façon disproportionnée plus abondants aux faibles abondances de reproducteurs. En fait, dans quatre des six cours d'eau, nous trouvons des preuves que les saumons peuvent contrôler l'exportation nette de P aux faibles abondances; ce sont des indications du renversement de la « courroie de transmission » des nutriments.

[Traduit par la Rédaction]

Introduction

Species can control fluxes of nutrients and energy across ecosystem boundaries through their own movements (Lundberg and Moberg 2003; Polis et al. 2004). Nutrients can be liberated in the recipient ecosystem when individuals of the species die or excrete there. For example, nesting seabirds import marine-derived nutrients to roosting and nesting islands, where their guano fuels terrestrial communities (Sánchez-Piñero and Polis 2000). It follows that the loss of these species that link ecosystems may have profound consequences; for example, seabird population declines have led to dramatic changes in the community composition and productivity of island ecosystems (Croll et al. 2005; Young et al. 2010).

Pacific salmon (*Oncorhynchus* spp.) represent one of the most well-known examples of biotic control of ecosystem fluxes. These anadromous species grow large in the ocean and subsequently migrate to coastal fresh waters where they spawn, often at high abundance. Through this migration,

Received 22 November 2010. Accepted 26 March 2011. Published at www.nrcresearchpress.com/cjfas on 4 July 2011.
J22128

Paper handled by Associate Editor Bror Jonsson.

J.W. Moore.* Department of Ecology and Evolutionary Biology, University of California, Santa Cruz, CA 95060, USA.
S.A. Hayes and C.J. Michel. NOAA Fisheries, Southwest Fisheries Science Center, Santa Cruz, CA 95060, USA.
W. Duffy. USGS California Cooperative Fish and Wildlife, Humbolt State University, Arcata, CA 95521, USA.
S. Gallagher. California State Department of Fish and Game, 32330 North Harbor Drive, Fort Bragg, CA 95437, USA.
D. Wright. Campbell Timberlands Management, LLC, P.O. Box 1228, Fort Bragg, CA 95437, USA.

Corresponding author: Jonathan W. Moore (e-mail: jwmoore@sfu.ca).

*Current address: Simon Fraser University, Earth$_2$Ocean research group, 8888 University Drive, Burnaby, BC V5A 1S6, Canada.

Can. J. Fish. Aquat. Sci. **68**: 1161–1170 (2011) doi:10.1139/F2011-054 Published by NRC Research Press

anadromous salmon can act as a "conveyor belt" of nutrients and energy, moving the nutrients and energy that make up their bodies from marine to coastal freshwater ecosystems (Larkin and Slaney 1997; Gresh et al. 2000; Naiman et al. 2002). In spawning habitats with high densities of salmon, salmon-derived nutrients such as nitrogen (N) and phosphorus (P) can comprise a large component of ecosystem nutrient budgets (Naiman et al. 2002; Schindler et al. 2003). N and P are commonly limiting nutrients in coastal fresh waters (Elser et al. 2007; Sanderson et al. 2009). Studies in regions with high abundances of salmon have found that their nutrients directly and indirectly subsidize a variety of aquatic and riparian species, ranging from bears to insects to plants (e.g., Cederholm et al. 1999; Wipfli and Baxter 2010). Even in highly altered river systems such as those that flow through agricultural areas in central California, salmon-derived resources are heavily used by a variety of riparian scavengers (Merz and Moyle 2006).

Anadromous salmon also export nutrients from fresh waters as outmigrating juvenile salmon, not only acting as importers of nutrients to fresh waters when adults migrate in from the ocean to spawn (Moore and Schindler 2004). Juvenile salmon spend up to several years feeding and growing in fresh waters prior to outmigration. This outmigration of juvenile salmon, or smolts, represents the movement of nutrients and energy from freshwater coastal ecosystems to marine ecosystems. Few studies have calculated both nutrient import and export due to salmon migrations. For semelparous species, the net flux of salmon nutrients can be calculated as the import by spawners minus the export by smolts. Studies on these anadromous and semelparous species have found that spawners generally import more nutrients than smolts export but that these patterns are influenced by density-dependent feedbacks (Moore and Schindler 2004; Scheuerell et al. 2005). Specifically, Moore and Schindler (2004) found that P import is approximately six times greater than export for Alaskan sockeye (*Oncorhynchus nerka*) populations, and Scheuerell et al. (2005) found import is approximately five times greater than export for Chinook salmon (*Oncorhynchus tshawytscha*) in the Snake River basin.

Many salmon populations have declined over the last century because of a suite of human impacts, especially towards the southern extent of their range, such as in California (Gustafson et al. 2007). These salmon declines have raised concerns about the loss of salmon-derived nutrients and corresponding potential declines in coastal freshwater productivity (e.g., Stockner et al. 2000). How do patterns of import and export change at low salmon abundance? Moore and Schindler (2004) proposed that export would be proportionally more important at lower population sizes because of density dependence, and Scheuerell et al. (2005) found evidence of this relationship for Snake River Chinook. Thus, net import of nutrients may decline faster than anticipated as salmon populations decline. It is even possible that at low abundances salmon become net exporters of nutrients — reversing the direction of the conveyor belt of marine-derived nutrients, stripping nutrients out of freshwater systems at low abundances. Thus, there remains great uncertainty into how these patterns of flux might change as salmon populations decline.

For iteroparous species with more complicated life histories, there is potential for a lower import–export ratio, as adults can survive spawning to migrate back out to the ocean. While fluxes have never before been quantified for iteroparous Pacific salmonids (i.e., steelhead (or sea-run rainbow trout), *Oncorhynchus mykiss*), previous research on iteroparous Atlantic salmon (*Salmo salar*) found that they can either act as a net importer (Lyle and Elliott 1998; Jonsson and Jonsson 2003) or net exporter of nutrients (Nislow et al. 2004). Thus, different species with different life histories may exhibit fundamentally different patterns of nutrient import and export.

Our goal was to quantify annual nutrient fluxes by multiple salmon species over recent decreases in salmon population abundances. In coastal California, where streams contain coho salmon (*Oncorhynchus kisutch*), steelhead trout (*O. mykiss*), and to a lesser extent, Chinook salmon (*O. tshawytscha*), populations have been declining. Of great conservation concern are coho salmon in the California coastal region, listed as federally Threatened or Endangered depending on the location (Federal Register 2005), which have rapidly declined in abundance over 2008–2010 (Miller 2010). Central California represents the southern extent of coho salmon in North America. For some spawning populations, there is concern that these populations will go extinct in the near future without human intervention (Miller 2010). It is thought that this recent decline is due to the combination of the legacy of past human degradation of freshwater habitats coupled with poor ocean conditions (Miller 2010). Using salmon abundance data from this period of population declines, we used a mass-balance approach to examine recent changes in nutrient fluxes in six coastal California streams. We asked the question, how did patterns of nutrient fluxes change over the recent collapse of California salmon populations? In particular, we examined the possibility that density-dependent processes could drive disproportionately rapid loss of net nutrient import. We also examined the role of multiple salmon species in contributing to nutrient fluxes during this period.

Materials and methods

Study systems

We compiled data on coho salmon (six streams), steelhead (five streams), and Chinook salmon (one stream) from six study streams (Table 1); five of these streams (the exception being Little River) represent all of the life-cycle monitoring stations (adult and smolt abundance) of the developing California Coastal Salmon Monitoring Plan (Adams et al. 2011). These stations consist of both adult upstream traps and downstream smolt traps. Adult escapement in Little River is based on redd counts (Gallagher et al. 2010). Adult traps are monitored from mid-November through late March. Downstream smolt traps are operated from early March until early June (Gallagher and Wright 2009). These streams are dominated by coniferous redwood forests (*Sequoia sempervirens*); stream lengths accessible to anadromous fishes range from 6 to 117 km, flow directly into the ocean, and are groundwater-fed with peak flows in winter following heavy rains (Table 1).

Annual abundances of smolts and adults (spawners) of each species were obtained using standard population estimation techniques (Johnson et al. 2007). Each of the life-cycle monitoring stations consists of a downstream smolt trap and

Table 1. Study streams, ordered from north (top) to south (bottom).

Stream	Flow ($m^3 \cdot s^{-1}$)[a]	Size (km)[b]	Diadromous salmonids	Years
Prairie Creek	0.05–8.80	21	Chinook, coho, steelhead[c]	2001–2008
Pudding Creek	0.01–7.65	18	Coho, steelhead	2006–2009
Noyo River	0.16–33.41	117	Coho, steelhead	2001–2009
Caspar Creek	0.01–5.92	14	Coho, steelhead	2002–2009
Little River	0.01–3.35	6	Coho, steelhead	2002–2009
Scott Creek	0.013–17	23	Coho, steelhead	2006–2009

[a] Range of observed stream flow.

[b] River kilometres accessible to spawning salmon.

[c] We did not include steelhead in our calculations of nutrient fluxes in Prairie Creek because monitoring only occurred during a subset of the available years. Steelhead were also not as abundant as Chinook and coho and thus did not contribute as much to nutrient fluxes.

an upstream migrant trap to catch emigrating adults. Smolt traps were generally monitored daily during the outmigration season. Trap efficiency tests were performed by experimental releases of marked smolts. Annual estimates of smolt abundance were obtained by extrapolating observed numbers based on these trap efficiency estimates. Annual adult estimates were generally obtained by combining observed numbers of upstream migrants with estimates based on mark and recapture techniques (Szerlong and Rundio 2008). More information on these life-cycle monitoring stations and these study streams can be found in Hayes et al. (2008), Gallagher and Wright (2009), Gallagher et al. (2010), and Campbell Timberland Management (2008).

Quantifying nutrient fluxes

We calculated the nutrient fluxes due to the migrations of salmon, following Moore and Schindler (2004) and Scheuerell et al. (2005). Similarly, we focused our analyses on P as a key limiting nutrient (Elser et al. 2007; Sanderson et al. 2009). In six northern California streams the N:P ratio was extremely high (total P and total N averaged 9.05 and 305.00 $\mu g \cdot L^{-1}$, respectively; Wilzbach et al. 2005), suggestive of P limitation in these streams. For each species, we estimated annual import (I) of P during year t as the product of the number of adults (A), their average mass (m_A), and the proportion of P in their bodies (p_A)

$$(1) \qquad I_t = A_t m_A p_A$$

For semelparous species, export of P during the year (E_t) is also the product of the number of outmigrating smolts (S), their average mass (m_S), and the proportion of P in their bodies (p_S).

$$(2) \qquad E_t = S_t m_S p_S$$

For iteroparous steelhead that can survive spawning, export was calculated as

$$(3) \qquad E_t = S_t m_S p_S + A_t m_A p_A kb$$

with the second half of the equation representing export from outmigrating, postspawning adults, or kelts, given their P concentration (p_A), the probability of surviving spawning (k), and the proportional change in mass during the spawning process (b). We estimate net annual flux as the difference between import (I_t) and export (E_t). These calculations of P flux could easily be translated to nitrogen flux by using N:P ratios.

We used previously published information as well as our own data to estimate parameters. Through comparing masses of individually marked steelhead before and after spawning (S.A. Hayes, unpublished data), we estimated the mass of postspawning steelhead to be 73% of prespawning fish (value of parameter b). We estimated the proportion of steelhead surviving spawning (k) at 0.62 through using mark–recapture estimates of adult steelhead from Scott Creek. Specifically, using the program MARK (White and Burnham 1999), we used a spatially explicit form of the Cormack–Jolly–Seber (CJS) model (Cormack 1964; Jolly 1965) for species that express an obligate migratory behavior, where recaptures are structured spatially along a migratory corridor (Burnham 1987). The model incorporates upstream and downstream migrating steelhead that were known to be missed by the weir, thus enabling maximum-likelihood estimates for the capture efficiency of the weir. Finally, correcting actual upstream and downstream steelhead counts at the weir with their respective capture efficiencies allows the estimate of total escapement and total kelt outmigration, the difference of which is the total steelhead carcasses remaining in the watershed. Through communications with other steelhead biologists, this estimate of spawning survival meshes well with other estimates that range from 0.5–0.85 (T. Seamons, University of Washington, School of Aquatic and Fishery Sciences, Seattle, Washington, personal communication, 2010; Mayer et al. 2008; S. Gallagher, unpublished data). We assumed that P concentrations for adults (p_A) and smolts (p_S) were 0.38% and 0.43% of mass, respectively, following Moore and Schindler (2004) and Scheuerell et al. (2005).

Although in some cases individual fish mass was directly measured, lengths were more often collected on a subset of individuals. Owing to the nonlinearity of length–mass relationships, we used a bootstrapping algorithm for this conversion. We drew iteratively from the observed mean and standard deviation of length and converted those draws to masses using length–mass regressions. We used an average of 5000 draws as the average mass. Fish sizes were not collected for some species in some years; for these we used the average size and standard deviation for that species based on other years from the same system. We restricted our analyses of fluxes to the years when we possessed full information on adult and smolt abundance for all major species (Table 1).

Quantifying dynamics in nutrient flux

We calculated patterns of P flux based on both an annual basis and on a brood-year basis. On an annual basis, net P flux is simply equal to I_t minus E_t. We used "salmon year" as the appropriate period; for example, fish that returned to spawn in December 2008 were considered part the 2009 salmon year. We also compared import and export on a brood-year basis; we compared parental nutrients (I_t) to the nutrients that their offspring would export (E_{t+1} for coho and E_{t+2} for steelhead; these lags reflect the dominant life histories). We did not lag nutrient export by steelhead kelts because they migrate back to the ocean in the same year they migrate to fresh water to spawn. The calculation of brood-year P fluxes allowed us to investigate potential density dependence in patterns of nutrient flux. To quantify patterns of density dependence, we fit Beverton–Holt functions where instead of recruits as a function of spawners, export was a function of import (Moore and Schindler 2004). We fit this function using the nls (nonlinear least-squares) procedure in R (R Development Core Team 2010). We restricted this function-fitting to systems with at least 7 years of data (excluding Scott and Pudding creeks). The Beverton–Holt model did not converge for Prairie Creek, so these results are not included.

To compare patterns of fluxes across species and streams, we compared total import versus total export summed across the whole time series for a given species and a given stream. As an index of change in abundance and nutrients, we calculated the proportional decrease in abundance and nutrients of each time series, comparing the average of the oldest two time points with the average of the two most recent time points.

We acknowledge that these calculations have some uncertainty associated with them. All parameter estimates have some uncertainty. Furthermore, population estimates of smolts and spawners were made using the best available salmon population estimation techniques, which do have uncertainty. While variation in these parameters and inputs may change some of the detailed output, we believe that these would not systematically change the results.

Results

Across the six focal stream systems in coastal California, there were substantial decreases in annual nutrient import associated with migratory salmonids over the last decade. With the exception of the most northern of the study streams (Prairie Creek), all streams had annual import of thousands of grams of P that declined by at least one order of magnitude between 2001 and 2009 (Fig. 1). For example, in Caspar Creek from 2002 to 2005, salmon migrations led to the net annual import of 1346 to 7115 g P. In contrast, in 2009 salmon only led to the net import of 36.1 g P in Caspar Creek. Salmon actually acted as net exporters of nutrients in two of the six streams (Scott and Pudding creeks) in 2009. Specifically, we estimate that salmon migration led to the net export of 110 and 18 g P in Scott and Pudding creeks, respectively.

Changes in annual nutrient import were driven by dynamics within and across species. For example, in Little River, a declining trend in import by steelhead populations through time is masked somewhat by variability in abundance (Fig. 2*a*). However, in a given year, steelhead smolts and kelts exported most (68% if import and export are summed across years) of the P that was imported by spawning adults, and steelhead export exceeded import in 2009 (Fig. 2*a*). In contrast, in the early half of the decade, coho salmon imported much more P than steelhead did, primarily because of the higher abundance of coho (Fig. 2*b*). During earlier years with higher adult abundances, coho smolts exported little P relative to that imported. However, coho adult spawners declined by 95% over the time series, decreasing import. Furthermore, smolts exported relatively more P as populations declined. As a result, there was a decrease in net salmon import of P from over 1000 g P per year during the first half of the decade to less than 40 g P per year during the last 3 years of data (Fig. 1*c*).

Density-dependent processes led to nonlinear relationships between brood-year import and export. For example, for coho salmon in Little River, smolts exported a higher fraction of the nutrients that were imported by their parents at low spawning population sizes (Fig. 3*a*). This relationship was strongly nonlinear, approximated by a power function (slope = 9.17, exponent = –0.85, $R^2 = 0.87$). Specifically, smolts exported less than 5% of parental nutrients, except at low spawner abundance, when they were observed to export up to 97% of the amount of parental P. This is likely driven by the combination of two density-dependent processes. First, there was strong density dependence in the relationship between the number of spawners and the number of smolts produced — few spawners produced disproportionately many smolts, following a Beverton–Holt relationship (Fig. 3*b*). Second, there was a negative relationship between the number of smolts and their size in a given year, presumably driven by density-dependent growth (Fig. 3*c*; $F_{[1,8]} = 11.58$, $R^2 = 0.59$, $p = 0.009$).

Patterns of density dependence in nutrient import vs. export varied across streams and species (Fig. 4). We analyzed three streams for each species; the other streams either had insufficient data to try to parameterize these relationships or models did not converge. According to model fits, coho export saturated quickly in two of the three systems (Fig. 4*a*), while steelhead export showed less nonlinearity (Fig. 4*b*). For steelhead, model fits predicted that one of the three streams (Noyo River) will enter the net export parameter space at low abundances (at approximately 47 adult steelhead; Fig. 4*b*). Coho are also predicted to become a net exporter in a second system (Little River), but only at an exceedingly low abundance threshold (of approximately two spawners; Fig. 4*a*). Thus, at lower spawner abundances, density dependence drives a relative increase in export compared with import, thereby contributing to nonlinearity in the relationship between spawner abundance and net import.

The three species of salmonids had different relationships between import vs. export (Fig. 5*a*). Spawning adults of the two semelparous species imported much more than their smolts exported; export represented 12% of import for Chinook and 9.6% ± 10.8% for coho (mean ± 1 standard deviation). In contrast, steelhead, which export nutrients both as outmigrating smolts as well as adults that have survived spawning (kelts), exported 63.7% ± 9.8% of the P that is imported by spawning adults. In other words, steelhead export the equivalent of the majority of the nutrients that they import.

In the last decade, across the different species and study streams, there were large decreases in spawner abundances (Fig. 5*b*). The two semelparous species decreased more than

Fig. 1. Annual phosphorus flux due to migration of Pacific salmon in six coastal California streams. Filled circles show total annual net P flux, while the open circles show the total flux due to coho salmon. The dotted line through flux = 0 is where import is equal to export; points above this line indicate net import, points below this line indicate net export. Note the different *y* axis scale on different panels.

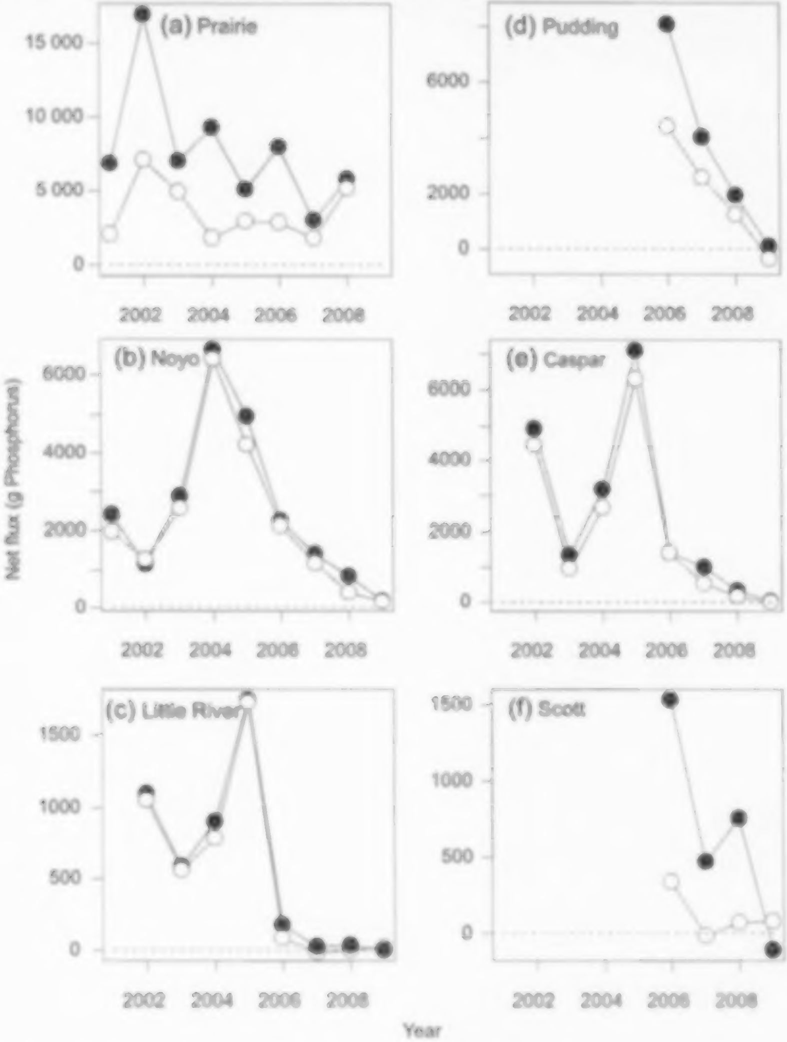

iteroparous steelhead. Specifically, Chinook decreased by 85% in the only stream in which they were present, and coho populations decreased by an average of 68% ± 28% across all streams. When the northernmost site was excluded (Prairie Creek), the average coho decline was 77%. In contrast, steelhead populations decreased by 46% ± 29%. We also note that the shorter time series did not show as large a decrease because of data truncation of the population decline.

Discussion

Over the last decade, populations of anadromous salmonids, especially coho (Miller 2010), have decreased precipitously in coastal California streams. Using a mass-balance approach to estimate P import and export, we found that these decreases in adult returns have driven a corresponding decrease in nutrient import to these coastal fresh waters. Depending on the stream, annual net P import has declined by roughly an order of magnitude over the last decade. Historical records of salmon populations from these watersheds are sparse, which makes it difficult to put these contemporary population decreases into context. We can gain some perspective into historic steelhead and salmon populations and nutrient import in one of our study streams (Scott Creek) from a century ago. This stream was historically used as a location to collect coho and steelhead eggs to jumpstart a hatchery operation. California Fish and Game Commission kept archives of the number of eggs collected from this watershed. For example, in 1909, personnel collected eggs from an estimated 437 female steelhead and 518 female coho from Scott Creek (California Fish and Game Commission 1910), assuming that steelhead average 5000 eggs and

Fig. 2. Phosphorus flux due to migrations of salmon in Little River. Filled circles show import of phosphorus via spawners, and the open circles show the export due to outmigrating smolts or kelts for steelhead (*a*) and coho (*b*).

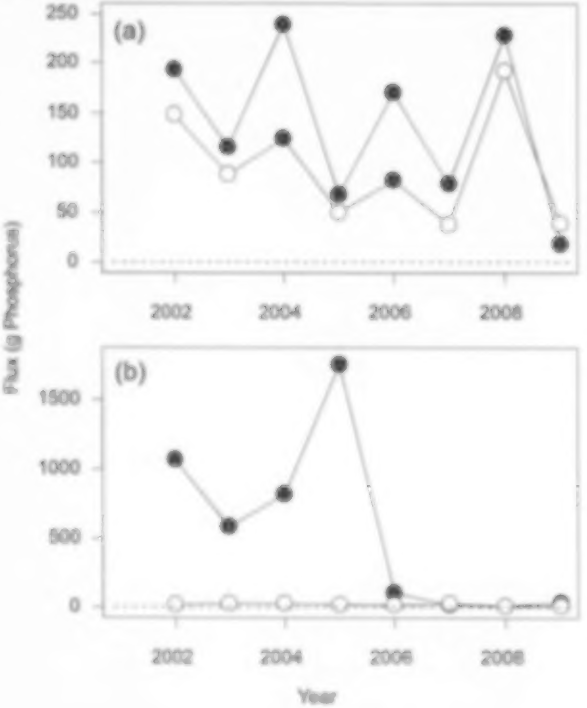

Fig. 3. Density dependence in nutrient import and export of coho salmon in Little River. Each point represents a different brood year. (*a*) The relationship between import by spawners for a given brood year and the proportion of that amount of nutrients that were exported by the resultant smolts. The line represents the best-fit exponential relationship. (*b*) The relationship between the number of spawning adults and the number of outmigrating smolts in the subsequent year. The line represents the best-fit Beverton–Holt relationship. (*c*) Average smolt size as a function of the number of smolts in that year. Also shown is the best-fit line.

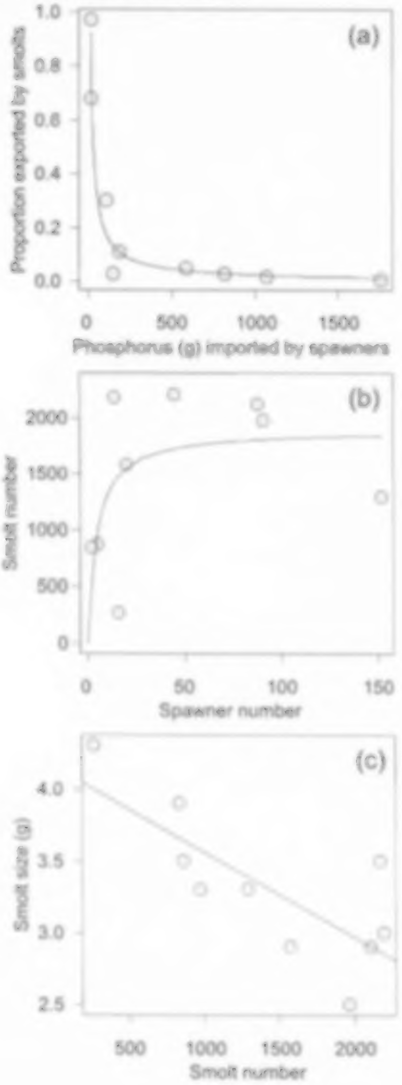

coho average 2700 eggs (D. Streig, Monterey Bay Salmon and Trout Project, 825 Big Creek Road, Davenport, CA 95017, USA, unpublished data). If we conservatively assume a 50:50 sex ratio and that every single female fish was harvested, this equates to an annual import of 16 246 g P. The highest annual import observed in this study in Scott Creek was 2964 g P during 2006, representing 18% of 1909 import. Since 2006, import has decreased even further; most recently in 2009 salmon imported only 372 g P, 6% of historic import. To put these fluxes in context of a previous experiment, Wipfli et al. (2004) found that the addition of 22.2 g P·m^{-2} in Alaskan systems drove a significant increase in juvenile salmon body condition. Thus, 16 246 g P could "fertilize" at least 732 m^2 of Scott Creek at this concentration. We note that these numbers are for import only and do not consider export dynamics; these patterns of flux would be accentuated if export were considered. Thus, the recent decrease in salmon-derived nutrients is likely only the tail end of a century-long process of declines (Gustafson et al. 2007).

As salmon populations decrease, density-dependent processes can shift the patterns of nutrient fluxes. Specifically, salmon exported relatively more nutrients at low spawner densities, as proposed by Moore and Schindler (2004) and documented by Scheuerell et al. (2005) for Snake River Chinook. In addition, density dependence in survival and growth of alewife (*Alosa pseudoharengus*) may drive a similar nonlinear relationship between import and export for these anadromous fish (West et al. 2010). We found that for both coho salmon and steelhead, export became relatively more important in a strongly nonlinear relationship as spawner populations decreased. These patterns were driven by the combination of two density-dependent relationships; juvenile fish were disproportionately more abundant as well as larger at low spawner densities. While this density dependence in

Fig. 4. Density dependence in salmon nutrient import and export across streams and species for coho (*a*) and steelhead (*b*). Shown are the fitted Beverton–Holt relationships of phosphorus import and phosphorus export for that brood year, assuming outmigrating fish are 1 and 2 years old for coho and steelhead, respectively. Solid line is for Caspar Creek, dashed line is Noyo River, and dotted line is Little River. The region where export is greater than import (net export) is portrayed with the gray polygon. Note the different *x* and *y* axes on the two panels.

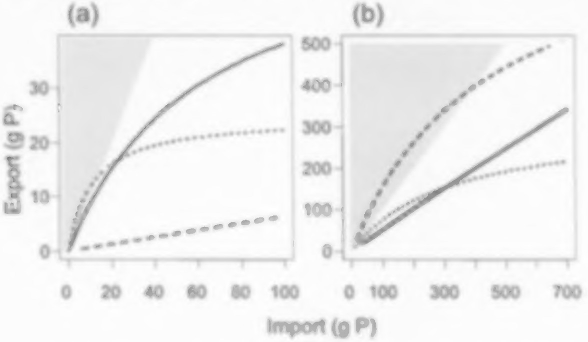

Fig. 5. Box and whisker plots of species-specific patterns of nutrient flux and population dynamics. Box plots show the distribution of observed values across the different stream systems. Only one stream had a Chinook population. (*a*) The proportion of imported nutrients that were exported, averaged across the time series for the different stream systems. (*b*) The proportional decrease in abundance of the different species over the course of the time series. The dotted line at 0 indicates the value where there was no change in abundance over the time series; dotted line at 1.0 indicates complete extirpation.

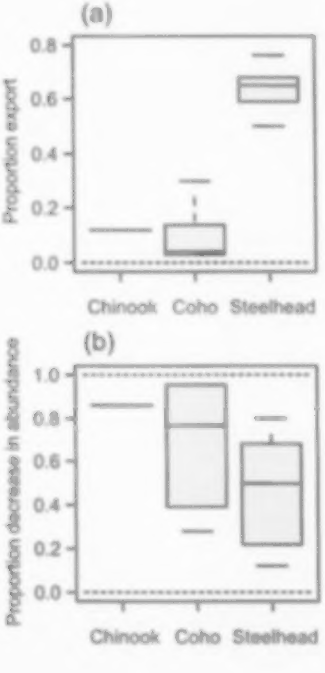

Fig. 6. Scatterplot showing the proportional decrease in abundance and the proportional decrease in net P flux, with each point representing a different stream. The dotted line at 1:1 indicates the predicted change in net P flux, if it was a linear relationship with abundance. Thus, points above this line indicate greater than predicted decrease in nutrients.

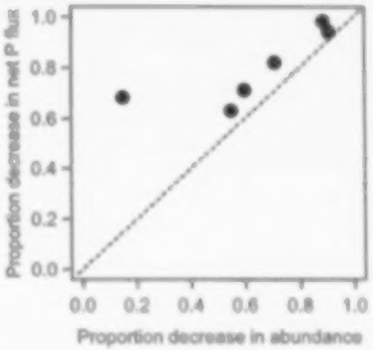

growth and survival can help salmon populations recover quickly from low abundances, these density-dependent processes also can increase nutrient export relative to import at low salmon abundance. Not surprisingly, as different streams and species have different patterns of density dependence, different streams and species also exhibited different nonlinear patterns of import and export. As we observed for two streams in 2009 (Scott and Pudding creeks) and predicted for another two streams based on model fits (Noyo and Little rivers), salmon can change from being net importers to net exporters of nutrients at low abundances. In other words, at low abundances, salmon can reverse their ecological function, stripping nutrients out of coastal fresh waters.

We found that even though nutrient import and export by the different species were driven by their abundance and body size, patterns of net flux that also incorporated export were more complicated. Semelparous Chinook and coho salmon imported 8.3 and 10.4 times, respectively, more than they exported, while the iteroparous steelhead exported the majority of the amount that they imported (importing only 1.6 times more than exporting). Thus, different species with different life histories exhibit different patterns of nutrient transport. The semelparous species also decreased more in abundance over the time series. Regardless of the mechanism driving different apparent vulnerability, the species that import more nutrients were also the species that decreased the most dramatically. Thus, this study represents an example of how species vulnerability may be positively related to their potential ecosystem impact, which can exacerbate the ecosystem consequences of biodiversity loss (Zavaleta et al. 2009).

Net import of nutrients declines more rapidly than salmon population abundance, driven by the combination of density-dependent processes (growth and survival in juveniles) and differential species vulnerability (Fig. 6). Total adult anadromous salmon abundance declined by 15%–91% (mean = 64%), depending on stream, but net P import declined even more, a decrease ranging from 63% to 98% (mean = 80%) (Fig. 6). This is now the second documented pathway by which the loss of the function performed by migratory salmon decreases disproportionately rapidly as populations decrease. Previously, Moore et al. (2008) found that subsidies of salmon eggs to resident fishes were also a positive nonlinear function of salmon density due to habitat saturation. Thus, if salmon populations decline, their subsidies to fresh waters decline even faster than would be predicted based on a simple linear function (Fig. 6). As a result, previous estimates of nutrient loss due to salmon declines (e.g., Gresh et al. 2000) are likely underestimates of the relative change in net nutrient flux.

There is still great uncertainty regarding the ecosystem consequences of salmon subsidies (Schindler et al. 2003; Janetski et al. 2009). Salmon-derived nutrients such as P can directly and indirectly fuel coastal food webs (Stockner et al. 2000; Naiman et al. 2002; Schindler et al. 2003). Alternatively, salmon nest-digging can be a substantial disturbance of benthic communities in spawning habitats (e.g., Peterson and Foote 2000; Moore and Schindler 2008). Thus, migratory salmonids not only deliver material subsidies (e.g., nutrients in carcasses) but also can modify key processes in coastal ecosystems (sensu Flecker et al. 2010). The mass-balance approach we used is a basic "ecosystem" ecology approach, calculating what comes in and what comes out, but does not examine the ecological consequences of those nutrient fluxes. The full ecological consequences of population declines of salmon will depend on the response variable and be driven by nonlinear dynamics such as those documented here and the potentially complex propagation of direct and indirect pathways, all likely modified by the environmental context (Tiegs et al. 2008; Janetski et al. 2009; Holtgrieve et al. 2010). Thus, management actions that attempt to replace the lost function of salmon, such as artificial nutrient additions, are not replicating the real complexity of the impacts of salmon (Compton et al. 2006). For example, nutrient enhancement programs often use the past salmon escapement to estimate the appropriate nutrient load (Washington Department of Fish and Wildlife 2004), but these calculations ignore the potentially important export of nutrients by outmigrating smolts.

The salmon densities and thus nutrient fluxes in these California systems that we observed are much lower than those observed in regions with more abundant salmon populations, such as Alaska. However, salmon nutrient fluxes still likely represent a major contribution to P budgets of these small streams. While we lack the data to create complete nutrient budgets, we can estimate the daily flux of P in streams during low flow periods as the product of the P concentration and the minimum observed discharge. If we use published P concentration data from nearby California streams (Wilzbach et al. 2005) and low summer discharge data from all streams, we can estimate the daily flux of P to be between 17.8 and 285.5 g P·day^{-1} for the different streams, scaling to stream discharge. The maximum annual net flux from salmonids for each stream thereby represents around between 23 and 473 days of watershed P flux during the low water period. However, it is important to note that this region is dominated by a Mediterranean climate, with discharges during irregular winter storms that can exceed 200 times that of low summer flows; watershed loading of P is going to be dominated by high discharges in winter. For example, maximum annual net P flux from salmonids for the streams represents between 0.1 and 1.1 days of watershed P flux during peak discharge. Thus, the degree to which salmon nutrient fluxes influence these California freshwater and riparian systems remains unknown. For example, Wilzbach et al. (2005) did not observe substantial impacts of experimental salmon carcass addition and suggested northern California streams may be light-limited. Even if the ecological consequences of the nutrient fluxes that we describe here are small, it is still important to understand that anadromous salmon populations at low abundances may switch their ecological function and reverse the direction of the conveyor belt of nutrients.

Human activities are altering global nutrient cycling through direct inputs (e.g., fertilizers) as well as by altering abundances of the organisms that control those cycles (Vitousek et al. 1997; McIntyre et al. 2007; Maranger et al. 2008). By linking ecosystems, migratory species can perform key roles in nutrient cycling (Lundberg and Moberg 2003; Willson et al. 2004; Flecker et al. 2010). There is increasing appreciation that a diverse set of migratory species can contribute to nutrient cycling in coastal fresh waters, including salmon, alewife (Durbin et al. 1979; Walters et al. 2009; West et al. 2010), Arctic charr (*Salvelinus alpinus*) (Swanson et al. 2010), and shrimp (Greathouse et al. 2006). Populations of many migratory fishes are declining (Limburg and Waldman 2009; Humphries and Winemiller 2009). It is easy to imagine that a migratory life cycle, which exposes the species to barriers as well as potential degradation in multiple habitats, would increase their vulnerability to population decline (Wilcove and Wikelski 2008). Decreases in migratory fish populations can alter nutrient fluxes in a nonlinear manner with relatively unknown consequences for coastal ecosystems.

Acknowledgements

Too many individuals to mention by name from the following entities helped collect data used in this study: California Department of Fish and Game, Campbell Timberlands Management, NOAA Fisheries Santa Cruz, and the Pacific States Marine Fisheries Commission; be assured we value your help. We specifically thank Scott Harris, Shaun Thompson, Wendy Holloway, and Chris Hannon. Any use of trade names is for descriptive purposes only and does not imply endorsement by the US government. California Fisheries Restoration Grant Program funded much of the field sampling, and NOAA Fisheries Santa Cruz and University of California Santa Cruz provided financial support. We appreciate generously shared insight from experts of steelhead biology, namely George Pess, Todd Seamons, and Kent Mayer. We appreciate insightful comments from Dave Beauchamp, Mark Novak, Corey Phillis, Daniel Schindler, Mark Wipfli, and several anonymous reviewers on earlier drafts of this manuscript.

References

Adams, P.B., Boydstun, L.B., Gallagher, S.P., Lacy, M.K., McDonald, T., and Shaffer, K.E. 2011. California coastal salmonid population monitoring: strategy, design, and methods. California Department of Fish and Game. Fish Bull. 180.

Burnham, K.P. 1987. Design and analysis methods for fish survival experiments based on release–recapture. American Fisheries Society, Bethesda, Md.

California Fish and Game Commission. 1910. The twenty-first biennial report of the Board of Fish and Game Commissioners of the State of

California for the years 1909–1910. *Edited by* W.W. Shannon. Sacramento, Calif.

Campbell Timberland Management. 2008. Pudding Creek Coho Salmon Project. Annual report. Prepared by Campbell Timberland Management LLC, Fort Bragg, Calif.

Cederholm, C.J., Kunze, M.D., Murota, T., and Sibatani, A. 1999. Pacific salmon carcasses: essential contributions of nutrients and energy for aquatic and terrestrial ecosystems. Fisheries, **24**: 6–15.

Compton, J.E., Andersen, C.P., Phillips, D.L., Brooks, J.R., Johnson, M.G., Church, M.R., Hogsett, W.E., Cairns, M.A., Rygiewicz, P.T., McComb, B.C., and Shaff, C.D. 2006. Ecological and water quality consequences of nutrient addition for salmon restoration in the Pacific Northwest. Front. Ecol. Environ. **4**(1): 18–26. doi:10.1890/1540-9295(2006)004[0018:EAWQCO]2.0.CO;2.

Cormack, R.M. 1964. Estimates of survival from the sighting of marked animals. Biometrika, **51**(3/4): 429–438. doi:10.2307/2334149.

Croll, D.A., Maron, J.L., Estes, J.A., Danner, E.M., and Byrd, G.V. 2005. Introduced predators transform subarctic islands from grassland to tundra. Science (Washington, D.C.), **307**(5717): 1959–1961. doi:10.1126/science.1108485. PMID:15790855.

Durbin, A.G., Nixon, S.W., and Oviatt, C.A. 1979. Effects of the spawning migration of the alewife, *Alosa pseudoharengus*, on freshwater ecosystems. Ecology, **60**(1): 8–17. doi:10.2307/1936461.

Elser, J.J., Bracken, M.E.S., Cleland, E.E., Gruner, D.S., Harpole, W.S., Hillebrand, H., Ngai, J.T., Seabloom, E.W., Shurin, J.B., and Smith, J.E. 2007. Global analysis of nitrogen and phosphorus limitation of primary producers in freshwater, marine and terrestrial ecosystems. Ecol. Lett. **10**(12): 1135–1142. doi:10.1111/j.1461-0248.2007.01113.x. PMID:17922835.

Federal Register. 2005. Endangered and threatened species: final listing determinations for 16 ESUs of west coast salmon, and final 4(*d*) protective regulations for threatened salmonid ESUs. Federal Register, Washington, D.C. **70**: 37160–37204.

Flecker, A.S., McIntyre, P.B., Moore, J.W., and Anderson, J.T. 2010. Migratory fishes as material and process subsidies in riverine ecosystems. Am. Fish. Soc. Symp. **73**: 559–592.

Gallagher, S.P., and Wright, D.W. 2009. Coastal Mendocino County salmonid life cycle and regional 383 monitoring: monitoring status and trends. California State Department of Fish and Game, Coastal 384 Watershed Planning and Assessment Program, Fortuna, Calif. Available from http://www.coastalwatersheds.ca.gov/Watersheds/NorthCoast/MendocinoCoastalStreams/MendocinoCoastAdditionalDocuments/tabid/169/Default.aspx.

Gallagher, S.P., Adams, P.B., Wright, D.W., and Collins, B.W. 2010. Performance of spawner survey techniques at low abundance levels. N. Am. J. Fish. Manage. **30**(5): 1086–1097. doi:10.1577/M09-204.1.

Greathouse, E.A., Pringle, C.M., McDowell, W.H., and Holmquist, J.G. 2006. Indirect upstream effects of dams: consequences of migratory consumer extirpation in Puerto Rico. Ecol. Appl. **16**(1): 339–352. doi:10.1890/05-0243. PMID:16705984.

Gresh, T., Lichatowich, J., and Schoonmaker, P. 2000. An estimation of historic and current levels of salmon production in the Northeast Pacific ecosystem: evidence of a nutrient deficit in the freshwater systems of the Pacific Northwest. Fisheries, **25**: 15–21.

Gustafson, R.G., Waples, R.S., Myers, J.M., Weitkamp, L.A., Bryant, G.J., Johnson, O.W., and Hard, J.J. 2007. Pacific salmon extinctions: quantifying lost and remaining diversity. Conserv. Biol. **21**(4): 1009–1020. doi:10.1111/j.1523-1739.2007.00693.x. PMID:17650251.

Hayes, S.A., Bond, M.H., Hanson, C.V., Freund, E.V., Smith, J.J., Anderson, E.C., Ammann, A.J., and MacFarlane, R.B. 2008. Steelhead growth in a small central California watershed: upstream and estuarine rearing patterns. Trans. Am. Fish. Soc. **137**(1): 114–128. doi:10.1577/T07-043.1.

Holtgrieve, G.W., Schindler, D.E., Gowell, C., Ruff, C.P., and Lisi, P.J. 2010. Stream geomorphology regulates the effects of ecosystem engineering and nutrient enrichment by Pacific salmon on periphyton. Freshw. Biol. **55**: 2598–2611. doi:10.1111/j.1365-2427.2010.02489.x.

Humphries, P., and Winemiller, K.O. 2009. Historical impacts on river fauna, shifting baselines, and challenges for restoration. Bioscience, **59**(8): 673–684. doi:10.1525/bio.2009.59.8.9.

Janetski, D.J., Chaloner, D.T., Tiegs, S.D., and Lamberti, G.A. 2009. Pacific salmon effects on stream ecosystems: a quantitative synthesis. Oecologia, **159**(3): 583–595. doi:10.1007/s00442-008-1249-x. PMID:19132408.

Johnson, D.H., Shrier, B.M., O'Neal, J.S., Knutzen, J.A., Augerot, X., O'Neil, T.A., and Pearsons, T.N. 2007. Salmonid field protocols handbook: techniques for assessing status and trends in salmon and trout populations. American Fisheries Society, Bethesda, Md.

Jolly, G.M. 1965. Explicit estimates from capture–recapture data with both death and immigration-stochastic model. Biometrika, **52**(1/2): 225–247. doi:10.2307/2333826. PMID:14341276.

Jonsson, B., and Jonsson, N. 2003. Migratory Atlantic salmon as vectors for the transfer of energy and nutrients between freshwater and marine environments. Freshw. Biol. **48**(1): 21–27. doi:10.1046/j.1365-2427.2003.00964.x.

Larkin, G.A., and Slaney, P.A. 1997. Implications of trends in marine-derived nutrient influx to south coastal British Columbia salmonid production. Fisheries, **22**: 16–24.

Limburg, K.E., and Waldman, J.R. 2009. Dramatic declines in North Atlantic diadromous fishes. Bioscience, **59**(11): 955–965. doi:10.1525/bio.2009.59.11.7.

Lundberg, J., and Moberg, F. 2003. Mobile link organisms and ecosystem functioning: implications for ecosystem resilience and management. Ecosystems, **6**(1): 87–98. doi:10.1007/s10021-002-0150-4.

Lyle, A.A., and Elliott, J.M. 1998. Migratory salmonids as vectors of carbon, nitrogen, and phosphorus between marine and freshwater environments in north-east England. Sci. Total Environ. **210–211**: 457–468.

Maranger, R., Caraco, N., Duhamel, J., and Amyot, M. 2008. Nitrogen transfer from sea to land via commercial fisheries. Nat. Geosci. **1**(2): 111–112. doi:10.1038/ngeo108.

Mayer, K., Schuck, M., and Iversen, P. 2008. Assessing salmonids in the Asotin watershed. Washington Department of Fish and Wildlife Report, US Department of Energy, Portland, Ore.

McIntyre, P.B., Jones, L.E., Flecker, A.S., and Vanni, M.J. 2007. Fish extinctions alter nutrient recycling in tropical freshwaters. Proc. Natl. Acad. Sci. U.S.A. **104**(11): 4461–4466. doi:10.1073/pnas.0608148104. PMID:17360546.

Merz, J.E., and Moyle, P.B. 2006. Salmon, wildlife, and wine: marine-derived nutrients in human-dominated ecosystems of central California. Ecol. Appl. **16**(3): 999–1009. doi:10.1890/1051-0761(2006)016[0999:SWAWMN]2.0.CO;2. PMID:16826998.

Miller, G. 2010. In central California, coho salmon are on the brink. Science (Washington, D.C.), **327**(5965): 512–513. doi:10.1126/science.327.5965.512. PMID:20110475.

Moore, J.W., and Schindler, D.E. 2004. Nutrient export from freshwater ecosystems by anadromous sockeye salmon (*Oncorhynchus nerka*). Can. J. Fish. Aquat. Sci. **61**(9): 1582–1589. doi:10.1139/f04-103.

Moore, J.W., and Schindler, D.E. 2008. Biotic disturbance and benthic community dynamics in salmon-bearing streams. J. Anim.

Ecol. **77**(2): 275–284. doi:10.1111/j.1365-2656.2007.01336.x. PMID:18081781.

Moore, J.W., Schindler, D.E., and Ruff, C.P. 2008. Habitat saturation drives thresholds in stream subsidies. Ecology, **89**(2): 306–312. doi:10.1890/07-1269.1. PMID:18409419.

Naiman, R.J., Bilby, R.E., Schindler, D.E., and Helfield, J.M. 2002. Pacific salmon, nutrients, and the dynamics of freshwater and riparian ecosystems. Ecosystems, **5**(4): 399–417. doi:10.1007/s10021-001-0083-3.

Nislow, K.H., Armstrong, J.D., and McKelvey, S. 2004. Phosphorus flux due to Atlantic salmon (*Salmo salar*) in an oligotrophic upland stream: effects of management and demography. Can. J. Fish. Aquat. Sci. **61**(12): 2401–2410. doi:10.1139/f05-006.

Peterson, D.P., and Foote, C.J. 2000. Disturbance of small-stream habitat by spawning sockeye salmon in Alaska. Trans. Am. Fish. Soc. **129**(4): 924–934. doi:10.1577/1548-8659(2000)129<0924:DOSSHB>2.3.CO;2.

Polis, G.A., Power, M.E., and Huxel, G.R. 2004. Food webs at the landscape level. University of Chicago Press, Chicago, Ill.

R Development Core Team. 2010. R: a language and environment for statistical computing. R Foundation for Statistical Computing, Vienna, Austria.

Sánchez-Piñero, F., and Polis, G.A. 2000. Bottom-up dynamics of allochthonous input: direct and indirect effects of seabirds on islands. Ecology, **81**: 3117–3132.

Sanderson, B.L., Coe, H.J., Tran, C.D., Macneale, K.H., Harstad, D.L., and Goodwin, A.B. 2009. Nutrient limitation of periphyton in Idaho streams: results from nutrient diffusing substrate experiments. J. N. Am. Benthol. Soc. **28**(4): 832–845. doi:10.1899/09-072.1.

Scheuerell, M.D., Levin, P.S., Zabel, R.W., Williams, J.G., and Sanderson, B.L. 2005. A new perspective on the importance of marine-derived nutrients to threatened stocks of Pacific salmon (*Oncorhynchus* spp.). Can. J. Fish. Aquat. Sci. **62**(5): 961–964. doi:10.1139/f05-113.

Schindler, D.E., Scheuerell, M.D., Moore, J.W., Gende, S.M., Francis, T.B., and Palen, W.J. 2003. Pacific salmon and the ecology of coastal ecosystems. Front. Ecol. Environ. **1**(1): 31–37. doi:10.1890/1540-9295(2003)001[0031:PSATEO]2.0.CO;2.

Stockner, J.G., Rydin, E., and Hyenstrand, P. 2000. Cultural oligotrophication: causes and consequences for fisheries resources. Fisheries, **25**: 7–14.

Swanson, H.K., Kidd, K.A., and Reist, J.D. 2010. Effects of partially anadromous arctic charr (*Salvelinus alpinus*) populations on ecology of coastal arctic lakes. Ecosystems, **13**(2): 261–274. doi:10.1007/s10021-010-9316-7.

Szerlong, R.G., and Rundio, D.E. 2008. A statistical modeling method for estimating mortality and abundance of spawning salmon from a time series of counts. Can. J. Fish. Aquat. Sci. **65**(1): 17–26. doi:10.1139/F07-141.

Tiegs, S.D., Chaloner, D.T., Levi, P., Rüegg, J., Tank, J.L., and Lamberti, G.A. 2008. Timber harvest transforms ecological roles of salmon in southeast Alaska rain forest streams. Ecol. Appl. **18**(1): 4–11. doi:10.1890/07-0655.1. PMID:18372551.

Vitousek, P.M., Aber, J.D., Howarth, R.W., Likens, G.E., Matson, P.A., Schindler, D.W., Schlesinger, W.H., and Tilman, D.G. 1997. Human alteration of the global nitrogen cycle: sources and consequences. Ecol. Appl. **7**: 737–750.

Walters, A.W., Barnes, R.T., and Post, D.M. 2009. Anadromous alewives (*Alosa pseudoharengus*) contribute marine-derived nutrients to coastal stream food webs. Can. J. Fish. Aquat. Sci. **66**(3): 439–448. doi:10.1139/F09-008.

Washington Department of Fish and Wildlife. 2004. Protocols and guidelines for distributing salmonid carcasses, salmon carcass analogs, and delayed release fertilizers to enhance stream productivity in Washington State. Washington Department of Fish and Wildlife, Seattle, Wash.

West, D.C., Walters, A.W., Gephard, S., and Post, D.M. 2010. Nutrient loading by anadromous alewife (*Alosa pseudoharengus*): contemporary patterns and predictions for restoration efforts. Can. J. Fish. Aquat. Sci. **67**: 1211–1220. doi:10.1139/F10-059.

White, G.C., and Burnham, K.P. 1999. Program MARK: survival estimation from populations of marked animals. Bird Study, **46**: 120–138.

Wilcove, D.S., and Wikelski, M. 2008. Going, going, gone: Is animal migration disappearing? PLoS Biol. **6**(7): e188. doi:10.1371/journal.pbio.0060188. PMID:18666834.

Willson, M.F., Gende, S.M., and Bisson, P.A. 2004. Anadromous fishes as ecological links between ocean, fresh water, and land. *In* Food webs at the landscape level. *Edited by* G.A. Polis, M.E. Power, and G.R. Huxel. University of Chicago Press, Chicago, Ill. pp. 284–300.

Wilzbach, M.A., Harvey, B.C., White, J.L., and Nakamoto, R.J. 2005. Effects of riparian canopy opening and salmon carcass addition on the abundance and growth of resident salmonids. Can. J. Fish. Aquat. Sci. **62**(1): 58–67. doi:10.1139/f04-177.

Wipfli, M.S., and Baxter, C.V. 2010. Linking ecosystems, food webs, and fish production: subsidies in salmonid watersheds. Fisheries, **35**(8): 373–387.

Wipfli, M.S., Hudson, J.P., and Caouette, J.P. 2004. Restoring productivity of salmon-based food webs: contrasting effects of salmon carcass and salmon carcass analog additions on stream-resident salmonids. Trans. Am. Fish. Soc. **133**(6): 1440–1454. doi:10.1577/T03-112.1.

Young, H.S., McCauley, D.J., Dunbar, R.B., and Dirzo, R. 2010. Plants cause ecosystem nutrient depletion via the interruption of bird-derived spatial subsidies. Proc. Natl. Acad. Sci. U.S.A. **107**(5): 2072–2077. doi:10.1073/pnas.0914169107. PMID:20133852.

Zavaleta, E., Pasari, J., Moore, J., Hernández, D., Suttle, K.B., and Wilmers, C.C. 2009. Ecosystem responses to community disassembly. Ann. N.Y. Acad. Sci. **1162**(1): 311–333. doi:10.1111/j.1749-6632.2009.04448.x. PMID:19432654.

Estimating multifleet catchability coefficients and natural mortality from fishery catch and effort data: comparison of Bayesian state–space and observation error models

Shijie Zhou, André E. Punt, Roy Deng, and Janet Bishop

Abstract: Catchability and natural mortality are key quantities in fisheries stock assessment. However, it is difficult to estimate these two parameters simultaneously using only fishery catch and effort data. A Bayesian state–space modified delay–difference model is outlined that can estimate time series of catchability by fleet as well as natural mortality. This model, and three variants thereof, is fitted to data for grooved tiger prawns (*Penaeus semisulcatus*) in Australia's Northern Prawn Fishery during the period of the year when there is little recruitment. A model that allows for both observation and process error and estimates natural mortality is best, in terms of model selection criteria as well as fit diagnostics. The posterior median estimate for catchability for the primary target fleet ranges from 6.15×10^{-4} to 1.09×10^{-4} during 1980–2007, while the posterior median estimate for catchability for a fleet with *P. semisulcatus* as its byproduct is about 20% of that for the primary fleet. Fishing efficiency increased at approximately 2% annually during 1980–2007, while the weekly natural mortality is estimated to be 0.053 week^{-1}.

Résumé : La capturabilité et la mortalité naturelle sont deux quantités essentielles dans l'évaluation des stocks de pêche. Il est, cependant, difficile d'estimer ces deux variables simultanément à partir de seulement les données de capture et d'effort de pêche. Nous présentons un modèle bayésien modifié d'état–espace et de délai différence qui peut estimer des séries chronologiques de capturabilité par la flotte de pêche, ainsi que la mortalité naturelle. Nous ajustons ce modèle et trois de ses variae la pêche commerciale nordique de crevettes (*Penaeus semisulcatus*) de l'Australie durant la période de l'année où il y a peu de recrutement. Un modèle qui tient compte à la fois des erreurs d'observation et de traitement et qui estime la mortalité naturelle fonctionne le mieux, en ce qui a trait aux critères de sélection des modèles et aux caractères diagnostics de l'ajustement. L'estimation a posteriori de la médiane de la capturabilité par la flotte qui cible principalement les crevettes varie de $6,15 \times 10^{-4}$ à $1,09 \times 10^{-4}$ entre 1980 et 2007, alors que l'estimation a posteriori de la médiane de la capturabilité par la flotte qui récolte *P. semisulcatus* comme capture accessoire est d'environ 20 % de celle de la flotte principale. L'efficacité de la pêche a augmenté d'environ 2 % par année de 1980 à 2007, alors que la mortalité naturelle hebdomadaire est estimée à 0,053 semaine^{-1}.

[Traduit par la Rédaction]

Introduction

Stock assessments provide the basis for applying harvest control rules and hence providing fisheries management advice. In general, stock assessment involves fitting population dynamics models to available data using nonlinear regression methods. Many stock assessments involve a large number of parameters to adequately describe the underlying biological processes and mimic the available data. Some of these parameters, such as growth, fecundity, and natural mortality, are usually not estimated from the data used when fitting the model, but are instead prespecified based on auxiliary information. However, these estimates can be highly consequential in terms of the outcomes of the assessment. Specifically, catchability (*q*, the constant of proportionality between an index of abundance — such as catch per unit effort (CPUE) or from a survey — and abundance) and the instantaneous rate of natural mortality (*M*) have been prespecified in assessments of prawns (e.g., Dichmont et al. 2003) and crabs (e.g., Zheng and Siddeek 2010). Errors in the prespecified values

Received 16 September 2010. Accepted 24 March 2011. Published at www.nrcresearchpress.com/cjfas on 5 July 2011.
J22018

Paper handled by Associate Editor Carl Walters.

S. Zhou, R. Deng, and J. Bishop.* CSIRO Marine and Atmospheric Research, Ecosciences Precinct, GPO Box 2853, Brisbane, QLD 4001, Australia.
A.E. Punt. Wealth from Oceans Flagship, CSIRO Marine and Atmospheric Research, GPO Box 1538, Hobart TAS 7001, Australia; School of Aquatic and Fishery Sciences, Box 355020, University of Washington, Seattle, WA 98195-5020, USA.

Corresponding author: Shijie Zhou (e-mail: Shijie.zhou@csiro.au).

*Present address: 20 Tooth Street, Nobby, QLD 4360, Australia.

Can. J. Fish. Aquat. Sci. **68**: 1171–1181 (2011) doi:10.1139/F2011-052 Published by NRC Research Press

for q and M can lead to biased estimates for key model outputs such as optimal yield, biomass, fishing mortality, and ultimately, recommended harvest levels (Dichmont et al. 2003).

There are several ways to estimate q and M (Quinn and Deriso 1999; Arreguin-Sanchez 1996; Hewitt and Hoenig 2005). However, these methods tend to be subject to considerable uncertainty (e.g., Salthaug and Aanes 2003; Zheng 2003; Walters and Hilborn 2005). The depletion model (Rider et al. 1994; Volstad et al. 2000; Burridge et al. 2003) is the most common of the "statistical" models used to estimate q. However, this model commonly assumes a "closed" population, i.e., the effects of growth, natural mortality, and recruitment are negligible compared with those of fishing mortality. Violation of the assumption of a closed population results in bias in estimated parameters, and variants of the depletion model have been developed to account for some of these factors (e.g., Rago et al. 2006; Walter et al. 2007).

Wang (1999) attempted to use a depletion model to estimate catchability and natural mortality simultaneously for a prawn species using maximum likelihood. However, the results were highly uncertain, and natural mortality was consequently fixed. Further, most depletion-type models (e.g., McAllister et al. 2004; Zhou et al. 2007, 2008) assume that the dynamics of the population are deterministic, i.e., no account is taken of process error in the dynamics of the population, and consequently attribute all differences between model predictions and observations to observation error. Finally, open-population depletion models can lead to parameter estimates that are highly uncertain depending on assumptions and the extent to which biomass is reduced during the modelled period (Wang 1999; Robert et al. 2010) because of high confounding between natural mortality and catchability.

We outline a method based on a Bayesian state–space model that addresses the bulk of the concerns above and apply it to data for a commercially valuable prawn species (grooved tiger prawns, *Penaeus semisulcatus*) in Australia's Northern Prawn Fishery (NPF). The reproductive dynamics of the grooved tiger prawn are described by Crocos (1987); each year class typically consists of two main cohorts: one born in spring (August to October) and another born in late summer (January and February). Juveniles leave the estuarine nursery grounds and disperse to the deeper offshore waters. The method we describe allows for growth (and in principle recruitment) and natural mortality during the period analyzed, takes account of both observation and process error, can make use of catch rate data from multiple fleets, allows for changes over time in catchability owing to the impact of changes over the year in fishing efficiency, and is formulated within a Bayesian hierarchical framework so data from multiple years can be analyzed simultaneously.

Materials and methods

There are two submodels in a state–space model: one that describes dynamics of the population during the period modelled (the "process model") and another that describes how the data relate to the predictions of the model (the "observation model"). Error is accounted for in both models.

The process model

The population model was modified from the Allen–Clark delay–difference model (Quinn and Deriso 1999) and accounts for growth, recruitment, and natural and fishing mortality. The fishery and recruitment are assumed to occur in the middle of each time step, while growth and natural mortality are assumed to occur continuously throughout each time step. The short time step of 1 week minimizes potential impacts of this assumption on parameter estimation. The dynamics of biomass are only modelled for part of the year (in this case when there is little evidence for recruitment), so no attempt is made to link the biomass from one year to the next. The change in biomass from one time step to the next (taken here to be a week) is given by

$$(1)\qquad B_{y,w} = [B_{y,w-1}\,\mathrm{e}^{-0.5M}(1+0.5\rho_{w-1}) - C_{y,w-1} + R_{y,w-1}]\,\mathrm{e}^{-0.5M}(1+0.5\rho_{w-1})\,\mathrm{e}^{\varepsilon^{B}_{y,w}}$$

where $B_{y,w}$ is the biomass at the start of week w of year y, $C_{y,w}$ is the observed catch by all fleets during week w of year y, ρ_w is a measure of the growth during week w, $R_{y,w}$ is the recruitment during week w of year y, $\varepsilon^{B}_{y,w}$ is the process error for week w of year y, $\varepsilon^{B}_{y,w} \sim N(0;\sigma^2_B)$, and σ^2_B determines the extent of process error in the dynamics. Natural mortality and growth are assumed to be constant over the modelled period.

Observation model

The data available for parameter estimation are catch rates from one or more fleets, each of which could have a different catchability coefficient. The model for the catch rate for fleet f during week w of year y, $U_{y,w,f}$, is

$$(2)\qquad U_{y,w,f} = q_{y,f}B_{y,w}\,\mathrm{e}^{-0.5M}(1+0.5\rho_w)\,\mathrm{e}^{\varepsilon^{U}_{y,w,f}},\qquad \varepsilon^{U}_{y,w,f} \sim N(0,\sigma^2_{U,f})$$

where $q_{y,f}$ is the catchability coefficient for fleet f and year y, and $\sigma^2_{U,f}$ is the variation in the error due to observing catch rate as well as due to environmental, behavioural, and fleet dynamic factors.

$$(3)\qquad q_{y,f} = \frac{1}{1+\mathrm{e}^{-(a_f+b_f y)}}\,\mathrm{e}^{\varepsilon^{q}_{y,f}},\qquad \varepsilon^{q}_{y,f} \sim N(0,\sigma^2_{q,f})$$

a_f and b_f are the parameters that define the deterministic relationship between catchability and time for fleet f, and $\sigma^2_{q,f}$ defines the extent to which catchability varies about the deterministic trend for fleet f. Note that $\sigma^2_{q,f}$ and $\sigma^2_{U,f}$ are distinguishable because $\sigma^2_{q,f}$ pertains only to between-year variation, while $\sigma^2_{U,f}$ pertains to variation among weeks and years. Equation 3 is flexible, ensures $q_{y,f}$ is always positive, and allows for changes in catchability over time due to technology improvement and increases in knowledge about the fished stock; these are factors known to cause changes in fishing efficiency in many fisheries, including Australia's NPF (Marchal et al. 2007; Ellis and Wang 2007; Bishop et al. 2008). These past analyses of efficiency changes in the NPF suggest a logistic-like function with time.

Parameter estimation

The parameters of the process and observation models (Table 1) are either prespecified based on auxiliary information (growth) or estimated within a Bayesian hierarchical

Table 1. Parameters, priors, and hyperpriors.

Parameter	Treatment
Prespecified parameters	
Growth rate, ρ_c	Prespecified
Estimated parameters	
Initial biomass	$B_{y,1} \sim \text{Lognormal}(\mu_{B1}, \sigma_{B1})$
Process error	$\varepsilon^{B}_{y,w} \sim N(0, \sigma^2_B)$
Catchability deviation	$\varepsilon^{q}_{y,f} \sim N(0, \sigma^2_{q,f})$
Observation error	$\varepsilon^{U}_{y,w,f} \sim N(0, \sigma^2_{U,f})$
a_f	$a_f \sim N(0, 10^2)$
b_f	$b_f \sim N(0, 10^2)$
Natural mortality (if estimated)	$M \sim \text{Lognormal}[\tilde{M}, \log(\tilde{\sigma}^2 + 1)]$; $\tilde{M} / \tilde{\sigma}$ prespecified
Hyperparameters	
Variation in process error	$\sigma^2_B \sim$ inverse gamma(0.001, 0.001)
Variation in observation error	$\sigma^2_{U,f} \sim$ inverse gamma(0.001, 0.001)
Variance in catchability deviations	$\sigma^2_{q,f} \sim$ inverse gamma(0.001, 0.001)
Between-year mean for $B_{y,1}$	$\mu_{B1} \sim N(7.5, \sigma^2_{\mu_{B1}})$
Between-year variation in $B_{y,1}$	$\sigma^2_{B1} \sim$ inverse gamma(0.001, 0.001)
Prior variance for μ_{B1}	$\sigma^2_{\mu_{B1}} \sim$ half-Cauchy, $\frac{\lvert\theta_{B1}\rvert}{\sqrt{v_{B1}}}$
Parameters of the half-Cauchy	$\theta_{B1} \sim N(0, 5^2)$; $v_{B1} \sim$ inverse gamma(0.5, 0.5)

Fig. 1. Box plot of mass versus week by sex for *Penaeus semisulcatus*. The data were based on length measurements from 14 years of commercial catch sampling and scientific surveys in the Northern Prawn Fishery (NPF). The whiskers extend 1.5 times the interquartile range. The solid lines are linear regression lines of mass on week. The 95% confidence intervals were too narrow to be visually distinguished from the fitted lines.

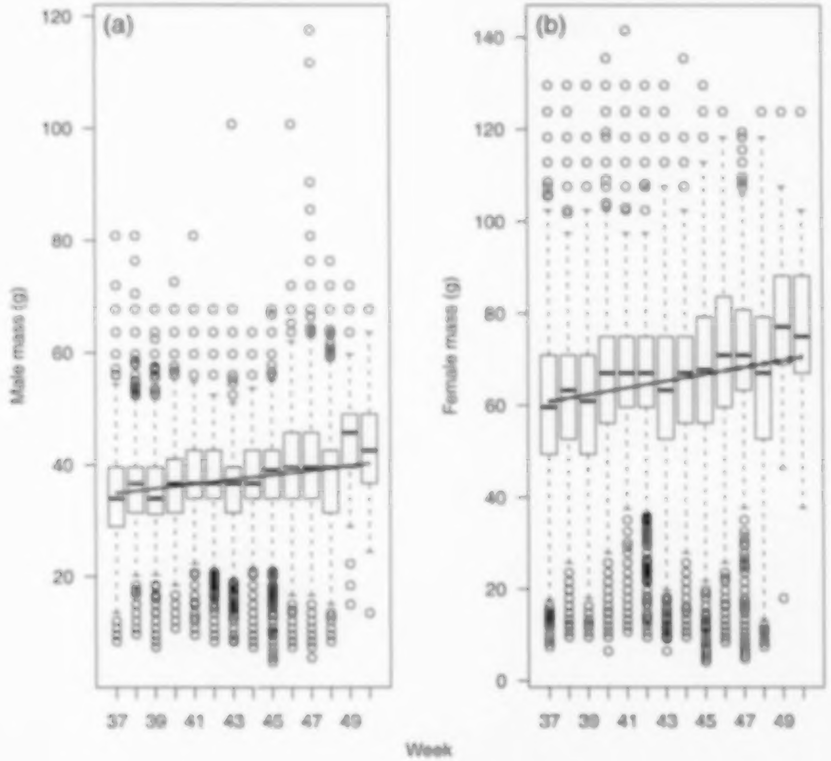

framework. The parameters that determine growth are calculated using the changes in relative mass between weeks $w-1$ and w (a reasonable assumption given that population consists essentially of only a single cohort):

$$(4)\qquad \rho_w = (W_w - W_{w-1})/W_{w-1}$$

where W_w is the expected mass of a prawn during week w under the assumption of an equal sex ratio, estimated here from the sampled average lengths by sex and week:

$$(5)\qquad W_w = 0.5\sum_{s=m,f} W_{w,s}$$

where $W_{w,s}$ is mass of animals of sex s during week w estimated from fishery and survey data (see eq. 9 below).

The priors for the parameters and the hyperparameters (Table 1) are generally assumed to be uninformative. Specifically, the priors for the variance parameters are assumed to be inverse gamma with parameters selected to be uninformative (Harley and Myers 2001; Su et al. 2001), while the priors for the parameters that determine how catchability changes over time are set to uninformative normal distributions. The biomass at the start of the first week of the period modelled is assumed to be drawn from a normal distribution, the mean and variance of which are, respectively, normally and half-Cauchy distributed. The half-Cauchy is a special case of the conditionally conjugate, folded-noncentral-t family of distributions. It has been shown that assuming a half-Cauchy distribution for variance parameters of hyperpriors that are estimated from a small number of groups is superior to assuming other noninformative prior distributions (Gelman 2006).

Natural mortality is either assumed to be prespecified to the value used in recent stock assessments (0.045 week^{-1}; Wang 1999; Dichmont et al. 2003) or estimated with a lognormal prior distribution. The sensitivity of the results to a prior mean for M of 0.025, 0.05, and 0.10 week^{-1} and a prior coefficient of variation (CV) of 0.3 and 1.0 is explored.

The parameters were sampled from the joint posterior distribution using a Bayesian Markov chain Monte Carlo algorithm, as implemented in WinBUGS (Spiegelhalter et al. 2003). WinBUGS represents variance parameters using precisions, which are the inverses of variances, i.e., $\tau = 1/\sigma^2$. Accordingly, we used τ values for the variances in eqs. 1, 2, and 3. Combining the hyperpriors, priors, and likelihood, the joint posterior distribution for all the parameters was then

$$(6)\qquad P(q_{y,f}, \tau_{q,f}, a_f, b_f, B_{y,1}, \tau_{B1}, B_{y,w}, \tau_B, M, \tau_{U,f} \mid U_{y,w,f}, \rho_w)$$
$$\propto P(\mu_{B1})P(\tau_{B1})P(a_f)P(b_f)P(\tau_{q,f})P(M)\tau_{U,f}\prod_y\left[P(q_{y,f} \mid a_f, b_f, \tau_{q,f})P(B_{y,1} \mid \mu_{B1}, \tau_{B1})\prod_w\prod_f P(U_{y,w,f} \mid q_{y,f}, B_{y,1}, \rho_w, M, \tau_{U,f})\right]$$

Alternative models

The state–space (hereafter SS) model described above recognizes that uncertainty exists in both the population dynamics and the observation process. In contrast, traditional depletion models assume that the population dynamics are deterministic and all error is associated with the observations. Four models are therefore considered that explore whether natural mortality is estimated or prespecified and whether or not allowance is made for process error: (1) state–space model, natural mortality estimated (SS+M); (2) state-space model, natural mortality prespecified (SS); (3) observation error only, natural mortality estimated (OE+M); (4) observation error only, natural mortality prespecified (OE).

Model diagnostics and comparison

The Bayesian analyses for each model were based on three chains, each with a burn-in of 20 000 cycles followed by a further 50 000 cycles, with the samples used for inference based on every 10th cycle (resulting in 15 000 samples from three chains). Trace plots were evaluated as an initial way to determine whether convergence had taken place, and the Gelman–Rubin diagnostic statistic (Best et al. 1996) was used for further convergence diagnosis.

The fits of the four models to the data were evaluated using a graphical assessment of the 95% prediction credibility intervals and Kolmogorov–Smirnov (KS) two-sample tests (Sheskin 1997). These statistics were calculated from posterior predictive distributions for the fleet-specific weekly catch rates. The posterior predictive distribution for each catch rate data point was obtained by sampling parameters from eq. 7, which summarizes all of the information about a "new" catch rate point, $U^{\mathrm{pred}}_{y,w,f}$, given the observed data, priors, and likelihood:

$$(7)\qquad P(U^{\mathrm{pred}}_{y,w,f} \mid \mathbf{U}, \rho) = \int P(U^{\mathrm{pred}}_{y,w,f}, \underline{\theta})P(\underline{\theta} \mid \mathbf{U}, \rho)\,\mathrm{d}\underline{\theta}$$

where $\underline{\theta}$ denotes all parameters, including model parameters and hyperparameters, and $\mathbf{U}$ is the observed catch rate data. The 2.5th, 50th, and 97.5th percentiles from the posterior predictive distribution are plotted together with the observed CPUE for visual inspection.

The nonparametric KS two-sample test was used to test the hypothesis that the predicted catch rate for each replicated sample and the observed catch rate were from the same distribution. The proportion of replicates in which the null hypothesis was rejected at α was defined as the overall KS p value:

$$(8)\qquad p_f^{\mathrm{KS}} = \frac{1}{n}\sum_y\sum_w I(p_{y,w,f} < \alpha)$$

where n was the total number of data points for fleet f, I was the indicator function that took the value of 1 when its argument was true and zero otherwise, and $p_{y,w,f}$ was the probability value from the KS test for each year, week, and fleet.

The deviance information criterion (DIC) (Spiegelhalter et al. 2003) was used to compare the four alternative models. The best model was the one that had the smallest value of DIC.

Application to grooved tiger prawns in Australia's NPF

Australia's NPF can be divided into "subfisheries". The major division of this fishery is between that which targets common (*Penaeus merguiensis*) and red-legged banana prawns (*Penaeus indicus*) and that which targets grooved (*P. semisulcatus*) and brown tiger prawns (*Penaeus esculentus*). The analyses of this paper aim to estimate q and M for *P. semisulcatus* because the reproductive pattern for this species is well-known so that weeks during which little recruitment occurs can be identified (Crocos 1987; Wang 1999). There is no known deliberate targeting of individual tiger prawn species, but because the two species have different spatial and temporal distributions, fishing when and where one species occurs may lead to some catch of the other species, albeit with lower catchability. For the purposes of this paper, therefore, we distinguish two tiger prawn "fleets". The grooved tiger prawns are targeted by the grooved tiger prawn fleet, but are also caught by the brown tiger fleet. Hence, the former is referred to as the target fleet and the latter as the byproduct fleet. The subfishery for banana prawns is not considered in this paper because it has low incidental catch of tiger prawns. However, the catch of tiger prawns during the banana subfishery is included in the total catch used when updating the population dynamics. The tiger prawn subfishery was open year-round before 1987, but has taken place from August to November since then.

The data on catch and effort used to fit the model were obtained from fishery logbooks. The raw catch and effort data in the logbooks are not recorded by species. However, algorithms have been developed that can reliably split the species-combined catches into catch (and effort) by two tiger prawn species in 6 nmi × 6 nmi (1 nautical mile = 1.852 km) grids throughout the NPF (Venables and Dichmont 2004). Monthly surveys of juvenile tiger prawns (Somers et al. 1987) show that tiger prawns recruit to the fishery during the warmer months of the year (January–February). The period modelled is selected so that recruitment is negligible (i.e., $R_{y,w} = 0$ in eq. 1). This assumption is also supported by the results of scientific surveys and commercial fishery data that show that catch rate generally decreases steadily from September (about week 35) to December (week 51) (Crocos and van der Velde 1995).

Wang (1999) used weeks 40–47 to estimate catchability for 1989 to 1993 and assumed recruitment was negligible during these weeks. The historical weekly CPUE data show a clear depletion process between weeks 38 and 49 for most years, although the timing of the onset of the decline varies somewhat among years. The analyses of this paper are therefore based on this latter period, with some years having fewer weeks because weeks at the beginning or end of the period are excluded based on the criteria that the catch rate for the primary target fleet in the second week and the final week should not increase more than 10% over that for the previous week. On average, the catch during the period used for analysis comprises about 50% of the total annual catch (range 35% to 70%).

The size of a grooved tiger prawn increases during the fishing season (Fig. 1). The weekly rate of growth was estimated using 9 years (1979–1990 (except 1981, 1982, and 1986 with no data); 27 248 measurements) of data on carapace length collected from commercial vessels in the Gulf of Carpentaria and data collected during scientific surveys (2002–2008 (except 2005 and 2006); 27 507 measurements). The individual length measurements were converted into masses using mass–length relationship parameters (Punt et al. (2009); α and β were, respectively, 0.002659 and 2.648 for females and 0.001955 and 2.746 for males). A linear model fits the mass data well (Fig. 1):

$$\begin{aligned} (9)\qquad \text{Male}: \quad & W_{w,m} = 19.79 + 0.410w \\ & (p < 2.2 \times 10^{-16}, \text{df} = 48\,887) \\ \text{Female}: \quad & W_{w,f} = 32.93 + 0.752w \\ & (p < 2.2 \times 10^{-16}, \text{df} = 46\,581) \end{aligned}$$

Wang (1999) estimated natural mortality for *P. semisulcatus* to lie between 0.03 and 0.065 week^{-1} using a maximum likelihood method and 5 years of catch and effort data. Consequently, recent stock assessments for tiger prawns (Wang and Die 1996; Dichmont et al. 2003) have been based on M = 0.045 week^{-1}. There was little effect on the results of the prior mean for M when the CV of the prior for M was set to 1.0, an essentially noninformative prior. However, the posterior distributions for the SS+M and OE+M models were more different than when a more informative prior was used (i.e., CV for M = 0.3). We focus on the results for a mean M of 0.045 week^{-1} and CV of 0.3, a relatively strong informative prior based on existing knowledge (Wang 1999; Wang and Ellis 2004) because one of the advantages of the Bayesian approach is its capability to incorporate prior knowledge. The value for M in models in which M was prespecified (SS and OE) was set to 0.045 week^{-1} for consistency with this.

Results

Model diagnostics and comparison

Visually, the four models fitted the weekly catch rates data well; it was difficult to visually distinguish the posterior median time trajectories of catch rate among the models (see Figs. 2 and 3 for the fits to the catch rates for the target and byproduct fleets for models SS+M and OE+M). The posterior predictive distributions showed that the model mimicked the observed catch rates very well (Figs. 2 and 3), although (and as expected), the posterior predictive distributions for the byproduct fleet are much wider than those for the target fleet.

The results of the KS two-sample test were similar for the SS and OE models (irrespective of whether M was estimated or prespecified). The overall p values for all models were greater than 0.95, implying that in less than 5% of cases could the null hypothesis (that the observed data came from the predictive distribution) be rejected.

The DIC increased from SS+M, to SS, OE+M, and OE (Table 2, column ΔDIC). The relative difference from the best to the other models was 244 or more, indicating that model SS+M was better (Spiegelhalter et al. 2003). The posterior estimates of the observation error variance were similar irrespective of whether M was estimated or prespecified, but,

Fig. 2. Observed (*x*) and posterior median (solid line) catch per unit effort (CPUE) and their 2.5 and 97.5 posterior predictive percentiles (dashed lines) for the target fleet (grooved tiger fleet) from model SS+M (state–space model with natural mortality estimated). The dark dotted line is the median of the posterior from model OE+M (observed error model with natural mortality estimated).

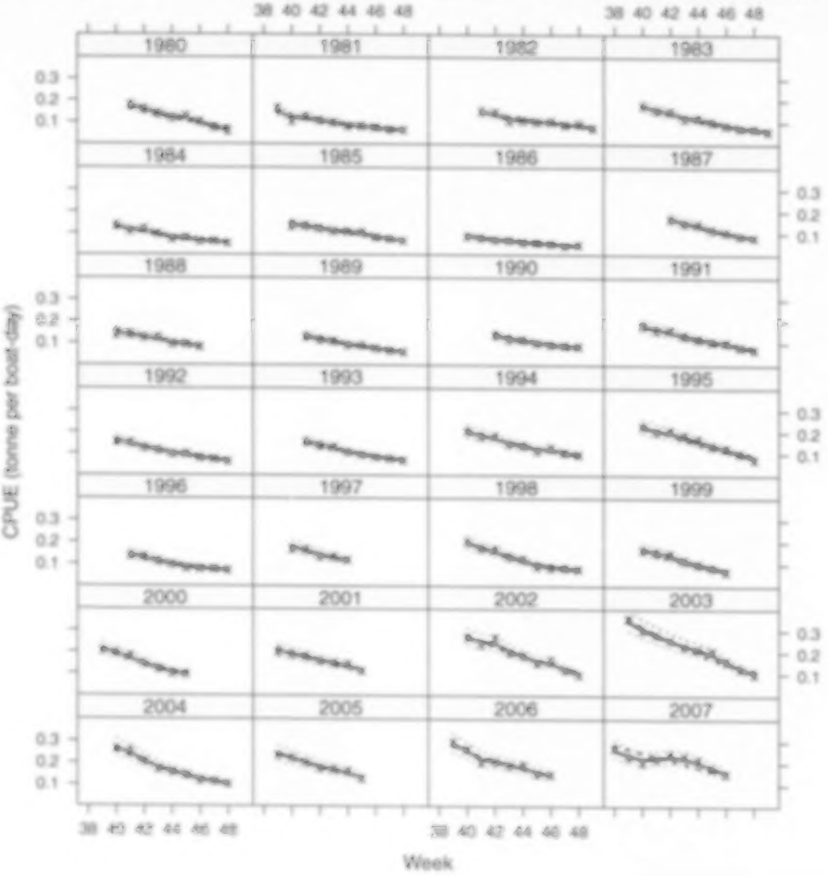

and as expected, the state–space models estimated smaller values for σ_U^2 for both fleets than the observation error models (Table 2). Within the same type of models, models with *M* estimated led to higher correlations between $B_{y,1}$ vs. q_{gv} (gv = grooved tiger prawn fleet). Given that the SS+M model was best, the results reported in the following sections are primarily for this model.

Catchability

The posterior median estimates of catchability for the target fleet ranged between 6.15 × 10^{-5} and 1.09 × 10^{-4} during 1980–2007. Catchability is estimated to have increased over time, particularly for the target fleet (Fig. 4). The posterior median for b_y from the SS+M model was 0.021 (95% credible interval 0.009 to 0.032), i.e., catchability increased by on average 2.1% per annum over the period 1980 to 2007. There were some differences in the estimates of the time series of catchability coefficients between the state–space and observation error models, with the latter suggesting a higher rate of increase in catchability, particularly for the target fleet (Fig. 4). Because of correlation, prespecifying M = 0.045 week^{-1} (which is smaller than the value estimated by SS+M model) caused estimated q to shift in the opposite direction. The SS models led to estimates of catchability with greater precision than the OE models for both fleets (Table 2). The catchability coefficient for 1993 has special importance for this fishery because it is a reference value for the stock assessment. The posterior median for this catchability coefficient from the SS+M model was 8.08 × 10^{-5} (95% credible interval 5.03 × 10^{-5} to 1.22 × 10^{-4}), which is slightly smaller than the value derived by Wang (1999) and currently used in assessments (8.8 × 10^{-5}).

The estimated byproduct catchability coefficient (q_{bn}–catchability of grooved tiger prawn in the brown tiger fleet) was smaller than the catchability coefficient for the target (grooved) fleet, ranging from 1.20 × 10^{-5} to 2.76 × 10^{-5} (Fig. 4). The posterior median for b_y for the byproduct fleet was 0.019 (95% credible interval 0.004 to 0.034), suggesting that catchability for the byproduct fleet increased by 1.9% on average each year. However, the trend in catchability for the byproduct fleet was not as clear as that for the target fleet (Fig. 4). The ratio q_{bn} / q_{gv} from the SS+M model varied between 0.18 and 0.30 with a mean of 0.24. This ratio was 0.20 for 1993, which compares with the value assumed in assess-

Fig. 3. Observed (x) and posterior median (solid line) catch per unit effort (CPUE) and their 2.5 and 97.5 posterior predictive percentiles (dashed lines) for the byproduct fleet (brown tiger fleet) from model SS+M (state–space model with natural mortality estimated). The dark dotted line is the median of the posterior from model OE+M (observed error model with natural mortality estimated).

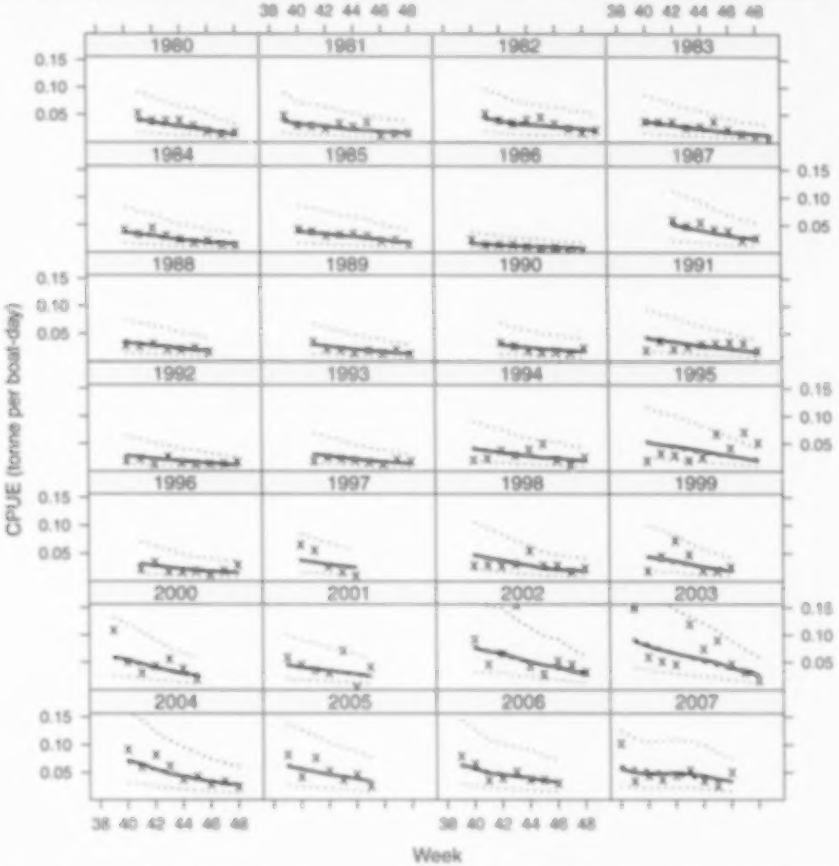

Table 2. Posterior medians for the variance parameters (gv = grooved tiger prawn fleet, bn = brown tiger prawn fleet) for the four models, along with the ΔDIC values, and the posterior correlations among initial biomass and catchability.

	Process error	Observation error			Catchability		Correlation	
Model	σ_B^2	$\sigma_{U,gv}^2$	$\sigma_{U,bn}^2$	ΔDIC	$\sigma_{q,gv}^2$	$\sigma_{q,bn}^2$	$M \sim q_{gv}$	$B_{1,1} \sim q_{gv}$
SS+M	0.0038	0.0034	0.1510	0	0.0127	0.0378	–0.86	–0.90
SS	0.0038	0.0034	0.1512	244	0.0130	0.0390	—	–0.77
OE+M	—	0.0071	0.1524	268	0.0208	0.0577	–0.82	–0.93
OE	—	0.0072	0.1525	355	0.0204	0.0572	—	–0.92

Note: SS+M, state–space model, natural mortality estimated; SS, state–space model, natural mortality prespecified; OE+M, observation error only, natural mortality estimated; OE, observation error only, natural mortality prespecified.

ments of 0.1. The posterior median for the extent of observation error for the byproduct fleet, expressed as variance, was 44 (state–space models) or 21 (observation error models) times larger than that for the target fleet (Table 2).

Natural mortality

The posterior distributions for weekly natural mortality from the state–space and observation error models overlapped. However, the distribution was narrower and its median larger for the state–space model than that for the observation error model (Fig. 5). The posterior medians (and their 95% credible intervals) were, respectively, 0.053 week^{-1} (0.028 to 0.078) and 0.042 week^{-1} (0.024 to 0.070) for the SS+M and OE+M models.

Discussion

We successfully applied a Bayesian hierarchical state–space model to estimate key quantities for fish stock assessment (natural mortality and time trends in catchability for

Fig. 4. Posterior time trajectories for catchability (target fleet top panel; byproduct fleet bottom panel) from the SS and OE models, with associated 95% credibility intervals for the SS+M model.

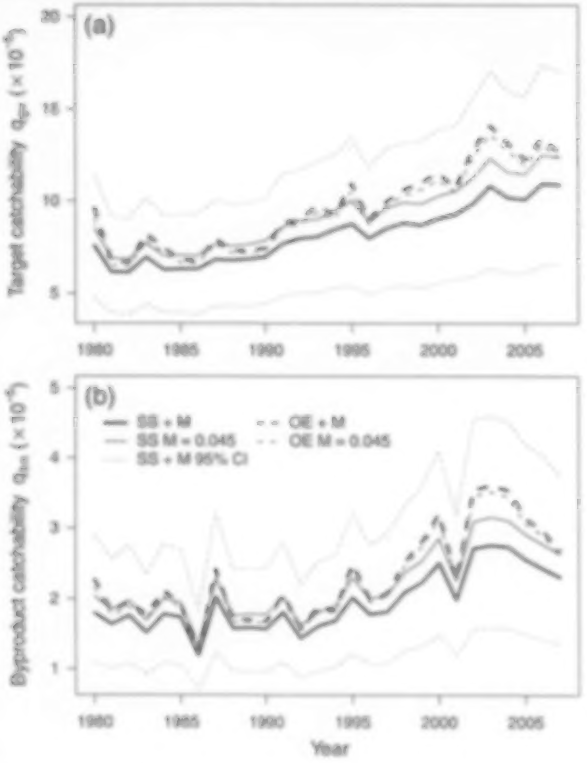

Fig. 5. Marginal posterior distributions for the natural mortality (solid line = SS+M model, thick dashed line = OE+M model) and the prior distribution assumed for *M* (thin dashed line). The shaded areas on *x* axis are 95% credible intervals: the grey area is for the SS+M model and the hatched area is for the OE+M model.

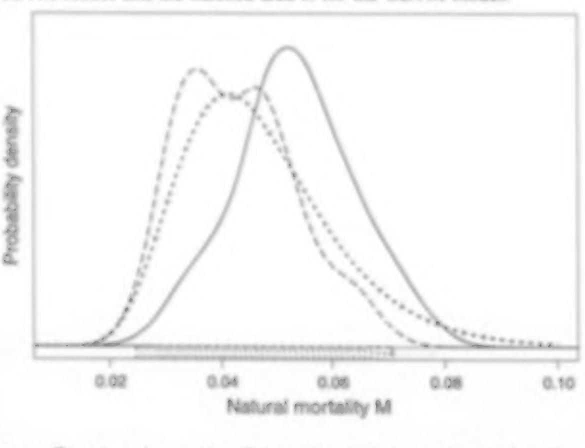

two fleets) using only fishery-dependent catch and effort data. The state–space models were superior to the observation error models. Specifically, the state–space models, which included variability in the population dynamics as well as in the catch process, led to narrower posterior distributions for all parameters and smaller DIC values. Zhou et al. (2009) found similar advantages of state–space over observation error formulations for assessments based on biomass dynamics models.

Fig. 6. Time series of catchability from the SS+M model (this study), the Base Case Low and Base Case High fishing power series (Bishop et al. 2008), and Wang's (1999) estimates of catchability. The plus sign (+) is year 1993.

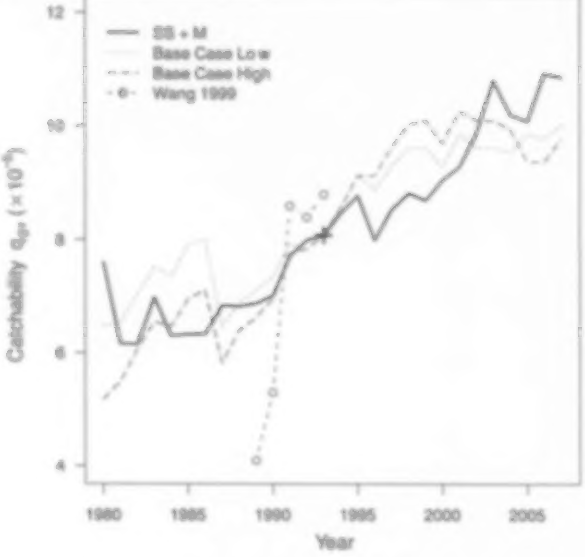

It is challenging to estimate catchability and natural mortality simultaneously using only catch and effort data. Wang (1999) developed a maximum likelihood approach to estimate *q* and *M* for the grooved tiger prawns by year for 1989 to 1993, but had to set *M* at three levels when estimating catchability because the *M* estimate was highly uncertain. In contrast, the Bayesian hierarchical models of this paper allowed both *q* and *M* to be estimated with reasonable precision. We also tested this method using simulations based on true parameter values similar to those obtained from the application (*q*, *M*, biomass, variances, etc.) and implemented the simulations in the similar procedure as described in the methods section. The posterior medians for natural mortality had a relative deviation of less than 2% from the true value, while the posterior medians for catchability had a relative deviation of –2% to 10%, and their 95% credible intervals included the true values. Changing the mean of the informative prior on *M* from 0.5 to 0.005 week^{-1} (a 100-fold difference), with a prior standard error of 0.3, resulted in a mean (over 15 000 simulations) posterior median for *M* of 0.046 and 0.034 week^{-1}, respectively (37% relative deviation), indicating relative insensitivity to the informative prior.

Our estimated posterior median catchability for the target fleet varied between 6.15×10^{-5} and 1.09×10^{-4} during 1980–2007. However, these estimates will be negatively biased if some recruitment occurred during the modelled period and positively biased if the catch rate indices reflect local depletion, i.e., the population in the fished area does not mix well with that in unfished areas. The posterior median estimate for *q* in 1993 of 8.08×10^{-5} was close to the estimate of *q* for 1993 obtained by Wang (1999) (8.8×10^{-5}) and is also comparable to an estimate of *q* for 1993 obtained using a biomass dynamics model (Zhou et al. 2009). However, the estimates of *q* for 1989 and 1990 were higher than Wang's (Fig. 6). The estimates of *q* from this paper changed more smoothly over time than those of Wang (1999), which is an expected result given that data for all of the years are analyzed simultaneously and are related stochastically to underlying deterministic trends in catchability (eq. 3). The catchability coefficient for the byproduct fleet is much lower than that for the target fleet. The ratio of byproduct to target catchability for 1993 was 0.2, which is the same as an estimate of this ratio from a biomass dynamics model (Zhou et al. 2009).

The estimates of byproduct catchability are much less precise than those of target catchability. The spatial distribution of the byproduct fleet relative to the distribution of grooved tiger prawns must be an important factor affecting weekly variation in byproduct catchability. Also, the catch rate patterns for the byproduct fleet for some years may not reflect the true depletion because this fleet changes its movement dynamics over time. This suggests that assessments involving indices based on the target and byproduct fleets should weight these indices differently (giving greater weight to the former).

The state–space model provided posterior median estimates of weekly *M* larger than 0.05 week^{-1}, even though the prior for *M* had its mode at 0.045 week^{-1}. Wang (1999) obtained a median estimate of natural mortality of 0.063 week^{-1}. However, he believed that the true value of *M* should be less than this, but at least 0.03 week^{-1}. Since then, weekly natural mortality has been assumed to be 0.045 week^{-1} in assessments for tiger prawns in Australia's NPF. Subsequently, Wang and Ellis (2004) estimated *M* and growth parameters for grooved tiger prawn using length–frequency data. Their estimated *M* ranged from 0.052 to 0.083 week^{-1}, with a mean of 0.067 week^{-1}. Using tagging data and trawl survey data, Somers and Kirkwood (1991) found that very few grooved tiger prawns survived beyond 18 months in the northwestern Gulf of Carpentaria, the major area of abundance for *P. semisulcatus* in the NPF (Somers et al. 1987). Using Hoenig's method (Hoenig 1983), longevity of 18 months is equivalent to a weekly *M* of 0.055 week^{-1}. From these studies, we conclude that *M* for grooved tiger prawns is likely to be larger than 0.045 week^{-1}.

Catch and effort data exist for the years 1970–1979. However, attempts to include these data in the analyses resulted in very uncertain results. There may be several reasons for this, including that the fishery operated year round during these years, fishing effort was low, there is less evidence for depletion in these years, and the quality of the catch and effort data for these early years is likely much poorer than for more recent years.

The results herein suggest an increase in catchability (and hence efficiency) over time for both fleets. Catchability is directly linked to fishing power (efficiency); the latter is affected by many factors, including gear, technology improvement, and skippers' knowledge (Bishop et al. 2008). Other studies found that it was very difficult to estimate the change in fishing efficiency for the tiger prawn fishery (Bishop et al. 2000, 2008). Different models produced a range of results, but there is considerable certainty that efficiency has increased substantially over the last 30 years (Robins et al. 1998; Kompas et al. 2004; Bishop et al. 2008). Historical estimates of fishing power, found by linear regressions or deterministic accounting, range quite widely: from 4.4% to 10.3% per year on average between 1971 and 1986, and 0.3% to 11.7% per year on average between 1987 and 1999 (Bishop et al. 2008). Two of the resulting models, "Base Case Low" and "Base Case High", have been used in recent annual stock assessments (Dichmont et al. 2003). The "envelope" of average change in catchability (Base Case Low to Base Case High) from 1980 to 2007 was 1.79% and 2.82% per year (Bishop et al. 2008). The up and down trend, but overall a lack of noteworthy increase in catchability, during the 1980s (Fig. 6) may have resulted from constant change in management and fleet structure, particularly a reduction in the average swept area per vessel balanced against an increased application of innovative aids to searching. The estimates of catchability from the Bayesian hierarchical models were similar to those from the latter two models (Fig. 6). Although the analyses on which the two catchability series are based used catch and effort data, the analyses of Bishop et al. (2008) also incorporated data on fleet renewal, within-vessel changes in swept area performance, catch efficiency, searching aids and skipper experience, and expert knowledge of trawl fishing and the fishery. The fact that the results of Bayesian hierarchical are similar to those of Bishop et al. (2008) is encouraging.

The comparison of Bayesian hierarchical state–space model with methods that require extensive data suggests this model could be applied to other fisheries that have limited data. The depletion method has been widely used in fisheries assessment (Cowx 1983; Young et al. 2004; Wright et al. 2006). However, process error has rarely been accounted for and natural mortality is either assumed negligible or prefixed as a known constant because of estimation difficulties (e.g., McAllister et al. 2004; Rago et al. 2006; Haakana and Huuskonen 2008). The method described in this paper would be useful for data-limited fisheries, particularly for short-lived species with high natural mortality and a short fishing season.

Acknowledgements

We thank Malcolm Haddon and Natalie Dowling (CSIRO Marine and Atmospheric Research) and two anonymous reviewers for their thorough review and constructive comments on the previous version of the manuscript. This research was supported by CSIRO Wealth from Ocean Flagship

References

Arreguin-Sanchez, F. 1996. Catchability: a key parameter for fish stock assessment. Rev. Fish Biol. Fish. **6**: 221–242. doi:10.1007/BF00182344.

Best, N., Cowles, M.K., and Vines, K. 1996. CODA convergence diagnosis and output analysis software for Gibbs sampling output. MRC Biostatistics Unit, Cambridge, UK.

Bishop, J., Die, D., and Wang, Y.G. 2000. A generized estimating equations approach for analysis of the impact of new techonology on a trawl fishery. Aust. N.Z. J. Statist. **42**(2): 159–177. doi:10.1111/1467-842X.00116.

Bishop, J., Venables, W.N., Dichmont, C.M., and Sterling, D.J. 2008.

Standardizing catch rates: is logbook information by itself enough? ICES J. Mar. Sci. **65**(2): 255–266. doi:10.1093/icesjms/fsm179.

Burridge, C.Y., Rr. Pitcher, C., Wassenberg, T.J., Poiner, I.R., and Hill, B.J. 2003. Measurement of the rate of depletion of benthic fauna by prawn (shrimp) otter trawls: an experiment in the Great Barrier Reef, Australia. Fish. Res. **60**(2–3): 237–253. doi:10.1016/S0165-7836(02)00179-0.

Cowx, I.G. 1983. Review of the methods for estimating fish population size from survey removal data. Fish. Manag. **14**: 67–82.

Crocos, P. 1987. Reproductive dynamics of the grooved tiger prawn, *Panaeus semisulcatus*, in the north-western Gulf of Carpentaria, Australia. Aust. J. Mar. Freshwater Res. **38**(1): 79–90. doi:10.1071/MF9870079.

Crocos, P.J., and van der Velde, T.D. 1995. Seasonal, spatial and interannual variability in the reproductive dynamics of the grooved tiger prawns, *Penaeus semisulcatus* in Albatross Bay, Gulf of Carpentaria, Australia: the concept of effective spawning. Mar. Biol. **122**: 557–570. doi:10.1007/BF00350678.

Dichmont, C.M., Punt, A.E., Deng, A., Dell, Q., and Venables, W. 2003. Application of a weekly delay-difference model to commercial catch and effort data for tiger prawns in Australia's Northern Prawn Fishery. Fish. Res. **65**(1–3): 335–350. doi:10.1016/j.fishres.2003.09.024.

Ellis, N., and Wang, Y.-G. 2007. Effects of fish density distribution and effort distribution on catchability. ICES J. Mar. Sci. **64**: 178–191.

Gelman, A. 2006. Prior distributions for variance parameters in hierarchical models. Bayes. Anal. **1**: 515–534. doi:10.1214/06-BA117A.

Haakana, H., and Huuskonen, H. 2008. Effects of intensive fishing on the perch population in a large oligotrophic lake in eastern Finland. Fish. Res. **91**(2–3): 144–150. doi:10.1016/j.fishres.2007.11.014.

Harley, S.J., and Myers, R.A. 2001. Hierarchical Bayesian models of length-specific catchability of research trawl surveys. Can. J. Fish. Aquat. Sci. **58**(8): 1569–1584. doi:10.1139/cjfas-58-8-1569.

Hewitt, D.A., and Hoenig, J.M. 2005. Comparison of two approaches for estimating natural mortality based on longevity. Fish Bull. **103**: 433–437.

Hoenig, J.M. 1983. Empirical use of longevity data to estimate mortality rates. Fish Bull. **82**: 898–903.

Kompas, T., Che, T.N., and Grafton, R.Q. 2004. Technical efficiency effects of input controls: evidence from Australia's banana prawn fishery. Appl. Econ. **36**(15): 1631–1641. doi:10.1080/0003684042000218561.

Marchal, P., Andersen, B., Caillart, B., Eigaard, O., Guyader, O., Hovgaard, H., Iriondo, A., Le Fur, F., Sacchi, J., and Santurtún, M. 2007. Impact of technological creep on fishing effort and fishing mortality, for a selection of European fleets. ICES J. Mar. Sci. **64**: 192–209.

McAllister, M.K., Hill, S.L., Agnew, D.J., Kirkwood, G.P., and Beddington, J.R. 2004. A Bayesian hierarchical formulation of the De Lury stock assessment model for abundance estimation of Falkland Islands' squid (*Loligo gahi*). Can. J. Fish. Aquat. Sci. **61**(6): 1048–1059. doi:10.1139/f04-084.

Punt, A.E., Buckworth, R.C., Dichmont, C.M., and Ye, Y. 2009. Performance of methods for estimating size–transition matrices using tag–recapture data. Mar. Freshw. Res. **60**(2): 168–182. doi:10.1071/MF08217.

Quinn, T.J., II, and Deriso, R.B. 1999. Quantitative fish dynamics. Oxford University Press, New York.

Rago, P.J., Weinberg, J.R., and Weidman, C. 2006. A spatial model to estimate gear efficiency and animal density from depletion experiments. Can. J. Fish. Aquat. Sci. **63**(10): 2377–2388. doi:10.1139/F06-121.

Rider, S.J., Maceina, M.J., and Lowery, D.R. 1994. Comparisons of cove rotenone and electrofishing catch-depletion estimates to determine abundance of age-0 largemouth bass in unvegetated and vegetated areas. J. Freshwat. Ecol. **9**(1): 19–27. doi:10.1080/02705060.1994.9664423.

Robert, M., Faraj, A., McAllister, M.K., and Rivot, E. 2010. Bayesian state–space modelling of the De Lury depletion model: strengths and limitations of the method, and application to the Moroccan octopus fishery. ICES J. Mar. Sci. **67**(6): 1272–1290. doi:10.1093/icesjms/fsq020.

Robins, C.M., Wang, Y.-G., and Die, D. 1998. The impact of global positioning systems and plotters on fishing power in the northern prawn fishery, Australia. Can. J. Fish. Aquat. Sci. **55**(7): 1645–1651. doi:10.1139/cjfas-55-7-1645.

Salthaug, A., and Aanes, S. 2003. Catchability and the spatial distribution of fishing vessels. Can. J. Fish. Aquat. Sci. **60**(3): 259–268. doi:10.1139/f03-018.

Sheskin, D. 1997. Handboook of parametric and nonparametric statistical procedures. CRC Press, Boca Raton, Fla.

Somers, I., and Kirkwood, G. 1991. Population ecology of grooved tiger prawn, *Penaeus semisculcatus*, in the north-western Gulf of Carpentaria, Australia: growth, movement, age structure, and infestation by the Bopyrid parasite *Epipenaeon ingens*. Aust. J. Mar. Freshwater Res. **42**(4): 349–367. doi:10.1071/MF9910349.

Somers, I.F., Crocos, P.J., and Hill, B.J. 1987. Distribution and abundance of the tiger prawns *Penaeus esculentus* and *P. semisulcatus* in the north-western Gulf of Carpentaria, Australia. Aust. J. Mar. Freshwater Res. **38**(1): 63–78. doi:10.1071/MF9870063.

Spiegelhalter, D., Thomas, A., Best, N., and Lunn, D. 2003. WinBUGS user manual, V.1.4. MRC Biostatistics Unit, Cambridge, UK.

Su, Z., Adkison, M.D., and van Alen, B.W. 2001. A hierarchical Bayesian model for estimating historical salmon escapement and escapement timing. Can. J. Fish. Aquat. Sci. **58**(8): 1648–1662. doi:10.1139/cjfas-58-8-1648.

Venables, W., and Dichmont, C.M. 2004. A generalized linear model for catch allocation: an example from Australia's Northern Prawn Fishery. Fish. Res. **70**(2–3): 409–426. doi:10.1016/j.fishres.2004.08.017.

Volstad, J.H., Sharov, A.F., Davis, G., and Davis, B. 2000. A method for estimating dredge catching efficiency for blue crabs, *Callinectes sapidus*, in Chesapeake Bay. Fish Bull. **98**: 410–420.

Walter, J.F., Hoenig, J.M., and Gedamke, T. 2007. Correcting for effective area fished in fishery-dependent depletion estimates of abundance and capture efficiency. ICES J. Mar. Sci. **64**(9): 1760–1771. doi:10.1093/icesjms/fsm147.

Walters, C.J., and Hilborn, R. 2005. Exploratory assessment of historical recruitment patterns using relative abundance and catch data. Can. J. Fish. Aquat. Sci. **62**(9): 1985–1990. doi:10.1139/f05-105.

Wang, Y.G. 1999. A maximum-likelihood method for estimating natural mortality and catchability coefficient from catch-and-effort data. Mar. Freshw. Res. **50**(4): 307–311. doi:10.1071/MF97140.

Wang, Y.G., and Die, D. 1996. Stock–recruitment relationships of the tiger prawns (*Penaeus esculentus* and *Penaeus semisulcatus*) in the Australian Northern Prawn Fishery. Mar. Freshw. Res. **47**(1): 87–95. doi:10.1071/MF9960087.

Wang, Y.G., and Ellis, N. 2004. Maximum likelihood estimation of mortality and growth with individual variability from multiple length–frequency data. Fish Bull. **103**: 380–391.

Wright, I., Caputi, N., and Penn, J. 2006. Depletion-based population estimates for western rock lobster (*Panulirus cygnus*) fishery in Western Australia. NZ J. Mar. Freshw. Res. **40**(1): 107–122. doi:10.1080/00288330.2006.9517406.

Young, I.A.G., Pierce, G.J., Daly, H.I., Santos, M.B., Key, L.N., Bailey, N., Robin, J.-P., Bishop, A.J., Stowasser, G., Nyegaard, M., Cho, S.K., Rasero, M., and Pereira, J.M.F. 2004. Application of depletion methods to estimate stock size in the squid *Loligo forbesi* in Scottish waters (UK). Fish. Res. **69**(2): 211–227. doi:10.1016/j.fishres.2004.04.013.

Zheng, J. 2003. Uncertainties of natural mortality estimates for eastern Bering Sea snow crab, *Chionoecetes opilio*. Fish. Res. **65**(1–3): 411–425. doi:10.1016/j.fishres.2003.09.029.

Zheng, J., and Siddeek, M.S.M. 2010. Bristol Bay red king crab stock assessment in spring 2010. *In* Stock assessment and fishery evaluation report for king and tanner crab fisheries of the Bering Sea and Aleutian Islands. North Pacific Fishery Management Council, Anchorage, Alaska. pp. 134–246.

Zhou, S., Dichmont, C., Burridge, C., Venables, W., Toscas, P., and Vance, D. 2007. Is catchability density-dependent for schooling prawns? Fish. Res. **85**(1–2): 23–36. doi:10.1016/j.fishres.2006.11.034.

Zhou, S., Vance, D.J., Dichmont, C.M., Burridge, C.Y., and Toscas, P.J. 2008. Estimating prawn abundance and catchability from catch-effort data: comparison of fixed and random effects models using maximum likelihood and hierarchical Bayesian methods. Mar. Freshw. Res. **59**: 1–9. doi:10.1071/MF07090.

Zhou, S., Punt, A.E., Deng, R., Dichmont, C.M., Ye, Y., and Bishop, J. 2009. Modified hierarchical Bayesian biomass dynamics model for assessment of short-lived invertebrates: a comparison for tropical tiger prawns. Mar. Freshw. Res. **60**(12): 1298–1308. doi:10.1071/MF09022.

Ocean circulation, Stokes drift, and connectivity of western rock lobster (*Panulirus cygnus*) population

Ming Feng, Nick Caputi, James Penn, Dirk Slawinski, Simon de Lestang, Evan Weller, and Alan Pearce

Abstract: An individual-based model, incorporating outputs of a data-assimilating hydrodynamic model, was developed to investigate the role of ocean circulation in the recruitment processes of western rock lobster (*Panulirus cygnus*) during its 9- to 11-month larval phase off the west coast of Australia. During austral summer, strong northward alongshore winds aid the offshore movement of early-stage model larvae from midshelf hatching sites into open ocean; during austral winter, eastward flows that feed the enhanced Leeuwin Current facilitate onshore movement of late-stage larvae towards nearshore habitats. Stokes drift induced by swells from the Southern Ocean is critical to retain larvae off the west coast. Diurnal migration and temperature-dependent growth are also important. Model larvae hatched in late spring – early summer grow faster because of longer exposure to warm summer temperature, which allows them to be transported towards the coast by the strong onshore flows in winter and reduces their natural mortality. Preliminary source–sink relationship indicates that the population was well mixed off the coast, with higher likelihood of settlement success from hatching sites in the north, mostly due to higher surface temperature. Weighted with the breeding stock distribution, the area between 27.5°S and 29.5°S, including the Abrolhos Islands, is the most important hatching area to the success of settlement.

Résumé : Nous avons mis au point un modèle basé sur l'individu qui intègre les résultats d'un modèle hydrodynamique d'incorporation de données afin de déterminer le rôle de la circulation océanique sur les processus de recrutement de la langouste d'Australie (*Palinurus cygnus*) durant sa phase larvaire de 9–11 mois au large de la côte occidentale de l'Australie. Durant l'été austral, de puissants vents vers le nord le long de la côte favorisent le déplacement au large des larves de premiers stades du modèle à partir de leurs sites d'éclosion au milieu de la plate-forme vers la haute mer. Durant l'hiver austral, les flots vers l'est qui alimentent le courant accru de Leeuwin facilitent les déplacements côtiers des larves de stades avancés vers les habitats près des rives. La dérive de Stokes provoquée par des lames provenant de l'Océan austral est de grande importance pour retenir les larves loin de la côte occidentale. Les migrations journalières et la croissance dépendante de la température sont aussi importantes. Les larves du modèle écloses à la fin du printemps et au début de l'été grandissent plus rapidement à cause de leur exposition prolongée à la température plus élevée d'été, ce qui leur permet d'être transportées vers la côte par les forts courants dirigés vers le bord en hiver et réduit leur mortalité naturelle. Une relation préliminaire de type source–puits indique que la population est bien mélangée au large de la côte, avec une plus forte vraisemblance du succès de l'établissement à partir des sites d'éclosion du nord, à cause surtout de la température de surface plus élevée. Compte tenu de la répartition du stock reproducteur, la région située entre 27,5°S et 29,5°S, y compris les îles Abrolhos, constitue la région d'éclosion la plus importante en ce qui a trait au succès de l'établissement.

[Traduit par la Rédaction]

Introduction

Recruitment process for western rock lobster (*Panulirus cygnus*) fishery off the lower west coast of Western Australia (WA) has been found to be strongly influenced by the physical environment, with sea surface temperature (SST), the Leeuwin Current, and westerly winds being highly associated with interannual variation in puerulus settlements of western rock lobster off the coast. SST in February–April is found to be significantly correlated with puerulus settlements later in the year, and with a stronger, southward-flowing Leeuwin Current, puerulus settlements in the southern locations tend to be relatively higher (Caputi et al. 2001). Westerly winds in late winter – spring also affect puerulus settlements (Caputi et al. 2010*a*). Puerulus settlements are in turn well correlated with lobster catches 3 to 4 years later (Caputi et al. 1995; de Lestang et al. 2009*a*), which generate revenues up to AU$200–300 million annually.

The very low puerulus settlements recorded in the 2007–2008 and 2008–2009 seasons (with 2008–2009 being the lowest in 40 years) have not followed the historical environmental correlations and indicates the need for an improved understanding of the recruitment process in this nationally important fishery. The breakdown in the historical correla-

Received 18 October 2010. Accepted 24 March 2011. Published at www.nrcresearchpress.com/cjfas on 6 July 2010.
J22072

Paper handled by Associate Editor David Brickman.

M. Feng, D. Slawinski, and E. Weller. CSIRO Marine and Atmospheric Research, Underwood Avenue, Floreat, WA 6014, Australia.
N. Caputi, J. Penn, S. de Lestang, and A. Pearce. Western Australian Fisheries and Marine Research Laboratories, Department of Fisheries, Western Australia, P.O. Box 20, North Beach, WA 6920, Australia.

Corresponding author: Ming Feng (e-mail: Ming.Feng@csiro.au).

doi:10.1139/F2011-065
Published by NRC Research Press

tions between environmental factors and puerulus settlements suggests that other unidentified physical factors may play a role. It has also raised the possibility that breeding stock, although at historically acceptable levels across most of the fishery (de Lestang et al. 2009*b*), may in some way have contributed to the settlement downturn. In particular, there is a need to better understand the source–sink relationship (i.e., contributions to recruitment (puerulus settlements) from breeding stocks in different sections of the fishery). To address these specific issues, an individual-based model (IBM) approach has been adopted, taking advantage of our improved oceanographic knowledge, the availability of a state-of-art data-assimilating hydrodynamic model, and a thorough review of larval behaviours of western rock lobster. This modelling approach is the only practical method to assess the possible impact of regional depletion of breeding stocks or to identify the combination of oceanographic factors that may have caused the unprecedented low settlement that occurred in 2007–2008 and 2008–2009.

IBMs that embed biological particles into simulated ocean circulation fields have been shown to have the capacity to provide important insights into potential patterns of transport and connectivity in populations of marine organisms with planktonic life stages (Cowen et al. 2006; Paris et al. 2007). An IBM was used to investigate larval transport and connectivity patterns in the Gulf of Maine lobster population and found that abundance patterns of competent (to settle) model larvae closely resemble observed, alongshore patterns of lobster settlement density, so that connectivity and potential transport mechanisms can be assessed (Xue et al. 2008; Incze et al. 2010).

The first IBM developed to investigate the larval phase of the western rock lobster incorporated satellite-based ocean currents and larval behaviour and was capable of moving large numbers of early-stage larvae (phyllosoma) offshore from breeding areas along the continental shelf and returning them to the west coast as puerulus some 9–11 months later (Griffin et al. 2001). While this model was a major step forward in the oceanographic sense, the authors noted that their model involved a number of simplifications and was not able to fully replicate the observed geographic distribution of puerulus settlements or the interannual variability in settlements.

In this study, the Griffin et al. (2001) model framework has been expanded based on recent developments in ocean models (Schiller et al. 2008) and satellite data. The new IBM also takes into account information from a review of the historical and recent *P. cygnus* literature on the behaviour of the phyllosoma and puerulus stages. The results from the IBM have been assessed for realism against the spatial and temporal distributions of the phyllosoma larvae from historical field surveys and the general puerulus settlement patterns along the WA coastline (Phillips et al. 1979; Caputi et al. 2001, 2010*b*). The outputs from the IBM have been used to provide a preliminary assessment of the source–sink relationship between regional breeding stocks and puerulus settlement across the fishery and the key factors that may be affecting this relationship.

Physical environment off the west coast of Western Australia

The poleward-flowing Leeuwin Current dominates the ocean circulation along the coast of WA. This atypical eastern boundary current deepens the thermocline and nitrocline off the coast of WA (Thompson 1984), suppressing productivity on the continental shelf and causing the oligotrophic marine environment off the coast (Koslow et al. 2008).

Seasonal variations in the strength of the Leeuwin Current are predominantly driven by seasonal variations of surface winds off the west coast of WA (Smith et al. 1991; Feng et al. 2003). During the austral summer, strong southerly to southeasterly winds prevail, while during the winter half of the year the winds are much weaker and are from the west to southwest, particularly in the southern section of the coast (Fig. 1). The Leeuwin Current is therefore stronger during the austral winter compared with the austral summer, when pulses of northward winds balance the meridional pressure gradient that drives the Leeuwin Current. These summer winds also drive the episodic northward inshore currents (Cresswell et al. 1989) and offshore (westward) surface Ekman transport (Fig. 2). In addition to the Leeuwin Current, the west coast is greatly influenced by open ocean waves (swells), mostly arriving from the southwest because of storm activities in the Southern Ocean. In winter, strong westerly winds associated with storm fronts occur off the lower west coast, so that the wave energy is also stronger, with a large wave height magnitude of 4–5 m in the area of the lobster settlement compared with typically less than 3 m in summer (Fig. 1).

El Niño Southern Oscillation (ENSO)-related upper ocean variations propagate poleward as internal coastal Kelvin waves along the northwest to west WA coasts (Meyers 1996; Feng et al. 2003). These waves generate higher coastal sea levels (increasing the depth of the thermocline) and induce strong Leeuwin Current flows during the La Niña years. Conversely, lower sea levels (and shallower thermocline) and weaker Leeuwin Current occur during the El Niño years (Feng et al. 2003, 2005). Interannual variations of SST off the lower west coast are strongly affected by the Leeuwin Current advection (Feng et al. 2008). Anomalous SST in the tropical eastern Indian Ocean associated with an Indian Ocean Dipole acts to trigger Rossby wave propagation in the upper troposphere and the development of easterly wind anomalies off the lower WA coast during the austral winter (E. Weller, M. Feng, H. Hendon, J. Ma, S.-P. Xie, and N. Caputi, personal communication, 2011). A positive Indian Ocean Dipole event is often associated with an enhancement of the Leeuwin Current in the year following the event (Feng et al. 2008).

Recruitment processes for western rock lobster

Spawning female lobsters through the main distribution of the stock along the lower west coast are typically found in depths from about 40 to 80 m and are associated with reef habitats (Melville-Smith et al. 2009). Exceptions to this general pattern are breeding in shallower depths through the Abrolhos Islands and on some deeper reefs north of the Abrolhos (Chubb et al. 1994). More than 50% of the breeding stock is distributed around the Abrolhos Islands region, 28°S–29°S (Fig. 3*b*). There is a regular migration of immature lobsters from the inshore nursery reefs to the offshore reef breeding areas in November–December each year. This offshore movement can also involve a substantial northward movement where the migrating lobster reach the shelf edge

Fig. 1. Surface wind speeds (*a*, *b*) and significant wave height (contour in metres) and direction (*c*, *d*) off the west coast of Western Australia (WA) during the austral summer (December–February) and winter (June–August).

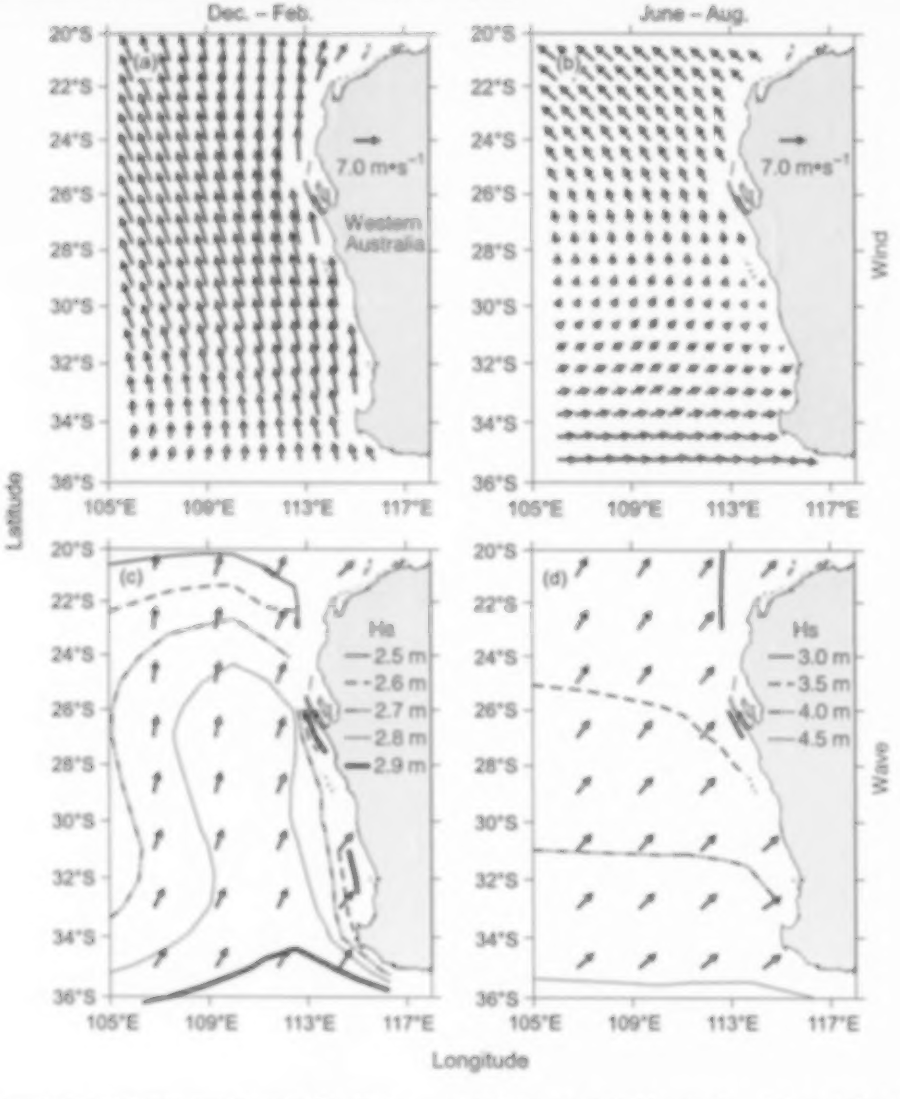

and result in large numbers of lobsters reaching the Big Bank area (~27°S) at the northern limit of the fishery (Chubb et al. 1994).

From the monthly catch rates of berried females (Chubb 1991) and allowing a 1-month lag for the typical incubation time at summer temperatures (Chittleborough 1976), the monthly distribution of hatching of phyllosoma larvae are approximately 3%, 15%, 36%, 23%, 20%, and 3% for the 6 months from October to March. During the summer hatching period, the strong alongshore winds, weak Leeuwin Current, and weak wave energy aid the offshore transport of the early stage phyllosoma (Fig. 2*a*). Offshore movement of the first stage phyllosoma has been estimated to occur at a minimum rate of about 5 km per day (Rimmer 1980).

Nine development stages in the phyllosoma phase have been identified (Braine et al. 1979), through a development period of about 9–11 months with variable time spent in each stage (Chittleborough and Thomas 1969; Phillips et al. 1979). Phyllosoma typically undergo diurnal vertical migrations and descend to increasing daylight depths with age (Rimmer and Phillips 1979). At night phyllosoma move into the surface layers (less than 20 m) and tend to concentrate in the upper few metres, particularly under calm conditions, and then they descend to deep layers during daylight (e.g., Fig. 4). Moonlight level and sea state also substantially influenced the position of phyllosoma in the water column at night. Stage I phyllosoma spend more time close to the surface than at later stages as a result of a more positive phototactic response (Ritz 1972; Rimmer 1980).

The growth rate of the early stage phyllosoma was found to be temperature-dependent (Marinovic et al. 1994). Liddy et al. (2004) compared growth rates of phyllosoma at 19, 22,

Fig. 2. Schematics of surface currents along the west coast of Western Australia (WA) during (*a*) the austral summer (December–February) and (*b*) winter (June–August). The hatched area in panel (*a*) denotes the release sites of particles in the individual-based model (IBM), and the hatched area in panel (*b*) denotes the June–July distribution of high-abundance, late-stage phyllosoma from historical observations (adapted from Phillips et al. 1979). Note that the abundance distribution is not uniform in the region. The broad arrows in the figures denote general directions of particle transport by ocean currents during the two opposite seasons.

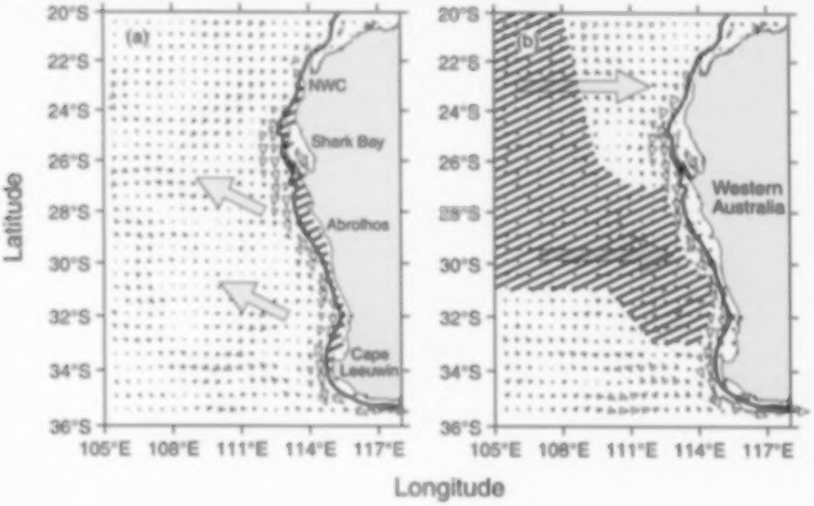

and 25 °C and suggested that growth from hatching to Stage III took about 60 days at 19 °C, 36 days at 22 °C, and 28 days at 25 °C. The optimal temperature for growth was suggested to be in the range 22 to 23 °C, which is in keeping with the SST recorded in the area off the middle west coast where the phyllosoma spend much of their time (Phillips et al. 1979). These temperatures for optimal growth are also supported by Caputi et al. (2001), who showed that high puerulus settlement years were generally associated with higher February–April SSTs (in the areas occupied by the phyllosoma) of about 22 to 22.5 °C, while low settlement years were typically associated with temperatures below 21 °C.

The numbers of phyllosoma surviving over time will also be a function of the level of "natural" mortality being experienced. While phyllosoma appear to be able to survive a wide range of oceanographic conditions between 21°S and 35°S (Chittleborough and Thomas 1969), survival is likely to be influenced by temperature (i.e., ability to feed), which has a range of 28 °C off the North West Cape (NWC) in the north and 15 °C off the south coast. Predation of phyllosoma by plankton-feeding fish species is also likely and is supported by observations that few phyllosoma apart from the hatching Stage I (or late larval stages) are found on the shelf, where fish (predator) abundance is highest. An indication of the likely natural mortality rate is provided by the phyllosoma catches from a series of surveys (Rimmer and Phillips 1979), which suggested a decline in numbers by about 85% to 90% over the 9-month period, corresponding to progression from Stages II to VIII. Metamorphosis of the Stage VIII phyllosoma to puerulus also requires a build up of nutritional reserves (Phillips and McWilliam 2009), so that the nonfeeding puerulus has sufficient energy reserves to migrate to coastal settlement areas.

While the westward wind-driven surface currents (0–20m) during the summer hatching season appear to be the mechanism to assist the offshore migration of the phyllosoma out into the eastern Indian Ocean, the eastward surface currents occurring during the austral winter appear to be the mechanism that facilitates the movement of late stage phyllosoma back to the shelf edge and allows them to metamorphose into puerulus and settle in the coastal habitats (Fig. 2*b*).

Because most puerulus are found near or on the shelf break (Phillips and McWilliam 2009), it appears that successful metamorphosis mostly occurs when the Stage IX phyllosoma are carried close to the shelf break. The most likely trigger for metamorphosis is the nutritional state of the phyllosoma (Phillips and Pearce 1997), and satellite chlorophyll data show chlorophyll concentrations (likely to correspond to phytoplankton and zooplankton abundance) are highest along the edge of the shelf during late winter – spring (Feng et al. 2007; 2009).

Relatively few swimming stage puerulus have been caught, and these were mostly captured at night on the shelf at subsurface levels between 15 and 25 m (Ritz 1972) and during new moon (Phillips et al. 1978). These records suggest that migration towards the coast occurs subsurface, although the largest catch recorded at night by Ritz (1972) was near the surface under storm conditions. Active swimming on the surface has been observed close to shore and near settlement habitats (Ritz 1972; Phillips and Olsen 1975). Because the puerulus stage does not feed, the time available from metamorphosis to settlement on the coast, based on nutritional reserves (Lemmens 1994), is likely to be a maximum of about 21 days, assuming that the puerulus are swimming intermittently. Substantial puerulus settlement has only been recorded in shallow reef and sea-grass areas in depths of less than 5 m

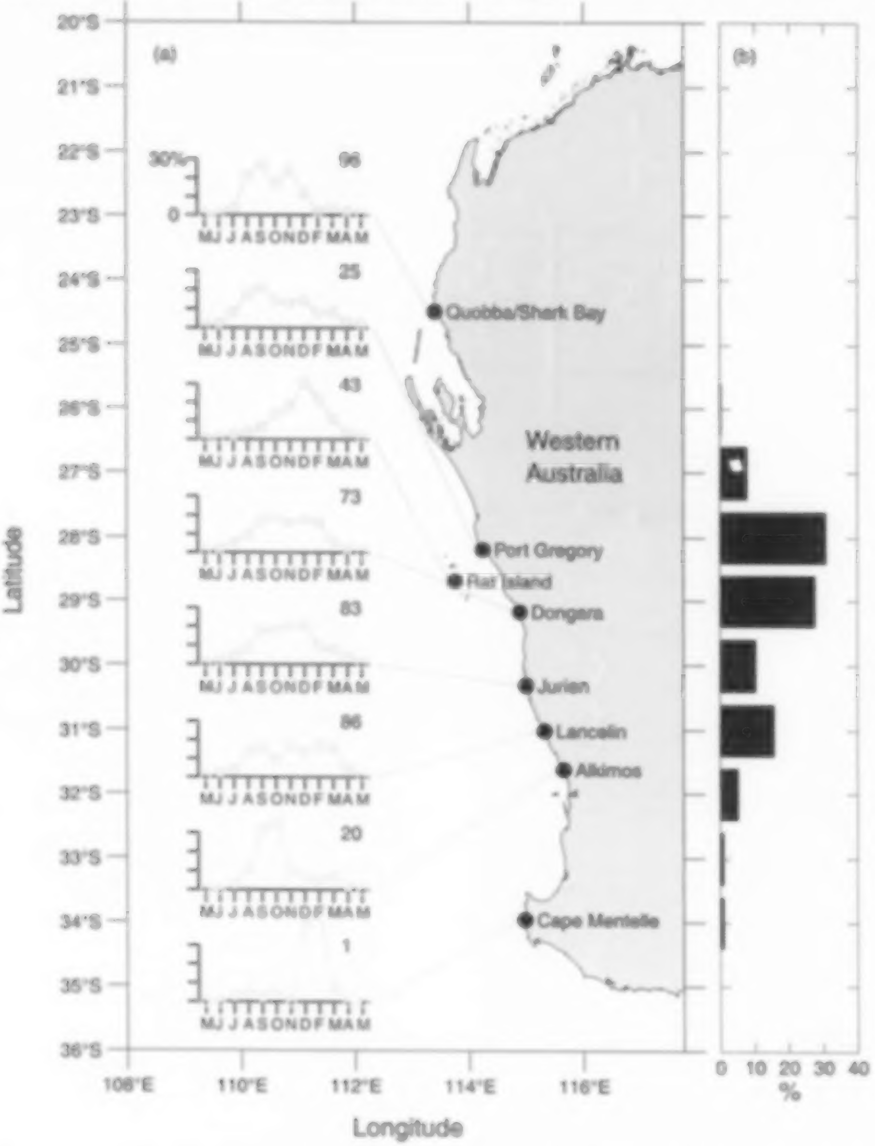
(a)
(b)
20°S
21°S
22°S
23°S
24°S
25°S
26°S
27°S
28°S
29°S
30°S
31°S
32°S
33°S
34°S
35°S
36°S
Latitude
30%
0
96
25
43
73
83
86
20
1
M J J A S O N D F M A M
Quobba/Shark Bay
Western Australia
Port Gregory
Rat Island
Dongara
Jurien
Lancelin
Alkimos
Cape Mentelle
108°E
110°E
112°E
114°E
116°E
Longitude
0 10 20 30 40
%

Fig. 3. (*a*) Average monthly settlement rates (2000–2001 to 2008–2009 settlement seasons) for western rock lobster (*Panulirus cygnus*) pueruli as percentages of total settlements (average number per collector shown to right of histogram, months abbreviated to first letter) at each collector site along the west coast of Australia. Note in 2005 the Shark Bay South Passage site was replaced by the Quobba site, so the two have been treated as a one site average. (Note the Rat Island site is in the central group of the Abrolhos Islands.) (*b*) Relative latitudinal contributions to overall breeding stock of western rock lobster (source: S. de Lestang).

(Jernakoff 1990), with high numbers occurring on artificial seaweed collectors between 25°S and 31°S (Fig. 3*a*).

IBM development

Physical models

The Bluelink reanalysis (BRAN) model used in this study is based on a global ocean model, OFAM (ocean forecasting Australia model), and has been developed for the Australian region (Schiller et al. 2008). BRAN uses the European Centre for Medium-Range Weather Forecasts reanalysis data for wind stress and heat and freshwater flux forcing at the sea surface and assimilates satellite altimeter and other in situ data (Oke et al. 2008). BRAN was used to create a 1993 to May 2008 archive of daily values of ocean properties, including ocean currents, salinity, and temperature in three dimensions — resolved at 10 km horizontally and 10 m vertically (in the upper ocean; i.e., to 300 m) for the eastern Indian Ocean study region. For the recent period (i.e., from May 2008 to 2009) where BRAN was not available,

Fig. 4. A schematic diagram representing the IBM model depths occupied by each category of phyllosoma and puerulus. The two lines are used to mimic the diurnal migration of the particles at each category, and they represent the upper and lower depth (m) limits of particle distributions. D denotes daytime and N denotes nighttime. The stippled area denotes a depth zone below the Leeuwin Current or shelf bottom; particles are motionless in this layer.

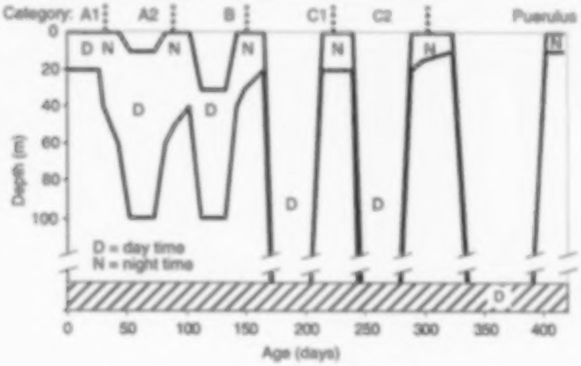

an equivalent forecast product based on BRAN (Brassington et al. 2007) has been used.

BRAN was selected as it appears to reasonably capture the average seasonal variations of the Leeuwin Current (e.g., Feng et al. 2010) along the west coast of Australia. The BRAN modelled currents and ocean temperature on seasonal and subseasonal (from days to weeks) time scales have also been validated with shipboard and mooring observations off the coast, showing that it has substantial skills in replicating the broader water movement off WA (A. Pearce, D. Slawinski, and M. Feng, unpublished data). However, it appears that BRAN has underestimated the wind-driven surface currents, especially those on the continental shelf (e.g., Capes Current). To adjust for this anomaly, QuikScat satellite-derived wind data has been used to generate a correction to the BRAN surface currents. The QuickScat-derived twice-daily global wind speed data at 1/4 degree by 1/4 degree resolution has been averaged into daily values and smoothed in time using a seven-point Hanning filter. The correction term was calculated using 1% and 3% of the wind speed and 20 degrees to the left of wind direction (e.g., Jenkins 1987) and applied to areas deeper and shallower, respectively, than 200 m. The correction is then interpolated onto the BRAN velocity grid and applied in the 0–20 m layer.

To further improve the surface water movements, the WAVEWATCH III model (WW3) incorporating significant wave height, wave period, and direction data (Tolman 2002) has been used to derive Stokes drift velocities in the surface layer (0–20 m) off the coast of WA. For this purpose the WW3 data from 1997 onwards were converted to daily means and then interpolated onto the BRAN velocity grid. In the wave propagation direction, the Stokes drift velocity can be calculated as

$$U_s = \frac{(ak)^2 C_P \cosh[2k(z+H)]}{2\sinh^2(kH)}$$

Here, $C_P = \sigma/k$ is the phase speed of the waves (m·s^{-1}), $\sigma^2 = gk\tanh(kH)$, where a is the wave height (m), k is the wave number, z is the water depth, which is zero at sea surface, and H is the ocean bottom depth. Using the WW3 data, $a = H_S/2$, and $\sigma = 2\pi/T_S$, where H_S is the significant wave height, and T_S is the significant wave period (Monismith and Fong 2004).

IBM of "super (larval) particles" and model runs

Larval development stage, horizontal and vertical positions in the water column, and mortality were represented by an IBM of particles (groups of larvae, each particle represented a large number of individual larvae, following the method of Xue et al. 2008), and coupled with the physical model outputs. In the IBM, 10 particles were released daily at three depths at each 0.1° latitude along the coast between 22°S and 35°S. Equal numbers of particles were released in the model from 16 October of year (–1) to 15 March of year (0) to cover the full hatching season. The three designated release depths were 40, 60, and 80 m, except in the Big Bank area (27°S) north of the Abrolhos Islands, where they were released in about 100 m, instead of 80 m (Fig. 2*a*). Each particle in the model was developed through time according to the rate specified by the IBM, which takes into account the ambient temperature.

The use of uniform releases of particles by both latitude and spawning depth zones in the IBM was adopted to allow for further investigation of a number of biological factors potentially influencing settlements. This was achieved through postmodel analysis of a much smaller data set of only the successfully settled particles, which allowed rapid investigation of the impacts of a range of factors such as time of hatching, release depth, spawner abundance, etc. To simplify the modelling and reporting, a new "category" system was devised to represent groups of phyllosoma and puerulus stages that could be assigned similar biological characteristics – behaviour in the model. Category A, B, and C particles represent the early (stages I, II, and III), middle (IV, V, VI), and late (VII, VIII, IX) stages of phyllosoma, respectively. Natant (or swimming) puerulus were designated as D1 particles and the settled puerulus as D2. Category A was further separated into A1 (stage I, newly hatched phyllosoma) and A2 (stages II, III). Category C was separated into C1 (stages VII, VIII) and C2 (stage IX) where an extended period waiting for metamorphosis could occur in the model. The average durations for each particle category in the IBM were set to approximate field observations (Chittleborough and Thomas 1969; Phillips et al. 1979; Table 1).

Following the approach of Griffin et al. (2001), particles in the IBM spend 8 h in the surface layer at night, 8 h at depth during the day, and 8 h (4 h descending and 4 h ascending) in transitions (Table 1; Fig. 4). After hatching, the first category particles (A1) stay in the surface 20 m at all times. For all later categories, three vertical profiles of particle distributions in the upper 20 m are used when applying wave-induced Stokes drift movements: Distribution I assumes evenly distributed particles in the surface–20 m layer, while Distributions II and III have exponential vertical distributions by assuming particles have skewed distribution towards the sea surface (Table 1), as occurs during calm conditions at night. To simplify the IBM, the effects of sea state and lunar cycle on vertical distributions of phyllosoma have not been included in the model at this stage.

Table 1. Depth ranges of diurnal vertical migrations by larval stage and time of day.

	Category A			Category C	
	A1	A2	Category B	C1	C2
Duration (days)	30	60	60	120	<150
Daytime (0900–1700)	0–20 m	10–100 m[a]	30–100 m[b]	Below Leeuwin Current[c]	
Transition time (1700–2100 and 0500–0900)	0–20 m	0–100 m	0–100 m	Surface to below Leeuwin Current[d]	
Nighttime (2100–0500)	0–20 m	0–60 m[e]	0–40 m[f]	0–20 m	
Near surface profile[g]	I	I	II	III	

[a] 50% of the larvae are in 10–50 m and 50% in 50–100 m.

[b] 50% in 30–60 m and 50% in 60–100 m.

[c] Stationary.

[d] Use one third of 0–100 m BRAN velocity to transport particles.

[e] 50% in 0–20 m and 50% in 20–60 m.

[f] 50% in 0–10 m and 50% in 10–40 m.

[g] I: even distribution; II and III: exponential distributions with e-folding scales of 10 and 3 m, respectively.

To assess the effect of temperature on growth, the model has incorporated temperature-dependent growth for category A, B, and C1 particles as follows:

$$G_s = \frac{(T - T_0)}{P_s(T_1 - T_0)}$$

where T is the 0–30 m average BRAN temperature that particles experience, T_0 and T_1 are the nominal minimum and average temperatures, respectively, that the particles experience during each category of their life cycle, and P_s is the number of days that the particles spend during each category at the nominal temperatures (Table 2). On average particles are able to reach category C2 in 270 days; at a warmer average temperature of 23 °C it takes about 240 days and at 20 °C it takes about 315 days. There is no growth if the temperature is below 15 °C, and the growth rate does not increase further if the temperature is above 26 °C. Constant growth is assumed for category C2, and D1 has a maximum life of 21 days or until they reach shallow habitat of <40 m to become D2 and are assumed to have successfully settled. Metamorphosis of C2 particles to D1 was triggered by any C2 particle intersecting the 200 m depth contour. D1 particles are assumed to swim directly toward the coast (i.e., 26 degrees north of east) during each 8 h night at a speed of 15 cm·s^{-1}. Any D1 particles that have not crossed the 40 m depth contour during a 21-day period will perish. The maximum age of the particles is 420 days.

The advection scheme used in the IBM is fourth-order Runge–Kutta method, and the horizontal diffusivity, K_m, is assumed to be 1 m^2·s^{-1}, to add extra diffusivity in the IBM, which is usually underestimated in the offline particle tracking. The IBM uses a 1 h time step to calculate particle movement. The simulation of the western rock lobster puerulus settlement processes has been undertaken for nine settlement seasons, from 2000–2001 to 2008–2009, which represents a range of years of good and poor settlement. For each settlement season, the model simulation is carried out for the period of 16 October of year (–1) to 31 March of year (+1), which represents the approximate start of the egg release and the end of the puerulus settlement recorded in the field, respectively.

Table 2. Parameters used in the IBM growth equation.

Category	P_s (days)	T_1 (°C)	T_0 (°C)
A	90	21.5	10
B	60	22.4	10
C1	120	21.4	10

The model was run with all particles being of equal rank and experiencing limited mortality. Category A particles are allowed to survive on the shelf for up to 15 days, while instant mortality is applied to categories B and C1 when they come onto the shelf. Category A to C particles can survive in ambient temperatures <16 °C, but perish if they are there for more than 14 days. Particles perish if they stay in temperatures <15 °C for more than 7 days. Also if the particles move out of the model domain, 18°S–40°S, 101°E–129°E, they are assumed to have perished.

From the IBM outputs, an average of 1758 particles or about 0.3% were recorded as settling on the coast out of a total of 585 000 released each settlement season. A smaller number of particles, 19 on average, also settled on the south coast each season. Among the unreturned particles, about 442 500, or 75.6%, died at A1, as shelf currents were unable to move them offshore within the 15-day survival limit. The total mortality on the shelf–land for particles in all categories was about 90.8%, and 3.7% of the particles were also lost by drifting out of the model domain. A further 4.0% of particles did not reach a position to undergo metamorphosis to D1 within the 420-day survival limit, and about 1.4% of total released particles remained "alive" within the model domain at the end of the IBM simulation.

The IBM results on successful settlements (time, location) were stored and processed postmodel run by weighting (multiplying) hatching rates and natural mortality rate. The postmodel processing include (*i*) weighting the particles at the time of their release according to monthly hatching rates, (*ii*) applying an additional mortality term (to incorporate a background level of natural mortality) as a function of category A duration (between 60 and 120 days), with an e-folding time scale of 15 days, and (*iii*) latitudinal distribution of breeding stock (numbers hatching) as in Fig. 3*b*.

Fig. 5. Nine-year average monthly counts of different categories of particles from November near the start of the hatching season to March near the end of settlement season. (Note the D1 particle (puerulus equivalent) counts have been multiplied by 200 to enable the monthly pattern to be visible.)

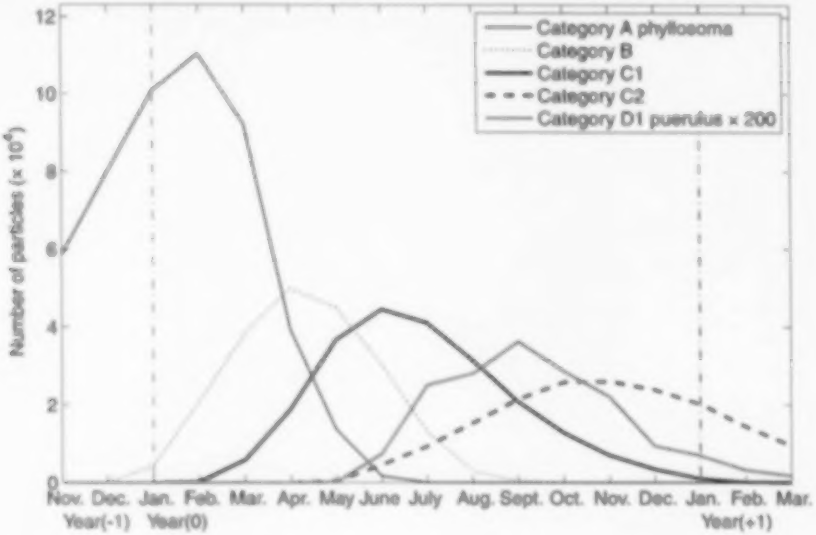

Assessment of IBM outputs

Seasonal and spatial distribution of IBM particle categories

Particle abundance of individual categories from the IBM (Fig. 5) compared well with monthly phyllosoma patterns observed during 1973–1977 (Phillips et al. 1979). Peak particle numbers for category A occurred in February (i.e., the end of the hatching season) in the model domain and had largely disappeared after May. The peak numbers of category B occurred in April, though large numbers were present between February and June. Very few of these middle stages were taken in field surveys; however, their field presence ceased at about the same time as category B particles in the model (i.e., they had largely disappeared by September). C1 particles peaked and became dominant in June–July, and C2 particles first started to appear in May–June and reach peak numbers in October–November. Small numbers of D1 particles started to appear in the model domain in June, and their peak occurrence was in September. The monthly occurrence of D1 particles was consistent with puerulus collector data, with most of the model settlement occurring before December (Fig. 3*a*). The average particle duration to settlement was 307 days, or about 10 months, which is consistent with the observed period from peak hatching (December) to the peak of puerulus settlement (September). The peak distribution of particle settlement occurs between 270 and 330 days, or 9–11 months, which is also consistent with the field data.

The spatial pattern of daily visits of successfully settled particles has the highest rate between the Abrolhos Islands and Fremantle (28°S–32°S; Figs. 6*a* and 6*b*). While most particles were located in the offshore regions, early D2 settlers near NWC (22°S), Shark Bay (26°S), Abrolhos, Jurien, and Fremantle were also indicated in the daily visit pattern. The total (successful and unsuccessful) particle distribution resembled the observed phyllosoma distribution in June–July period (Figs. 6*c* and 2*b*). It appears that particles west of 108°E or north of 24°S during June–July are less likely to return to coastal regions, despite the high concentrations of phyllosoma found in these areas during historic surveys (data from Phillips et al. 1979 superimposed on Fig. 2*b*).

Factors affecting IBM particle settlement

Time of hatching was found to influence settlement success. The IBM results, with equal daily particle releases (unweighted), suggest that settlement success rate was highest for particles released in October (half month) and declined through to March. The majority of successfully settled particles were released during the first half of the hatching season (i.e., from mid-October to December; Fig. 7*a*). The early-released particles experience a longer period in the warmer temperatures during the summer season, which enables them to "grow" faster and be at a stage able to metamorphose to puerulus, when the strongest onshore flows occur during the winter to early spring months. When the settled particle numbers are weighted with monthly hatching rates, the successful particles show a peak hatch time in December. More than three quarters of successful settlements were from November and December releases (Fig. 7*b*). This pattern was only slightly changed by the additional inclusion of the particle duration (mortality) weighting.

Release latitude in the IBM also affects success of particle settlement. The unweighted distribution of settling particles shows two major source areas, a northern area between 23°S and 25°S and a larger southern area between about 28°S and 34°S. Within the southern release area, two distinct peaks also occur around 28°S and 33°S (Fig. 8*a*). After weighting to take into account the observed monthly hatching pattern, there was little change in this pattern. However, when particle duration mortality was also taken into account, the success rate in the northern area is enhanced and a general decrease

Fig. 6. June–July (*a*) spatial distribution and (*b*) latitudinal visit rates (visits per day in every 0.5° grid) of successfully settled particles averaged over the nine model years; and (*c*) latitudinal visit rates for all particles (both settled and unsettled).

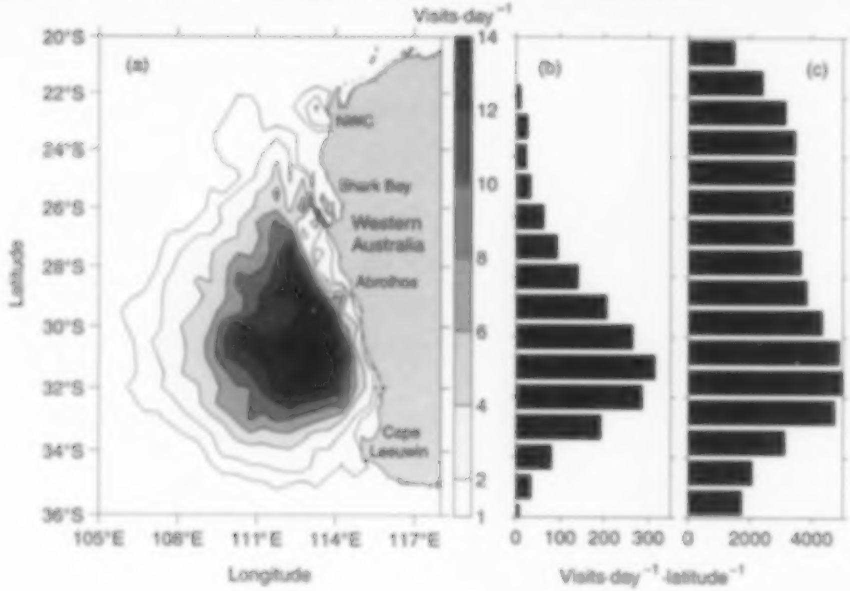

in settlement success from north to south becomes evident (Fig. 8*b*). The declining trend in success from north to south appears to result from the particles released in the north experiencing high temperatures and therefore having shorter overall pelagic larval duration. In comparison, particles released further south tend to experience colder temperatures, resulting in longer larval duration and therefore receive a higher natural mortality in the model.

To compare with observed spatial patterns of puerulus settlement (e.g., Fig. 3a), the IBM results are further scaled with the latitudinal distribution to the breeding stock as in Fig. 3*b*. Whereas nearly 60% of the breeding stock is located near the Abrolhos region (28°S–29°S), about three quarters of the successful settlements were originated from that region after considering all the weighting factors (Fig. 8*c*). Also, noticeably, the shelf regions north of 27°S and south of 32°S are no longer major sources of successful particle settlements. When scaled by the latitudinal breeding stock distribution, the successful rate for the December releases was also further enhanced (Fig. 7*c*).

Comparison of the successful settlement rates for particles released at different depths suggests that the success rates were much higher for the 60 and 80–100 m releases compared with those in 40 m, as particles released at inner shelf depth take longer to exit the shelf and are therefore subject to additional mortality in the model. The low likelihood of successful returns for particles released at Northwest Cape (22° S), near Shark Bay (26°S), and off Cape Leeuwin, 34°S (Fig. 8*b*) is due to particles being only released very close to the coast at these locations and therefore have a greater chance of hitting the coast (Fig. 2*a*).

The unweighted data showing the latitude of model puerulus settlements suggests that the mean latitude for successful settlement is at about 30.4°S, with the main settlement region centred between the Abrolhos Islands (28°S–29°S) in the north and Perth (32°S) region in the south (Fig. 9*a*). There are also three other regions where peaks occur (i.e., Coral Bay (23°S), South of Shark Bay (26°S), and near the Capes (34°S) region). This distribution bears some similarity to the spatial distribution derived from puerulus collectors, with the exception of the settlement south of 32°S that is consistently low (e.g., Fig. 3*a*). Weighting the model settlements with monthly hatching rate does not modify the settlement pattern, whereas adding the weighting factor of pelagic larval duration mortality causes the likelihood of successful settlement in the north to increase, while the successful settlement in the south is reduced (Fig. 9*b*). The overall settlement structure under this arrangement has more resemblance to the spatial distribution from puerulus collector observations, which may indicate the importance of environmental effects of growth–survival on the particle settlement. The scaling with the latitudinal breeding stock distribution gives more weight to the settlements between Abrolhos (28°S–29°S) and Perth (32°S) (Fig. 9*c*), but retains the over-representation of settlement in the southern Capes (34°S).

The daily pattern of settlement from the IBM suggests that particles begin settling in June and continue until March (not shown), as indicated in D1 distribution in Fig. 5. After applying the weighting and scaling factors, most of the particle settlement occurs from August to December, with a distinct peak occurring in September–October north of Abrolhos (28°S–30°S) and a broader peak spanning from September to almost December in the south (30°S–32°S) (Fig. 10). The difference in IBM settlement patterns between the north and south reflects the relative advantages of fast growth by phyllosoma that are released and therefore spend more time in the high ambient temperature in the offshore north region, as reflected in the puerulus collector observations (e.g., Fig. 3*a*).

Fig. 7. Release months for successfully settled IBM particles along the west coast of Western Australia (WA) averaged over the nine model years: (*a*) unweighted distribution, (*b*) weighted for monthly hatching rate and for natural mortality at category A, and (*c*) same as panel (*b*) but with additional scaling using the breeding stock distribution in Fig. 3*b*.

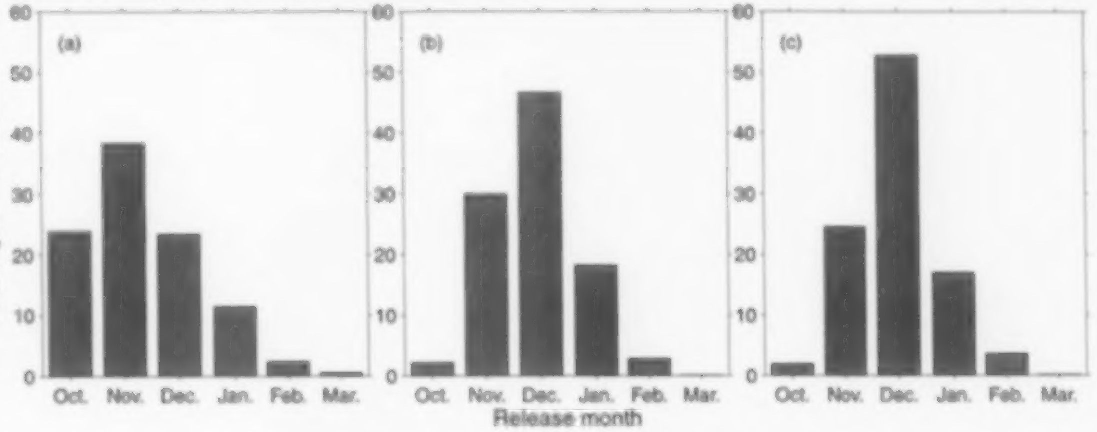

Fig. 8. Release latitudes (by half-degree grids) for successfully settled IBM particles along the west coast of Western Australia (WA) averaged over the nine model years: (*a*) unweighted distribution, (*b*) weighted for monthly hatching rate and natural mortality, and (*c*) same as panel (*b*) but with additional scaling using the breeding stock distribution in Fig. 3*b*.

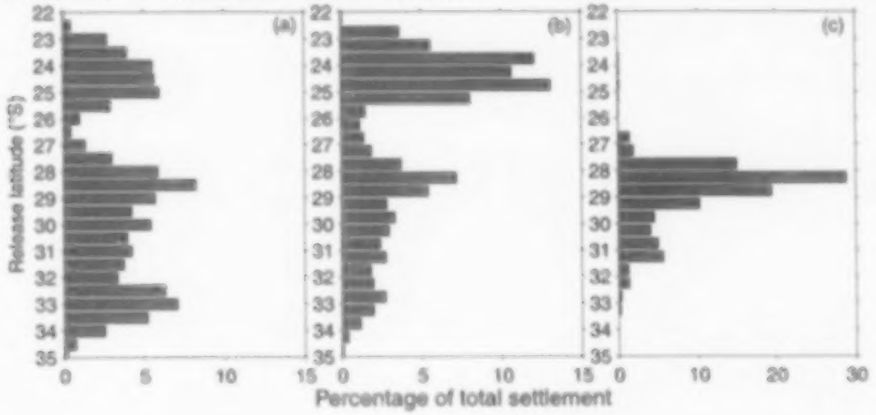

The postmodel analyses elucidate the dual role of ocean temperature on the particle settlements in our model. High temperature results in increased growth rate, such that the stage of particle development has advanced sufficiently to allow for successful later settlement if they are transported into coastal regions by the strong onshore ocean current during the austral winter. Faster growth with higher temperatures also reduces the particle duration, which lowers the natural mortality and which is applied to all particles from age 300 days onwards. These temperature effects enhance the success rate for more northern releases (i.e., into warmer waters) and cause relatively more particles to settle earlier in the settlement season.

Source–sink relationship of particle settlements

To assess the source (hatching) and sink (puerulus settlement) locations along the coastline, the successfully settled particles from uniform releases have been grouped according to their release and settlement latitudes. These source–sink data from the model, averaged over the 9 years have then been weighted with monthly hatching rates and natural mortality linked to category A duration to provide a preliminary view of the relative success of sources throughout the full latitudinal species range (Fig. 11*a*).

These data suggest that two areas of the coast have the potential to be major sources of successful settlement: a northern area between 23°30′S and 25°30′S (between NWC and northern Shark Bay), and a southern area between 27.5°S and 33°S. Within the southern area, the section of the middle of the west coast between 28°S and 29°S (including the offshore Abrolhos region) was the most important source region. Further, particles released from the northern source area were likely to supply successful settlements all along the coast (i.e., from NWC to Cape Leeuwin), with peaks in the Shark Bay and Geraldton–Abrolhos regions. Particles released off the middle of the west coast region were more likely to result in settlements in a broad area south of 28°30′ S, but with a peak on the coast around 29°S (i.e., in the area

Fig. 9. Settlement latitudes (by half-degree grids) for successfully settled IBM particles along the west coast of Western Australia (WA) averaged over the nine model years: (*a*) unweighted distribution, (*b*) same as panel (*a*) but weighted for monthly hatching rate and for natural mortality, and (*c*) same as panel (*b*) but with additional scaling using the breeding stock distribution in Fig. 3*b*.

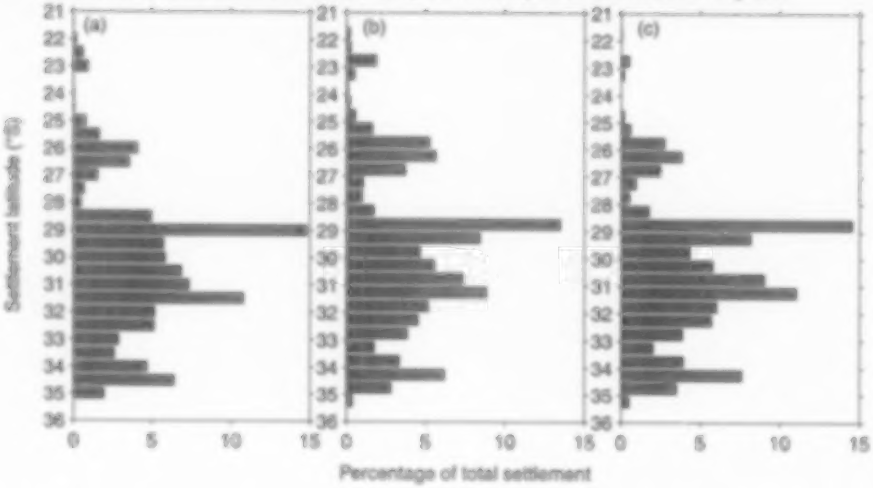

Fig. 10. Monthly IBM particle settlement rates along two latitude bands (solid line, 28°S–30°S; dashed line, 30°S–32°S) during the settlement season (May–March) after weighting with monthly hatching rate, natural mortality for category A, and the latitudinal distribution of breeding stock.

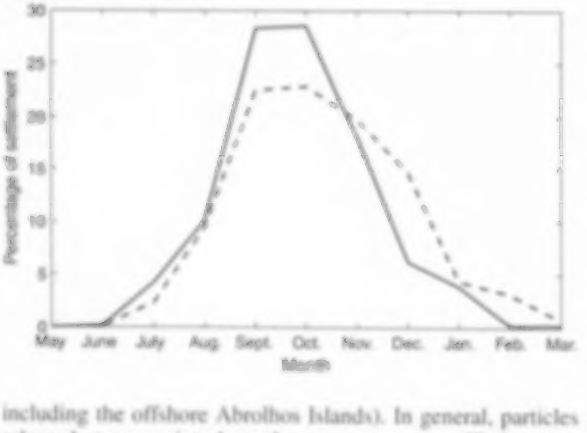

including the offshore Abrolhos Islands). In general, particles released at any point along the coast were more likely to return to the same region or further south than settle north of their release location. These IBM results showing that northern released particles are more likely to result in successful settlements are a reflection of the influence of the southward-flowing Leeuwin Current in the model.

To further assess the source–sink relationship for the stock, the sources of particle settlement were scaled to take into account the general latitudinal distribution of breeding stock (e.g., Fig. 3*b*). This weighting results in the southern source region between 27.5°S (Kalbarri) and 31.5°S (Lancelin) becoming the main and only section of the coastline to generate major particle settlement (Fig. 11*b*). That is, very low breeding stock abundance from Shark Bay north (25°S) to NWC (22°S), an area on the edge of the stock's geographic distribution, removes this area as a source of substantial model settlement. While all of the southern source sites are important within the general southern region, the release latitudes between 27.5°S and 29°S are shown to be the more important sources of particle settlement for all coast regions. This northern section of the southern source region includes the offshore Abrolhos Islands, which have relatively high breeding stock levels (Chubb 1991) and contain a major part of the breeding biomass. These areas, being close to the edge of shelf, are also more likely to be the source of successfully settling particles in the model.

Effects of Stokes drift

To assess the overall effect of the surface waves, a parallel IBM run has been carried out removing the wave-induced Stokes drift in the model. For this assessment we compare the winter particle distributions and settlement locations generated by the two simulations (i.e., with and without Stokes drift effects).

With Stokes drift, the latitudinal distributions of the category C particles in June–July are centred around 22°S–33°S (e.g., Fig. 6c), largely consistent with late Stage (VI to IX) phyllosoma spatial distributions (Rimmer and Phillips 1979). Without Stokes drift effect, the category C particles have a more southern distribution, skewed toward 30°S–32°S (not shown). The average latitudes of all category C particles during this period are 27.6°S and 28.6°S for the IBM simulations with and without Stokes drift, respectively, so that the net effect of Strokes drift is to shift the particle population by about a 100 km northward and retain the particle population off the west coast.

As a consequence of the northward shift of the category C particle distribution (due to Stokes drift), the mean latitude of settling particles (category D1) is at 29.7°S, more than 150 km northward compared with the simulation without Stokes drift (Figs. 12*a* and 12*b*). With the Stokes drift effect, the central region of the settlements is located between the Abrolhos and Fremantle regions, and the settlements in the southern Capes region are substantially reduced. The model

Fig. 11. Source and sink relations along the west coast of Western Australia (WA) in half-degree latitude boxes for successfully settling IBM particles averaged over the nine model years: (*a*) weighted by monthly hatching rate and category A particle duration, which affects the mortality rate, (*b*) same weighting as panel (*a*), but with additional weighting by the breeding stock distribution in Fig. 3*b*. (Both plots are scaled by their maximum values.)

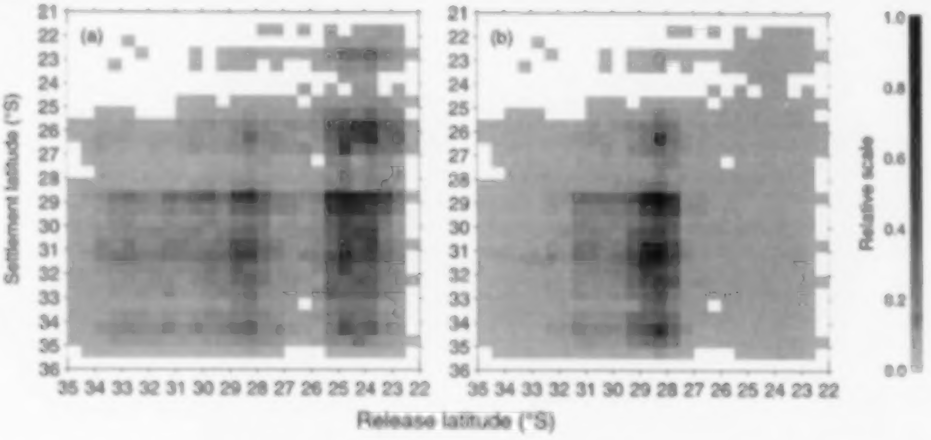

Fig. 12. Latitudinal distribution of successfully settled IBM particles along the west coast of Western Australia (WA) averaged over the nine model years: (*a*) with Stokes drift incorporated in the IBM and (*b*) without the Stokes drift effect, and their comparison with observed settlements that are binned onto the half-degree segments off the coast (*c*).

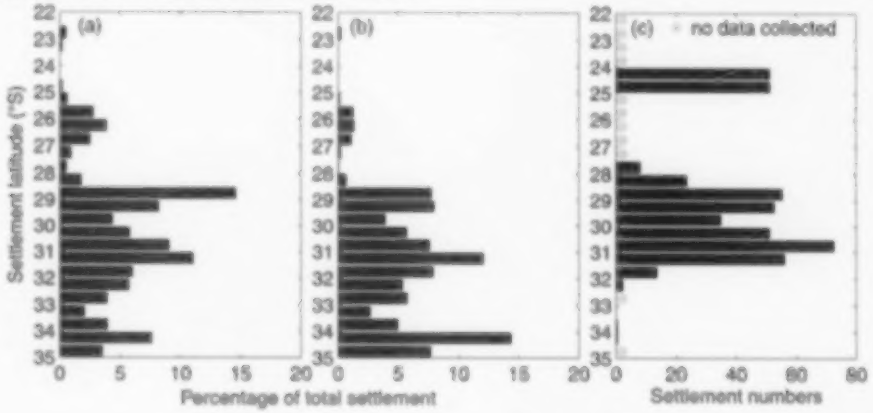

outputs are more consistent with the puerulus collector data (Fig. 12*c*) compared with the simulation without Stokes drift. Although the model fails to settle particles between 24°S and 25°S, (puerulus settlement in this area has only been recorded over a short period), the model with Stokes drift has relatively high settlement near Shark Bay. Overall, the model has overcome one of the important issues of settlement being too far south in the previous model (Griffin et al. 2001).

Another important effect of including the Stokes drift in the IBM is that the total number of surviving category C particles in June–July is about 60% higher without Stokes drift compared with with Stokes drift. This indicates that the onshore wave action during the summer hatching period of the particles (Fig. 1*c*) traps more newly hatched particles on the shelf and increases their overall mortality. On the other hand, there were similar total particle numbers settling in these two simulations (not shown), which indicates that including Stokes drift results in higher winter onshore wave action driving more particles toward the coast, and this compensates for the increased mortality at time of hatching. Thus, variations and changes in the wave climate in the Southern Ocean may affect their overall effects on particle settlement rate off the coast.

The modelled pattern of particle settlement along the coast (Fig. 12*a*) is generally consistent with the observed puerulus settlement distribution (Fig. 12*c*) and catches in the fishery. Additionally, it also shows a series of peaks, which are consistent both with and without the Stokes drift effect (Figs. 12*a* and 12*b*). These distinct peaks in IBM settlement suggest that the particles are not being randomly distributed along the coast, and oceanographic factors other than wave action are involved. One likely cause of these peaks or distinct bands in the particle settlement along the coast are the observed surface eastward jets in the southeast Indian Ocean (e.g., the Eastern Gyral Current (off NWC), the broad eastward flow in the south subtropical Indian Ocean (off Abrolhos–Perth), and the South Indian Countercurrent (off the Capes)). The other likely cause is the semipermanent meander structure in the Leeuwin Current (e.g., Fig. 2*b*). Both factors would have been incorporated in the IBM through the BRAN inputs. The potential impact of these factors will be investigated when the IBM is further developed to examine interannual variability in puerulus settlement.

Discussion

An improved IBM for investigating phyllosoma transport and puerulus settlement processes for western rock lobster stock has been developed. Innovations include the use of daily outputs from a hydrodynamic model to provide the three-dimensional wind- and density-driven horizontal velocity fields, corrected with additional surface Ekman flows and Stokes drift. As in the Griffin et al. (2001) model, advection alone did not produce a realistic distribution of particle settlement relative to puerulus collector catches along the coast. The Stokes drift effect due to surface waves was found to be a key factor in maintaining the latitudinal position of particle population, overcoming the problem in the previous model of too many particles being swept onto the south coast and out of the natural settlement zone. Similarly, the increased growth and subsequent increased survival of the phyllosoma associated with water temperature was an important component of the model, which resulted in a more realistic distribution of particle settlement along the coast.

The modelling indicates that early phyllosoma release (mid-October to December) is likely to result in a greater chance of survival for puerulus than late release (January to mid-March). These early-released particles experience a longer period of warmer temperatures during the summer, which enables them to grow faster and hence increase their survival to the settling stage. The potential positive effects of warmer water temperatures and early hatching on the model puerulus settlement are supported by the relationship between the annual level of puerulus settlement and average day of the year that settlement occurs (Caputi et al. 2001). That is, good settlement (e.g., 50% above average) in a year is associated with a peak in settlement about 1 month earlier compared with a low settlement year.

The outputs from the model in the 9 years simulated also suggest a declining trend in the likelihood of settlement success from releases north to south. This appears to result from the model particles released in the north tending to experience higher temperature and therefore have shorter overall durations compared with those released further south. After scaling for the latitudinal distribution of breeding stock, the model suggests that the coastline between Kalbarri and Fremantle is the major source area for the entire coast, and within this area the region from 27.5°S to 29.5°S, which includes the Abrolhos Islands, clearly becomes the most important source of particle settlement.

Further development

While the IBM model settlement outputs with the Stokes drift are now much closer to the patterns observed for the field, the model continues to settle more particles on the southern section of the west coast near Cape Leeuwin than occurs at the field collector sites. A number of aspects of larval behaviour in the IBM can be further improved to help replicate the interannual variation in puerulus settlement that is the main focus of the next stage of development of the IBM. The 8 h block distribution approach used to simplify the diurnal vertical migration may be underestimating the vertical extent of larval distribution during the daytime and could be improved by shorter time steps. The effects of sea state (wind and wave) and moonlight level on the diurnal movements and distribution of phyllosoma in the surface layers at night have also been shown to be important (Rimmer and Phillips 1979). Incorporation of sea state and moonlight levels in the model has the potential to move the phyllosoma depth distributions to slightly deeper levels at night but may also result in the daytime depth arc being moved downward during the bright moonlight periods. All of these additional phyllosoma behaviour-related factors have the capacity to alter particle movements in the IBM and potentially improve its ability to replicate interannual variability in settlement. Similarly, most of the natural mortality in the current IBM occurs through particles failing to move off the shelf after hatching and then again at the end of the cycle through failing to settle. Further development of this aspect of the IBM is necessary and could also help address the interannual variability issue.

The eastern Indian Ocean area, where the phyllosoma spend most of their development time (Phillips et al. 1979), has extremely low productivity, which suggests that phyllosoma growth may be food-limited, which is in turn likely to be linked to the success of metamorphosis to the nonfeeding puerulus stage (Phillips and McWilliam 2009) and successful settlement. The model currently uses interception with the 200 m depth isobath (shelf edge) as a proxy for food availability and the trigger for metamorphosis, but does not include any direct measures of ocean productivity–food. Field survey data (Tranter and Kerr 1969) has indicated that chlorophyll *a* peaked in the region in May–June, with zooplankton peaking 2–3 months later in August–September. Satellite monitoring data has confirmed this general seasonal pattern that chlorophyll levels are highest in winter months, suggesting that zooplankton will peak in spring, assuming the lag in zooplankton abundance by Tranter and Kerr (1969). Satellite data (Caputi et al. 2010*b*) has also indicated that chlorophyll levels are higher on the shelf at all times, but with considerable seasonal variability. The incorporation of both seasonal and interannual parameters for productivity based on satellite chlorophyll monitoring could substantially improve the model's response to environmental changes and potentially its ability to replicate interannual variability in puerulus settlement.

Acknowledgements

Funding support for the project from the Fisheries Research and Development Corporation, the Western Australian Department of Fisheries (DoF), and CSIRO Marine and Atmospheric Research is gratefully acknowledged. The authors also acknowledge the participants of the two workshops involved in the development of this project, particularly the contributions of the reviewers, Bruce Phillips and David Griffin. Also acknowledged are the major contributions to the project from the Bluelink (BRAN) model developers in CSIRO and Australian Bureau of Meteorology, the satellite data providers (e.g., NASA), WW3 model, Western Australian Marine Science Institution, and CSIRO Wealth from Oceans National Research Flagship. Finally, the authors also thank the internal reviewers at CSIRO and the Western Australian Fisheries and Marine Research Laboratories (DoF), Rick Fletcher and Mervi Kangas, and three anonymous reviewers. We thank Huijie Xue and Alejandro Sanchez for sharing some of their programming codes.

References

Braine, S.J., Rimmer, D.W., and Phillips, B.F. 1979. An illustrated key and notes on the phyllosoma stages of western rock lobster *Panulirus cygnus* George. CSIRO Division of Fisheries and Oceanography, Rep. 102.

Brassington, G.B., Pugh, T., Spillman, C., Schulz, E., Beggs, H., Schiller, A., and Oke, P.R. 2007. BLUElink: Development of operational oceanography and servicing in Australia. J. Res. Pract. Inf. Tech. **39**(2): 151–164.

Caputi, N., Brown, R.S., and Chubb, C.F. 1995. Regional prediction of the western rock lobster, *Panulirus cygnus*, catch in Western Australia. Crustaceana, **68**(2): 245–256. doi:10.1163/156854095X00142.

Caputi, N., Chubb, C., and Pearce, A. 2001. Environmental effects on the recruitment of the western rock lobster, *Panulirus cygnus*. Mar. Freshw. Res. **52**(8): 1167–1174. doi:10.1071/MF01180.

Caputi, N., Melville-Smith, R., de Lestang, S., Pearce, A., and Feng, M. 2010*a*. The effect of climate change on the western rock lobster (*Panulirus cygnus*) fishery of Western Australia. Can. J. Fish. Aquat. Sci. **67**(1): 85–96. doi:10.1139/F09-167.

Caputi, N., Feng, M., Penn, J.W., Slawinski, D., de Lestang, S., Weller, E., and Pearce, A. 2010*b*. Evaluating source–sink relationships of the western rock lobster fishery using oceanographic modelling (FRDC Project 2008/087). Fisheries Research Report, Department of Fisheries, Western Australia.

Chittleborough, R.G. 1976. Breeding of *Panulirus longipes cygnus* George under natural and controlled conditions. Aust. J. Mar. Freshw. Res. **27**(3): 499–516. doi:10.1071/MF9760499.

Chittleborough, R.G., and Thomas, L.R. 1969. Larval ecology of the Western Australian marine crayfish, with notes upon other panulirid larvae from the eastern Indian Ocean. Aust. J. Mar. Freshw. Res. **20**(3): 199–223. doi:10.1071/MF9690199.

Chubb, C.F. 1991. Measurement of spawning stock levels for the western rock lobster *Panulirus cygnus*. Rev. Invest. Mar. **12**: 223–233.

Chubb, C.F., Barker, E.H., and Dibden, C.J. 1994. The Big Bank region of the limited entry fishery for the western rock lobster, *Panulirus cygnus*. Issue 101, Fisheries Research Report, Department of Fisheries, Western Australia.

Cowen, R.K., Paris, C.B., and Srinivasan, A. 2006. Scaling of connectivity in marine populations. Science (Washington, D.C.), **311**(5760): 522–527. doi:10.1126/science.1122039. PMID: 16357224.

Cresswell, G.R., Boland, F.M., Peterson, J.L., and Wells, G.S. 1989. Continental shelf currents near the Abrolhos Islands, Western Australia. Aust. J. Mar. Freshw. Res. **40**(2): 113–128. doi:10.1071/MF9890113.

de Lestang, S., Caputi, N., and Melville-Smith, R. 2009*a*. Using fine-scale catch predictions to examine spatial variation in growth and catchability of *Panulirus cygnus* along the west coast of Australia. N.Z. J. Mar. Freshw. Res. **43**(1): 443–455. doi:10.1080/00288330909510013.

de Lestang, S., Thomson, A., and Rossbach, M. 2009*b*. West coast rock lobster fishery status report. *In* State of the fisheries report 2008/09. *Edited by* W.J. Fletcher and K. Santoro. Department of Fisheries, Western Australia. pp. 18–28.

Feng, M., Meyers, G., Pearce, A., and Wijffels, S. 2003. Annual and interannual variations of the Leeuwin Current at 32°S. J. Geophys. Res. **108**(C11): 3355. doi:10.1029/2002JC001763 .

Feng, M., Wijffels, S., Godfrey, S., and Meyers, G. 2005. Do eddies play a role in the momentum balance of the Leeuwin Current? J. Phys. Oceanogr. **35**(6): 964–975. doi:10.1175/JPO2730.1.

Feng, M., Majewski, L., Fandry, C., and Waite, A. 2007. Characteristics of two counter-rotating eddies in the Leeuwin Current system off the Western Australian coast. Deep Sea Res. Part II Top. Stud. Oceanogr. **54**(8–10): 961–980. doi:10.1016/j.dsr2.2006.11.022.

Feng, M., Biastoch, A., Boning, C., Caputi, N., and Meyers, G. 2008. Seasonal and interannual variations of upper ocean heat balance off the west coast of Australia. J. Geophys. Res. **113**(C12): C12025. doi:10.1029/2008JC004908.

Feng, M., Waite, A.M., and Thompson, P.A. 2009. Climate variability and ocean productivity in the Leeuwin Current system off the west coast of Western Australia. J. R. Soc. West. Aust. **92**: 67–81.

Feng, M., Slawinski, D., Beckley, L., and Keesing, J. 2010. Retention and dispersal of shelf waters influenced by interactions of ocean boundary current and coastal geography. Mar. Freshw. Res. **61**(11): 1259–1267. doi:10.1071/MF09275.

Griffin, D.A., Wilkin, J.L., Chubb, C.F., Pearce, A.F., and Caputi, N. 2001. Ocean currents and the larval phase of Australian western rock lobster, *Panulirus cygnus*. Mar. Freshw. Res. **52**(8): 1187–1199. doi:10.1071/MF01181.

Incze, L., Xue, H., Wolff, N., Xu, D., Wilson, C., Steneck, R., Wahle, R., Lawton, P., Pettigrew, N., and Chen, Y. 2010. Connectivity of lobster (*Homarus americanus*) populations in the coastal Gulf of Maine. Part II. Coupled biophysical dynamics. Fish. Oceanogr. **19**(1): 1–20. doi:10.1111/j.1365-2419.2009.00522.x.

Jenkins, A. 1987. Wind and wave induced currents in a rotating sea with depth-varying eddy viscosity. J. Phys. Oceanogr. **17**(7): 938–951. doi:10.1175/1520-0485(1987)017<0938:WAWICI>2.0.CO;2.

Jernakoff, P. 1990. Distribution of newly settled western rock lobsters *Panulirus cygnus*. Mar. Ecol. Prog. Ser. **66**: 63–74. doi:10.3354/meps066063.

Koslow, J.A., Pesant, S., Feng, M., Pearce, A., Fearns, P., Moore, T., Matear, R., and Waite, A. 2008. The effect of the Leeuwin Current on phytoplankton biomass and production off Southwestern Australia. J. Geophys. Res. **113**(C7): C07050. doi:10.1029/2007JC004102.

Lemmens, J.W. 1994. The Western rock lobster *P. cygnus*: feeding biology and energetics of the puerulus stage. Ph.D. thesis, The University of Western Australia, Perth, Australia.

Liddy, G.C., Phillips, B.F., and Maguire, G.B. 2004. Effects of temperature and food density on the survival and growth of early stage phyllosoma of the western rock lobster, *Panulirus cygnus*. Aquaculture, **242**(1–4): 207–215. doi:10.1016/j.aquaculture.2004.05.034.

Marinovic, B., Lemmens, J.W.T.J., and Knott, B. 1994. Larval development of *Ibacus peronii* Leach (Decapoda: Scyllaridae) under laboratory conditions. J. Crustac. Biol. **14**(1): 80–96. doi:10.2307/1549057.

Melville-Smith, R., de Lestang, S., and Thomson, A. 2009. Spatial and temporal changes in egg production in the western rock lobster (*Panulirus cygnus*) fishery. N.Z. J. Mar. Freshw. Res. **43**(1): 151–161. doi:10.1080/00288330909509989.

Meyers, G. 1996. Variation of Indonesian throughflow and the El Niño Southern Oscillation. J. Geophys. Res. **101**(C5): 12255–12263. doi:10.1029/95JC03729.

Monismith, S.G., and Fong, D.A. 2004. A note on the potential transport of scalars and organisms by surface waves. Limnol. Oceanogr. **49**(4): 1214–1217. doi:10.4319/lo.2004.49.4.1214.

Oke, P.R., Brassington, G.B., Griffin, D.A., and Schiller, A. 2008. The Bluelink ocean data assimilation system (BODAS). Ocean Model. **21**(1–2): 46–70. doi:10.1016/j.ocemod.2007.11.002.

Paris, C.B., Chérubin, L.M., and Cowen, R.K. 2007. Surfing, spinning, or diving from reef to reef: effects on population connectivity? Mar. Ecol. Prog. Ser. **347**: 285–300. doi:10.3354/meps06985.

Phillips, B.F., and McWilliam, P.S. 2009. Spiny lobster development: where does successful metamorphosis to the puerulus occur? A review. Rev. Fish Biol. Fish. **19**(2): 193–215. doi:10.1007/s11160-008-9099-5.

Phillips, B.F., and Olsen, L. 1975. Swimming behaviour of puerulus larvae of western rock lobster. Aust. J. Mar. Freshw. Res. **26**(3): 415–417. doi:10.1071/MF9750415.

Phillips, B.F., and Pearce, A.F. 1997. Spiny lobster recruitment off Western Australia. Bull. Mar. Sci. **61**: 21–41.

Phillips, B., Rimmer, D., and Reid, D. 1978. Ecological investigations of the late-stage phyllosoma and puerulus larvae of the western rock lobster *Panulirus longipes cygnus*. Mar. Biol. **45**(4): 347–357. doi:10.1007/BF00391821.

Phillips, B.F., Brown, P.A., Rimmer, D.W., and Reid, D.D. 1979. Distribution and dispersal of phyllosoma larvae of the western rock lobster, *Panulirus cygnus*, in the south-eastern Indian Ocean. Aust. J. Mar. Freshw. Res. **30**: 773–783. doi:10.1071/MF9790773.

Rimmer, D.W. 1980. Spatial and temporal distribution of early-stage phyllosoma of western rock lobster, *Panulirus cygnus*. Aust. J. Mar. Freshw. Res. **31**(4): 485–497. doi:10.1071/MF9800485.

Rimmer, D.W., and Phillips, B.F. 1979. Diurnal migration and vertical distribution of phyllosoma larvae of the western rock lobster *Panulirus cygnus*. Mar. Biol. **54**(2): 109–124. doi:10.1007/BF00386590.

Ritz, D. 1972. Behavioural response to light of the newly hatched phyllosoma larvae of *Panulirus longipes cygnus*. J. Exp. Mar. Biol. Ecol. **10**(2): 105–114. doi:10.1016/0022-0981(72)90096-2.

Schiller, A., Oke, P.R., Brassington, G., Entel, M., Fiedler, R., Griffin, D.A., and Mansbridge, J.V. 2008. Eddy-resolving ocean circulation in the Asian–Australian region inferred from an ocean reanalysis effort. Prog. Oceanogr. **76**(3): 334–365. doi:10.1016/j.pocean.2008.01.003.

Smith, R.L., Huyer, A., Godfrey, J.S., and Church, J. 1991. The Leeuwin Current off Western Australia, 1986–1987. J. Phys. Oceanogr. **21**(2): 323–345. doi:10.1175/1520-0485(1991)021<0323:TLCOWA>2.0.CO;2.

Thompson, R.O.R.Y. 1984. Observations of the Leeuwin Current off Western Australia. J. Phys. Oceanogr. **14**(3): 623–628. doi:10.1175/1520-0485(1984)014<0623:OOTLCO>2.0.CO;2.

Tolman, H.L. 2002. User manual and system documentation of WAVEWATCH III version 2.22. NOAA/NWS/NCEP/MMAB Tech. Note 222.

Tranter, D.J., and Kerr, J.D. 1969. Seasonal variations in the Indian Ocean along 110°E. V. Zooplankton biomass. Aust. J. Mar. Freshw. Res. **20**(1): 77–84. doi:10.1071/MF9690077.

Xue, H., Incze, L.S., Xu, D., Wolff, N., and Pettigrew, N.R. 2008. Connectivity of lobster populations in the coastal Gulf of Maine: Part I: Circulation and larval transport potential. Ecol. Model. **210**(1–2): 193–211. doi:10.1016/j.ecolmodel.2007.07.024.

Home range of European lobster (*Homarus gammarus*) in a marine reserve: implications for future reserve design

Even Moland, Esben Moland Olsen, Kristian Andvord, Jan Atle Knutsen, and Nils Chr. Stenseth

Abstract: Marine reserves are perceived as a critical component in successful rebuilding of overharvested marine populations. Such efforts can be particularly successful in species with limited movement rates. However, long-term data on movement is sparse for most marine species. Here, we investigated space use in European lobster (*Homarus gammarus*) by ultrasonic tracking in a reserve on the Norwegian Skagerrak coast from September 2006 to August 2007. Over the period, 95% of tagged lobsters remained either within the reserve or near reserve boundaries. Home range estimates based on a kernel density estimator of the 95% utilization distribution ranged from 5728 to 41 548 m^2 (mean 19 879 ± 2152 m^2 standard error), representing 0.57%–4.15% of the reserve area (1 km^2), with no significant difference among males, non-ovigerous females, and ovigerous females for an overlapping observation period of 242 days. Logistic regression predicted average time to reach 50% and 95% of minimum convex polygon home range area at 98 and 259 days, respectively. These results show that European lobsters can be resident with limited home ranges. Small coastal reserves can be designed to afford complete or partial protection by letting boundaries engulf or intersect patches of habitat preferred by this species.

Résumé : Les réserves marines sont perçues comme une composante essentielle pour la reconstruction des populations marines surexploitées. De telles initiatives peuvent avoir du succès particulièrement chez les espèces à taux de déplacement limité. Il n'existe cependant que peu de données sur les déplacements à long terme chez la plupart des espèces marines. Nous étudions l'utilisation de l'espace chez des homards européens (*Homarus gammarus*) suivis par ultrasons dans une réserve sur la côte de Skagerrak en Norvège de septembre 2006 à août 2007. Durant cette période, 90 % des homards marqués sont demeurés ou bien à l'intérieur de la réserve ou près de ses frontières. Les estimations des aires vitales basées sur un estimateur du noyau de densité de 95 % de la distribution de l'utilisation varient de 5728 à 41 548 m^2 (moyenne de 19 879 ± 2152 m^2 erreur standard), ce qui représente 0,57–4,15 % de la surface de la réserve (1 km^2), sans différence significative entre les mâles et les femelles, ni entre les femelles non ovigères et les femelles ovigères sur une période d'observation superposée de 242 jours. Une régression logistique prédit que le temps moyen nécessaire pour atteindre 50 % et 95 % de la surface du polygone convexe minimal de l'aire vitale est respectivement de 98 et 259 jours. Ces résultats montrent que les homards européens peuvent résider dans une aire vitale restreinte. On peut donc aménager de petites réserves côtières pour fournir une protection totale ou partielle en s'assurant que leurs frontières contiennent ou recoupent des taches de l'habitat préféré de cette espèce.

[Traduit par la Rédaction]

Introduction

Marine reserve effects commonly include increased density, biomass, and average size of target species within boundaries (e.g., Halpern 2003; Claudet et al. 2008; Lester et al. 2009), and studies that document supplement to fished stocks in surrounding areas (i.e., spillover) are few but accumulating (e.g., Abesamis and Russ 2005; Goñi et al. 2006; Stobart et al. 2009). Fisheries typically remove large and old individuals, leading to "longevity overfishing" (Berkeley et al. 2004; Beamish et al. 2006). Importantly, as marine reserves counteract the effects of longevity overfishing (i.e., restore and maintain broad size structure and age structure in harvested species), they simultaneously protect against strong fisheries-

Received 1 November 2010. Accepted 24 March 2011. Published at www.nrcresearchpress.com/cjfas on 5 July 2011.
J22096

Paper handled by Associate Editor Bernard Sainte-Marie.

E. Moland. Institute of Marine Research, Flødevigen, N-4817 His, Norway.
E.M. Olsen. Institute of Marine Research, Flødevigen, N-4817 His, Norway; Centre for Ecological and Evolutionary Synthesis (CEES), Department of Biology, University of Oslo, P.O. Box 1066 Blindern, N-0316 Oslo, Norway.
K. Andvord. Ministry of Fisheries and Coastal Affairs, P.O. Box 8118 Dep, N-0032 Oslo, Norway.
J.A. Knutsen. Department of Environment, County Governor of Aust-Agder, P.O. Box 788 Stoa, N-4809 Arendal, Norway.
N.C. Stenseth. Centre for Ecological and Evolutionary Synthesis (CEES), Department of Biology, University of Oslo, P.O. Box 1066 Blindern, N-0316 Oslo, Norway.

Corresponding author: Even Moland (e-mail: even.moland@graduates.jcu.edu.au).

Can. J. Fish. Aquat. Sci. **68**: 1197–1210 (2011) doi:10.1139/F2011-053 Published by NRC Research Press

based selection for earlier maturation (Baskett et al. 2005). Because of this, marine reserves are now perceived as an integral part of ecosystem-based fisheries management and a critical component of successful rebuilding efforts (e.g., Lubchenco et al. 2003; Francis et al. 2007; Worm et al. 2009).

Recent studies have demonstrated reserve effects in a range of coastal species from spiny lobsters to large predatory fishes (e.g., Roberts et al. 2001; Russ et al. 2008; Barrett et al. 2009). Species that are expected to demonstrate the strongest response to protection are those that are subject to high levels of fishing mortality and have low rates of movement relative to the size of the refuge (Kelly and MacDiarmid 2003). Thus, knowledge regarding target species movement patterns is central in determining the population response to marine reserves (e.g., DeMartini 1993; Attwood and Bennett 1995; Guénette and Pitcher 1999). A recognized challenge to predicting the success of marine reserves as a fisheries management tool is the lack of data on target species' spatiotemporal distribution (Sale et al. 2005). Moreover, knowledge regarding home range, activity patterns, habitat preference, and the nature and magnitude of movements between fished and unfished areas is central for successful reserve design (Kramer and Chapman 1999; Lowe et al. 2003; Moffitt et al. 2009).

Home ranges link the movement of animals to the distribution of resources necessary for survival and reproduction (Börger et al. 2008). Home ranges are dynamic properties influenced by individual characteristics, such as ontogeny, sex, and reproductive state (Bradbury et al. 1995; Kramer and Chapman 1999; Boydston et al. 2003), and also by food availability and abiotic conditions (Reese 1989; Clark and Green 1990; Nemtzov 1997). Home ranges have been estimated for a range of fish species in both tropical (e.g., Zeller 1997; Heupel et al. 2004; Jones 2005) and temperate waters (e.g., Lowe et al. 2003; Topping et al. 2005; Espeland et al. 2007). In the past, limited attention has been devoted to studies specifically addressing home range behaviour in commercially exploited decapods (but see Chittleborough 1974; Herrnkind 1980). However, recent studies that examined movement patterns of American lobsters (*Homarus americanus*) documented both resident and transient behaviours in coastal populations (e.g., Bowlby et al. 2007; Geraldi et al. 2009). Relatively recent developments in ultrasonic tracking technology have also generated novel insights in the home range behaviour of lobster species (e.g., Bertelsen and Hornbeck 2009; Scopel et al. 2009).

European lobsters (*Homarus gammarus*) are large decapod crustaceans of ecological and commercial importance, distributed from the north of Norway to Morocco in North Africa (Triantafyllidis et al. 2005). Historically, the Skagerrak region supported a viable population of the species, but over the last 30–40 years catches have plummeted (Agnalt et al. 2007). Currently, the stock figures in the Norwegian Red List as "near threatened" according to the IUCN (International Union for Conservation of Nature) criteria (Oug et al. 2010). The downward trend in catches is mirrored in standardized self-sampling catch-per-unit-effort data collected in Skagerrak since 1928, suggesting that the lobster population is presently at a historical low level (Pettersen et al. 2009).

In September 2006, four experimental lobster reserves (size 0.5–1 km^2) were established along the Norwegian Skagerrak coast to generate knowledge regarding population dynamics, behaviour, and the development of local lobster populations in areas unaffected by extractive fishing. The reserves were established based on consultations with local fishers, and policing of the lobster reserves are performed by the Coast Guard, by local police, and by local fishers operating near the respective areas (Pettersen et al. 2009).

The European lobster is considered a nocturnal animal (Mehrtens et al. 2005; Childress and Jury 2006). Light hours are generally spent solitary inside shelters on rocky bottoms, and activity increases at sunset and continues during dark hours (Smith et al. 1998, 1999). The benefit of the diel activity pattern is probably reduced predation risk from visual predators at night, but increased prey availability at night could also make foraging during dark hours more energetically effective and further promote nocturnal activity (Smith et al. 1999). Traditional mark–recapture studies suggest that European lobsters rarely move more than a few kilometres, for periods up to years (e.g., Dannevig 1936; Smith et al. 2001; Agnalt et al. 2007). Aside from providing coarse-scale information on movement, mark–recapture studies can yield important insights in population parameters such as growth rates, recruitment, and natural and fishing mortality (see e.g., Dunnington et al. 2005). However, space use and residency at higher spatiotemporal resolutions is still poorly investigated in European lobster (but see van der Meeren 1997; Smith et al. 1998).

Here, we have taken advantage of ultrasonic tracking technology in a recently established lobster reserve in coastal Skagerrak to assess long-term site fidelity in European lobster in their natural habitat, undisturbed by fishing gears. The focal objective of the present study was to assess whether the habitat included within reserve boundaries matched areas of consistent use by lobsters throughout four seasons.

Materials and methods

The study was conducted in the Flødevigen lobster reserve (58°25′N, 8°45′E) on the Norwegian southeastern Skagerrak coast (Fig. 1) from September 2006 to August 2007. This reserve is 1 km^2 in size and located in the waters outside the Norwegian Institute of Marine Research, Flødevigen marine research station. The reserve includes the entire Flødevigen bay and extends southeastward, including several small islets and one larger island, Ærøya. The bathymetry in the reserve is shaped by glacial scouring, with a main gully gaining depth as it cuts from northwest to southeast, emptying into the deeper basin north of Ærøya. Depths increase gradually and range from 0 to <50 m. The greatest depths are found on the reserve boundary perpendicular to the steep slope on the exposed side of the Ærøya Island (Fig. 1). The upper 1–5 m of substrate within the Flødevigen reserve are mostly rocky habitat dominated by macro-algae. Photosynthetic communities become gradually sparser down to 10 m and are more or less absent at greater depths, except for the exposed southeastern side of Ærøya Island, which contains a lush kelp forest that extends down to 10–12 m. SCUBA surveys performed prior to reserve establishment also revealed a topography consisting of rock faces and ledges with rocks or boulder fields of varying size at the base. In deeper basins and flat areas, the bottom consists of soft sediments. The

Fig. 1. Study area: the Flødevigen lobster reserve (*a*) on the Norwegian Skagerrak coast (*b*); Swe: Sweden. Insert in panel (*b*): the Scandinavian Peninsula (Norway and Sweden), Denmark, and the location of the Skagerrak Sea. Isobaths shown are the 5, 10, 20, 30, and 40 m depth contours. Black rectangle in panel (*a*) is the location of Institute of Marine Research Flødevigen Marine Research Station.

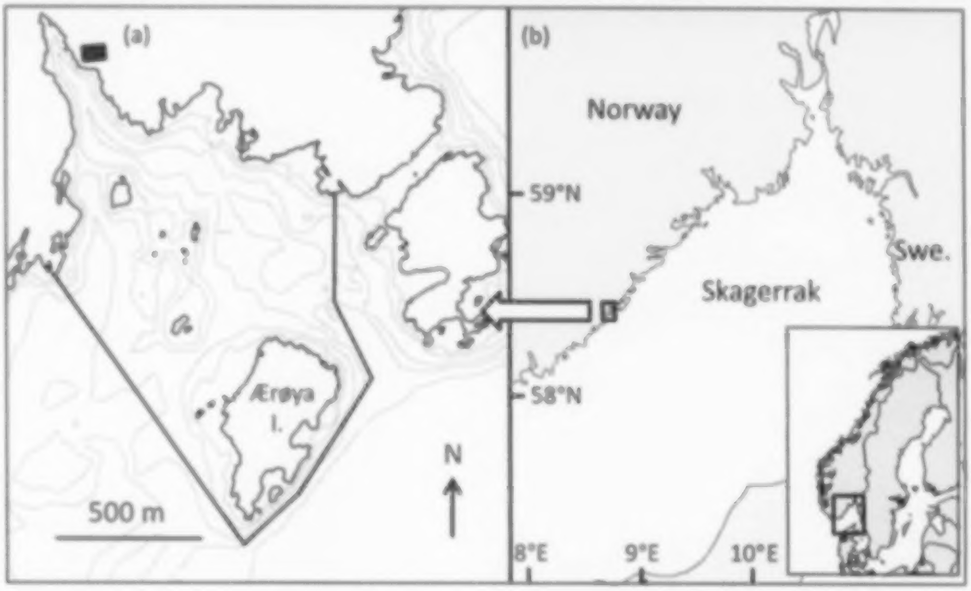

area harbours typical lobster habitats representative of coastal Skagerrak, which was one of the selection criteria used when the experimental reserves were established (Pettersen et al. 2009). In the reserve, fishing for *H. gammarus* is prohibited by exclusion of all types of standing gears (nets, pots, traps). Conducting the study in this area thus allowed space use and residency of lobsters to be studied without potential removal of individuals by fishing and without behaviours influenced by baited traps.

A total of 20 individual *H. gammarus* were tagged between 5 September and 17 October 2006 (Table 1). Lobsters were caught with mackerel-baited parlour pots deployed at depths between 10 and 30 m and soaked overnight. Captured lobsters were sexed and measured (carapace length). Carapace length (CL, mm) was measured from the rear of the eye socket to the posterior margin of the carapace to the nearest millimetre using vernier callipers, and sex was determined by examination of the first pair of pleopods. The 20 lobsters used in this study consisted of eight males, four nonovigerous females, and seven ovigerous females (Table 1). We selected individuals from different areas and depths throughout the reserve. Except for ovigerous females, we made efforts to select recently moulted individuals based on the visual appearance of exoskeletons (i.e., we chose individuals with a "fresh" appearance, free from any kind of biofouling). Visual inspection confirmed that eggs in all ovigerous females were in "stage I" according to Pandian (1970) and thus expected to hatch during spring–summer in the following year (2007). Thus, the ovigerous females selected would not moult until the following year, subsequent to the hatching of eggs. The capture position for each lobster was recorded with a handheld global positioning system (GPS) receiver. Immediately after capture, lobsters were brought back to the laboratory on shore and equipped with V13 high power coded acoustic transmitters (diameter 13 mm, length 36 mm, mass in seawater <6 g, Vemco Division, Amirix Systems Inc., Halifax, Canada) emitting on 69 kHz. Tags were set to transmit at a randomized interval between 40 and 120 s and had an expected battery life of 320 days. A tag harness was constructed by inserting the tag into a piece of soft plastic tubing (2 cm long). This was attached with a cable tie threaded through two holes punched in the piece of tubing, between the most robust denticles on the middle segment (carpus) of the crusher claw limb (Fig. 2). Tags were attached with the transmitting end of the tag pointing towards the posterior to minimize the probability for damage to the tag through wear during digging behaviour and entering–exiting of shelters. The actual tag-attachment procedure did not exceed 5 min. After tagging, lobsters were brought back to the reserve and gently released from the surface at their respective recorded capture positions. The attached tags did not appear to influence behaviour or manoeuvrability of lobsters as evidenced by observations in the laboratory prior to the field study (see also; Cowan et al. 2007). Note that tags would eventually be lost after moulting. As part of a mark–recapture survey conducted annually in the lobster reserves by the Norwegian Institute of Marine Research, all lobsters caught during the sampling received a T-bar anchor tag (TBA1, 30 mm × 2 mm, Hallprint Pty. Ltd, Holden Hill, South Australia) with printed information about the ongoing project. The T-bar anchor tag was inserted in the ventral musculature between the cephalotorax and first abdominal segment, to the right side of the midline using a standard tag applicator. Placing the tag in this area ensures its retention through the moulting process (Agnalt et al. 2007).

Tracking was conducted from a motor craft with a handheld directional hydrophone (model VH 110, Vemco) coupled

Table 1. Summary details of 20 *Homarus gammarus* equipped with V13 tags.

Lobster No.	Body size (mm CL)	Sex and state	Date released	Days monitored	Position fixes	Net movement (m)
1	91	O-F	5 Sept. 2006	281	53	61
2	104	M	5 Sept. 2006	281	53	379
3	89	M	5 Sept. 2006	274	53	96
4	88	O-F	5 Sept. 2006	354	71	233
5	92	O-F	5 Sept. 2006	354	68	58
6	108	F	5 Sept. 2006	281	52	34
7*	90	O-F	5 Sept. 2006	—	—	—
8	103	F	12 Oct. 2006	319	65	64
9	105	F	12 Oct. 2006	318	62	105
10	74	M	12 Oct. 2006	246	48	164
11	90	M	12 Oct. 2006	246	47	59
12	102	O-F	12 Oct. 2006	319	62	8
13	91	F	12 Oct. 2006	318	63	22
14	87	O-F	12 Oct. 2006	317	62	318
15	117	O-F	13 Oct. 2006	305	61	20
16	93	M	13 Oct. 2006	246	47	210
17	97	M	13 Oct. 2006	242	51	209
18	91	M	13 Oct. 2006	318	64	29
19	104	O-F	17 Oct. 2006	316	35	98
20	88	M	17 Oct. 2006	315	61	87

Note: CL, carapace length; M, male; F, female; O-F, ovigerous female.

*Lobster No. 7 was not heard after its release and thus not included in the data analyses.

Fig. 2. A Vemco V13 acoustic transmitter and harness attached to the middle segment (carpus) of the left cheliped in a European lobster (*Homarus gammarus*). Note the placement of the cable tie between two denticles, which prevents the harness from sliding towards the carpus' tapered end. (Photo by E. Moland.)

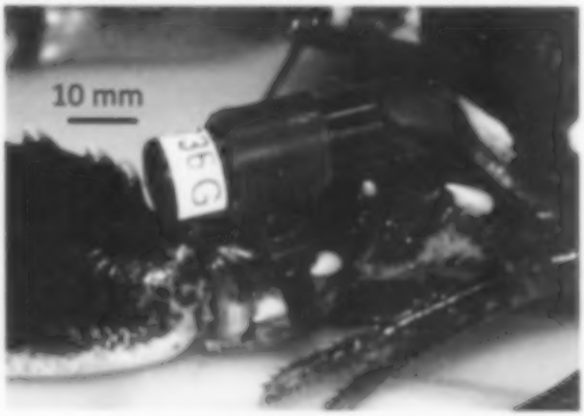

to an ultrasonic receiver with a built-in GPS receiver (model VR 100, Vemco). This field work was conducted, on average, every 5 days throughout the duration of the study around midday (between 10 am and 2 pm) when lobster activity was expected to be minimal. We aimed to collect a minimum sample of 50 position fixes per individual. Tracking was carried out only when weather and sea state allowed accurate positional fixes to be obtained. Individual lobsters were located in a random order in each tracking session. Position fixes were accepted only when high signal strength (≥80%) was obtained at the minimum receiver gain setting (00). We tested the accuracy of positional fixes by spot tests (n = 5) involving SCUBA and careful deployment of a weighted bottom rope from the surface at recently recorded positions. Upon location of the focal lobster, we measured the shortest distance from the lobster to the bottom rope marker. These tests revealed that lobsters, when located by SCUBA, were positioned 4 to10 m (mean 7.0 ± 1.14 m SE) away from the deployed bottom marker and thus the recently recorded GPS position.

From 2 July to 17 August 2007, we tracked 10 individuals at daytime (defined as above) and nighttime (between 1 h after sundown to 1 h before sunrise) two to five times per week to obtain information on the diel range in movement. For this period we (*i*) estimated individual daytime and nighttime home ranges by applying the minimum convex polygon (MCP) estimator (Mohr 1947), (*ii*) quantified the overlap between the two, and (*iii*) the proportion of nighttime position fixes found within the daytime home range. In addition, (*iv*) we estimated diel range in movement as "day night distance" measured as the shortest distance between the daytime and nighttime position fixes obtained consecutively during this period.

Although we began tracking lobsters the day after tagging, we omitted position fixes obtained during the first week after tagging to ensure that lobsters had resumed normal activity. We assumed moulting, tag loss, or mortality if no movement was detected over five consecutive tracking sessions. Using SCUBA, we attempted to confirm the status of non-moving lobsters or tags. The SCUBA searches had three possible outcomes: (1) the lobster with tag intact was located in a den (tracking continued); (2) the tag with harness was located on the substratum (confirming tag loss due to moulting); or (3) neither tag nor lobster was located. In the latter case, tracking ensued through the next five sessions. If the status remained inconclusive (no movement during 10 consecutive tracking sessions), we terminated tracking and removed positions recorded since movement stalled in the analysis.

We estimated long-term MCP home ranges for each individual and also a kernel density estimator of the utilization distribution (UD) (Worton 1989). In the latter case we defined the home range as the smallest area containing 95% of the estimated utilization distribution (UD95). In addition, core areas were defined as the smallest area containing 50% of the utilization distribution (UD50). Data was processed within the R software (version 2.3.1; R Development Core Team 2007). UDs were estimated with fixed kernels. For the purpose of unbiased comparison between individuals, kernel shape (the smoothing parameter) was standardized (i.e., we found a common smoothing parameter ($h0 = 25$) that produced a biologically meaningful kernel shape to the plots of all individuals), avoiding oversmoothing and kernel shapes that included substantial sections of dry land. The alternative would involve selection of kernel bandwidth based on the unique spatial configuration of position fixes in each individual, resulting in a unique smoothing parameter in each case (e.g., least-squares cross-validation; Worton 1989; Gitzen et al. 2006). A sample size of 30–50 is commonly recommended for home range estimates based on kernel density estimation to be valid (Kernohan et al. 2001). In cases where MCP home ranges included sections of dry land (islands or land masses), the area of such overlap was quantified and subtracted from the MCP estimates. As position fixes represent direct observations of lobster locations, all were included in the MCP home range estimates (i.e., no position fixes were considered as biologically unrealistic outliers).

For statistical analyses of individual variation in home range, we used an observation period of 242 days during October 2006 – June 2007 for which we had overlapping data with approximately equal sample size from 18 individuals (see Results section). The 18 individuals consisted of eight males, four non-ovigerous females, and six ovigerous females. We used classical linear models (McCullagh and Nelder 1999) to analyse effects of body size, sex, and reproductive state on home range and core area. We considered these tests relevant as a means to evaluate to what degree there are general patterns to home range behaviour in the species. First, we tested for an effect of body size (CL) on UD95 home range area using the following model structure:

$$(1) \qquad \mathrm{UD95}_{is} = \beta_0 + \beta_1(\mathrm{CL}_{is}) + \beta_S + \varepsilon_i$$

where β_0 is the intercept, β_1 is the slope relating to body size (CL), β_S is a three-level factor describing sex or reproductive state (S) where male is the reference level, and ε_i is the error term. Second, we tested for an effect of body size (CL) on UD50 core area (KUD50) using the same model structure as eq. 1:

$$(2) \qquad \mathrm{UD50}_{is} = \beta_0 + \beta_1(\mathrm{CL}_{is}) + \beta_S + \varepsilon_i$$

Third, we tested for an effect of body size (CL) on MCP home range area using the same model structure as eqs. 1 and 2:

$$(3) \qquad \mathrm{MCP}_{is} = \beta_0 + \beta_1(\mathrm{CL}_{is}) + \beta_S + \varepsilon_i$$

Residual plots indicated that models fitted the data adequately.

We developed the following method to examine the rate at which home range area expanded with time and test whether our monitoring duration was sufficient to effectively capture the home range of each of our study animals: (*i*) We calculated the stepwise increase in MCP home range area with each position fix as the proportion of total estimated MCP home range area (from 0 to 1) for each individual lobster. (*ii*) We plotted the proportional data against monitoring duration (days). Although the resultant curves varied among individuals, most described a sigmoid-like shape. (*iii*) We used generalized linear models with a logit link (McCullagh and Nelder 1999) to perform logistic regressions on the proportional MCP home range area data for each individual. Residual plots indicated that models fitted the data adequately for some individuals. However, as the shape of the curves describing the proportional increase in MCP area with time varied substantially, the model fit was less than adequate for others. However, we concluded that the overall fit was sufficient to justify inclusion of this analysis. A logistic curve is biologically meaningful in relation to animal space use, as home range area is bound to reach an asymptote. We performed the logistic regressions with the following model structure:

$$(4) \qquad \mathrm{logit}(p\mathrm{MCP})_i = \beta_0 + \beta_1(\mathrm{Day}_i) + \varepsilon_i$$

in which the response variable is proportion of MCP home range area (pMCP), β_0 is the intercept, β_1 is the slope relating to monitoring duration (Day), and ε_i is the error term. The fitted regression was then used to estimate the time required to reach 50% and 95% of the annual MCP home range.

Results

Nineteen out of 20 lobsters tagged inside the Flødevigen reserve remained within or near the reserve throughout their monitoring durations. One individual was not heard of after release (lobster No. 7). The number of position fixes recorded for remaining individuals ranged from 35 to 71, with a mean of 57 (Table 1). The particularly low number of position fixes recorded in a single individual (Table 1, lobster No. 19) was due to signal loss perhaps caused by the destruction of the tag by the individual itself or by another lobster. Fortuitously, this individual was recaptured later in the study in a fyke net research survey (targeting cod) within the reserve and equipped with a new tag. However, because of a 154-day break in monitoring, the total number of position fixes amounted to 35. Monitoring duration ranged from 242 to 354 days (median 315 days). Observed net movement during the observation period ranged from 8 to 379 m (mean 119 ± 24 m standard error, SE), thus indicating long-term attachment to limited parts of the study area (Table 1).

The total UD95 home range area (estimated for the entire observation period) ranged from 5728 to 41 548 m^2, representing 0.57% to 4.15% of the reserve area (1 km^2) (Table 2; Fig. 3). The largest UD95 home range area was >7 times greater than the smallest. Total UD50 core area ranged from 1321 to 8715 m^2. The largest UD50 core area was >6.5 times greater than the smallest. Total MCP home range area ranged from 2657 to 93 670 m^2, representing 0.30% to 9.37% of the reserve area. The largest MCP home range area was thus more than an order of magnitude (35 times) greater than the smallest. Both the smallest and the largest UD95, UD50, and

Table 2. Home range summary statistics for 19 *Homarus gammarus* monitored within the Flødevigen lobster reserve during September 2006 – August 2007.

Lobster No.	Area within UD95 (m^2)	Area within UD50 (m^2)	50%:95% ratio (%)	Area within MCP (m^2)	UD95 in % of MR	MCP in % of MR	MCP outside MR (%)
Male							
2	29 018	5 630	19.40	58 463	2.90	5.85	—
3	17 595	3 182	18.08	16 030	1.76	1.60	96.0
10	23 540	5 553	23.60	20 753	2.35	2.08	76.0
11	10 564	1 942	18.38	5 943	1.06	0.60	73.7
16	17 080	2 238	13.10	14 596	1.71	1.46	50.7
17	19 031	3 734	19.62	23 481	1.90	2.35	—
18	25 078	3 554	14.17	31 564	2.51	3.16	—
20	28 091	4 533	16.14	26 823	2.81	2.68	17.7
Mean±SE	21 250±2 224	3 796±487	17.81±1.18	24 703±5 571	2.12±0.22	2.47±0.56	
Female							
6	12 873	2 880	22.37	7 768	1.29	0.78	97.4
8	20 579	4 027	19.57	26 131	2.10	2.61	—
9	26 326	4 406	16.74	26 840	2.63	2.68	3.0
13	10 036	2 571	25.62	6 983	1.00	0.70	—
Mean±SE	17 454±3 702	3 471±442	21.07±1.90	16 931±5 521	1.75±0.37	1.69±0.55	
Ovigerous female							
1	6 222	1 323	21.26	2 993	0.62	0.30	—
4	33 861	6 994	20.66	43 271	3.39	4.33	—
5	14 566	2 345	16.10	11 596	1.46	1.16	47.7
12	15 142	3 019	19.94	10 463	1.51	1.05	72.4
14	41 548	8 715	20.98	93 679	4.15	9.37	32.8
15	5 728	1 321	23.06	2 657	0.57	0.26	—
19	20 826	4 716	22.64	14 831	2.08	1.48	—
Mean±SE	19 700±5 125	4 062±1 088	20.66±0.87	25 638±12 466	1.97±0.37	2.56±1.25	
Overall mean±SE	19 879±2 152	3 825±440	19.55±0.76	23 411±5 086	1.99±0.22	2.34±0.51	

Note: UD95 and UD50, kernel density estimator of the 95% and 50% utilization distribution, respectively; MCP, minimum convex polygon; MR, marine reserve area; MCP outside, minimum convex polygon outside marine reserve borders (in individuals with home ranges straddling reserve boundaries).

MCP areas were found in ovigerous females (Table 2). Average total UD95 home range area was largest in males, followed by ovigerous females and non-ovigerous females (Table 2). Average total UD50 core area was largest in ovigerous females, followed by males and non-ovigerous females (Table 2). The UD50%:UD95% ratio ranged from 14.17% to 25.62%, indicating that some individuals used the space within their home range more evenly than others (Table 2). Average total MCP home range area was higher in ovigerous females, followed by males and non-ovigerous females (Table 2).

Home ranges of 10 individuals straddled the reserve boundary, and some had a major part of their home range area outside the reserve (Table 2). The majority of these individuals were residents of the steep slope on the southeastern side of Ærøya Island (Fig. 3). The other group exhibiting straddling home ranges were residents of the gully and bay to the north of Ærøya Island. Here, the reserve boundary intersects lobster habitat as it runs south–east to north–west along the middle of the gully and then turns northward to connect with land (Fig. 3).

During the observation period of 242 days for which we had overlapping and continuous data from 18 individuals, the number of recorded position fixes ranged from 46 to 51 (mean 47.8 ± 0.4 SE). During this observation period, there was no statistically significant effect of body size, sex, or reproductive state on UD95 home range area, UD50 core area, or MCP home range area (Fig. 4, $p > 0.5$).

Daytime and nighttime MCP home ranges estimated for the 10 individuals monitored intensively from 2 July to 17 August 2007 were similar in size on average (Table 3). The two home ranges were usually somewhat differently configured but with considerable overlap (mean 58.4% ± 7.8% SE). In eight individuals the majority of nighttime position fixes were located within the daytime MCP home range (mean 66.3% ± 4.9% SE). In six individuals the nighttime home range estimate was larger than that of daytime (Table 3). Average diel range in movement (i.e., the distance between consecutively obtained daytime and nighttime position fixes) ranged from 16.0 to 107.9 m (Table 4).

A conspicuous long-range shift in location, resulting in a substantial home range and core area expansion, was evident in two ovigerous females. In one 87 mm individual (Table 1, lobster No. 14), this shift involved a sudden migration in mid-April 2007 from a location at approximately 40 m depth on the steep slope outside Ærøya Island to a much shallower location 300 m to the northwest near the northern corner of the island, where she took up residence (Fig. 5). Suspecting that she would hatch her eggs in this location, we inspected her using SCUBA on 7 June 2007. We located her in a den at 15 m depth and confirmed that her eggs were close to

Fig. 3. Plots showing home ranges calculated for the entire monitoring duration based on a kernel estimator of the 95% utilization distribution (UD95) in 19 lobsters monitored by ultrasonic tracking within the Flødevigen lobster reserve during September 2006 – August 2007. Stippled black line: reserve boundary. Isobaths are the 5, 10, 20, 30, and 40 m depth contours. Note that depth increases gradually to >80 m beyond the 40 m contour.

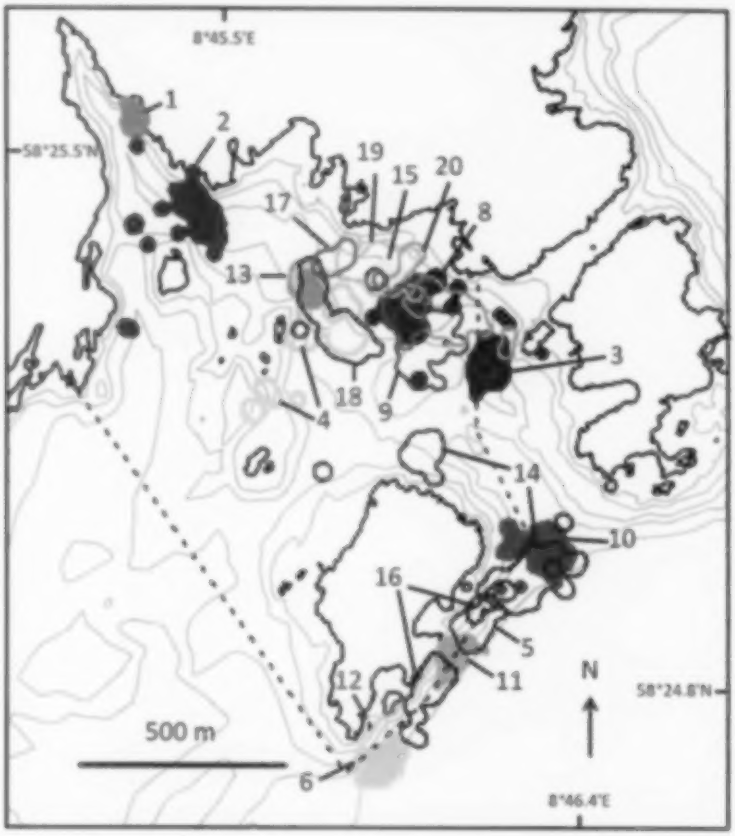

hatching. She remained in this location until early August when she was located further west on one occasion before she returned to her former location in deeper water outside Ærøya Island. In early June 2007, another 88 mm female (Table 1, lobster No. 4) began transmitting from the edge of a shallow basin 250 m southwest of the reserve centre where she had been residing in the preceding months. From then on she would be located in the new part of her home range on alternate tracking days. We were successful in locating her (using SCUBA) in the old part of her home range on 28 June 2007 (at 12 m depth) and confirmed that her eggs were close to hatching. As we were curious to know what drove her commuting behaviour, we also attempted to locate her in the new part of her home range. Unfortunately, these attempts were unsuccessful. However, we did find tracks made by a large decapod crustacean and evidence of digging activity in the soft silt that constituted the substratum in the shallow (10 m), flat basin she frequented. During our SCUBA search in the basin, we noticed a number of shells from dead, burrowing echinoids (*Echinocardium* sp.), suggesting that they were plentiful there (see Fig. 5). Although anecdotal, these observations may suggest that she somehow discovered this food source and thus developed the habit of commuting to this area to forage on burrowing echinoids. One plausible explanation why she commuted rather than taking up residence in this area could be, simply, that it was suboptimal as lobster habitat. The behaviours exhibited by these two individuals contributed profoundly to the relatively large average UD95, UD50, and MCP areas and the large SEs associated with these, estimated for ovigerous females (see Table 2).

Plots of the temporal increase in proportion MCP home range described sigmoid-like curves for most individuals (Fig. 6). The logistic regression model fitted to the temporal increase in proportion MCP home range area generated predicted time to 50% and 95% MCP home range that matched the data reasonably well (Fig. 6; Table 5). However, in some cases, the model extrapolated predicted time to 95% MCP home range beyond the actual monitoring duration (i.e., reflecting that MCP home range area had not yet levelled out within the observation period for these individuals; Table 5). Average time required to reach 50% and 95% MCP home range was 98 and 259 days, respectively.

Discussion

The results presented herein represent novel findings, as they embody, to the best of our knowledge, the first annual

Fig. 4. Estimates of UD95 home range area (*a*–*b*), UD50 core area (*c*–*d*), and MCP home range area (*e*–*f*) for eight male (M), four female (F), and six ovigerous female (O-F) lobsters monitored during a 242-day overlapping observation period (October 2006 – June 2007).

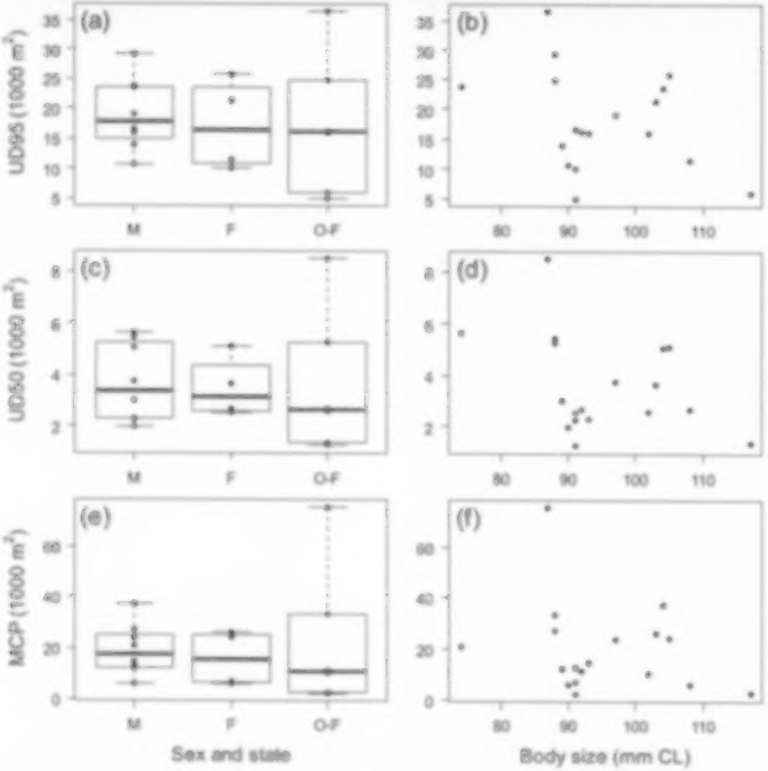

Table 3. Home range summary statistics for a subset of 10 lobsters monitored at daytime and nighttime within the Flødevigen lobster reserve from 2 July to 17 August 2007.

	Daytime		Nighttime			
Lobster No.	Position fixes	MCP (m²)	Position fixes	MCP (m²)	Overlap (%)	Nighttime position fixes within daytime MCP (%)
4	19	20 917	18	28 797	45.4	50.0
5	27	1 256	19	677	83.5	79.0
8	25	2 583	20	4 727	53.7	70.0
9	21	1 047	20	5 636	16.7	35.0
12	26	1 601	23	1 728	58.9	69.6
13	26	5 505	20	1 973	65.9	80.0
14	24	50 488	19	26 859	95.0	84.2
18	29	34 820	19	23 961	85.5	73.7
19	25	8 773	22	14 920	34.0	68.2
20	25	1 004	15	1 792	44.3	53.3
Mean±SE	24.7±0.9	12 799±5 458	19.5±0.7	11 107±3 618	58.4±7.8	66.3±4.9

Note: MCP, minimum convex polygon; Overlap, percent of nighttime MCP home range overlapping daytime MCP home range area.

home range estimates for European lobster. While some preceding studies have been successful in obtaining repetitive locations of individual European lobsters, the duration of sampling was either too short (van der Meeren 1997) or the study was not designed to assess home range size (Smith et al. 1998, 1999). Moreover, this study revealed that long-term tracking is possible and that monitored individuals were resident in the area. We discuss our findings in relation to reserve design in coastal marine habitats.

The differences in home range size estimates obtained during the entire study period illustrate tremendous amounts of variability between individuals, as well as between the two estimators. In seven lobsters, the MCP estimator generated the larger estimate of home range size, whereas in 12 lobsters

Table 4. Diel movement summary statistics for a subset of 10 lobsters monitored at daytime and nighttime within the Flødevigen lobster reserve from 2 July to 17 August 2007.

Lobster No.	DND (m)	SD	*n*
4	31.5	31.3	10
5	16.0	12.6	16
8	21.6	14.0	16
9	37.6	30.3	12
12	10.9	7.0	17
13	19.9	11.9	14
14	24.6	20.6	13
18	107.9	74.9	15
19	45.2	31.8	15
20	23.9	18.2	13

Note: DND, mean day night distance (m) measured as the shortest distance between consecutive daytime and nighttime position fixes; SD, standard deviation; *n*, number of consecutive day–night observations per individual over the monitoring period.

the larger estimates were generated by the UD95 estimator. However, overall, the UD95 was the more conservative estimator of home range size. The MCP estimator will greatly inflate home range size if activity centres are spaced wide apart or in cases with occasional excursive position fixes. In contrast, the UD95 estimator generated home range sizes up to two times larger than the MCP estimator in cases where position fixes were relatively evenly spaced. To a large degree, the latter characteristic of the UD95 estimator was driven by our decision to use a common smoothing parameter for all lobsters. There are few studies to which we can compare our estimates. However, Stone and O'Clair (2002) reported an average MCP home range size of 33 600 m^2 for eight native ovigerous female Dungeness crabs (*Cancer magister*), another large decapod species, during the first 100 days of their acoustic tracking study in an Alaskan estuary. In comparison, the average MCP home range size for seven ovigerous females was 25 638 m^2 in the present study, suggesting similar types of movement pattern across species.

Herein we adopted a primarily Lagrangian (individual-based) approach to study detailed movement patterns in European lobster. In light of the innate limitations posed by this approach, future work aiming to gain a broader understanding of the population dynamics of this species in particular areas (e.g., within reserves and control areas) might benefit from the more Eulerian approach adopted in mark–recapture studies of other large decapod crustacean species (e.g., Bell et al. 2003; Etherington et al. 2003; Dunnington et al. 2005). Although the latter method will typically yield lower spatial resolution concerning movement patterns, there are clear advantages in terms of information gained from large sample size and recaptures obtained over longer terms. For example, recent Eulerian studies that examined larger scale movement patterns of American lobsters revealed both resident and transient coastal population components (Bowlby et al. 2007; Geraldi et al. 2009). To date there is no evidence for this behavioural dichotomy in coastal populations of European lobster.

We found no effect of body size, sex, or reproductive state on home range or core area size. Scopel et al. (2009) estimated daily (24 h) UD95 home ranges in the sister species American lobster and reported no significant differences between sexes and no relationship between lobster size and home range size. Similarly, Bertelsen and Hornbeck (2009) estimated MCP home ranges in the Caribbean spiny lobster (*Panulirus argus*) and reported no significant differences between sexes and no relationship between lobster size and home range size. For terrestrial animals, it is commonly acknowledged that home range size scales with animal size, as larger animals require more food and thus larger areas for foraging (McNab 1963; Reiss 1988; McLoughlin and Ferguson 2000). In contrast, the available data for decapod species suggest poor correlation among locomotor activity, home range size, and body size. Some studies reported no relationship (Gherardi et al. 2000; Golet et al. 2006; Scopel et al. 2009), whereas others found smaller animals moved farther (Linnane et al. 2005; Kelly and MacDiarmid 2003; Bertelsen and Hornbeck 2009) or had larger home ranges (Stone and O'Clair 2002). We note that the limited sample size ($n = 18$) and narrow range in body size evaluated in our study means that only major effects can be detected statistically. Hence, body size, sex, and reproductive state could still influence lobster home ranges to some extent.

The long-term home range estimates presented here were based on daytime observations of lobsters' locations, a time during which activity is minimal and behaviour is presumably dominated by sheltering within dens (Smith et al. 1999; Mehrtens et al. 2005; Childress and Jury 2006). That said, we observed large lobsters (>90 mm CL) out on the open substratum in broad summer daylight during the SCUBA work conducted in this study. Such observations indicate that the nocturnal activity rhythm reported for this species (e.g., Mehrtens et al. 2005) is not entirely rigid. For comparison, large amounts of variability in the daily activity patterns have been demonstrated in wild American lobster by Golet et al. (2006). In their telemetry study, five out of 44 lobsters (11%) moved significantly more during the day than during the night. Consequently, we cannot distinguish whether the daytime position fixes obtained in this study represent sheltering locations or instances of movement on the substratum. Most likely they represent a mixture of the two, where the majority of position fixes obtained during the winter (February and March) represent sheltering locations, as this is a time of minimal activity in the species. Considering the absence of long-term nighttime observations, this study lacks an important aspect of lobster behaviour. However, the short-term movement data obtained during the seven summer weeks during which lobsters were tracked during both daytime and nighttime indicate that nighttime activity occurred mostly in near proximity to where lobsters were located during daytime. We note that only one individual (lobster No. 18) had an estimated average diel range in movement >50 m during a time of year when lobster activity in this area is moving towards its maximum because of increasing water temperatures throughout the water column. Most likely, our study animals displayed nighttime movement that may have extended beyond the estimated long-term home ranges. Still, the short-term movement data support our study design as successful in documenting residency and long-term home range behaviour in European lobster.

The lobsters studied herein had home ranges located in

Fig. 5. UD95 home range (perimeter encircling all points), UD50 core area (in grey), and position fixes (black points) in two ovigerous female lobsters (*a*: lobster No. 4, *b*: lobster No. 14) monitored in the Flødevigen reserve. Grey arrow in panel (*a*) denotes the extent of the repeated "commuting" behaviour observed in lobster No. 4 towards the end of the study. Grey arrows in panel (*b*) denote the home range relocation exhibited by lobster No. 14 during spring and summer 2007. After having spent the spring–summer and hatched her eggs in the northern (shallow) area, she returned to the southern (deeper) area. Black line in panel (*b*) is the reserve boundary. Numbers in grey are contour depths (m).

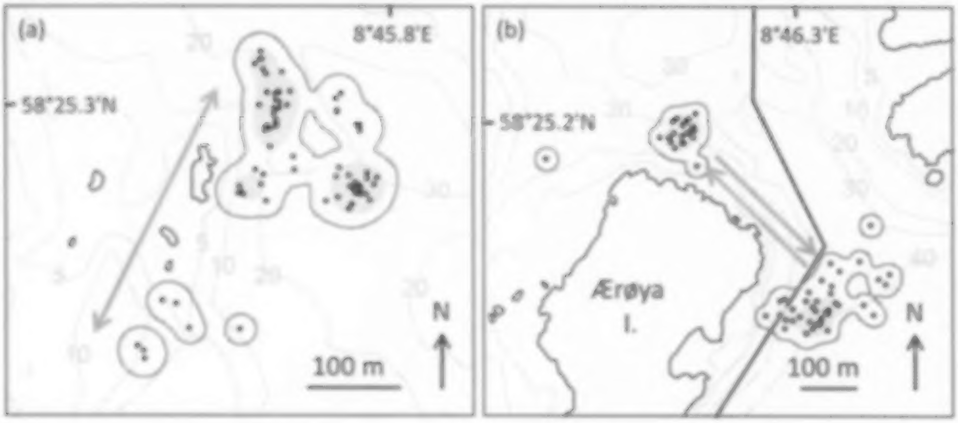

Fig. 6. Plots showing the cumulative increase in proportional MCP home range area for 19 European lobsters, throughout their respective monitoring durations. Lobsters were tracked by ultrasonic telemetry within Flødevigen lobster reserve during September 2006 – August 2007. Position fixes were obtained every 5 days throughout the observation period.

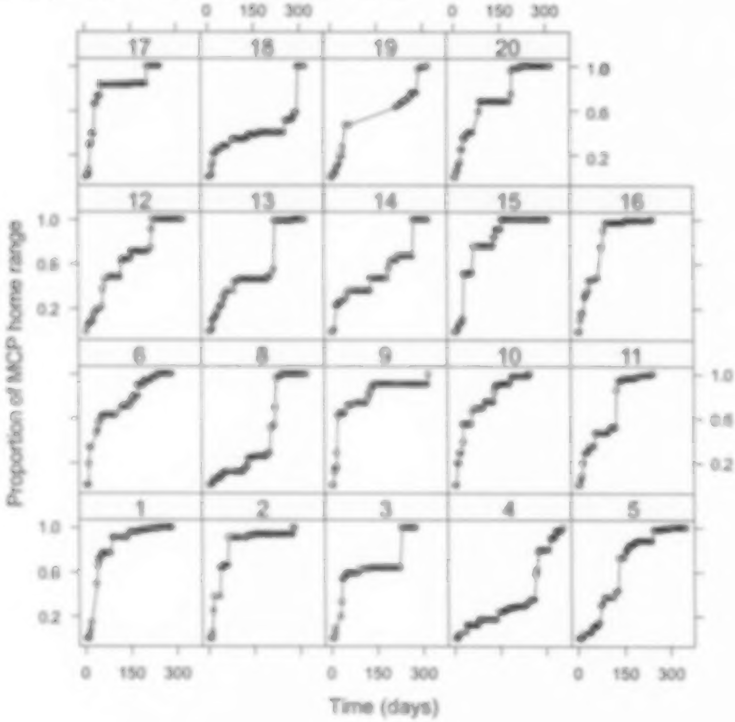

habitat with differing slope and rugosity. We note that the horizontal projection of home range areas used here has resulted in estimates that are biased low in cases where lobsters resided in particularly steep habitat. For species that are fully bottom dwelling, such as most large decapod crustaceans, it would be useful to project home range areas onto a three-dimensional model of the habitat and thus obtain a more realistic estimate of home range size in future studies.

Our study animals displayed limited net movement during the observation period, which is a good indicator of long-

Table 5. Estimates of time (days) required to observe 50% ($MCP50_T$) and 95% ($MCP95_T$) of the minimum convex polygon home range in European lobster.

Lobster No.	$MCP50_T$	SE	$MCP95_T$	SE
1	41.7	15.2	128.4	29.2
2	33.9	26.0	183.8	41.2
3	84.2	29.2	329.2*	77.1
4	227.1	19.7	415.0*	52.0
5	122.9	14.8	229.9	27.3
6	60.6	22.8	217.2	42.8
8	179.0	13.6	284.2	28.9
9	32.7	35.6	263.6	59.2
10	54.0	19.6	184.1	36.4
11	79.3	15.3	182.1	29.3
12	111.2	16.7	242.2	32.8
13	135.3	17.5	294.2	41.2
14	147.3	22.4	367.5*	61.9
15	64.7	12.9	146.1	24.6
16	49.9	12.3	113.4	23.8
17	46.5	21.2	195.0	41.5
18	212.8	34.4	548.4*	137.6
19	87.6	33.4	370.4*	63.3
20	87.6	17.6	222.3	34.0

Note: Estimates were generated from logistic regressions performed on data from 19 *Homarus gammarus* tracked within the Flødevigen lobster reserve in coastal Skagerrak. SE, standard error.

*Cases where the model extrapolated estimates beyond actual observation time (see also Fig. 6).

term site attachment. Such behaviour has previously been demonstrated based on traditional mark–recapture methods (Dannevig 1936; Smith et al. 2001; Agnalt et al. 2007) and electromagnetic telemetry (Smith et al. 1998, 1999). The shortest distance from first to last position fix over the monitoring period was only 8 m. The well-being of this particular female was confirmed as she was caught (within her home range) during the annual trap survey in the reserve, conducted shortly after the termination of this study. Although European lobsters are certainly capable of migrations (e.g., Smith et al. 2001), we found no evidence of a common behaviour involving seasonal migration from shallower areas within the bay into deeper waters outside Ærøya Island. This finding is in agreement with studies suggesting that a wide range of lobster species have at least a proportion of their populations that remain resident (see e.g., Barrett et al. 2009; Bowlby et al. 2007; Geraldi et al. 2009).

On average, it took 98 days to reach 50% of the annual MCP home range and 259 days to reach the 95% level. The number of locations needed for MCP home range estimates to reach asymptotic levels will depend on observation duration and study species. Authors have proposed that 100–200 locations are often needed (see Kernohan et al. 2001 and references therein). In the case of the European lobster, our study suggests that about 50–70 observations spread over roughly 300 days will be sufficient in most cases (although in a few cases, an asymptotic level was not reached even though the lobsters were tracked for up to 1 year). We note that an observation time of 1 year is but a limited part of a lobster's lifetime and that one thus should be cautious when generalizing the time to reach an asymptotic home range from a small sample of study animals.

This study provides empirical field data that are potentially valuable for deciding the size and location of future marine reserves for this species. Home ranges were all of limited size relative to reserve area (0.57%–4.15%), which implies that even small experimental reserves may be well suited in, for example, capture–mark–recapture studies aimed at examining long-term effects of protection on demographic rates. In contrast, Dunnington et al. (2005) observed high turnover of American lobster populations on study areas comparable in size to the present study. Yet, the movement pattern observed herein indicates that European lobster can potentially recover in abundance to natural levels in marine reserves of limited size despite intense fishing pressure in adjoining areas. Rowe (2001) reported on a mark–recapture study on American lobster conducted inside and outside small no-take reserves in Bonavista Bay, Newfoundland. The majority of recaptures (58.7%) were in close proximity to their original capture locations. Among individuals that moved, 77.1% travelled less than 1000 m. Similarly, she suggested that no-take reserves of limited size can offer increased survival to lobsters and thus may provide benefits to fisheries. However, habitat type may have profound influence on movement patterns in lobsters. In another tagging study, Geraldi et al. (2009) found that American lobsters caught and released on sediment moved farther and faster than lobsters initially caught in traps on rocky substrate. Importantly, 10 of the 19 lobsters observed in the present study had home ranges that straddled the reserve boundary, some with considerable proportions of their home range area outside the reserve. Considering the limited home range areas exhibited by these lobsters, the configuration of the Flødevigen reserve could easily be modified to include the areas utilized outside reserve boundaries. Seven out of the 10 straddling lobsters had home ranges situated on a steep slope largely consisting of a boulder field. Clearly, these individuals utilized the full extent of this habitat, as reflected in home ranges extending into deeper water, well beyond the reserve boundary. This observation supports the conclusions made by Freeman et al. (2009) that if marine reserves aim to conserve species at all times, their boundaries should follow barriers to species movement. However, if cross-boundary movement of harvestable individuals associated with certain habitat (i.e., spillover) is a management goal for fisheries purposes, then boundaries should be designed to intersect that habitat.

The limited long-term movement revealed in this study suggests that heavily fished areas are unlikely to receive substantial replenishment via movement of adult lobsters from protected areas. However, this study was conducted in a recently established reserve in which the protected population still resembles that of the outside depleted state. It remains to be tested whether the observed movement patterns remain the same or will be altered if the protected population recovers in abundance to natural levels. Theory might suggest increased movement over time owing to a process termed "demographic diffusion", proposed and experimentally evaluated for American lobster, where larger lobsters leave or avoid areas of high lobster population density and intense competition for areas of low population density and relaxed competition (Steneck 2006).

In conclusion, the observations presented here suggest that (*i*) if the management objective is to ensure long-term protection, then future reserves for European lobster should be designed to include complete patches of habitat preferred by this species, and (*ii*) the reserves should in general be somewhat larger than the present one and include deeper habitat if possible. That said, the observed combination of relatively limited home ranges and the temporal stability of their locations within the year of study suggest that even small coastal reserves (≈1 km^2 in size), given a proper design, may realistically protect fractions of European lobster populations.

Acknowledgements

We kindly thank S.E. Enersen and H. Knutsen for assistance with capture and tracking of lobsters and members of the Institute of Marine Research dive team: Ø. Paulsen and P. Baardsen, for assistance during underwater work. S.H. Espeland played a central role in developing R code. W.H. Watson III shared important insights regarding the noble art of lobster tracking, and the paper benefited from discussions with M.R. Heupel, S.H. Jury, and C.A. Simpfendorfer and thoughtful reviews provided by two anonymous reviewers. This study was financed by the Research Council of Norway through grant Nos. 173432/S40 and 201917/V50.

References

Abesamis, R.A., and Russ, G.R. 2005. Density-dependent spillover from a marine reserve: long-term evidence. Ecol. Appl. **15**(5): 1798–1812. doi:10.1890/05-0174.

Agnalt, A.L., Kristiansen, T.S., and Jorstad, K.E. 2007. Growth, reproductive cycle, and movement of berried European lobsters (*Homarus gammarus*) in a local stock off southwestern Norway. ICES J. Mar. Sci. **64**(2): 288–297. doi:10.1093/icesjms/fsl020.

Attwood, C.G., and Bennett, B.A. 1995. Modelling the effect of marine reserves on the recreational shore-fishery of the South-Western Cape, South Africa. S. Afr. J. Mar. Sci. **16**(1): 227–240. doi:10.2989/025776195784156458.

Barrett, N., Buxton, C., and Gardner, C. 2009. Rock lobster movement patterns and population structure within a Tasmanian Marine Protected Area inform fishery and conservation management. Mar. Freshw. Res. **60**(5): 417–425. doi:10.1071/MF07154.

Baskett, M.L., Levin, S.A., Gaines, S.D., and Dushoff, J. 2005. Marine reserve design and the evolution of size at maturation in harvested fish. Ecol. Appl. **15**(3): 882–901. doi:10.1890/04-0723.

Beamish, R.J., McFarlane, G.A., and Benson, A. 2006. Longevity overfishing. Prog. Oceanogr. **68**(2–4): 289–302.

Bell, M.C., Eaton, D.R., Bannister, R.C.A., and Addison, J.T. 2003. A mark–recapture approach to estimating population density from continuous trapping data: application to edible crabs, *Cancer pagurus*, on the east coast of England. Fish. Res. **65**(1–3): 361–378. doi:10.1016/j.fishres.2003.09.026.

Berkeley, S.A., Hixon, M.A., Larson, R.J., and Love, M.S. 2004. Fisheries sustainability via protection of age structure and spatial distribution of fish populations. Fisheries, **29**(8): 23–32.

Bertelsen, R.D., and Hornbeck, J. 2009. Using acoustic tagging to determine adult spiny lobster (*Panulirus argus*) movement patterns in the Western Sambo Ecological Reserve (Florida, United States). N.Z. J. Mar. Freshw. Res. **43**(1): 35–46. doi:10.1080/00288330909509980.

Börger, L., Dalziel, B., and Fryxell, J. 2008. Are there general mechanisms of animal home range behaviour? A review and prospects for future research. Ecol. Lett. **11**(6): 637–650. doi:10.1111/j.1461-0248.2008.01182.x. PMID:18400017.

Bowlby, H.D., Hanson, J.M., and Hutchings, J.A. 2007. Resident and dispersal behaviour among individuals within a population of American lobster *Homarus americanus*. Mar. Ecol. Prog. Ser. **331**: 207–218. doi:10.3354/meps331207.

Boydston, E.E., Kapheim, K.M., Szykman, M., and Holekamp, K.E. 2003. Individual variation in space use by female spotted hyenas. J. Mammal. **84**(3): 1006–1018. doi:10.1644/BOS-038.

Bradbury, C., Green, J.M., and Brucelockhart, M. 1995. Home ranges of female cunner, *Tautogolabrus adspersus* (Labridae), as determined by ultrasonic telemetry. Can. J. Zool. **73**(7): 1268–1279. doi:10.1139/z95-151.

Childress, J.M., and Jury, S.H. 2006. Behaviour. *In* Lobsters: biology, management, aquaculture and fisheries. *Edited by* B.F. Phillips. Blackwell Publishing, Oxford, UK. pp. 78–112.

Chittleborough, R.G. 1974. Home range, homing and dominance in juvenile western rock lobsters. Aust. J. Mar. Freshw. Res. **25**(2): 227–234. doi:10.1071/MF9740227.

Clark, D., and Green, J.M. 1990. Activity and movement patterns of juvenile Atlantic cod, *Gadus morhua*, in Conception Bay, Newfoundland, as determined by sonic telemetry. Can. J. Zool. **68**(7): 1434–1442. doi:10.1139/z90-214.

Claudet, J., Osenberg, C.W., Benedetti-Cecchi, L., Domenici, P., Garcia-Charton, J.A., Perez-Ruzafa, A., Badalamenti, F., Bayle-Sempere, J., Brito, A., Bulleri, F., Culioli, J.M., Dimech, M., Falcon, J.M., Guala, I., Milazzo, M., Sanchez-Meca, J., Somerfield, P.J., Stobart, B., Vandeperre, F., Valle, C., and Planes, S. 2008. Marine reserves: size and age do matter. Ecol. Lett. **11**(5): 481–489. doi:10.1111/j.1461-0248.2008.01166.x. PMID:18294212.

Cowan, D.F., Watson, W.H., III, Solow, A.R., and Mountcastle, A.M. 2007. Thermal histories of brooding lobsters, *Homarus americanus*, in the Gulf of Maine. Mar. Biol. **150**(3): 463–470. doi:10.1007/s00227-006-0358-5.

Dannevig, A. 1936. Lobster and lobster culture. *In* Report on Norwegian Fishery and Marine Investigations. Vol. 4, Issue 12.

DeMartini, E.E. 1993. Modeling the potential of fishery reserves for managing Pacific coral reef fishes. Fish. Bull. **91**(3): 414–427.

Dunnington, M.J., Wahle, R.A., Bell, M.C., and Geraldi, N.R. 2005. Evaluating local population dynamics of the American lobster, *Homarus americanus*, with trap-based mark–recapture methods and seabed mapping. N.Z. J. Mar. Freshw. Res. **39**(6): 1253–1276. doi:10.1080/00288330.2005.9517391.

Espeland, S.H., Gundersen, A.F., Olsen, E.M., Knutsen, H., Gjosaeter, J., and Stenseth, N.C. 2007. Home range and elevated egg densities within an inshore spawning ground of coastal cod. ICES J. Mar. Sci. **64**(5): 920–928. doi:10.1093/icesjms/fsm028.

Etherington, L.L., Eggleston, D.B., and Stockhausen, W.T. 2003. Partitioning loss rates of early juvenile blue crabs from seagrass habitats into mortality and emigration. Bull. Mar. Sci. **72**(2): 371–391.

Francis, R.C., Hixon, M.A., Clarke, M.E., Murawski, S.A., and Ralston, S. 2007. Fisheries management — ten commandments for ecosystem-based fisheries scientists. Fisheries, **32**(5): 217–233.

Freeman, D.J., MacDiarmid, A.B., and Taylor, R.B. 2009. Habitat patches that cross marine reserve boundaries: consequences for the lobster *Jasus edwardsii*. Mar. Ecol. Prog. Ser. **388**: 159–167. doi:10.3354/meps08122.

Geraldi, N.R., Wahle, R.A., and Dunnington, M. 2009. Habitat effects on American lobster (*Homarus americanus*) movement and density: insights from georeferenced trap arrays, seabed mapping, and tagging. Can. J. Fish. Aquat. Sci. **66**(3): 460–470. doi:10.1139/F09-011.

Gherardi, F., Barbaresi, S., and Salvi, G. 2000. Spatial and temporal patterns in the movement of *Procambarus clarkii*, an invasive crayfish. Aquat. Sci. **62**(2): 179–193. doi:10.1007/PL00001330.

Gitzen, R.A., Millspaugh, J.J., and Kernohan, B.J. 2006. Bandwidth selection for fixed-kernel analysis of animal utilization distributions. J. Wildl. Manage. **70**(5): 1334–1344. doi:10.2193/0022-541X(2006)70[1334:BSFFAO]2.0.CO;2.

Golet, W.J., Scopel, D.A., Cooper, A.B., and Watson, W.H., III. 2006. Daily patterns of locomotion expressed by American lobsters (*Homarus americanus*) in their natural habitat. J. Crustac. Biol. **26**(4): 610–620. doi:10.1651/S-2729.1.

Goñi, R., Quetglas, A., and Reñones, O. 2006. Spillover of spiny lobsters *Palinurus elephas* from a marine reserve to an adjoining fishery. Mar. Ecol. Prog. Ser. **308**: 207–219. doi:10.3354/meps308207.

Guénette, S., and Pitcher, T.J. 1999. An age-structured model showing the benefits of marine reserves in controlling overexploitation. Fish. Res. **39**(3): 295–303. doi:10.1016/S0165-7836(98)00173-8.

Halpern, B.S. 2003. The impact of marine reserves: Do reserves work and does reserve size matter? Ecol. Appl. **13**(1): S117–S137. doi:10.1890/1051-0761(2003)013[0117:TIOMRD]2.0.CO;2.

Herrnkind, W.F. 1980. Spiny lobsters: patterns of movement. *In* The biology and management of lobsters. *Edited by* J.S. Cobb and B.F. Phillips. Academic Press, New York. pp. 349–407.

Heupel, M.R., Simpfendorfer, C.A., and Hueter, R.E. 2004. Estimation of shark home ranges using passive monitoring techniques. Environ. Biol. Fishes, **71**(2): 135–142. doi:10.1023/B:EBFI.0000045710.18997.f7.

Jones, K.M.M. 2005. Home range areas and activity centres in six species of Caribbean wrasses (Labridae). J. Fish Biol. **66**(1): 150–166. doi:10.1111/j.0022-1112.2005.00589.x.

Kelly, S., and MacDiarmid, A.B. 2003. Movement patterns of mature spiny lobsters, *Jasus edwardsii*, from a marine reserve. N.Z. J. Mar. Freshw. Res. **37**(1): 149–158. doi:10.1080/00288330.2003.9517153.

Kernohan, B.J., Gitzen, R.A., and Millspaugh, J.J. 2001. Analysis of animal space use and movements. *In* Radio tracking and animal populations. *Edited by* J.J. Millspaugh and J.M. Marzluff. Academic Press, San Diego, Calif. pp. 125–166.

Kramer, D.L., and Chapman, M.R. 1999. Implications of fish home range size and relocation for marine reserve function. Environ. Biol. Fishes, **55**(1–2): 65–79. doi:10.1023/A:1007481206399.

Lester, S.E., Halpern, B.S., Grorud-Colvert, K., Lubchenco, J., Ruttenberg, B.I., Gaines, S.D., Airame, S., and Warner, R.R. 2009. Biological effects within no-take marine reserves: a global synthesis. Mar. Ecol. Prog. Ser. **384**: 33–46. doi:10.3354/meps08029.

Linnane, A., Dimmlich, W., and Ward, T. 2005. Movement patterns of the southern rock lobster, *Jasus edwardsii*, off South Australia. N.Z. J. Mar. Freshw. Res. **39**(2): 335–346. doi:10.1080/00288330.2005.9517314.

Lowe, C.G., Topping, D.T., Cartamil, D.P., and Papastamatiou, Y.P. 2003. Movement patterns, home range, and habitat utilization of adult kelp bass *Paralabrax clathratus* in a temperate no-take marine reserve. Mar. Ecol. Prog. Ser. **256**: 205–216. doi:10.3354/meps256205.

Lubchenco, J., Palumbi, S.R., Gaines, S.D., and Andelman, S. 2003. Plugging a hole in the ocean: the emerging science of marine reserves. Ecol. Appl. **13**(1): S3–S7. doi:10.1890/1051-0761(2003)013[0003:PAHITO]2.0.CO;2.

McCullagh, P., and Nelder, J.A. 1999. Generalized linear models. Chapman & Hall/CRC, London, UK.

McLoughlin, P.D., and Ferguson, S.H. 2000. A hierarchical pattern of limiting factors helps explain variation in home range size. Ecoscience, **7**(2): 123–130.

McNab, B.K. 1963. Bioenergetics and determination of home range size. Am. Nat. **97**(894): 133–140. doi:10.1086/282264.

Mehrtens, F., Stolpmann, M., Buchholz, F., Hagen, W., and Saborowski, R. 2005. Locomotory activity and exploration behaviour of juvenile Euroepan lobsters (*Homarus gammarus*) in the laboratory. Mar. Freshw. Behav. Physiol. **38**(2): 105–116. doi:10.1080/10236240500104101.

Moffitt, E.A., Botsford, L.W., Kaplan, D.M., and O'Farrell, M.R. 2009. Marine reserve networks for species that move within a home range. Ecol. Appl. **19**(7): 1835–1847. doi:10.1890/08-1101.1. PMID:19831073.

Mohr, C.O. 1947. Table of equivalent populations of North American small mammals. Am. Midl. Nat. **37**(1): 223–249. doi:10.2307/2421652.

Nemtzov, S.C. 1997. Intraspecific variation in home range exclusivity by female green razorfish, *Xyrichtys splendens* (family Labridae), in different habitats. Environ. Biol. Fishes, **50**(4): 371–381. doi:10.1023/A:1007319622028.

Oug, E., Vader, W., Brattegaard, T., Christiansen, M.E., Walseng, B., and Djursvoll, P. 2010. Crustacea. In The 2010 Norwegian Red List for species. *Edited by* J.A. Kålås, Å. Viken, S. Henriksen, and S. Skjelseth. Norwegian Biodiversity Information Centre, Trondheim, Norway. pp. 209–222.

Pandian, T.J. 1970. Ecophysiological studies on the developing eggs and embryos of the European lobster *Homarus gammarus*. Mar. Biol. **5**(2): 154–167. doi:10.1007/BF00352599.

Pettersen, A.R., Moland, E., Olsen, E.M., and Knutsen, J.A. 2009. Lobster reserves in coastal Skagerrak — an integrated analysis of the implementation process. *In* Integrated coastal zone management. *Edited by* E. Dahl, E. Moksness, and J. Støttrup. Wiley-Blackwell Publishing, London, UK. pp. 178–188.

Reese, E. 1989. Orientation and behaviour of butterflyfishes (family Chaetodontidae) on coral reefs: spatial learning of route specific landmarks and cognitive maps. Environ. Biol. Fishes, **25**(1–3): 79–86. doi:10.1007/BF00002202.

Reiss, M. 1988. Scaling of home range size: body size, metabolic needs and ecology. Trends Ecol. Evol. **3**(3): 85–86. doi:10.1016/0169-5347(88)90025-0. PMID:21227101.

Roberts, C.M., Bohnsack, J.A., Gell, F., Hawkins, J.P., and Goodridge, R. 2001. Effects of marine reserves on adjacent fisheries. Science (Washington, D.C.), **294**(5548): 1920–1923. doi:10.1126/science.294.5548.1920. PMID:11729316.

Rowe, S. 2001. Movement and harvesting mortality of American lobsters (*Homarus americanus*) tagged inside and outside no-take reserves in Bonavista Bay, Newfoundland. Can. J. Fish. Aquat. Sci. **58**(7): 1336–1346. doi:10.1139/cjfas-58-7-1336.

Russ, G.R., Cheal, A.J., Dolman, A.M., Emslie, M.J., Evans, R.D., Miller, I., Sweatman, H., and Williamson, D.H. 2008. Rapid increase in fish numbers follows creation of world's largest marine reserve network. Curr. Biol. **18**(12): R514–R515. doi:10.1016/j.cub.2008.04.016. PMID:18579091.

Sale, P.F., Cowen, R.K., Danilowicz, B.S., Jones, G.P., Kritzer, J.P., Lindeman, K.C., Planes, S., Polunin, N.V.C., Russ, G.R., Sadovy, Y.J., and Steneck, R.S. 2005. Critical science gaps impede use of no-take fishery reserves. Trends Ecol. Evol. **20**(2): 74–80. doi:10.1016/j.tree.2004.11.007. PMID:16701346.

Scopel, D.A., Golet, W.J., and Watson, W.H., III. 2009. Home range dynamics of the American lobster, *Homarus americanus*. Mar. Freshw. Behav. Physiol. **42**(1): 63–80. doi:10.1080/10236240902781498.

Smith, I.P., Collins, K.J., and Jensen, A.C. 1998. Movement and activity patterns of the European lobster, *Homarus gammarus*, revealed by electromagnetic telemetry. Mar. Biol. **132**(4): 611–623. doi:10.1007/s002270050426.

Smith, I.P., Collins, K.J., and Jensen, A.C. 1999. Seasonal changes in the level and diel patterns of activity in the European lobster

Homarus gammarus. Mar. Ecol. Prog. Ser. **186**: 255–264. doi:10.3354/meps186255.

Smith, I.P., Jensen, A.C., Collins, K.J., and Mattey, E.L. 2001. Movement of wild European lobsters *Homarus gammarus* in natural habitat. Mar. Ecol. Prog. Ser. **222**: 177–186. doi:10.3354/meps222177.

Steneck, R.S. 2006. Possible demographic consequences of intraspecific shelter competition among American lobsters. J. Crustac. Biol. **26**(4): 628–638. doi:10.1651/S-2753.1.

Stobart, B., Warwick, R., González, C., Mallol, S., Díaz, D., Reñones, O., and Goñi, R. 2009. Long-term and spillover effects of a marine protected area on an exploited fish community. Mar. Ecol. Prog. Ser. **384**: 47–60. doi:10.3354/meps08007.

Stone, R.P., and O'Clair, C.E. 2002. Behavior of female Dungeness crabs, *Cancer magister*, in a glacial southeast Alaska estuary: homing, brooding-site fidelity, seasonal movements, and habitat use. J. Crustac. Biol. **22**(2): 481–492. doi:10.1651/0278-0372(2002)022[0481:BOFDCC]2.0.CO;2.

R Development Core Team. 2007. R: A language and environment for statistical computing. R Foundation for Statistical Computing, Vienna, Austria. Available from http://www.r-project.org/.

Topping, D.T., Lowe, C.G., and Caselle, J.E. 2005. Home range and habitat utilization of adult California sheephead, *Semicossyphus pulcher* (Labridae), in a temperate no-take marine reserve. Mar. Biol. **147**(2): 301–311. doi:10.1007/s00227-005-1573-1.

Triantafyllidis, A., Apostolidis, A.P., Katsares, V., Kelly, E., Mercer, J., Hughes, M., Jørstad, K.E., Tsolou, A., Hynes, R., and Triantaphyllidis, C. 2005. Mitochondrial DNA variation in the European lobster (*Homarus gammarus*) throughout the range. Mar. Biol. **146**(2): 223–235. doi:10.1007/s00227-004-1435-2.

van der Meeren, G.I. 1997. Preliminary acoustic tracking of native and transplanted European lobsters (*Homarus gammarus*) in an open sea lagoon. Mar. Freshw. Res. **48**(8): 915–921. doi:10.1071/MF97126.

Worm, B., Hilborn, R., Baum, J.K., Branch, T.A., Collie, J.S., Costello, C., Fogarty, M.J., Fulton, E.A., Hutchings, J.A., Jennings, S., Jensen, O.P., Lotze, H.K., Mace, P.M., McClanahan, T.R., Minto, C., Palumbi, S.R., Parma, A.M., Ricard, D., Rosenberg, A.A., Watson, R., and Zeller, D. 2009. Rebuilding global fisheries. Science (Washington, D.C.), **325**(5940): 578–585. doi:10.1126/science.1173146. PMID:19644114.

Worton, B.J. 1989. Kernel methods for estimating the utilization distribution in home-range studies. Ecology, **70**(1): 164–168. doi:10.2307/1938423.

Zeller, D.C. 1997. Home range and activity patterns of the coral trout *Plectropomus leopardus* (Serranidae). Mar. Ecol. Prog. Ser. **154**: 65–77. doi:10.3354/meps154065.

Fatty acid signatures of Lake Michigan prey fish and invertebrates: among-species differences and spatiotemporal variability

Sergiusz J. Czesny, Jacques Rinchard, S. Dale Hanson, John M. Dettmers, and Konrad Dabrowski

Abstract: Lipid concentration and fatty acid composition of common prey species or taxonomic groups from four distinct regions of Lake Michigan were quantified (n = 894). We used a combination of parametric and nonparametric statistics to assess the differences in fatty acid signatures (FAS) among species and to evaluate intraspecies variation relative to interspecies variation in FAS. Discriminant function analysis performed on 13 species or taxa groups using the 18 most abundant fatty acids revealed clear separation among taxa, with overall classification success reaching 89%. Species were readily distinguished based on their overall fatty acid profile in spite of intraspecies variation (temporal, regional, and size-related). Among species sampled, pelagic and benthic clusters were formed based on the degree of fatty acid profile similarity. In alewife (*Alosa pseudoharengus*) and round goby (*Neogobius melanostomus*), fatty acid compositions differed with fish size, sampling location, and temporal variation; however, the magnitude of these differences was small relative to differences between species. Our results demonstrate the utility of fatty acid signatures in studies of food webs in large freshwater ecosystems. This study is also a necessary first step toward development of mechanistic research that investigates the effects of variation in fatty acids within the prey base on top predators.

Résumé : Nous avons mesuré les concentrations de lipides et la composition en acides gras des espèces ou groupes taxonomiques communs de proies (n = 894) dans quatre régions distinctes du lac Michigan. Une combinaison de méthodes statistiques paramétriques et non paramétriques nous ont servi à déterminer les différences dans les signatures d'acides gras (FAS) entre les espèces et d'évaluer la variation des FAS au sein des espèces relativement à la variation entre les espèces. Une analyse discriminante faite sur 13 espèces ou groupes taxonomiques avec les 18 acides gras les plus abondants présente une nette séparation entre les taxons avec un succès global de la classification de 89 %. Les espèces peuvent être clairement séparées d'après leur profil global d'acides gras malgré la variation intraspécifique (temporelle, régionale et reliée à la taille). Parmi les espèces échantillonnées, il se forme des regroupements pélagique et benthique d'après le degré de similarité de leurs profils d'acides gras. Chez le gaspareau (*Alosa pseudoharengus*) et le gobie à taches noires (*Neogobius melanostomus*), la composition en acides gras varie en fonction de la taille du poisson, du site d'échantillonnage et de la variation temporelle, mais l'importance de ces différences est faible par rapport aux différences entre les espèces. Notre étude démontre l'utilité des signatures d'acides gras dans les études de réseaux alimentaires dans les grands écosystèmes d'eau douce. Notre travail est aussi un premier pas essentiel dans la mise au point d'une recherche mécaniste qui étudie les effets de la variation des acides gras dans le contingent de proies sur les prédateurs supérieurs.

[Traduit par la Rédaction]

Introduction

Lake Michigan's food web has been, and is, undergoing major changes because of various anthropogenic stressors. Successful establishment of invasive species can exert both top-down and bottom-up effects with negative consequences to ecosystem function (Mills et al. 1993; Morrison et al.

Received 28 July 2010. Accepted 24 March 2011. Published at www.nrcresearchpress.com/cjfas on 14 July 2011.
J21942

Paper handled by Associate Editor Ralph Smith.

S.J. Czesny. Lake Michigan Biological Station, Illinois Natural History Survey, University of Illinois, 400 17th Street, Zion, IL 60099, USA.
J. Rinchard. Department of Environmental Science and Biology, The College at Brockport – State University of New York, 350 New Campus Drive, Brockport, NY 14420, USA.
S.D. Hanson. US Fish and Wildlife Service, Green Bay Fish and Wildlife Conservation Office, 2661 Scott Tower Drive, New Franken, WI 54229, USA.
J.M. Dettmers. Great Lakes Fishery Commission, 2100 Commonwealth Boulevard, Suite 100, Ann Arbor, MI 48105, USA.
K. Dabrowski. School of Environment and Natural Resources, The Ohio State University, 2021 Coffey Road, Columbus, OH 43210, USA.

Corresponding author: Sergiusz J. Czesny (e-mail: czesny@illinois.edu).

doi:10.1139/F2011-048

2000; Madenjian et al. 2008). Shifts in existing food web linkages may influence the pathways of energy and nutrient flow through the entire ecosystem. For millennia, energy in Lake Michigan has flowed through a pelagic food chain via phytoplankton, zooplankton, and pelagic planktivores, with a strong benthic link provided by *Diporeia hoyi*. In recent decades, alewife (*Alosa pseudoharengus*), rainbow smelt (*Osmerus mordax*), and bloater (*Coregonus hoyi*) were the most numerous planktivores, providing prey to pelagic salmonine piscivores (Madenjian et al. 2002; Mills et al. 2003). As part of this food web, key benthic–pelagic linkages occurred via the large, vertically migrating invertebrate *Mysis diliviana* and *Diporeia hoyi*. More recently, however, the structure and relative energy and nutrient flow has begun to change. Dreissenid mussels (zebra mussel *Dreissena polymorpha* and quagga mussel *Dreissena rostriformis bugensis*) and round goby (*Neogobius melanostomus*) are now integral components of Lake Michigan's ecosystem (Kuhns and Berg 1999; Clapp et al. 2001), resulting in a greater proportion of energy flow shifting to the benthic community and steadily diminishing productivity in the pelagic zone (Nalepa et al. 2009). Such changes in energy and nutrient flow at the ecosystem level impact top consumers that respond via their own population success to reduced pelagic prey species abundance. This has the effect of further destabilizing the food web through a reduction in top-down predatory pressure. Understanding how invasive species coexist within Lake Michigan food webs is essential for adequate management responses and conservation efforts.

A first step towards better understanding consequences of food web "reorganization" associated with non-native species invasions, and thus altered species assemblages, is to establish reliable means of delineating food webs' structure. Analysis of fatty acid signatures (FAS) can effectively mark trophic position in food web studies. Foraging patterns and overlaps in feeding niches among animals from various taxonomic groups as well as among members of the same taxa can be studied using this biochemical method. Diets of crustaceans (Brett et al. 2006), fish (Dalsgaard et al. 2003), birds (Raclot et al. 1998; Käkelä et al. 2006), and mammals (Iverson et al. 1997; Thiemann et al. 2008) have been reliably described using FAS. These signatures also enable detection of diet shifts within populations (Kirsch et al. 1998), including spatial (Iverson et al. 2002) or temporal (Budge et al. 2002) differences related to ontogenetic diet shifts, and variation in prey assemblages or foragers' migratory patterns (Thiemann et al. 2008). The utility of fatty acid profiles as food web markers depends on the assumption that each species has a distinct FAS. Although this assumption is relatively well documented in marine environments (for review see Budge et al. 2006), the utility of FAS has not been confirmed in large freshwater systems.

Along with their biomarker importance in aquatic food webs, fatty acids are key nutrients that influence physiological performance of aquatic organisms. They are a source of metabolic energy (β-oxidation of fatty acids, which provides ATP), components of cellular membranes (supporting membrane viscosity and permeability), and precursors of ecosanoids (e.g., controlling immune responses, ovulation, embryonic development, hatching, and early larval performance; Tocher 2003). In most animals, linoleic (18:2n-6) and linolenic (18:3n-3) acids are essential and must be obtained through diet because organisms without chlorophyll lack Δ12 and Δ15 desaturases required for their formations from 18:1n-9. These dietary essential fatty acids can be desaturated and elongated to form the physiologically essential polyunsaturated fatty acids (PUFA). The degree to which an animal can perform these conversions is dependent on the relative activities of fatty acid elongases and desaturases in their tissues. The activity of these enzymes depends on the extent to which the species can or cannot readily obtain the end products of these conversions from their natural diets (Tocher 2003), but may also change during the ontogeny (Henderson et al. 1995).

Lake Michigan, with its dynamic food web, history of invasions, size, and high profile as a commercial and conservation focal point, presents an interesting and unique study system to investigate the current state of food web linkages and test the utility of FAS as markers in freshwater environments. As a first step in this delineation, our objectives were the following: (*i*) assemble a FAS library to examine the degree of interspecific and intraspecific variability in lipid concentration and fatty acid profiles among common prey species of fish and macroinvertebrates in Lake Michigan; (*ii*) within this library, determine the extent of spatial and temporal variation in fatty acid profiles of two dominant non-native forage species in Lake Michigan: alewife (a pelagic species) and round goby (a benthic species); and (*iii*) assess variation in individual fatty acid concentrations as a function of body size and lipid concentration in both alewife and round goby.

Materials and methods

Sample collection

Forage fish, macroinvertebrates, and zooplankton were collected during lake trout (*Salvelinus namaycush*), yellow perch (*Perca flavescens*), and other fisheries surveys between 2002 and 2006 from the Illinois management unit (IL) of Lake Michigan (Fig. 1). Gill nets, bottom trawls, and seines were used to obtain forage fish species, while benthic core sampling and SCUBA gear were employed to collect macroinvertebrates and dreissenid mussels. Zooplankton was collected with horizontal and vertical plankton net (64 μm) hauls. Samples were obtained seasonally (spring, summer, and fall) between fall 2002 and summer 2006, and sampling effort was not standardized across seasons or years, but rather was focused on collection of 15 individuals within each species or taxonomic group (forage fish and larger macroinvertebrates) or enough material for three composite samples (zooplankton, dreissenid mussels, and other small invertebrate) during each sampling event (season within a year). To assess potential ontogenetic differences in lipid concentrations and FAS in alewife and round goby, we collected two size ranges. Size groupings for alewife were small (≤90 mm) and large (>90 mm), while round goby size groupings used 70 mm as the separation point; these values were based on published accounts of ontogenetic diet shifts within these species (Stewart and Binkowski 1986; Taraborelli and Schaner 2002).

In addition, we collected forage fish species and dreissenid mussels in 2006 and 2007 from fisheries assessments in management units MM3, WM5, and WM3 to contrast intraspe-

Fig. 1. Study area: Lake Michigan (inset shows location in the Great Lakes region of North America); shaded areas indicate management units where samples for lipids and fatty acid analysis were collected, while black dots approximate sampling sites within management units.

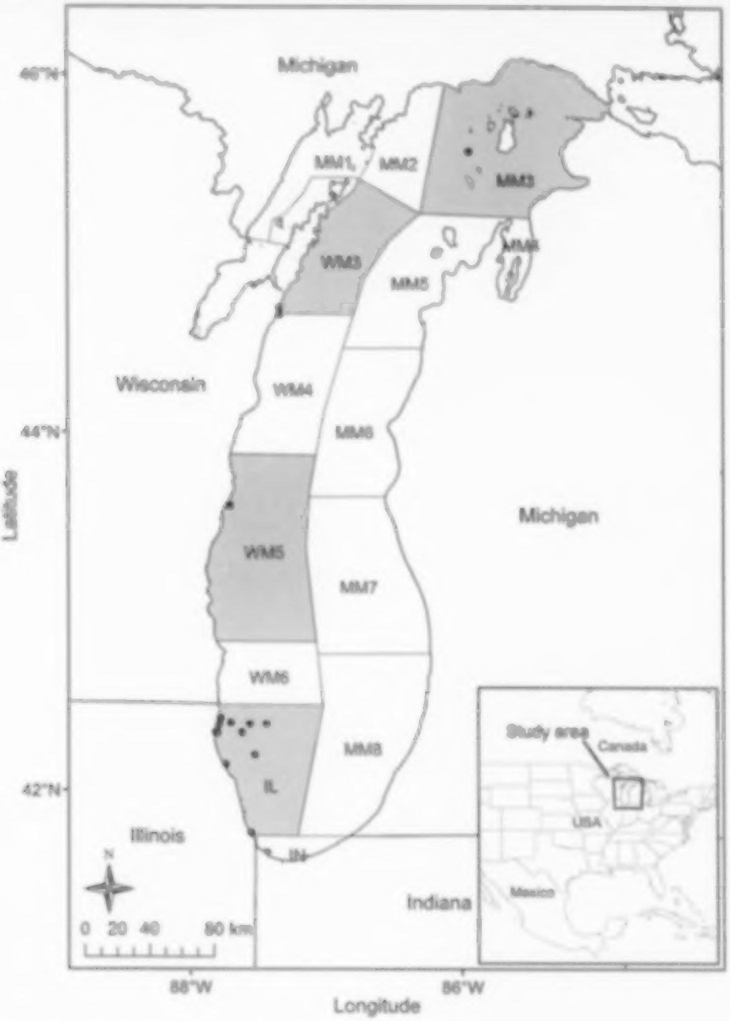

cies variation in FAS relative to spatial variation (Fig. 1). Immediately upon collection, all samples were frozen on dry ice, transferred to a bio-freezer (–80 °C), and stored until analysis (usually within 2–3 months). Only organisms alive at the time of collection were retained for analysis. A summary of all samples included in this study is presented in Table 1.

Lipid and fatty acid analysis

For analytical purposes, species or taxonomic groups were formed as follows: all fish were identified and grouped at the species level unless otherwise noted, while for practical reasons (time constraints related to identification and sorting) zooplankton, amphipods, arthropods, isopods, and dreissenid mussels (mostly *Dreissena r. bugensis* per Nalepa et al. 2009) were grouped and analyzed as such to ensure their freshness owing to the sensitive nature of fatty acid analysis. Individual fish were partially thawed, weighed to the nearest 0.1 g, measured for total length (mm), and cut into pieces <2 g and homogenized with a blender (Waring commercial blender, model 51B131, Fisher Scientific, Pittsburg, Pennsylvania). Individual invertebrates of the same species or taxonomic group, collected on the same date and site, were combined within a composite sample to acquire at least 1 g of material necessary for analysis. Crayfish species and dreissenid mussel samples were prepared by opening the carapace and shells, respectively, and removing all soft tissues for analysis.

Total lipids were extracted with chloroform–methanol (2:1, *v/v*) containing 0.01% butylated hydroxytoluene as an antioxidant (Folch et al. 1957). The organic solvent was evaporated under a stream of nitrogen and the lipid concentration determined gravimetrically. Fatty acid methyl esters (FAMEs) were prepared following the methods of Metcalfe and Schmitz (1961). FAMEs of samples collected prior to 2006 were separated using a gas chromatograph (GC) equipped

Table 1. Summary of samples (species and taxonomic groups) collected throughout the study.

Species	2002	2003	2004	2005	2006	2007	Total
Alewife ≤ 90 mm	***9f(IL)***	***10sp(IL)***, ***14s(IL)***, ***6f(IL)***	***12s(IL)***, ***9f(IL)***	***10sp(IL)***, ***8s(IL)***	***7s(IL)***, **38sp(MM3)**, **2s(WM3)**	**18sp(WM3)**	143
Alewife > 90 mm	—	**1s(IL)**	***10f(IL)***	***25sp(IL)***, ***17s(IL)***	***23s(IL)***, **15sp(MM3)**, **2s(WM3)**, **16f(WM3)**, **11sp(WM5)**	**19sp(WM3)**	139
Amphipods	*1s(IL)*	*2sp(IL)*, *3s(IL)*, *1f(IL)*	*1s(IL)*, *1f(IL)*	—	—	—	9
Arthropods	—	—	—	*2sp(IL)*	—	—	2
Bloater	—	—	**1s(IL)**	—	**29f(WM5)**	—	30
Crayfish spp.	—	***9sp(IL)***, ***10f(IL)***	***6sp(IL)***, ***1s(IL)***, ***7f(IL)***	***13sp(IL)***, ***1s(IL)***	—	—	47
Deepwater sculpin	—	—	—	—	**23sp(MM3)**	—	23
Isopods	—	*2s(IL)*	*4s(IL)*, *1f(IL)*	—	—	—	8
Johnny darter	—	—	*3s(IL)*, *3f(IL)*	—	—	—	6
Dreissenid mussels	—	—	***2s(IL)***	***6sp(IL)***, ***3s(IL)***	**4sp(MM3)**, **1sp(WM5)**	**3sp(WM3)**	19
Mysis diliviana	—	—	—	*3sp(IL)*, *5s(IL)*	—	—	8
Rainbow smelt	—	***4s(IL)***	***17s(IL)***	***6sp(IL)***, ***3s(IL)***	**21sp(MM3)**, **35f(WM3)**, **1sp(WM5)**	**17sp(WM3)**	104
Round goby ≤ 70 mm	—	—	***12f(IL)***	***21s(IL)***	***29sp(IL)***	—	62
Round goby > 70 mm	—	—	***6f(IL)***	***6sp(IL)***, ***15s(IL)***	***17u(IL)***, ***16sp(IL)***	**2sp(WM3)**	62
Slimy sculpin	—	—	—	—	**19sp(MM3)**, **9s(WM3)**	—	28
Spottail shiner	—	**1sp(IL)**, ***11s(IL)***	***2s(IL)***, ***8f(IL)***	***5s(IL)***	—	—	27
Stickleback spp.	—	***3s(IL)***	***6s(IL)***	**2s(IL)**	**10s(WM3)**	—	21
Yellow perch (adult)	—	—	—	—	***75sp(IL)***	—	75
Yellow perch (YOY)	—	—	***5s(IL)***, ***5f(IL)***	***21s(IL)***	—	—	31
Zooplankton	***3sp(IL)***, ***4s(IL)***	***3sp(IL)***, ***23s(IL)***	***7sp(IL)***, ***1s(IL)***	***2sp(IL)***, ***3s(IL)***	—	—	46

Note: Numbers represent sample size (*n*); lowercase letters represent seasons (sp, spring; s, summer; f, fall; u, unknown); and capital letters represent management units (MM, Michigan; WM, Wisconsin; IL, Illinois). Common font style is shared by samples included in particular statistical analyses: bold — discriminant function; italic — nonmetric multidimensional scaling (nMDS) in Illinois; underlined — nMDS regional.

with a flame ionization detector (Varian 3900 GC, Varian, Inc., Walnut Creek, California), a capillary column (Varian Chrompack capillary column (WCOT fused silica 100 m × 0.25 mm coating CPSIL 88 for FAME, DF = 0.2)), and an auto-injector (CP-8410 autoInjector, Varian, Inc.). The analysis of FAMEs from samples collected in 2006 and 2007 were performed with a Hewlett Packard 6890 GC (Palo Alto, California) equipped with a 7683 Series injector (Agilent Technologies, Palo Alto, California) interfaced to a Hewlett Packard 5973 mass selective detector. FAMEs were separated on an Omegawax 320 fused silica capillary column (30 m × 0.32 mm × 0.25 μm film thickness, Supelco, Bellefonte, Pennsylvania). In both GCs, the oven temperature was programmed from 175 °C for 26 min to 205 °C at 2 °C per min, then held at 205 °C for 24 min. Helium was used as the carrier gas at a rate of 1.8 mL·min^{-1}. For the GC with FID detector, the injector and detector temperatures were 270 and 300 °C, respectively, whereas for the GC – mass spectrophotometer (MS) the source and analyzer temperature of the MS was set at 230 °C.

Prior to transmethylation, a known amount of nonadecanoate acid (19:0, Nu-Check Prep Inc., Elysian, Minnesota), proportional to the amount of total lipids detected (8 mg per 50 mg of lipids) was added as an internal standard. The individual FAMEs were identified by comparing the retention times of authentic standard mixtures (FAME mix 37 components, Supleco) and with known spectrographic patterns of FAMEs. The FAMEs quantification was made by comparing their peak areas with that of the internal standard. All lipid and fatty acid data are expressed on the wet mass (wm) basis.

Statistical analysis

Discriminant function analysis (DFA) was used to determine which fatty acids most accurately separated species and (or) taxonomic groups and to test the predictive ability of FAS by assessing success rate of back-classification. To prevent misclassifications of subjects to groups with the largest variance, equality of covariance matrices is required. To achieve this requirement, the sample size of the smallest group has to be larger than the number of predictor variables (Stevens 1986). Thus, we limited the number of fatty acid variables to 18 (14:0, 16:0, 16:1n-9, 16:1n-7, 18:0, 18:1n-9, 18:1n-7, 18:2n-6, 18:3n-3, 18:4n-3, 20:1n-9, 20:4n-6, 20:4n-3, 20:5n-3, 22:4n-6, 22:5n-6, 22:5n-3, and 22:6n-3), allowing all aggregated species and taxonomic groups with sample size (n) of 18 or greater to be included in the analysis. Fatty acids listed above were selected based on the largest overall variance and an overall mean of >0.4% of total fatty acids across all species, accounting for nearly 97% of total fatty acids identified. Eight fish species were considered: alewife, round goby, rainbow smelt, spottail shiner (*Notropis hudsonius*), slimy sculpin (*Cottus cognatus*), deepwater sculpin (*Myoxocephalus thompsonii*), stickleback species, and yellow perch. Yellow perch were separated into adult and young of the year (YOY) to reflect their distinctly different diet, while ninespine sticklebacks (*Pungitius pungitius*) and threespine sticklebacks (*Gasterosteus aculeatus*) were combined to increase their sample size ($n \geq 18$). Crayfish, dreissenid mussels, and zooplankton samples were also included for a total of 13 groups in this analysis. Prior to DFA, percentage values for fatty acids were normalized using the log-ratio transformation (Aitchison 1986) according to the following equation: $X_{(\mathrm{trans})} = \ln(X_i / C_r)$, where X_i is a given fatty acid expressed as percentage of total fatty acids, $X_{(\mathrm{trans})}$ is the transformed fatty acid data, and C_r is the geometric mean of the 18 fatty acid variables. Wilks' λ was used to test the significance of the DFA to separate groups. The number of observations correctly classified was used to evaluate the performance of the DFA. Classifications were also cross-validated using a jackknife procedure, which allow us to determine into which group individuals were misclassified. While we are aware of other multivariate techniques that may be more suitable for analysis of compositional data (Jackson 1997), DFA has an advantage because of its predictive ability. The DFA was carried out with SPSS 17.0 (SPSS Inc., Chicago, Illinois).

Nonparametric methods were used to assess intraspecies group(s) variation relative to interspecies group(s) variation in FAS. Although nonparametric methods have no minimum sample size requirement, we only used species and taxonomic groups composed of at least three individual samples ($n \geq 3$) or alternatively samples consisting of a composite of individuals (zooplankton, dreissenid mussels, etc.). All nonparametric analyses were performed in PRIMER software v.6, Primer-E Ltd., Plymouth, UK) using untransformed data of the 28 detected fatty acids expressed as a percentage of total fatty acids, hereafter referred to as relative concentrations. We based our analysis on untransformed data to emphasize differences in pelagic and benthic species, as our goal is to provide a framework to interpret fatty acid signatures among top predators. Other applications such as distinguishing fatty acid profiles from species with similar ecological functions (e.g., alewives and rainbow smelt) may benefit from data transformation (e.g., square root, presence or absence, etc.) to place more emphasis on differences among less common fatty acids that may be more informative as biomarkers.

First, we analyzed samples collected from the Illinois management unit to address temporal and size-related variability in FAS. For alewife and round goby, groupings represented individuals, by size class, collected within the same season and year, hereafter termed sampling event, while data for other species were aggregated by year. Data for each grouping were averaged and a Bray–Curtis similarity matrix was computed. Cluster analysis was then used to generate similarity contours, whereby contours are drawn around samples (e.g., groupings) at an arbitrarily defined level of similarity between 0 and 100 (the number of clusters increases with the defined level of similarity). Nonmetric multidimensional scaling (nMDS) plots, with overlain similarity contours, were used to visualize the trophic pathways in two dimensions (e.g., conservation of fatty acids through the food web). The relative level of data distortion in each nMDS plot is described by a stress value, where stress values < 0.1 indicate an accurate representation of the data, while plots with stress values > 0.2 must be interpreted with caution. We then used individual (as opposed to group mean) FAS within the SIMPER routine to summarize which fatty acids contribute to dissimilarity between species groupings.

Alewife, round goby, rainbow smelt, and dreissenid mussels were collected from two or more management units and provided a basis to evaluate regional variation in FAS. For this analysis, data for each species were grouped by management unit and year. As before, we used nMDS plots and SIMPER output to describe the regional variation in FAS and specific fatty acid contributing to dissimilarity among species collected from different management units. We highlight the groups considered in the above described parametric and nonparametric analyses (Table 1).

Differences in total lipid concentration due to temporal variation and fish length were evaluated separately for alewife and round goby using an analysis of covariance. The relationship among relative fatty acid concentrations and fish length were investigated further with multivariate techniques. For alewife and round goby, we ran two-way nested analysis of similarity (ANOSIM) permutation tests (Clarke and Warwick 2001) to assess whether the fatty acid profiles varied temporally (essentially this corroborates the findings of the preceding analysis of covariance (ANCOVA) univariate analysis of total lipids but provides insight on specific fatty acid differences) or by size group. This analysis was restricted to samples collected within the Illinois management unit. The two-way ANOSIM uses a resemblance matrix, based on Bray–Curtis similarity of untransformed data in our study, and tests the null hypothesis that there are (*i*) no differences in similarity among FAS between sampling events within size classes and (*ii*) no differences in FAS similarity between size classes. Subsequent use of the SIMPER routine then outputs which specific fatty acids contribute to the dissimilarity between small and large size classes. Finally, we used simple regressions to investigate relationships among individual fatty acid concentration, body length, and total lipid for alewife and round goby.

Results

Weather and variable catch rates resulted in incomplete sampling among prey fish species and invertebrate groups across each season and year. A total of 597 samples from the Illinois management unit and 297 samples from other Lake Michigan management units (Fig. 1) were collected and analyzed for total lipid concentration and fatty acid composition representing 19 species or taxonomic groups. Nine fish species were sampled from the Illinois management unit, including five native species (e.g., johnny darter (*Etheostoma nigrum*), spottail shiner, ninespine stickleback, white sucker (*Catostomus commersonii*), and yellow perch) and four non-native species (e.g., alewife, rainbow smelt,

Table 2. Morphological characteristics, lipid concentration (expressed as percentage of wet mass) and fatty acid composition (percentage of total fatty acids detected) of fish species collected in the Illinois management unit (IL) from 2002 to 2006.

	Alewife	Johnny darter	Rainbow smelt	Round goby	Spottail shiner	Ninespine stickleback	Threespine stickleback	White sucker	Yellow perch (adult)	Yellow perch (YOY)
n	161	8	30	122	27	6	5	2	75	31
Length (mm)	10.8±0.3	6.0±0.5	6.6±0.2	7.5±0.2	7.1±0.3	5.2±0.8	5.8±0.2	NA	24.0±0.4	5.4±0.2
Mass (g)	11.8±1.0	1.7±0.3	1.3±0.2	8.1±1.0	3.9±0.6	1.2±0.3	1.5±0.2	1.6±0.3	171.1±12.0	1.5±0.2
Lipid (% wm)	4.1±0.2	7.1±0.5	3.8±0.3	3.8±0.1	4.9±0.3	5.9±0.5	7.6±1.5	3.1±0.1	3.3±0.2	3.3±0.2
Saturated fatty acids (%)										
12:0	0.1±0.0	0.1±0.0	0.1±0.0	0.1±0.0	0.2±0.0	0.1±0.0	0.1±0.0	0.2±0.0	0.1±0.0	0.2±0.0
14:0	3.1±0.1	2.2±0.2	2.5±0.2	1.8±0.0	2.0±0.1	2.0±0.4	3.5±0.2	2.2±0.0	2.0±0.1	2.0±0.1
15:0	0.3±0.0	0.1±0.1	0.4±0.1	0.6±0.0	0.1±0.0	0.4±0.2	0.0±0.0	0.2±0.2	0.3±0.0	0.7±0.1
16:0	19.0±0.2	18.3±0.8	18.4±0.3	14.7±0.2	17.0±0.4	18.3±1.3	15.2±0.7	18.0±0.1	16.4±0.2	19.1±0.5
17:0	0.4±0.0	0.6±0.2	0.5±0.1	0.8±0.0	0.5±0.1	0.4±0.1	0.2±0.1	0.3±0.0	0.2±0.0	0.5±0.0
18:0	5.3±0.2	3.1±0.3	4.3±0.2	5.6±0.1	5.5±0.2	4.9±0.7	3.5±0.3	6.3±0.0	3.8±0.1	5.7±0.3
Subtotal	28.2±0.2	24.5±1.0	26.1±0.4	23.6±0.3	25.2±0.6	26.1±1.6	22.4±0.7	27.1±0.1	22.7±0.3	28.2±0.6
Monounsaturated fatty acids (%)										
14:1	0.1±0.0	0.2±0.2	0.6±0.2	0.1±0.0	0.2±0.1	0.5±0.4	0.1±0.0	0.3±0.1	0.2±0.0	0.3±0.1
16:1n-9	0.9±0.0	1.0±0.2	0.6±0.1	1.5±0.1	0.9±0.1	0.9±0.2	0.7±0.2	1.0±0.0	1.2±0.0	0.7±0.1
16:1n-7	4.7±0.2	22.1±1.4	5.1±0.6	9.5±0.3	13.5±0.5	10.6±1.2	9.3±1.2	16.6±0.1	13.5±0.5	9.5±1.1
17:1	0.2±0.0	0.1±0.0	0.3±0.0	0.6±0.0	0.7±0.1	0.1±0.0	0.1±0.1	0.5±0.4	0.3±0.0	0.4±0.0
18:1n-9	13.0±0.4	11.4±0.7	8.2±0.3	11.8±0.2	13.6±0.6	12.0±1.4	10.3±0.3	6.9±0.4	13.9±0.3	8.9±0.4
18:1n-7	4.3±0.1	5.8±0.5	3.2±0.2	7.4±0.1	7.7±0.3	6.0±0.2	4.5±0.3	8.1±0.2	5.0±0.0	4.5±0.2
20:1n-9	2.0±0.1	1.0±0.1	2.4±0.2	1.4±0.1	0.7±0.0	1.1±0.2	2.2±0.2	1.3±0.0	0.6±0.0	1.3±0.0
22:1n-9	0.1±0.0	0.1±0.0	0.1±0.0	0.1±0.0	0.1±0.0	0.1±0.0	0.1±0.0	0.1±0.0	0.0±0.0	0.1±0.0
Subtotal	25.3±0.5	41.5±1.5	19.9±1.0	32.3±0.4	37.2±1.0	30.8±2.0	27.3±1.1	34.5±0.7	34.4±0.8	25.4±1.2
Polyunsaturated fatty acids (%)										
18:2n-6	4.1±0.1	4.5±0.3	4.4±0.2	4.5±0.1	4.3±0.2	3.8±0.7	7.5±0.4	2.7±0.0	2.9±0.1	4.3±0.2
11,14–18:2	0.4±0.0	0.4±0.0	0.3±0.0	0.4±0.0	0.3±0.0	0.4±0.1	0.3±0.1	0.4±0.0	0.1±0.0	0.6±0.0
18:3n-3	3.3±0.1	2.4±0.3	4.1±0.2	3.8±0.2	2.1±0.1	1.9±0.4	5.1±0.5	1.9±0.1	1.1±0.1	2.8±0.2
18:4n-3	0.6±0.0	0.4±0.1	0.3±0.0	0.9±0.0	0.6±0.1	0.4±0.1	0.4±0.1	0.4±0.1	0.4±0.0	0.4±0.0
20:2n-6	0.8±0.1	0.3±0.0	0.8±0.1	0.5±0.0	0.6±0.0	0.6±0.1	1.5±0.1	0.3±0.0	0.3±0.0	0.4±0.0
20:3n-6	0.6±0.0	0.3±0.0	0.5±0.1	0.3±0.0	0.4±0.0	0.5±0.1	1.5±0.3	0.3±0.0	0.1±0.0	0.3±0.0
20:4n-6	5.4±0.1	2.7±0.2	4.4±0.3	6.2±0.1	3.6±0.2	4.5±0.4	2.7±0.4	4.5±0.0	5.5±0.2	4.8±0.2
20:3n-3	0.2±0.0	0.2±0.1	0.4±0.0	0.2±0.0	0.1±0.0	0.2±0.1	0.2±0.1	0.0±0.0	0.2±0.0	0.2±0.0
20:4n-3	1.4±0.0	0.4±0.0	1.0±0.1	0.4±0.0	0.8±0.0	0.9±0.1	2.6±0.3	0.6±0.0	0.3±0.0	0.6±0.1
20:5n-3	7.5±0.1	9.5±0.6	11.0±0.3	12.3±0.2	10.1±0.3	11.2±1.1	7.2±0.6	11.9±0.0	8.5±0.2	10.4±0.3
22:4n-6	1.0±0.1	0.8±0.1	1.7±0.1	1.1±0.0	0.6±0.1	1.0±0.2	1.8±0.3	0.6±0.1	0.5±0.0	1.2±0.1
22:5n-6	3.0±0.1	0.5±0.1	3.4±0.2	1.5±0.1	1.5±0.3	1.6±0.3	3.2±0.2	0.5±0.1	1.6±0.1	2.8±0.2
22:5n-3	2.3±0.0	3.8±0.3	1.4±0.1	4.7±0.1	2.5±0.3	5.7±0.8	5.6±0.2	3.1±0.1	3.1±0.1	1.7±0.0
22:6n-3	15.5±0.5	7.8±1.0	19.8±0.8	6.8±0.4	9.9±0.7	10.2±1.5	10.9±0.7	11.0±0.6	18.1±0.5	15.6±0.6
Subtotal	46.4±0.5	33.8±1.9	53.4±1.1	43.9±0.4	37.4±0.9	42.7±2.3	50.3±1.5	38.2±0.5	42.6±0.7	46.0±0.8

Table 2 (*concluded*).

	Alewife	Johnny darter	Rainbow smelt	Round goby	Spottail shiner	Ninespine stickleback	Threespine stickleback	White sucker	Yellow perch (adult)	Yellow perch (YOY)
Sum n-3	31.0±0.4	24.4±1.7	37.9±0.8	29.2±0.4	26.1±0.7	30.4±2.4	32.0±0.5	28.9±0.3	31.6±0.6	31.5±0.6
Sum n-6	15.0±0.2	9.0±0.5	15.2±0.4	14.2±0.2	11.0±0.4	11.9±0.6	18.1±1.2	8.8±0.2	10.9±0.2	13.9±0.6

Note: Data are expressed as mean ± standard error. YOY, young of the year; wm, wet mass; NA, not available.

round goby, and threespine stickleback) (Table 2). For invertebrates, we collected seven components of Lake Michigan food web (Table 3). Sample collections from other management units included alewife, bloater, deepwater sculpin, ninespine stickleback, rainbow smelt, round goby, slimy sculpin, and dreissenid mussels (Table 4).

Mean lipid concentration of fish collected throughout the study period across all management units considered varied between 2.3% of wet mass in slimy sculpin from MM3 to 10.2% in bloater from WM5 (Tables 2 and 4). However, the within-species variation in total lipid concentration due to spatiotemporal factors can be quite substantial as shown for alewife (Fig. 2). Invertebrates generally had lower lipid concentration (~2%) except for crayfish (4.5%) (Tables 3 and 4). Twenty-eight fatty acids were routinely identified and quantified in all species. The most abundant fatty acids were generally similar across species, but at highly variable concentrations. Saturated fatty acids were predominantly represented by palmitic acid 16:0, and monounsaturated fatty acids were mostly represented by palmitoleic acid 16:1n-7 and oleic acid 18:1n-9. Among PUFA, most dominant were docosahexaenoic acid (DHA — 22:6n-3), eicosapentaenoic acid (EPA — 20:5n-3), arachidonic acid (ARA — 20:4n-6), and linoleic and linolenic acids. DHA was generally higher in fish associated with pelagic environment (alewife, rainbow smelt), while EPA was more concentrated among benthic-oriented fish species (round goby, deepwater sculpin). These trends, however, were dependent on spatiotemporal variation (i.e., slimy sculpin in MM3 *vs.* WM3). Predominance of EPA in PUFA was much stronger among invertebrates than fish, except for dreissenid mussels where DHA was found at higher concentrations (Table 3). Although PUFA were generally high in all analyzed groups, the proportions of particular PUFA varied substantially among them. The (n-3)/(n-6) ratios also varied considerably and ranged from 1.8 to 3.3 in fish and 1.5 to 3.1 in invertebrates.

DFA — broadscale classification of species by FAS

DFA performed on 13 species or taxa groups (with $n \geq 18$) using 18 of the most abundant fatty acids revealed relatively clear separation of investigated groups (Fig. 3). Twelve discriminant functions (DFs), or linear combinations of variables, were generated. The first two components derived from the DFA accounted for 55% of the variation (DF1 = 34.0% and DF2 = 19.9%) in fatty acid composition among the samples. Inclusion of DF3 (18.5%) and DF4 (8.8%) increased the cumulative variation explained to 81.2%. DF1 was defined by 16:1n-7, whereas DF2 separated groups based on the contrast in proportions of 22:6n-3 and proportions of 22:5n-6 (Fig. 3). The third and fourth functions discriminated proportions of 22:5n-3 and 18:1n-9, respectively. While bivariate plots, based solely on DF1 and DF2, showed clear separation among species, the use of only two DFs was insufficient to display distinct food web relationships (e.g., aggregations of species with similar trophic roles). Nevertheless, despite within-group variation, DFA classified them with 89% (761/857) overall success (Wilks' $\lambda = 0.001$; $P < 0.0001$). Cross-validation using jackknife procedure yielded 87% overall success rate in predicted group membership (Table 5). Of the small number of misclassified individuals, most were misclassified as species with likely overlapping diet (e.g., ale-

Table 3. Lipid concentration (expressed as percentage of wet mass) and fatty acid composition (percentage of total fatty acids detected) of invertebrates collected in the Illinois management unit (IL) from 2002 to 2006.

	Amphipods	Arthropods	Crayfish spp.	Dreissenid mussels	Isopods	*Mysis diliviana*	Zooplankton
n	9	2	47	11	7	8	46
Lipid (% wm)	2.8±0.3	2.6±0.4	4.5±0.3	1.1±0.1	2.0±0.2	3.1±0.3	2.2±0.2
Saturated fatty acids (%)							
12:0	0.3±0.0	0.1±0.0	0.2±0.0	1.0±0.1	0.2±0.0	0.1±0.0	0.1±0.0
14:0	1.8±0.4	9.2±1.4	1.4±0.1	3.5±0.4	2.0±0.0	4.4±0.5	4.9±0.4
15:0	1.0±0.5	0.3±0.0	0.3±0.1	2.5±0.5	0.2±0.1	0.5±0.1	0.3±0.1
16:0	18.2±0.8	18.9±0.3	16.9±0.5	18.7±0.8	19.6±0.6	18.1±0.7	21.7±0.4
17:0	0.3±0.1	0.1±0.0	0.5±0.1	0.4±0.1	0.1±0.1	0.2±0.0	0.2±0.0
18:0	2.0±0.1	2.0±0.0	3.3±0.2	2.9±0.1	3.5±0.4	1.4±0.2	3.4±0.1
Subtotal	23.6±0.8	30.6±1.0	22.6±0.6	29.0±0.7	25.6±0.7	24.7±0.4	30.7±0.6
Monounsaturated fatty acids (%)							
14:1	0.2±0.1	0.3±0.0	0.1±0.1	1.9±0.6	0.5±0.2	0.3±0.1	0.1±0.0
16:1n-9	0.5±0.1	0.7±0.0	1.9±0.3	1.6±0.1	0.8±0.2	0.9±0.1	0.8±0.1
16:1n-7	13.6±1.3	12.9±0.2	15.5±0.9	4.9±1.3	24.6±0.6	11.2±1.2	8.0±0.6
17:1	0.4±0.1	0.0±0.0	0.3±0.0	0.3±0.1	0.5±0.3	0.1±0.0	0.2±0.0
18:1n-9	16.1±0.5	15.9±0.1	13.1±0.5	6.4±0.2	9.9±0.6	12.0±0.8	7.1±0.3
18:1n-7	5.6±0.2	3.0±0.0	4.9±0.2	2.6±0.2	4.5±0.4	3.3±0.1	3.9±0.3
20:1n-9	0.9±0.1	2.1±0.0	1.0±0.1	2.7±0.2	1.2±0.1	2.7±0.5	4.9±0.2
22:1n-9	0.1±0.0	0.0±0.0	0.1±0.0	0.5±0.1	0.1±0.0	0.1±0.0	0.1±0.0
Subtotal	37.4±1.0	34.9±0.4	36.9±0.9	21.0±0.6	42.1±0.6	30.6±2.1	25.2±0.7
Polyunsaturated fatty acids (%)							
18:2n-6	5.8±0.6	3.2±0.1	5.0±0.4	3.9±0.2	4.4±0.4	3.4±0.3	6.5±0.1
11,14–18:2	0.5±0.0	0.6±0.0	0.3±0.0	0.3±0.1	0.8±0.0	0.6±0.1	0.7±0.1
18:3n-3	3.0±0.4	2.8±0.0	4.2±0.3	6.7±0.4	2.7±0.6	3.1±0.6	6.7±0.2
18:4n-3	0.6±0.0	1.2±0.0	0.8±0.1	2.5±0.5	0.1±0.0	1.1±0.1	0.3±0.1
20:2n-6	1.5±0.1	0.8±0.0	1.8±0.1	0.5±0.0	0.5±0.0	1.0±0.1	1.0±0.1
20:3n-6	0.6±0.1	0.7±0.0	0.8±0.0	0.1±0.0	0.3±0.1	1.0±0.4	0.8±0.1
20:4n-6	5.8±0.6	2.9±0.0	6.6±0.3	5.5±0.2	3.6±0.2	3.6±0.1	3.4±0.2
20:3n-3	0.1±0.0	0.1±0.0	0.1±0.0	0.1±0.1	0.0±0.0	0.1±0.0	0.1±0.0
20:4n-3	0.4±0.0	0.4±0.0	0.7±0.1	1.8±0.1	0.3±0.0	0.7±0.1	1.6±0.1
20:5n-3	15.2±0.6	14.5±0.3	13.7±0.4	7.6±0.3	16.0±0.7	16.5±0.9	10.3±0.5
22:4n-6	0.7±0.1	0.7±0.0	0.8±0.1	1.7±0.1	0.5±0.1	0.5±0.1	1.2±0.1
22:5n-6	0.5±0.1	1.2±0.0	1.1±0.1	6.9±0.2	0.4±0.1	1.5±0.2	2.9±0.2
22:5n-3	1.0±0.1	0.7±0.1	1.1±0.1	3.2±0.1	0.6±0.1	0.6±0.1	1.4±0.1
22:6n-3	3.6±0.4	4.6±0.1	3.7±0.3	9.4±0.4	2.3±0.4	11.2±1.5	7.2±0.5
Subtotal	39.1±1.6	34.5±0.7	40.5±0.9	50.1±0.9	32.4±1.0	44.8±1.8	44.2±0.7
Sum n-3	23.8±1.0	24.3±0.5	24.2±0.5	31.3±0.9	22.0±0.8	33.4±1.8	27.6±0.5
Sum n-6	14.9±1.0	9.6±0.2	16.0±0.7	18.6±0.5	9.6±0.4	10.9±0.5	15.8±0.4

Note: Data are expressed as mean ± standard error.

wives were misclassified as juvenile yellow perch, rainbow smelt, bloater, or spottail shiner, while round gobies were misclassified as slimy sculpin or stickleback species).

Analysis of interspecies groups variation in fatty acid compositions

Similarity among species and taxonomic group(s) mean fatty acid signatures for samples from the Illinois management unit are portrayed in an nMDS plot with overlain similarity contours to show the contrast in interspecies variation relative to temporal (sampling event) variation and size-related variation (Fig. 4). All species formed a single cluster below the 75% similarity level. Two clusters emerged at 75% similarity: one cluster encompassed zooplankton, dreissenid mussels, rainbow smelt, and alewife, while the second cluster was composed of benthic invertebrates (amphipods, arthropods, isopods, and *Mysis*), round goby, johnny darter, spottail shiner, adult yellow perch, and stickleback species. YOY yellow perch were variable; the 2005 year class grouped pelagically, while the 2004 year class was benthic. At 85% similarity, finer-scale clusters are evident, and SIMPER results indicated the zooplankton cluster was differentiated by a higher percentage of 16:0 and EPA, alewives and rainbow smelt were characterized by high concentrations of DHA and low concentrations of 16:1n-7, whereas round gobies and spottail shiners exhibited the reverse trend. Palmitoleic acid and DHA define the benthic and pelagic clusters, respectively, and notably these were the prominent fatty acid driving the first two DFs. Crayfish species, amphipods, and especially isopods exhibit the highest relative content of 16:1n-7.

Regional variation

FAS similarity among forage fish and dreissenid mussels collected within all management units generally show the clustering patterns as reported for the Illinois management unit (Fig. 5), though minor deviances from these patterns were noted. Rainbow smelt collected from the WM3 management unit in the spring of 2007 contained FAS more similar to round goby and stickleback species. However, rainbow smelt from this management unit sampled in the fall 2006 did group pelagically with rainbow smelt and alewife from other management units. Individual rainbow smelt within the WM3 2007 sample (spring) were smaller (89 ± 15 mm) than rainbow smelt in the WM3 2006 sample (116 ± 11 mm), and concentrations of 16:1n-7, 18:1n-7, 18:3n-3, and 22:6n-3 differed. Slimy sculpin from WM3 had a much lower concentration of DHA than slimy sculpin from MM3 (6.3% compared with 18.0%). Alewife, round goby, stickleback species, and dreissenid mussels did not show substantial variation in FAS across management units.

Alewife and round goby temporal and size-related variation in lipids and FAS

Alewife total lipid concentration varied temporally (across sample events) ($F = 10.7$, $P = 0.001$, df = 12), and fish length was a significant covariate ($F = 30.1$, $P = 0.001$, df = 1). Generally lipid concentration in alewives was lower in summer compared with fall, while spring concentrations were highly variable by year (Fig. 2). Multivariate analysis corroborated these results; the two-way nested ANOSIM indicated sample event (global R between sample events = 0.51, $P < 0.001$, 999 permutations) and size class (global R between size groups = 0.35, $P = 0.03$, 715 permutations) were significant factors affecting similarity levels among alewife fatty acid signatures (Fig. 6*a*; Table 6). SIMPER analysis showed that smaller alewives (≤90 mm) had higher percentages of DHA (mean of 17.4% ± 5.3% vs. 14.0% ± 7.4%) and decreased concentrations of oleic acid, 18:1n-9 (10.8% ± 2.8% vs. 15.2% ± 5.2%) compared with large alewives (>90 mm). Round goby were captured during only four sampling events within the Illinois management unit, and consequently our ANCOVA detected marginal evidence for temporal differences in round goby lipid concentration ($F = 2.6$, $P = 0.06$, df = 3), but length was a highly significant covariate ($F = 20.8$, $P = 0.001$, df = 1). However, the two-way ANOSIM indicated sample event (global R between sample events = 0.60, $P < 0.001$, 999 permutations) was significant but found no such relationship for size class (global R between size groups = 0.11, $P = 0.29$, 35 permutations) (Fig. 6*b*; Table 6).

To further examine variation in percent fatty acid concentrations and fish size, we present several examples of such relationships (Fig. 7). In alewife, 18:1n-9 proportion increased with size ($r^2 = 0.40$, $P < 0.001$), whereas 22:5n-6 and 22:6n-3 decreased in larger fish ($r^2 = 0.49$, $P < 0.001$ and $r^2 = 0.24$, $P < 0.001$, respectively) (Figs. 7*a* and 7*b*; 22:6n-3 not shown). In round goby, 16:1n-7 concentration increased with length ($r^2 = 0.39$, $P < 0.001$), whereas 18:0 decreased ($r^2 = 0.48$, $P < 0.001$) (Figs. 7*c* and 7*d*).

Lipid concentration, which tends to fluctuate during the year (see alewife seasonal changes in Fig. 2), also can affect relative proportions of fatty acids in fish tissues. As evidence of this dynamic, proportions of 18:2n-6 and 18:3n-3 in alewives increased with increasing total lipid concentration ($r^2 = 0.55$, $P < 0.001$ and $r^2 = 0.57$, $P < 0.001$, respectively) (Figs. 8*a* and 8*b*), whereas proportions of 20:4n-6 and 22:6n-3 decreased ($r^2 = 0.68$, $P < 0.001$ and $r^2 = 0.66$, $P < 0.001$, respectively) (Figs. 8*c* and 8*d*).

Discussion

This study represents the first large description of lipid concentration and fatty acid profiles among common species of prey fish and invertebrates in the Lake Michigan food web. Although several authors described the spatial–temporal dynamic of FAS among organisms in various marine environments (Iverson et al. 1997; Kirsch et al. 1998; Budge et al. 2002), this study provides the first comprehensive examination of FAS for multiple taxa representing a large freshwater ecosystem. Results presented herein not only permit differentiation of species and (or) taxonomic groups based on their FAS, but also describe diverse sources of within-species variability in fatty acid profiles related to size, region, season, and annum. Nevertheless, one must exercise caution when interpreting FAS results in the food webs because of the fact that internal biosynthetic capacities of most organisms have not yet been elucidated. Moreover, many species have very similar fatty acid profiles, making their use as biomarkers more difficult and not universally applicable (Dalsgaard et al. 2003).

General trends

FAS of organisms considered in this study were largely characterized by commonly occurring fatty acids from saturated fatty acids, monounsaturated fatty acids, and PUFA, such as 16:0, 16:1n-7, 18:1n-9, 18:3n-3, 20:5n-3, and 22:6n-3; however, we also noticed relatively high levels of fatty acids from the (n-6) family. Notably, 18:2n-6, 20:4n-6, and 22:5n-6 were found in appreciable concentrations among all organisms analyzed, which is consistent with the general notion that (n-6) fatty acids are relatively abundant in freshwater systems, while (n-3) fatty acids are dominant in both freshwater and marine environments.

Comparison of fatty acid profiles across species and taxonomic groups serves as a simple but useful indicator of the degree of similarity among animals that share common habitats or overlap foraging niches and yet often originate from different geographic areas within Lake Michigan. Discriminant analysis of the 13 most numerous species and taxonomic groups resulted in relatively high (89%) classification success. In spite of within-species or taxonomic group variation (temporal, regional, and size-related), species or taxonomic groups were readily distinguished based on their overall fatty acid profile. Similar, or higher, rates of classification success were reported in an analogous analyses conducted on marine fish and invertebrates (Budge et al. 2002; Iverson et al.

Table 4. Morphological characteristics, lipid concentration (expressed as percentage of wet mass) and fatty acid composition (percentage of units MM3, WM3, and WM5 from 2006 to 2007.

	Alewife			Bloater	Deepwater sculpin	Ninespine stickleback	Rainbow smelt		
	MM3	WM3	WM5	WM5	MM3	WM3	MM3	WM3	WM5
n	53	57	11	30	23	10	21	52	1
Length (mm)	8.0±0.2	12.0±0.5	16.1±0.3	25.4±0.8	8.7±0.5	5.9±0.3	11.9±0.4	10.7±0.2	16.0
Mass (mm)	4.5±0.3	18.9±2.1	34.7±1.4	170.6±14.7	6.6±0.9	1.3±0.2	7.9±0.9	9.1±0.4	26.2
Lipid (% wm)	4.3±0.3	3.5±0.3	5.0±0.9	10.2±0.8	3.1±0.2	4.1±0.4	2.6±0.2	4.9±0.2	4.5
Saturated fatty acids (%)									
12:0	0.0±0.0	0.0±0.0	0.0±0.0	0.2±0.0	0.2±0.0	0.0±0.0	0.0±0.0	0.2±0.0	0.1
14:0	3.1±0.1	2.5±0.2	3.4±0.9	4.3±0.1	3.2±0.2	2.1±0.3	2.9±0.2	3.3±0.1	3.9
15:0	0.5±0.0	0.4±0.0	0.4±0.0	0.4±0.0	0.4±0.0	0.3±0.0	0.4±0.1	0.4±0.0	0.3
16:0	15.8±0.2	18.3±0.3	16.3±0.4	13.1±0.3	15.4±0.3	15.4±0.3	16.2±0.3	13.9±0.1	13.5
17:0	0.7±0.0	0.6±0.0	0.5±0.0	0.4±0.0	0.3±0.0	0.7±0.1	0.5±0.1	0.5±0.0	0.2
18:0	4.3±0.1	5.7±0.2	4.3±0.2	3.0±0.1	3.8±0.3	6.0±0.4	3.6±0.1	3.7±0.2	2.4
Subtotal	24.4±0.3	27.4±0.3	25.0±0.5	21.3±0.3	23.2±0.3	24.5±0.5	22.5±1.0	22.0±0.2	20.4
Monounsaturated fatty acids (%)									
14:1	0.0±0.0	0.0±0.0	0.1±0.0	0.1±0.0	0.1±0.0	0.1±0.0	0.0±0.0	0.2±0.0	0.2
16:1n-9	0.6±0.0	0.7±0.0	0.8±0.1	0.2±0.0	0.7±0.0	0.7±0.0	0.7±0.1	0.6±0.0	0.6
16:1n-7	3.6±0.1	3.7±0.2	4.0±0.3	11.8±0.6	12.1±0.6	8.2±0.4	5.6±0.4	9.4±0.6	11.2
17:1	0.3±0.0	0.1±0.0	0.3±0.0	0.3±0.0	0.3±0.0	0.2±0.0	0.2±0.0	0.2±0.0	0.3
18:1n-9	11.5±0.3	13.8±0.8	18.8±0.8	23.8±0.7	14.4±0.3	11.4±0.6	10.5±0.7	14.6±0.4	24.7
18:1n-7	4.3±0.0	4.7±0.7	5.0±0.1	4.4±0.1	5.8±0.1	7.7±0.3	3.7±0.3	5.6±0.3	4.4
20:1n-9	1.4±0.1	1.1±0.1	1.5±0.1	2.1±0.1	1.0±0.0	1.1±0.1	0.7±0.1	1.4±0.1	1.2
22:1n-9	0.1±0.0	0.1±0.0	0.2±0.0	0.2±0.0	0.1±0.0	0.1±0.0	0.0±0.0	0.1±0.0	0.2
Subtotal	21.8±0.4	24.1±1.0	30.5±2.0	42.7±1.1	34.4±0.7	29.4±1.0	23.7±0.3	32.1±0.9	42.5
Polyunsaturated fatty acids (%)									
18:2n-6	4.3±0.1	3.4±0.2	4.0±0.3	3.6±0.1	2.6±0.2	3.4±0.3	3.7±0.3	5.3±0.2	3.9
11,14–18:2	0.1±0.0	0.1±0.0	0.1±0.0	0.2±0.0	0.2±0.0	0.2±0.0	0.1±0.0	0.2±0.0	0.1
18:3n-3	3.2±0.1	2.5±0.2	2.9±0.3	2.6±0.1	1.4±0.1	1.6±0.2	2.6±0.2	4.0±0.2	2.3
18:4n-3	1.8±0.1	1.2±0.1	1.4±0.2	1.4±0.1	1.5±0.1	0.8±0.1	1.4±0.1	2.2±0.2	1.3
20:2n-6	1.4±0.1	0.7±0.1	1.0±0.1	1.0±0.1	0.6±0.0	0.6±0.1	0.8±0.1	1.0±0.1	0.7
20:3n-6	0.3±0.0	0.2±0.0	0.2±0.0	0.4±0.0	0.0±0.0	0.2±0.0	0.1±0.0	0.4±0.0	0.1
20:4n-6	5.1±0.2	6.4±0.2	5.8±0.5	3.1±0.2	5.3±0.4	5.0±0.4	5.4±0.2	4.1±0.2	3.8
20:3n-3	1.4±0.1	0.7±0.1	0.9±0.1	0.7±0.1	0.4±0.0	0.6±0.1	0.8±0.1	1.0±0.1	0.5
20:4n-3	2.3±0.1	1.2±0.1	1.7±0.2	1.5±0.0	0.7±0.1	0.9±0.1	1.1±0.1	1.3±0.1	0.7
20:5n-3	9.0±0.2	8.8±0.2	8.3±0.2	7.7±0.1	15.1±0.3	11.5±0.7	10.8±0.4	11.2±0.2	9.3
22:4n-6	0.5±0.0	0.2±0.0	1.2±0.7	0.5±0.0	0.2±0.0	0.4±0.1	0.3±0.0	0.3±0.0	0.2
22:5n-6	4.0±0.1	2.4±0.1	2.1±0.2	1.4±0.1	0.8±0.0	1.8±0.2	2.9±0.1	1.4±0.1	1.5
22:5n-3	3.2±0.1	2.3±0.1	2.8±0.2	2.9±0.1	1.3±0.2	5.8±0.4	2.3±0.1	2.6±0.1	1.0
22:6n-3	17.3±0.5	18.4±1.1	12.2±1.4	8.9±0.3	12.2±0.7	13.3±0.9	22.5±1.0	11.0±0.6	11.6
Subtotal	53.8±0.4	48.5±0.8	44.5±2.2	35.9±0.8	42.4±0.6	46.0±0.8	54.9±0.9	45.8±1.0	37.0
Sum n-3	38.1±3.0	35.1±5.4	30.1±4.5	25.7±2.4	32.6±3.5	34.4±2.4	41.5±4.4	33.1±5.5	26.6
Sum n-6	15.6±1.0	13.3±1.1	14.3±3.0	10.0±2.1	9.6±2.1	11.4±1.1	13.3±1.6	12.5±2.2	10.3

Note: Data are expressed as mean ± standard error. NA = not applicable.

2002). In our study DFA, as one of the multivariate techniques, attempts to illustrate the degree of uniqueness of each subject based on a series of common traits. DFA was effective at evaluating broadscale differences but insufficient sample sizes, both temporally and spatially, precluded inferences on the importance of these sources of variability. This variation was addressed in our supporting nonparametric analysis, which used a fundamentally different approach based on the amount of similarity among species groups from each sampling event, by size class and management unit. Also, we were able to contrast similarity among fatty acid profiles of less commonly sampled species (e.g., spottail shiners, *Mysis diliviana*, amphipods, etc.). The nMDS plots of the similarity among group mean FAS resulted in a clear illustration of where species fit within pelagic and benthic clusters. While largely descriptive in nature, this nonparametric approach corroborated and expanded upon the results obtained with DFA, which provided a more ambiguous characterization of total fatty acids detected) of fish species and invertebrates collected in management

Round goby	Slimy sculpin		Dreissenid mussels		
WM3	MM3	WM3	MM3	WM3	WM5
2	19	9	4	3	1
12.9±2.5	7.1±0.2	6.2±0.5	NA	NA	NA
34.8±16.6	4.2±0.3	3.6±0.8	NA	NA	NA
2.6±0.8	2.3±0.2	4.8±0.5	1.0±0.2	0.8±0.1	0.7
0.0±0.0	0.1±0.0	0.2±0.0	0.0±0.0	0.0±0.0	0.1
1.1±0.1	1.7±0.2	1.9±0.1	3.1±0.2	1.7±0.1	1.9
0.4±0.1	0.4±0.0	0.3±0.0	0.6±0.1	2.1±0.1	0.4
15.8±1.8	15.2±0.2	16.0±0.3	18.2±1.4	19.8±0.4	20.7
1.0±0.2	0.6±0.0	0.3±0.0	0.7±0.1	0.6±0.0	0.7
4.6±1.0	6.0±0.3	4.2±0.3	2.9±0.4	3.3±0.1	3.9
23.0±3.0	24.0±0.3	22.8±0.5	25.6±1.9	27.5±0.5	27.6
0.0±0.0	0.0±0.0	0.1±0.0	0.0±0.0	0.0±0.0	0.9
0.0±0.0	1.1±0.1	0.5±0.1	0.3±0.0	0.2±0.1	0.3
8.8±2.0	6.5±0.5	21.9±1.1	9.9±1.4	8.0±0.2	5.8
0.2±0.2	0.2±0.0	0.2±0.1	0.0±0.0	0.0±0.0	0.0
10.3±1.6	9.8±0.4	11.7±0.6	8.6±0.3	6.6±0.7	12.1
7.4±0.8	5.2±0.3	2.7±0.1	2.3±0.2	2.3±0.1	3.5
1.6±0.7	1.9±0.1	0.8±0.1	5.5±1.3	5.5±0.4	1.4
0.0±0.0	0.1±0.0	0.0±0.0	0.0±0.0	0.0±0.0	0.0
28.3±5.3	24.8±0.8	42.1±1.3	26.5±0.5	22.6±0.4	24.0
3.2±0.6	2.0±0.2	2.7±0.1	5.7±0.1	3.0±0.2	6.1
0.0±0.0	0.1±0.0	0.2±0.0	0.1±0.0	0.0±0.0	0.0
0.0±0.0	0.8±0.1	1.1±0.1	5.8±0.7	4.0±0.1	6.7
0.9±0.4	0.5±0.1	0.8±0.1	5.3±1.4	1.4±0.0	3.1
0.3±0.3	0.5±0.1	0.2±0.0	0.3±0.1	0.0±0.0	0.3
0.1±0.1	0.1±0.0	0.2±0.0	0.0±0.0	0.0±0.0	0.0
8.5±0.9	10.0±0.5	4.0±0.3	3.6±0.8	6.7±0.3	4.6
0.1±0.1	0.2±0.1	0.1±0.0	0.0±0.0	0.0±0.0	0.0
0.1±0.1	0.3±0.1	0.1±0.0	0.2±0.1	0.0±0.0	0.3
13.3±0.8	10.6±0.5	14.1±0.5	9.1±1.9	9.5±0.2	7.1
1.4±0.3	0.8±0.1	0.3±0.0	0.9±0.4	2.3±0.2	1.0
2.8±0.2	2.4±0.4	0.2±0.0	5.1±1.3	6.9±0.4	6.1
8.8±0.6	4.9±0.3	4.6±0.1	2.6±0.3	6.1±0.2	3.8
9.2±1.7	18.0±0.9	6.3±0.7	9.1±0.2	10.1±0.2	9.4
48.7±2.3	51.2±0.8	35.0±1.0	47.9±1.5	49.9±0.8	48.4
32.4±3.5	35.3±3.6	27.1±2.5	32.2±7.6	31.0±0.6	30.3
16.3±0.3	15.8±2.5	7.6±0.9	15.6±4.8	18.9±1.4	18.1

food web relationships (e.g., aggregations of species with similar trophic roles) represented by plotting only the first two DFs.

Similar patterns of fatty acid profiles in species that are unrelated or occupy different trophic levels may be associated with one of two mechanisms related to horizontal or vertical nature of food web interactions. Organisms can either share common food resources (horizontal) or one group constitutes food for the other group (vertical). The first mechanism, portrayed by Budge et al. (2002), relates to common diet (e.g., planktivorous) shared among members of distinctly different families of fish (e.g., capelin, herring, and sand lance). Similar, horizontal patterns of food web interactions were illustrated among different species of Arctic amphipods (Auel et al. 2002). Both DFA and nonparametric analysis in the above study placed these horizontally related species in a common group that was distinct from other considered species. In our study, such delineation could be used to explain the relative close position of alewife, rainbow smelt, and some YOY yel-

Fig. 2. Boxplots (line, median; box, interquartile range (IR) centered at the median; whiskers 3 × IR centered at the median; circles are shown for outliers that fall outside of the whiskers) showing the variation in total lipid concentration among alewives sampled by season, year, and management unit.

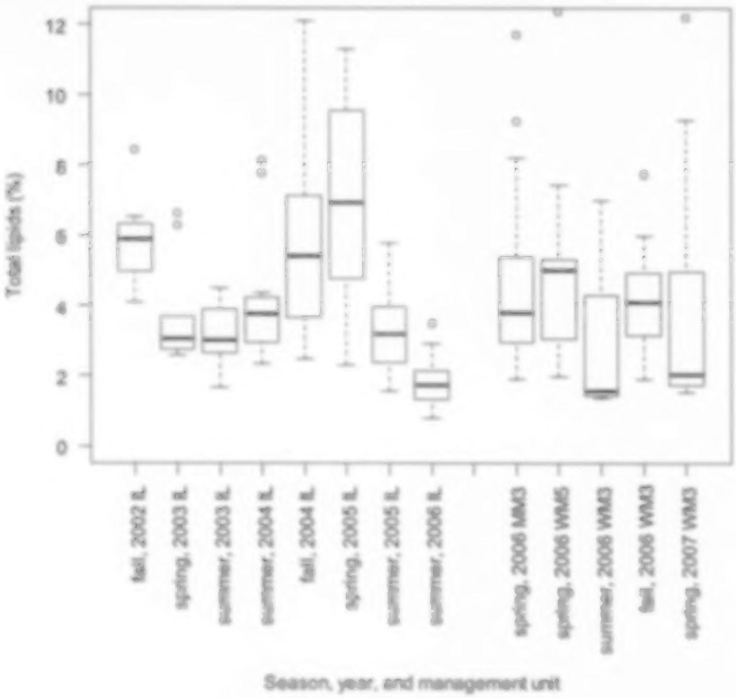

Fig. 3. Discriminant analysis of the 13 species or taxonomic groups (with $n \geq 18$) using 18 of the fatty acids selected based on the largest overall variance and an overall mean of >0.4% of total fatty acids across all groups. Plot shows the average scores of the first 2 of 12 discriminant functions that classified individuals to species or taxonomic groups with an 89% success rate.

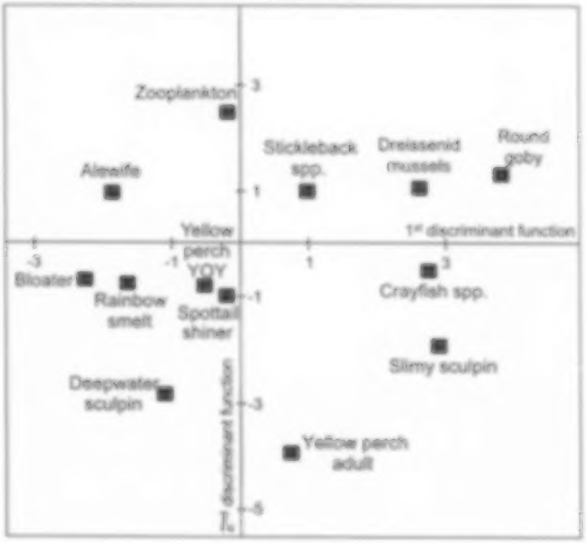

low perch. FAS similarity among these groups is most likely due to the same food base (zooplankton). Interestingly, the pelagic signature noted in 2005 YOY yellow perch sampled in the summer, presumably when they were actively feeding on zooplankton, differed from the benthic signature displayed by fish caught in late summer and fall of 2004, by which time they had attained a large enough size that macroinvertebrates were prominent potential prey items.

FAS of two unrelated species can also resemble each other when one species feeds predominantly on the other species. Such dietary dependence, reflected in similar FAS, has been demonstrated in a wide range of foragers. FAS of fish, birds, and mammals have all been reliably linked to fatty acid profiles of their food (Raclot et al. 1998; Iverson et al. 2002; Thiemann et al. 2008). Our study examined lower level prey fish and invertebrates (e.g., no top predator species) and does not provide unambiguous examples of such dietary dependence when DFA is applied and a wide range of fatty acids is considered. This is likely due to highly variable FAS among primary consumers and our inability to sample their FAS at seasonal intervals comparable to alewife and round goby. Recent diet studies show that Lake Michigan yellow perch consume round gobies and other benthic-oriented fish and macroinvertebrates compared with historical accounts when alewife and rainbow smelt were dominating their diet (Czesny et al. 2006; Truemper et al. 2006). Short-term feeding trials suggest adult yellow perch prefer to feed on alewives (Weber et al. 2010), yet we found they contained a benthic FAS, suggesting yellow perch are utilizing the recently expanding populations of round goby in the lake. Sea-

Table 5. Predicted group classification from discriminant function analysis of 13 species and taxa groups ($n \geq 18$); 89% (761/857) of individuals were correctly classified.

	Alewife	Round goby	Rainbow smelt	Yellow perch (adult)	Crayfish spp.	Zooplankton	Yellow perch (YOY)	Bloater	Slimy sculpin	Spottail shiner	Deepwater sculpin	Stickleback spp.	Dreissenid mussels	Total
Alewife	248	1	7	2	0	0	16	2	0	4	1	1	0	282
Round goby	0	114	0	2	0	0	0	0	5	0	0	3	0	124
Rainbow smelt	3	0	84	1	0	0	6	0	0	7	2	1	0	104
Yellow perch (adult)	0	0	0	70	0	0	0	0	4	0	1	0	0	75
Crayfish spp.	0	1	0	0	46	0	0	0	0	0	0	0	0	47
Zooplankton	0	0	0	0	4	40	2	0	0	0	0	0	0	46
Yellow perch (YOY)	0	0	1	2	0	0	25	2	0	2	0	0	0	31
Bloater	1	0	0	0	0	0	0	28	0	1	0	0	0	30
Slimy sculpin	0	1	0	0	0	0	0	0	26	0	0	1	0	28
Spottail shiner	0	0	0	1	0	0	1	0	0	23	0	2	0	27
Deepwater sculpin	0	0	0	0	0	0	0	0	1	0	22	0	0	23
Stickleback spp.	1	2	0	0	0	0	0	0	0	0	0	18	0	21
Dreissenid mussels	0	0	1	0	0	1	0	0	0	0	0	0	17	19

sonal movement of yellow perch, inshore in early spring and offshore in the fall, can also affect their fatty acid profiles because perch likely consume different prey nearshore compared with offshore. Thus, it may be informative to expand adult yellow perch sampling over the entire year. Supplementing fatty acid analyses with stomach content surveys when determining fish feeding patterns and use of a larger number of fatty acids to increase resolution, as suggested by Budge et al. (2002), is also recommended.

Sources of variation in lipids and FAS

Annual and seasonal variation in productivity at the base of aquatic food webs is tied to nutrient fluxes and physical conditions, which in turn affect food resources (quantitative and qualitative) for primary and secondary consumers. Total lipid concentration in fish varies seasonally and is reflective of food richness and reproductive cycle. Lipid concentration of alewife collected in spring, summer, and fall varied considerably, with lowest concentrations observed during summer months. Such a seasonal drop in the summer is consistent with earlier reports by Madenjian et al. (2000, 2002, 2006) and shows that Lake Michigan alewife condition fluctuates and reflects their variable feeding rates though the year (Stewart and Binkowski 1986) and reproductive cycle. Similar to alewife, round goby mean total lipid concentration also varied seasonally. Alewife, given its status as the preferred prey for Lake Michigan salmonines, has been better studied than recently established round goby, and yet the latter species is lately becoming an important component in the diets of top predators. Thus, potential differences in energy dynamic or other nutritional traits that differentiate these two species should be investigated in the context of nutritional value they provide for top predators. For example, it is quite conceivable to expect that round goby constitutes a viable prey, alternative to alewife, for lake trout that have been feeding on thiamine-depleting alosids for years. In fact, recent reports from Lakes Huron and Ontario suggested such a scenario where round goby could have been ameliorating the negative effects of alewife in lake trout diet (Fitzsimons et al. 2009, 2010).

Annual and seasonal variation in food quantity and quality is common in aquatic food webs because productivity is tied to annual variability in bottom-up and top-down pressures as well as varying physical conditions. This annual and seasonal variation in quantity and quality of food resources would be expected to influence fatty acid profiles of consumers. Availability of fatty acids, especially PUFA, at the bottom of the food web (i.e., primary producers) varies across seasons because PUFA synthesis is species-specific (Graeve et al. 2002; Reuss and Poulsen 2002). As such, different species of algae, which bloom in seasonal succession, synthesize PUFA at different rates. For example, diatoms, which bloom early in spring, are rich in EPA (Napolitano et al. 1994), while dinoflagellates contain high concentrations of DHA (Napolitano et al. 1995). Consequently, PUFA available to higher trophic levels (zooplankton, zooplanktivorous fish, and eventually piscivores) can be affected because their PUFA intake will depend on PUFA availability at lower trophic levels, as shown in laboratory experiments (Brett et al. 2006). Some field studies, however, suggest a less direct link between fatty acid concentration in seston and in zooplankton

Fig. 4. nMDS plot of group-averaged fatty acid signature data for samples from the Illinois management district. Alewife and round goby data were averaged by season–year and size class; all other data were averaged by species or taxa group and year. Solid and dashed ovals enclose clusters of group means with 75% and 85% similarities, respectively.

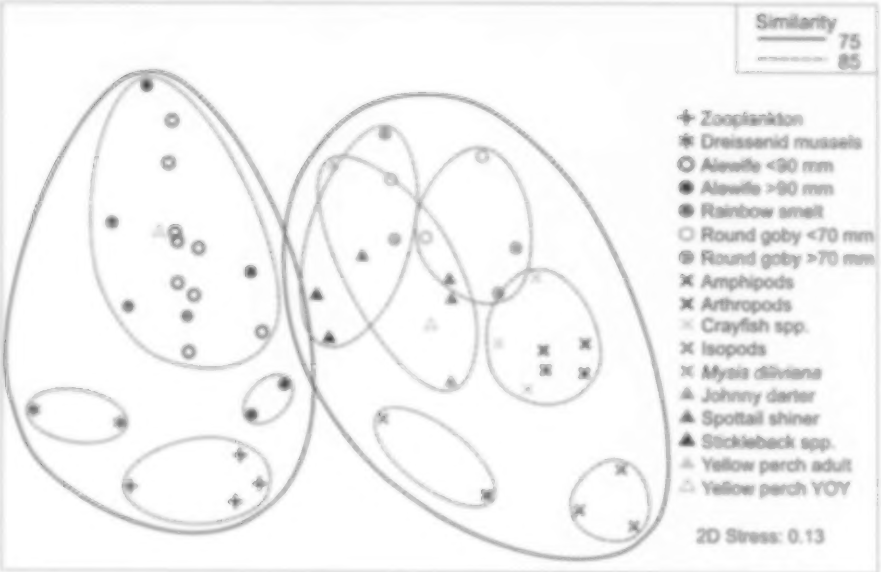

Fig. 5. nMDS plot of the similarity among annual group mean fatty acid signatures for alewife, round goby, and other selected species from different management units of Lake Michigan. Solid and dashed ovals enclose clusters of group means with 80% and 90% similarities, respectively.

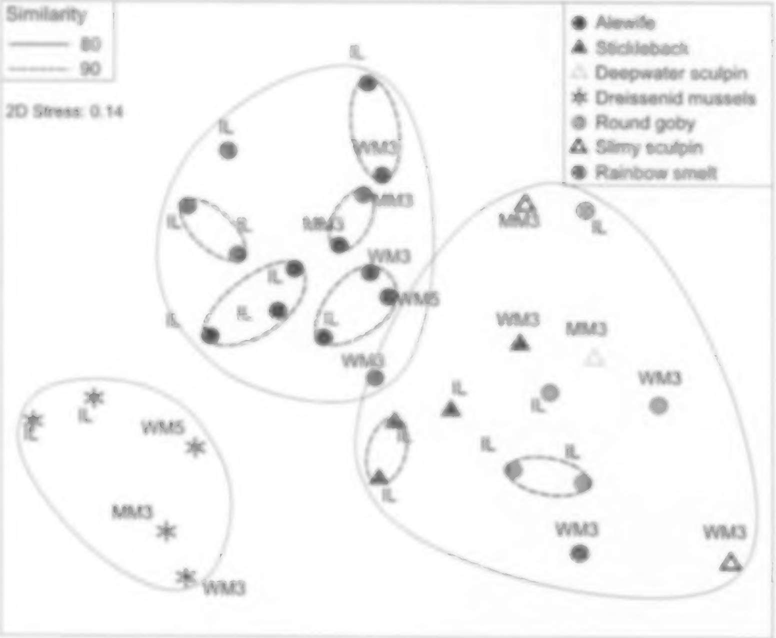

(Persson and Vrede 2006; Smyntek et al. 2008), which may be related to the fatty acid biosynthetic capacity of primary consumers. Our study reports annual mean FAS among zooplankton sampled throughout the water column, and we focus our analysis on the variability in fatty acid profiles among the more stable (e.g., longer-lived) secondary consumers. While we were unable to describe the variation in PUFA among primary consumers given this would require frequent sampling at multiple limnetic strata, we observed the concentrations of 16:1n-7, 18:1n-7, 18:3n-3, and 22:6n-3 were substantially

Fig. 6. nMDS plots showing similarity in fatty acid signatures among group means of alewife (*a*) and round goby (*b*) by sample event and size class. Solid and dashed ovals enclose clusters of group means with 80% and 90% similarities, respectively. Open and solid circles represent, respectively, large and small size classes of alewife and round goby.

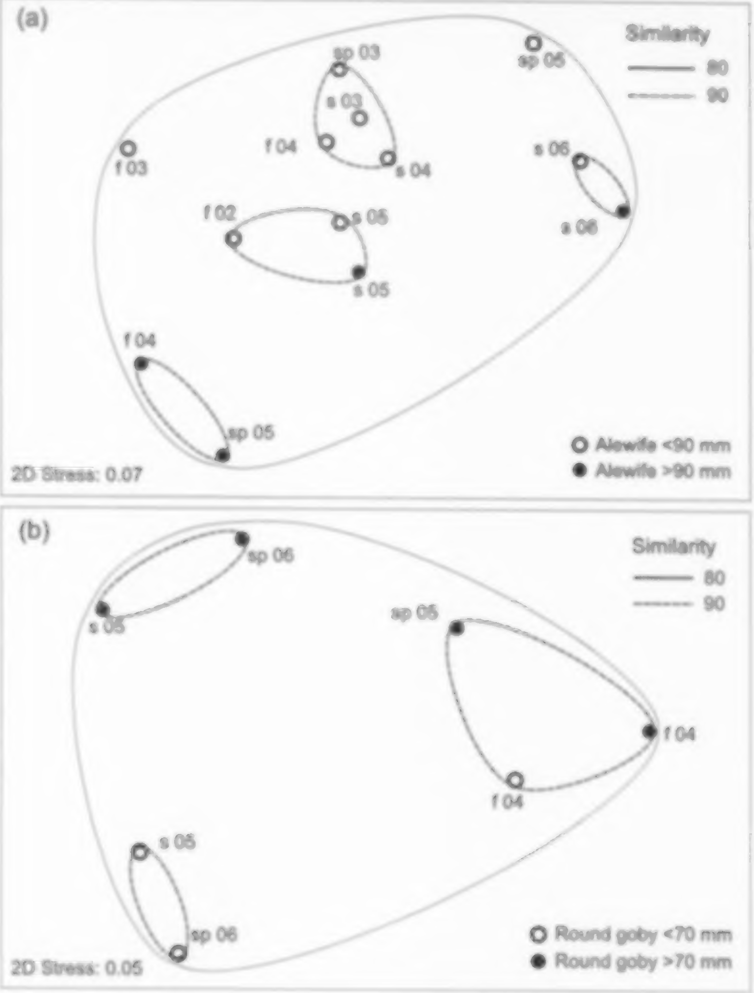

different in rainbow smelt sampled in two different years. This suggests that either rainbow smelt from WM3 sampled in spring of 2007 were at an ontogenetically earlier life stage and likely had not yet begun feeding offshore in the pelagic zone or that diatom abundance varied seasonally. On the other hand, differences in developmental stage do not explain deviations in slimy sculpin DHA concentration between sampling locations and rather suggest that regional variability may be a substantial source of variation though both samples remained within the benthic cluster with >80% similarity.

Varying PUFA concentrations in phytoplankton will also affect benthic organisms. Settling organic matter constitutes an important food resource for detrital-feeding invertebrates (Goedkoop and Johnson 1996), including dreissenid mussels. However, the amounts of PUFA reaching organisms at the bottom of the lake in the form of precipitating phyto-detritus may be changed because of rapid decomposition and oxidation (Frederickson et al. 1986). Thus, fish species associated with the benthic environment may contain different concentrations of PUFA compared with pelagic fish. In our study, within-species variation in FAS was apparent in alewife and round goby collected during three seasons. In both cases, fish captured through the year had distinctly different fatty acid profiles that likely resulted from changing availability of fatty acids in their food. Although, both alewife and round goby exhibited a sizable variation in FAS based on sampling period (sample event), in neither case were there consistent, seasonal, reoccurring patterns. This may be indicative of a system that is undergoing slow but constant succession rather than more cyclical seasonal fluctuations with regards to available pool of fatty acids.

Body size driven ontogenetic diet shifts and spatial heterogeneity in food resources can also influence fatty acid profiles. Alewife and round goby occupy and dominate

Table 6. Fatty acid concentration (percentage of total detected) in small and large alewife and round goby collected in Lake Michigan Illinois management unit.

	Alewife		Round goby	
	≤90 mm (*n* = 63)	>90 mm (*n* = 80)	≤70 mm (*n* = 63)	>70 mm (*n* = 52)
Saturated fatty acids				
12:0	0.1±0.1	0.1±0.1	0.1±0.1	0.1±0.0
14:0	2.9±1.3	3.3±1.6	1.6±0.3	2.0±0.5
15:0	0.2±0.2	0.4±0.2	0.7±0.3	0.6±0.2
16:0	18.9±2.0	18.8±2.1	14.9±2.1	14.2±1.9
17:0	0.3±0.2	0.5±0.2	1.0±0.5	0.7±0.3
18:0	5.1±1.5	5.5±2.5	6.3±1.4	4.6±0.8
Subtotal	27.6±0.4	28.6±0.3	24.6±0.4	22.1±0.4
Monounsaturated fatty acids				
14:1	0.2±0.3	0.2±0.3	0.1±0.1	0.2±0.1
16:1n-9	0.9±0.3	0.9±0.5	1.5±0.8	1.4±1.6
16:1n-7	4.3±1.8	4.8±2.1	8.3±2.5	11.4±2.7
17:1	0.2±0.1	0.3±0.2	0.6±0.5	0.7±0.4
18:1n-9	10.8±2.8	15.2±5.2	11.3±1.7	12.8±2.2
18:1n-7	4.3±0.9	4.4±0.7	7.8±1.3	7.1±1.5
20:1n-9	2.1±1.2	1.8±1.2	1.2±0.5	1.6±0.7
22:1n-9	0.1±0.1	0.1±0.1	0.1±0.1	0.2±0.1
Subtotal	22.8±0.6	27.7±0.8	31.0±0.5	35.3±0.6
Polyunsaturated fatty acids				
18:2n-6	4.3±1.0	4.0±1.2	5.0±1.6	4.1±1.2
18:3n-3	3.8±1.6	2.8±0.5	4.4±2.1	3.3±1.6
18:4n-3	0.4±0.4	0.8±0.5	1.0±0.5	0.9±0.3
20:2n-6	0.9±1.2	0.8±0.4	0.5±0.1	0.5±0.2
20:3n-6	0.6±0.3	0.6±0.6	0.3±0.1	0.2±0.2
20:4n-6	5.1±1.1	5.8±1.9	6.5±1.2	5.5±1.4
20:3n-3	0.1±0.1	0.3±0.2	0.2±0.1	0.2±0.1
20:4n-3	1.5±0.5	1.4±0.7	0.4±0.1	0.4±0.2
20:5n-3	7.7±2.0	7.3±1.7	12.4±1.7	12.2±2.3
22:4n-6	1.5±1.1	0.7±0.4	1.1±0.3	1.0±0.3
22:5n-6	3.6±0.7	2.6±0.8	1.4±1.0	1.6±1.1
22:5n-3	2.2±0.5	2.4±0.4	4.3±0.6	5.1±1.0
22:6n-3	17.4±5.3	14.0±7.4	6.5±3.8	6.9±4.5
Subtotal	49.6±0.7	43.7±0.6	44.4±0.4	42.6±0.8
Sum n-3	33.2±0.5	28.9±0.5	29.2±0.4	29.1±0.6
Sum n-6	16.1±0.3	14.4±0.2	14.8±0.2	13.1±0.3

distinctly different habitat and feed on distinctly different prey assemblages. Alewife is a pelagic species, whereas round goby is a benthic species with a strong competitive edge over native benthic-dwelling fish, in particular native sculpin species. Small alewives were shown to feed on cladocerans and copepods, whereas large individuals historically fed on *Diporeia* (Stewart and Binkowski 1986), but since the drastic decline of *Diporeia* (Nalepa et al. 1998, 2009) they now consume a more diverse diet composed of zooplankton, chironomids, and amphipods (Janssen and Luebke 2004). Small gobies rely on a variety of mobile invertebrates (chironomids, dipterans, cladocerans, and copepods), whereas larger gobies are known to consume mollusks (including dreissenid mussels) (French and Jude 2001; Taraborelli and Schaner 2002). In our study, two size classes of alewives and round gobies were defined based on the above mentioned studies (Stewart and Binkowski 1986; Taraborelli and Schaner 2002), but neither species FAS indicated such diet shifts during the ontogeny. Although we found size to be a major factor behind differences in total lipid concentrations in both species, no clear and consistent grouping by size emerged within FAS concntrations. These contradicting results likely stem from the use of size as a categorical variable in our nonparametric analysis of FAS compared with its use as a covariate in evaluating differences in total lipids. Linear relationships with a sizable "noise" between several fatty acids and fish size indicate a gradual transition rather than an abrupt switch from one food source to another would be a likely reason size classes did not group more clearly. Similarly, differences in FAS that are driven by changing diet were noted among YOY yellow perch that carried both pelagic (summer caught) and benthic (late summer – fall caught) signatures. Noteworthy is the fact that the relative differences in fatty acid composition in alewife and round goby related to their size or season were small in comparison with differences documented between them, which means that regardless of size and season they forage on a distinctly different prey base.

Fatty acids as biomarker and essential nutrients

Recently, it has been suggested that physiological measures can provide simple indicators necessary for cost-effective monitoring in the evaluation of fisheries sustainability (Young et al. 2006). In this context, fatty acids not only provide means to track trophic structure in aquatic ecosystems, but also enable a better understanding of physiological processes associated with the metabolism of fatty acids in many fish species and the possible consequences to populations dynamics. Such a link has been demonstrated by Ahlgren et al. (2005), where the imbalance of fatty acids (abnormally high DHA:ARA ratio) in the copepods of the southern Baltic Sea has been linked to the low concentration of ARA in phytoplankton. Similarly, in sockeye salmon (*Oncorhynchus nerka*), changes in dietary fatty acid intake associated with pelagic or benthic origin of their prey affected fatty acid composition of their bodies and slowed their growth (Ballantyne et al. 2003). In recently conducted experiments, we have found a direct link between dietary fatty acid intake and the quality of offspring produced by yellow perch broodstock (S. Czesny and J. Rinchard, unpublished data). In the field we have found differences in lake trout egg fatty acid composition between females spawned in different parts of Lake Michigan, which are likely related to dietary effects associated with heterogeneous prey assemblage throughout the basin (Czesny et al. 2009).

Given the background of recent shifts in food web structure, we stand in a unique position to investigate these changes in the context of food quality for top predators and its influence on physiological processes leading to reproductive success. In Lake Michigan, the predator balance is actively managed to sustain a recreational fishery for Chinook (*Oncorhynchus tshawytscha*) and other Pacific salmon while simultaneously restoring naturally reproducing lake trout populations (Eshenroder et al. 1995). Alewife as an established species, and round goby as a dynamically spreading one, are the prominent prey available to the top predators (e.g.,

Fig. 7. Correlations of individual fatty acids with total length in alewife (*a* and *b*) and in round goby (*c* and *d*). The fatty acids illustrated are significantly correlated with length.

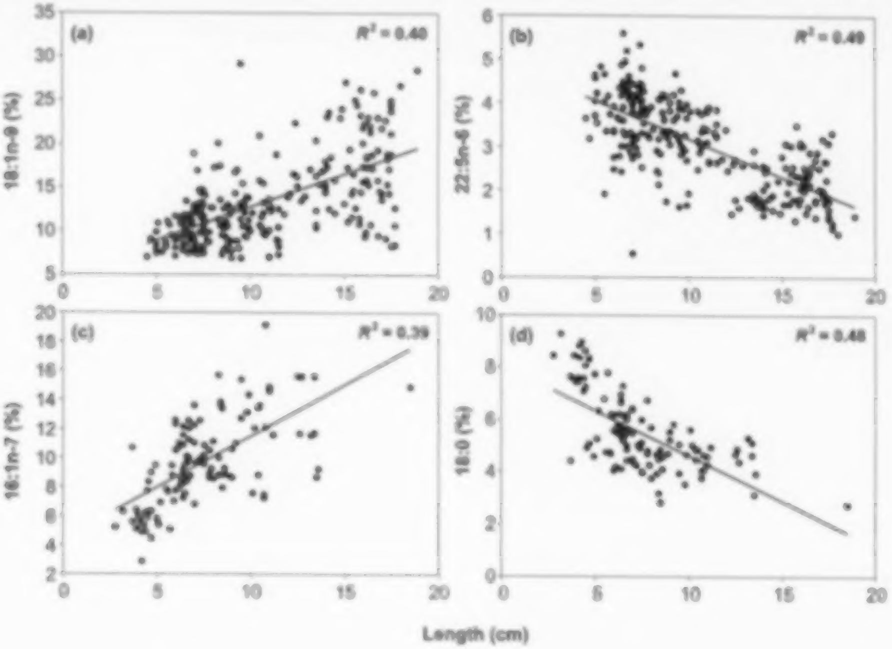

Fig. 8. Variation in the proportion of individual fatty acids as a function of total lipid concentration in alewife. The fatty acids presented here are significantly correlated with total lipid concentration.

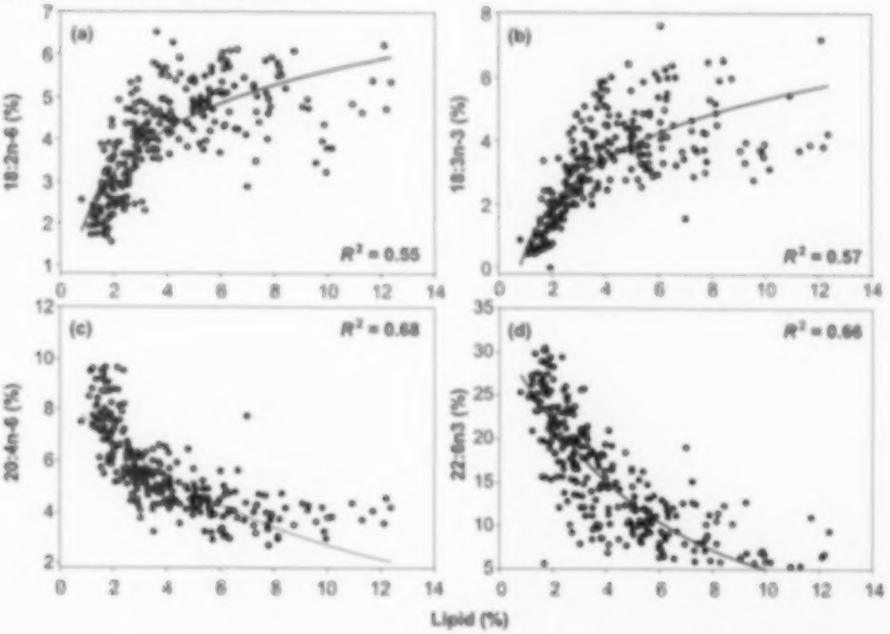

salmon, lake trout). Recent alewife population collapse in Lake Huron and nearly 70% decline in alewife biomass in Lake Michigan between 2003 and 2004 (Madenjian et al. 2009) suggest, based on our work, that the availability of fatty acids may change with these changes in prey assemblage. Evidence is mounting to suggest abundant alewife populations impede restoration of native species, including lake trout (Bunnell et al. 2006; Stockwell et al. 2009). Recent widespread findings of lake-spawned lake trout confirm that restoration is progressing in Lake Huron, and the timing of this undergoing recovery is coincident with the collapse of alewife and salmon populations (Riley et al. 2007). While quantitative estimates of predator consumption using fatty acid profiles can only be achieved with a combination of feeding experiments and food web modeling (Budge et al. 2002), we advocate that our findings provide a general baseline to assess food web relationships, as we have shown fatty acid profiles clearly segregate pelagic and benthic signatures among Lake Michigan prey species. The strong among-species differences in fatty acid profiles relative to size-driven, temporal, and spatial variability of within-species differences provide solid evidence that FAS may serve as a lake-wide tool to assess forage contributions to top predator diets and the impending physiological effects that may produce population-level responses.

Acknowledgements

We thank Kyle Ware (The Ohio State University) and Linda Begnoche (USGS – Great Lakes Science Center) for parts of the analysis. We also thank Charles Madenjian and David Bunnell (USGS – Great Lakes Science Center) for sample collection in MM3 management unit and the entire staff at the Lake Michigan Biological Station for long hours in the field collecting samples. Special thanks are extended to Deborah Lichti for database maintenance and Sara Creque for technical help with the manuscript. This study was supported by the Great Lakes Fishery Commission and the Great Lakes Fishery Trust Grant No. 292. The findings and conclusions in this article are those of the authors and do not necessarily represent the views of the US Fish and Wildlife Service.

References

Ahlgren, G., Van Nieuwerburgh, L., Wänstrand, I., Pedersén, M., Boberg, M., and Snoeijs, P. 2005. Imbalance of fatty acids in the base of the Baltic Sea food web — a mesocosm study. Can. J. Fish. Aquat. Sci. **62**(10): 2240–2253. doi:10.1139/f05-140.

Aitchison, J. 1986. The statistical analysis of compositional data. Chapman and Hall, New York.

Auel, H., Harjes, M., da Rocha, R., Stubing, D., and Hagen, W. 2002. Lipid biomarkers indicate different ecological niches and trophic relationships of the Arctic hyperiid amphipods *Themisto abyssorum* and *T. libellula*. Polar Biol. **25**: 374–383.

Ballantyne, A.P., Brett, M.T., and Schindler, D.E. 2003. The importance of dietary phosphorus and highly unsaturated fatty acids for sockeye (*Oncorhynchus nerka*) growth in Lake Washington — a bioenergetics approach. Can. J. Fish. Aquat. Sci. **60**(1): 12–22. doi:10.1139/f02-166.

Brett, M.T., Muller-Navarra, D.C., Ballantyne, A.P., Ravet, J.L., and Goldman, C.R. 2006. *Daphnia* fatty acid composition reflects that of their diet. Limnol. Oceanogr. **51**(5): 2428–2437. doi:10.4319/lo.2006.51.5.2428.

Budge, S.M., Iverson, S.J., Bowen, W.D., and Ackman, R.G. 2002. Among- and within-species variability in fatty acid signatures of marine fish and invertebrates on the Scotian Shelf, Georges Bank, and southern Gulf of St. Lawrence. Can. J. Fish. Aquat. Sci. **59**(5): 886–898. doi:10.1139/f02-062.

Budge, S.M., Iverson, S.J., and Koopman, H.N. 2006. Studying trophic ecology in marine ecosystems using fatty acids: a primer on analysis and interpretation. Mar. Mamm. Sci. **22**(4): 759–801. doi:10.1111/j.1748-7692.2006.00079.x.

Bunnell, D.B., Madenjian, C.P., and Claramunt, R.M. 2006. Long-term changes of the Lake Michigan fish community following the reduction of exotic alewife (*Alosa pseudoharengus*). Can. J. Fish. Aquat. Sci. **63**(11): 2434–2446. doi:10.1139/F06-132.

Clapp, D.F., Schneeberger, P.J., Jude, D.J., Madison, G., and Pistis, C. 2001. Monitoring round goby (*Neogobius melanostomus*) population expansion in eastern and northern Lake Michigan. J. Great Lakes Res. **27**(3): 335–341. doi:10.1016/S0380-1330(01)70649-1.

Clarke, K.R., and Warwick, R.M. 2001. Change in marine communities: an approach to statistical analysis and interpretation. 2nd ed. Primer-E, Plymouth Marine Laboratory, Plymouth, UK.

Czesny, S.J., Rinchard, J., Dabrowski, K., and Dettmers, J.M. 2006. Effects of exotic species and human impacts on essential fatty acid availability in the Lake Michigan food web. Great Lakes Fishery Trust Final Report. Available from http://www.glft.org/resourcelibrary/attachments/PROJECTS-404WebFile2002.292FinalReport.pdf.

Czesny, S.J., Rinchard, J., Dabrowski, K., and Dettmers, J.M. 2009. Pelagic and benthic food web shifts affect availability of polyunsaturated fatty acids to lake trout, implications for early life stages survival. Great Lakes Fishery Commission Project Completion Report. Available from http://www.glfc.org/research/reports/Czesny_2009.htm.

Dalsgaard, J., St. John, M., Kattner, G., Müller-Navarra, D., and Hagen, W. 2003. Fatty acid trophic markers in the pelagic marine environment. Adv. Mar. Biol. **46**: 225–340. doi:10.1016/S0065-2881(03)46005-7. PMID:14601414.

Eshenroder, R.L., Holey, M.E., Gorenflo, T.K., and Clark, R.D., Jr. 1995. Fish-community objectives for Lake Michigan. Great Lakes Fish. Comm. Spec. Publ. 95-3.

Fitzsimons, J.D., Clark, M., and Keir, M. 2009. Addition of round gobies to the prey communityof Lake Ontario and potential implications to thiamine status and reproductive success of lake trout. Aquat. Ecosyst. Health, **12**(3): 296–312. doi:10.1080/14634980903136453.

Fitzsimons, J.D., Brown, S., Brown, L., Honeyfield, D., He, J., and Johnson, J.E. 2010. Increase in lake trout reproduction in Lake Huron following the collapse of alewife: relief from thiamine deficiency or larval predation? Aquat. Ecosyst. Health, **13**(1): 73–84. doi:10.1080/14634980903581252.

Folch, J., Lees, M., and Sloane Stanley, G.H. 1957. A simple method for the isolation and purification of total lipids from animal tissues. J. Biol. Chem. **226**(1): 497–509. PMID:13428781.

Frederickson, H.L., Cappenberg, T.E., and de Leeuw, J.W. 1986. Polar lipid ester-linked fatty acid composition of Lake Vechten seston: an ecological application of lipid analysis. FEMS Microbiol. Ecol. **38**(6): 381–396. doi:10.1111/j.1574-6968.1986.tb01751.x.

French, J.R.P., III, and Jude, D.J. 2001. Diets and diet overlap of nonindigenous gobies and small benthic native fishes co-inhabiting the St. Clair River, Michigan. J. Great Lakes Res. **27**(3): 300–311. doi:10.1016/S0380-1330(01)70645-4.

Goedkoop, W., and Johnson, R.K. 1996. Pelagic–benthic coupling: profundal benthic community response to spring diatom deposition in mesotrophic Lake Erken. Limnol. Oceanogr. **41**(4): 636–647. doi:10.4319/lo.1996.41.4.0636.

Graeve, M., Kattner, G., Wiencke, C., and Karsten, U. 2002. Fatty acid composition of Arctic and Antarctic macroalgae: indicator of phylogenetic and trophic relationships. Mar. Ecol. Prog. Ser. **231**: 67–74. doi:10.3354/meps231067.

Henderson, R.J., Park, M.T., and Sargent, J.R. 1995. The desaturation and elongation of ^{14}C-labelled polyunsaturated fatty acids by pike

(*Esox lucius* L.) *in vitro*. Fish Physiol. Biochem. **14**(3): 223–235. doi:10.1007/BF00004313.

Iverson, S.J., Frost, K.J., and Lowry, L.F. 1997. Fatty acid signatures reveal fine scale structure of foraging distribution of harbor seals and their prey in Prince William Sound, Alaska. Mar. Ecol. Prog. Ser. **151**: 255–271. doi:10.3354/meps151255.

Iverson, S.J., Frost, K.J., and Lang, S.L.C. 2002. Fat content and fatty acid composition of forage fish and invertebrates in Prince William Sound, Alaska: factors contributing to among and within species variability. Mar. Ecol. Prog. Ser. **241**: 161–181. doi:10.3354/meps241161.

Jackson, D.A. 1997. Compositional data in community ecology: the paradigm or peril of proportions? Ecology, **78**(3): 929–940. doi:10.1890/0012-9658(1997)078[0929:CDICET]2.0.CO;2.

Janssen, J., and Luebke, M. 2004. Preference for rocky habitat by young-of-the-year yellow perch and alewives. J. Great Lakes Res. **30**(1): 93–99. doi:10.1016/S0380-1330(04)70332-9.

Käkelä, A., Crane, J., Votier, S.C., Furness, R.W., and Käkelä, R. 2006. Fatty acid signatures as indicators of diet in great skuas *Stercorarius skua*, Shetland. Mar. Ecol. Prog. Ser. **319**: 297–310. doi:10.3354/meps319297.

Kirsch, P.E., Iverson, S.J., Bowen, W.D., Kerr, S.R., and Ackman, R.G. 1998. Dietary effects on the fatty acid signature of whole Atlantic cod (*Gadus morhua*). Can. J. Fish. Aquat. Sci. **55**(6): 1378–1386. doi:10.1139/cjfas-55-6-1378.

Kuhns, L.A., and Berg, M.B. 1999. Benthic invertebrate community responses to round goby (*Neogobius melanostomus*) and zebra mussel (*Dreissena polymorpha*) invasion in southern Lake Michigan. J. Great Lakes Res. **25**(4): 910–917. doi:10.1016/S0380-1330(99)70788-4.

Madenjian, C.P., Elliott, R.F., DeSorcie, T.J., Stedman, R.M., O'Connor, D.V., and Rottiers, D.V. 2000. Lipid concentrations in Lake Michigan fishes: seasonal, spatial, ontogenetic, and long-term trends. J. Great Lakes Res. **26**(4): 427–444. doi:10.1016/S0380-1330(00)70706-4.

Madenjian, C.P., Fahnenstiel, G.L., Johengen, T.H., Nalepa, T.F., Vanderploeg, H.A., Fleischer, G.W., Schneeberger, P.J., Benjamin, D.M., Smith, E.B., Bence, J.R., Rutherford, E.S., Lavis, D.S., Robertson, D.M., Jude, D.J., and Ebener, M.P. 2002. Dynamics of the Lake Michigan food web, 1970–2000. Can. J. Fish. Aquat. Sci. **59**(4): 736–753. doi:10.1139/f02-044.

Madenjian, C.P., Pothoven, S.A., Dettmers, J.M., and Holuszko, J.D. 2006. Changes in seasonal energy dynamics of alewife (*Alosa pseudoharengus*) in Lake Michigan after invasion of dreissenid mussels. Can. J. Fish. Aquat. Sci. **63**(4): 891–902. doi:10.1139/f06-017.

Madenjian, C.P., O'Gorman, R., Bunnell, D.B., Argyle, R.L., Roseman, E.F., Warner, D.M., Stockwell, J.D., and Stapanian, M.A. 2008. Adverse effects of alewives on Laurentian Great Lakes fish communities. N. Am. J. Fish. Manage. **28**(1): 263–282. doi:10.1577/M07-012.1.

Madenjian, C.P., Bunnell, D.B., Holuszko, J.D., Desorcie, T.J., and Adams, J.V. 2009. Status and trends of prey fish populations in Lake Michigan, 2009. Great Lakes Science Center Report. US Geological Survey, Great Lakes Science Center, Ann Arbor, Michigan. Available from http://www.glsc.usgs.gov/_files/reports/2009LakeMichiganPreyfish.pdf.

Metcalfe, L.D., and Schmitz, A.A. 1961. The rapid preparation of fatty acid esters for gas chromatographic analysis. Anal. Chem. **33**(3): 363–364. doi:10.1021/ac60171a016.

Mills, E.L., Leach, J.H., Carlton, J.T., and Secor, C.L. 1993. Exotic species in the Great Lakes: a historic biotic crises and anthropogenic introductions. J. Great Lakes Res. **19**(1): 1–54. doi:10.1016/S0380-1330(93)71197-1.

Mills, E.L., Casselman, J.M., Dermott, R., Fitzsimons, J.D., Gal, G., Holeck, K.T., Hoyle, J.A., Johannsson, O.E., Lantry, B.F., Makarewicz, J.C., Millard, E.S., Munawar, I.F., Munawar, M., O'Gorman, R., Owens, R.W., Rudstam, L.G., Schaner, T., and Stewart, T.J. 2003. Lake Ontario: food web dynamics in a changing ecosystem, 1970–2000. Can. J. Fish. Aquat. Sci. **60**(4): 471–490. doi:10.1139/f03-033.

Morrison, H.A., Whittle, D.M., and Haffner, G.D. 2000. The relative importance of species invasions and sediment disturbance in regulating chemical dynamics in western Lake Erie. Ecol. Model. **125**(2-3): 279–294. doi:10.1016/S0304-3800(99)00189-1.

Nalepa, T.F., Hartson, D.J., Fanslow, D.J., Lang, G.A., and Lozano, S.J. 1998. Declines in benthic macroinvertebate populations in southern Lake Michigan, 1980–1993. Can. J. Fish. Aquat. Sci. **55**(11): 2402–2413. doi:10.1139/cjfas-55-11-2402.

Nalepa, T.F., Fanslow, D.L., and Lang, G.A. 2009. Transformation of the offshore benthic community in Lake Michigan: recent shift from the native amphipod *Diporeia* spp. to the invasive mussel *Dreissena rostiformis bugensis*. Freshw. Biol. **54**(3): 466–479. doi:10.1111/j.1365-2427.2008.02123.x.

Napolitano, G.E., Hill, W.R., Guckert, J.B., Stewart, A.J., Nold, S.C., and White, D.C. 1994. Changes in periphyton fatty acid composition in chlorine polluted streams. J. N. Am. Benthol. Soc. **13**(2): 237–249. doi:10.2307/1467242.

Napolitano, G.E., Heras, H., and Stewart, A.J. 1995. Fatty acid composition of freshwater phytoplankton during a red tide event. Biochem. Syst. Ecol. **23**(1): 65–69. doi:10.1016/0305-1978(95)93659-Q.

Persson, J., and Vrede, T. 2006. Polyunsaturated fatty acids in zooplankton: variation due to taxonomy and trophic position. Freshw. Biol. **51**(5): 887–900. doi:10.1111/j.1365-2427.2006.01540.x.

Raclot, T., Groscolas, R., and Cherel, Y. 1998. Fatty acid evidence for the importance of myctophid fishes in the diet of king penguins, *Aptenodytes patagonicus*. Mar. Biol. **132**(3): 523–533. doi:10.1007/s002270050418.

Reuss, N., and Poulsen, L.K. 2002. Evaluation of fatty acids as biomarkers for a natural plankton community. A field study of a spring bloom and a post-bloom period off West Greenland. Mar. Biol. **141**(3): 423–434. doi:10.1007/s00227-002-0841-6.

Riley, S.C., He, J.X., Johnson, J.E., O'Brien, T.P., and Schaeffer, J.S. 2007. Evidence of widespread natural reproduction by lake trout *Salvelinus namaycush* in the Michigan waters of Lake Huron. J. Great Lakes Res. **33**(4): 917–921. doi:10.3394/0380-1330(2007)33[917:EOWNRB]2.0.CO;2.

Smyntek, P.M., Teece, M.A., Schulz, K.L., and Storch, A.J. 2008. Taxonomic differences in the essential fatty acid composition of groups of freshwater zooplankton relate to reproductive demands and generation time. Freshw. Biol. **53**(9): 1768–1782. doi:10.1111/j.1365-2427.2008.02001.x.

Stevens, J. 1986. Applied multivariate statistics for the social sciences. Lawrence Erlbaum Associates, Mahwah, N.J.

Stewart, D.J., and Binkowski, F.P. 1986. Dynamics of consumption and food conversion by Lake Michigan alewives: an energetics-modeling synthesis. Trans. Am. Fish. Soc. **115**(5): 643–661. doi:10.1577/1548-8659(1986)115<643:DOCAFC>2.0.CO;2.

Stockwell, J.D., Ebener, M.P., Black, J.A., Gorman, O.T., Hrabik, T.R., Kinnunen, R.E., Mattes, W.P., Oyadomari, J.K., Schram, S.T., Schreiner, D.R., Seider, M.J., Sitar, S.P., and Yule, D.L. 2009. A synthesis of cisco recovery in Lake Superior: implications for native fish rehabilitation in the Laurentian Great Lakes. N. Am. J. Fish. Manage. **29**(3): 626–652. doi:10.1577/M08-002.1.

Taraborelli, A.C., and Schaner, T. 2002. Diet of the round goby in the Bay of Quinte, Lake Ontario. Chapter 16. Part III. Special studies.

In Lake Ontario Fish Communities and Fisheries: 2001 Annual Report of the Lake Ontario Management Unit, Ontario Ministry of Natural Resources, Picton, Ont., Canada.

Thiemann, G.W., Iverson, S.J., and Stirling, I. 2008. Polar bear diets and Arctic marine food webs: insights from fatty acid analysis. Ecol. Monogr. **78**(4): 591–613. doi:10.1890/07-1050.1.

Tocher, D.R. 2003. Metabolism and functions of lipids and fatty acids in teleost fish. Rev. Fish. Sci. **11**(2): 107–184. doi:10.1080/713610925.

Truemper, H.A., Lauer, T.E., McComish, T.S., and Edgell, R.A. 2006. Response of yellow perch diet to a changing forage base in southern Lake Michigan, 1984–2002. J. Great Lakes Res. **32**(4): 806–816. doi:10.3394/0380-1330(2006)32[806:ROYPDT]2.0.CO;2.

Weber, M.J., Dettmers, J.M., Wahl, D.H., and Czesny, S.J. 2010. Effects of predator–prey interactions and benthic habitat complexity on selectivity of a foraging generalist. Trans. Am. Fish. Soc. **139**(4): 1004–1013. doi:10.1577/T09-100.1.

Young, J.L., Bornik, Z.B., Marcotte, M.L., Charlie, K.N., Wagner, G.N., Hinch, S.G., and Cooke, S.J. 2006. Integrating physiology and life history to improve fisheries management and conservation. Fish Fish. **7**: 262–283.

Using acoustic data from fishing vessels to estimate walleye pollock (*Theragra chalcogramma*) abundance in the eastern Bering Sea

Taina Honkalehto, Patrick H. Ressler, Richard H. Towler, and Christopher D. Wilson

Abstract: Eastern Bering Sea walleye pollock (*Theragra chalcogramma*) support one of the world's largest fisheries. Because of walleye pollock's high recruitment variability and relatively short life span, timely and accurate abundance indices are needed for fisheries management. Walleye pollock are surveyed biennially with an acoustic-trawl (AT) survey and annually with a bottom trawl (BT) survey. The latter tracks the demersal portion of the population using chartered fishing vessels, whereas the AT survey tracks the younger, midwater portion using research vessels and is critical for evaluating prerecruit abundances. Acoustic data collected from commercial fishing vessels conducting the BT survey were analyzed to provide information on midwater walleye pollock abundance at relatively low cost. A retrospective analysis of AT survey data identified a suitable index area to track midwater walleye pollock abundance. The BT survey acoustic data in that area tracked the AT survey abundance and captured its broad spatial patterns. This study is unique because commercial vessel acoustic data were used to estimate a new annual abundance index whose performance can be evaluated by a biennial research vessel survey. The new index will benefit managers by providing more accurate information on near-term abundance trends when dedicated research ship time is not available.

Résumé : Les goberges d'Alaska (*Theragra chalcogramma*) de la partie est de la mer Béring supportent une des plus grandes pêcheries du monde. A cause de la très grande variabilité du recrutement et de la durée de vie relativement courte de la goberge, des indices d'abondance précis et fait au moment opportun sont nécessaires pour la gestion de la pêcherie. La population de goberges d'Alaska est échantillonnée tous les deux ans par une campagne en mer couplant des inventaires acoustiques et du chalutage (AC), et annuellement par une campagne de chalutage de fond (C). Cette dernière estime la proportion démersale en utilisant des navires de pêche commerciale affrétés, alors que la campagne AC estime la proportion pélagique des individus plus jeunes en utilisant des navires de recherche. Les campagnes AC sont d'une importance critique pour l'évaluation de l'abondance des pré-recrues. Les donnés acoustiques collectées à bord des navires de pêche commerciale réalisant les campagnes C ont été analysées pour fournir des informations à coût relativement modique sur l'abondance des goberges d'Alaska pélagiques. Une analyse rétrospective des données de campagne AC a identifié une zone indicatrice appropriée pour suivre l'abondance des goberges d'Alaska pélagiques; les données acoustiques de la campagne C dans cette zone suivent les abondances des inventaires de la campagne AC et en capturentles patrons spatiaux généraux. Notre étude est unique, car les données acoustiques des navires commerciaux sont utilisées pour estimer un nouvel indice annuel d'abondance dont la performance peut être évaluée tous les deux ans par une campagne en mer d'un navire de recherche. Le nouvel indice bénéficiera aux gestionnaires en fournissant des informations plus précises sur les tendances d'abondance à court terme lorsque du temps spécialisé de navire de recherche n'est pas disponible.

[Traduit par la Rédaction]

Introduction

Walleye pollock (*Theragra chalcogramma*) is an abundant, semidemersal gadid fish that inhabits the continental shelf waters of the North Pacific Ocean from Washington State, USA, north and west to Japan. In the US Exclusive Economic Zone within the eastern Bering Sea (EBS), this species supports one of the world's largest commercial fisheries (Food and Agriculture Organization of the United Nations 2009). Since the late 1970s, walleye pollock have been monitored by two fishery-independent summer surveys conducted by scientists from the National Oceanic and Atmospheric Administration's (NOAA) Alaska Fisheries Science Center (AFSC). One survey is dedicated primarily to evaluating walleye pollock abundance and uses acoustic-trawl (AT) methods deployed from NOAA research vessels. This biennial survey is costly but valuable because it covers the generally younger, midwater component of the walleye pollock stock. The other survey is multispecies and provides an index of the older, demersal component of the walleye pollock population. This annual survey uses area-swept bottom trawl (BT) survey methods aboard chartered commercial fishing vessels. Both surveys are critical to the assessment and management of

Received 1 July 2010. Accepted 24 March 2011. Published at www.nrcresearchpress.com/cjfas on 06 July 2011.
J21904

Paper handled by Associate Editor Josef Michael Jech.

T. Honkalehto, P.H. Ressler, R.H. Towler, and C.D. Wilson. National Marine Fisheries Service, Alaska Fisheries Science Center, Resource Assessment and Conservation Engineering Division, 7600 Sand Point Way NE, Seattle, WA 98115, USA.

Corresponding author: Taina Honkalehto (e-mail: Taina.Honkalehto@noaa.gov).

Can. J. Fish. Aquat. Sci. **68**: 1231–1242 (2011) doi:10.1139/F2011-050 Published by NRC Research Press

this stock (Ianelli et al. 2009). The walleye pollock population is highly variable and in recent years has declined following a period of below-average recruitment in 2001–2005, heightening the need for accurate and timely information on stock status (Ianelli et al. 2009). Annual acoustic data obtained from the commercial fishing vessels conducting the BT survey could provide an economic and timely way to augment the biennial fishery-independent data used to estimate the midwater component of the EBS walleye pollock stock.

Commercial fishing vessels have been used to collect acoustic data for fisheries research purposes where dedicated research vessels are not available. The use of these data from commercial fishing vessels has recently been reviewed (International Council for the Exploration of the Sea 2007) and remains an active area of research (e.g., Wyeth et al. 2000; Mackinson and van der Kooij 2006; Pena 2008). For example, acoustic data collected on commercial vessels during a fishing season have been used to estimate hoki (*Macruronus novaezelandiae*) biomass in New Zealand (O'Driscoll and Macaulay 2005) to characterize herring abundance indices in eastern Canada (Claytor and Allard 2001) and to examine commercial fishing effects on walleye pollock aggregations in the EBS (Barbeaux et al. 2005; Shen et al. 2009). Commercial vessel acoustic systems have also been used in directed studies to examine the behavioral response of fish to trawling vessels (De Robertis and Wilson 2006) and to study the effect of light intensity on walleye pollock availability to EBS AT and BT surveys (Kotwicki et al. 2009). Many commercial walleye pollock vessels in Alaska are equipped with Simrad ES60 echo sounders (Simrad, Kongsberg AS, Horten, Norway), which are capable of collecting and storing scientific quality acoustic data.

The goal of this project was to evaluate whether acoustic data collected aboard commercial fishing vessels during a BT survey could be used to create a reliable abundance index for the midwater portion of the walleye pollock stock, which was not targeted by this survey. The acoustic data were collected under methods quite different than those employed during dedicated AT surveys. For example, we had very limited control over the vessels used, the acoustic equipment used or frequency that the instruments were monitored during the cruise, and other day-to-day data collection operations. It was also not possible to directly sample the acoustic backscatter for species classification, nor run a trackline pattern recommended for a dedicated acoustic survey (Simmonds and MacLennan 2005). Nevertheless, the project was feasible because walleye pollock account for a large proportion of midwater backscatter in the EBS, the BT survey coverage was adequate, and the resulting index could provide data on a critical component of the walleye pollock population that would be otherwise unavailable during off-years for the AT survey.

Materials and methods

Surveys

The NOAA AT and BT walleye pollock stock assessment surveys take place in June and July, proceeding from east to west across the EBS shelf and slope during daylight hours (Fig. 1*a*). They cover regions between approximately the 50 and 1000 m isobaths (AT survey) and the 20 and 200 m isobaths (BT survey; Fig. 1*a*). The BT survey covers a larger total area than the AT survey to also monitor commercially important crab and other groundfish species. Methods for each survey are described briefly, as more detail is available elsewhere (Honkalehto et al. 2008; Lauth 2010).

The biennial AT survey is currently carried out aboard one of two NOAA research vessels (63–66 m in length) equipped with calibrated scientific echo sounders connected to split-beam transducers attached to a centerboard located 9 m below the water surface. The principal frequency used to survey walleye pollock is 38 kHz. Acoustic backscatter data were collected along parallel north–south transects spaced 37 km apart at a nominal vessel speed of 6.2 $m \cdot s^{-1}$ from about 14–16 m from the surface to within 0.5 m of the bottom, to maximum depths of 500 m. Midwater trawls are conducted to verify the species composition of the observed backscatter and to collect other biological information. Acoustic backscatter data are manually classified into taxonomic groups by trained analysts based on a visual examination of backscatter characteristics and on the species composition of midwater trawl catches. Walleye pollock length, mass, and age information from the trawls are then used to convert the echo integral data attributed to walleye pollock into numbers and mass of walleye pollock per unit area, which are expanded to represent the midwater component of the walleye pollock stock for the surveyed area. The demersal component of the walleye pollock stock is assessed by the BT survey as described below.

The annual BT survey is conducted aboard two chartered commercial fishing vessels (40–50 m in length) that deploy bottom trawls in a grid of 396 stations spaced 20 nautical miles (nmi) (37 km) apart, forming rows of 37 km × 37 km cells (Fig. 1*a*). About 280 cells overlap the AT survey trackline. Nominal vessel speeds range from about 1.5 $m \cdot s^{-1}$ when trawling to about 4.6–5.7 $m \cdot s^{-1}$ when free-running. The bottom trawl catch-per-unit effort for walleye pollock is used to estimate demersal biomass. BT survey vessels are typically equipped with commercial echo sounders and hull-mounted transducers located 4–5 m below the water surface.

Acoustic data collection and processing

Routine AT surveys were carried out in 2006–2009 using Simrad EK60 scientific echo sounders operating at 38 kHz and standard acoustic survey methods (Honkalehto et al. 2002, 2010). The Simrad acoustic systems were calibrated before, during, and after the surveys using standard sphere techniques (Foote et al. 1987).

Routine BT surveys were carried out in 2006–2009. For this project, acoustic data collected from the commercial vessels were required to be of higher quality than typically available from these platforms. Whereas on AT surveys acoustic data were collected, examined, and postprocessed in near real time by acoustics experts, on the chartered BT survey vessels large volumes of acoustic data were collected semi-automatically without immediate review by an acoustics expert. To obtain high-quality, midwater acoustic information, detailed protocols for data collection (International Council for the Exploration of the Sea 2007) and custom, semi-automated, data analysis software for postprocessing were developed. Collection of the acoustic data required close collaboration with BT survey vessel skippers and survey personnel regarding mutually acceptable data collection protocols and

Fig. 1. Study area showing (*a*) typical spatial coverage of the bottom trawl (BT) survey (squares) and acoustic-trawl (AT) survey (solid lines), (*b*) 2006 BT vessel tracks, (*c*) 2007 BT vessel track (only the vessel (one of two) that collected 38 kHz acoustic data is shown), and (*d*) 2008 BT vessel tracks. The 2009 vessel tracks (not shown) were very similar to 2006 and 2008. Shaded squares indicate index area cells where data were autoprocessed (dark gray) or hand-processed (medium gray). Also shown are depth contours (short dashes) and the boundary between the USA and the Russian Exclusive Economic Zone (long dashes). 1 nautical mile (nmi) = 1.852 km.

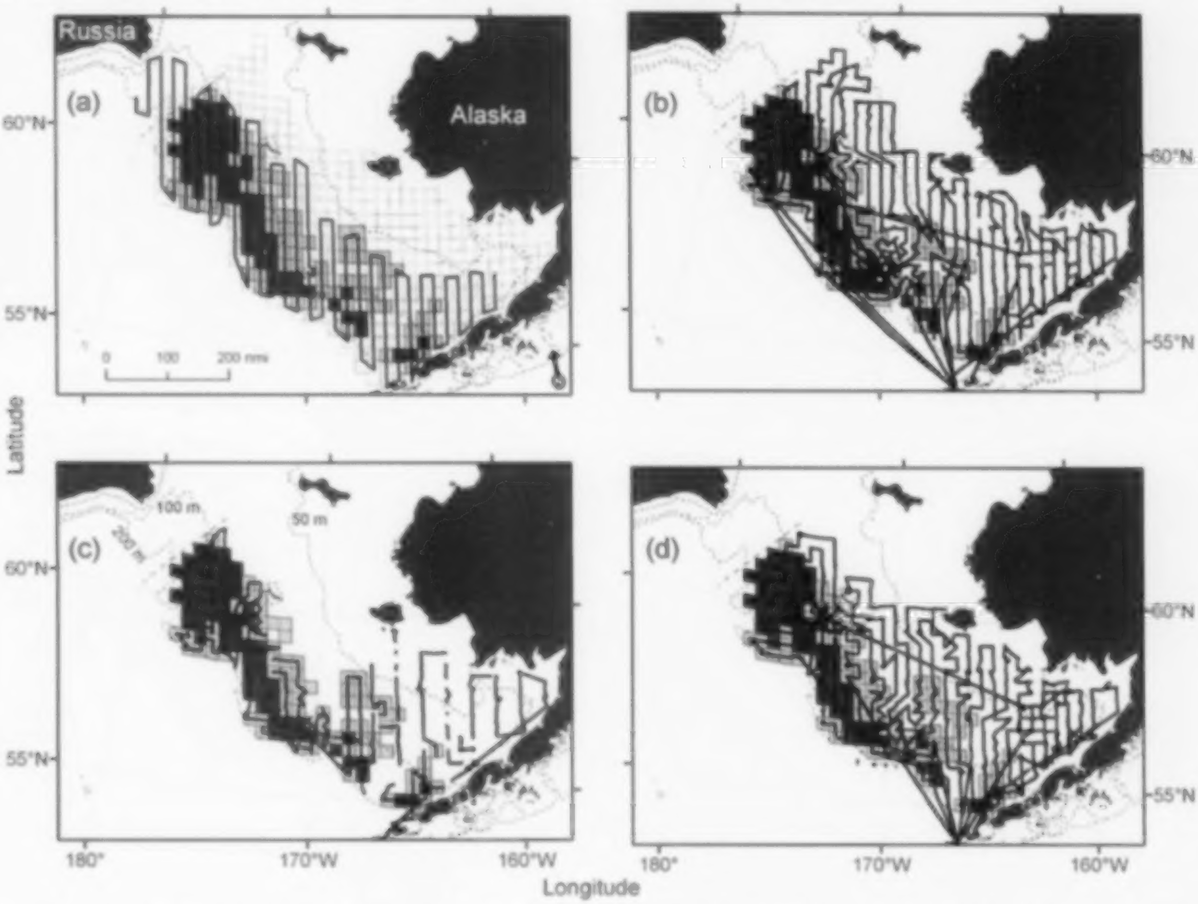

vessel logistics, in particular because acoustic data collection was not the primary BT survey objective. Common concerns affecting acoustic data quality included system installation issues; noise from various acoustic (other sounders, bubble sweepdown), electrical, or mechanical sources; intermittent navigation information; and inconsistent bottom tracking.

BT survey acoustic data were collected with Simrad ES60 commercial echo sounders and split-beam transducers operating at 38 kHz. Other acoustic devices aboard the vessels were either synchronized with the ES60 or turned off while data were collected to prevent interference. The Simrad acoustic systems were generally calibrated at the start and end of the surveys using standard sphere techniques (Foote et al. 1987); except for expediency, the vessels were drifting instead of anchored during the calibration. The standard target was suspended as close as possible to the main axis of the beam, and only detections close to the center of the beam (defined as a maximum applied beam compensation of ≤0.3 dB) were used to compute new gain values. Sound speed and absorption settings for processing BT survey acoustic data were based on prior EBS AT surveys. Upper and lower depth bounds for BT acoustic data collection were the same as those for the AT survey: from about 14–16 m from the surface to within 3 m of the bottom. A systematic ping-indexed bias present in ES60 raw data files was removed using either a Java utility (T. Ryan and R. Kloser, CSIRO Marine and Atmospheric Research, GPO Box 1538, Hobart 7001, Australia, personal communication, 2005) or a custom-written Matlab (The Mathworks, Natick, Massachusetts, USA) software program described below.

The hull-mounted transducers on BT survey vessels were more susceptible to the effects of air bubbles sweeping across the transducer face (bubble sweepdown) than the centerboard-mounted transducers on the AT survey vessel (Ona and Traynor 1990; Cox et al. 2006). These bubbles can cause attenuation of sound transmission and reception of echoes. Two simple data filters were developed to remove pings compromised by bubble sweepdown. For each ping in an ES60 raw data file, the transmit pulse S_v was tested for deviations greater than ±2% of the long-term mean from each BT survey, the same standard expected from experience with AT survey research vessel data. Pings exceeding this standard were removed. Also, a bottom echo filter removed pings having a weak bottom echo (mean $S_v < -40.0$ dB). As it was uncertain whether all pings compromised by bubble sweepdown were detected and removed by these filters, the filtered data files were used only if less than 15% of the pings in a raw file had been removed. Otherwise the entire data file was considered compromised and was excluded from further analysis.

Overall, the 2006 through 2009 field methods specific to the AT and BT surveys were similar across years, with slight variations in participating vessels and survey timing (Table 1; Figs. 1*b*, 1*c*, 1*d*; Honkalehto et al. 2010; Lauth 2010). Although two vessels were contracted to conduct the 2007 BT survey, only one was equipped with a 38 kHz echo sounder and used in this study.

To facilitate rapid processing of the large volumes of BT acoustic data, a customized postprocessing system called rawLoader was developed in MatLab. RawLoader was used to read Simrad ES60 (and ER60) .raw files, convert raw power and electrical angles, mask and filter data, apply calibration parameters, create analysis intervals (e.g., 0.5 nmi (0.93 km) elementary distance sampling units (EDSUs) along the vessel path and 10 m vertical depth bins), and perform echo integration. Additional features of rawLoader included automated removal of the systematic ping-indexed bias present in ES60 data, enhanced bottom detection, flagging of extreme high or low s_A (nautical area scattering coefficient ($m^2 \cdot nmi^{-2}$); MacLennan et al. 2002) value pings, and flexible ping filtering to remove most bubble sweepdown effects. Resulting echo integration information was stored in a relational database, and echogram image files were created to allow visual audits of the data. Echoview software (Myriax Pty., Ltd., Hobart, Tasmania, Australia) was used to analyze acoustic backscatter data where the presence of contaminant taxa required manual processing. As an initial quality control measure, rawLoader echogram images of all data were examined to detect large problems such as invalid bottom detections, acoustic interference, and non-walleye pollock backscatter.

Retrospective analysis

A retrospective analysis of AT survey data (1999–2004) was completed to explore ways to save time postprocessing the BT survey data. The analysis identified an index area on the EBS shelf where much of the acoustic backscatter at 38 kHz was attributed to walleye pollock. It also determined where the acoustic data could be automatically processed in the custom Matlab software or where the presence of substantial backscatter from other taxa required manual processing to identify and isolate walleye pollock backscatter. The suitability of the index area was assessed by testing the ability of its summed backscatter over a portion of the water column to track the AT survey walleye pollock biomass time series. Subsequently, the acoustic data inside the index area from the 2006–2009 BT surveys were used to generate a walleye pollock abundance index. This reduced the entire BT survey data set to a smaller geographic area, which expedited postprocessing and index computation.

The four most recent years of AT survey data available when this study began (1999, 2000, 2002, and 2004) were used for the retrospective analysis. These AT surveys were chosen because their start and end dates closely matched those of the bottom trawl surveys, and the methods used were most similar to current practices. All acoustic backscatter data (s_A) classified to taxonomic groups (e.g., walleye pollock, non-walleye pollock fish, near-surface fish – plankton mix) were stratified into 37 km × 37 km BT survey cells and reanalyzed as follows (Fig. 1*a*). First, cells were selected where AT survey walleye pollock backscatter was (*i*) present above a minimum level ($\geq 100\ s_A$) and (*ii*) the predominant fraction of total backscatter ($\geq 70\%$ of total s_A) in at least 1 of the 4 years. These presence and predominance criteria were chosen based on observations of walleye pollock backscatter over the EBS AT survey time series. The 138 cells that passed these thresholds were combined into an index area covering a little more than half of the normal AT survey area (Fig. 1*a*, shaded cells). Second, to determine whether cells could be automatically processed or required manual processing, the number of survey years (1–4) when each index cell met both area thresholds was noted; based on this categorization, the index area was divided into two subareas. Cells where walleye pollock backscatter passed the present and predominant thresholds for more than one survey year comprised the first subarea (about half of the index area; Fig. 1*a*), and all backscatter in the water column between 30 m from the surface and 3 m above bottom was automatically attributed to walleye pollock. Backscatter shallower than 30 m was excluded, as it typically comprises a variable mixture of other fishes and plankton. Cells where walleye pollock backscatter met the minimum thresholds in only one survey year comprised the second subarea. Here, backscatter attributed to non-walleye pollock targets was common throughout the water column, and thus more careful, manual processing was required to classify backscatter as walleye pollock. Finally, walleye pollock backscatter from the two index subareas was combined, and a walleye pollock abundance index (I_{AT}) for each year was computed from the AT survey backscatter data in the index area as follows:

$$I_{AT} = c\sum \bar{s}_{Aj} \tag{1}$$

where $\bar{s}_{Aj}$ is the average s_A attributed to walleye pollock from all 0.5 nmi (0.93 km) EDSUs in index area cell j ($m^2 \cdot nmi^{-2}$), c is cell area (= 400 nmi^2), and the summation is over all index area cells.

Two simple procedures were performed to validate the empirically chosen thresholds for walleye pollock backscatter presence ($\geq 100\ s_A$) and predominance ($\geq 70\%$ of total backscatter) that were used to define the index area and to evaluate how much manual versus automatic classification of walleye pollock was necessary in the retrospective analysis. First, higher and lower threshold combinations were systematically chosen, and the index area and values were recomputed and compared with those produced with the original thresholds. In the second procedure, an index of undifferentiated backscatter (I_{UDB}) was computed in the same way as I_{AT} (eq. 1), except that all AT survey backscatter between 30 m from the surface and 3 m off bottom in the entire index area was attributed to walleye pollock. The I_{UDB} (1999–2004) simulated the effect of automatically processing all index area data to test whether all data below 30 m could be classified

Table 1. Dates and vessels used for the Alaska Fisheries Science Center acoustic-trawl (AT) and bottom trawl (BT) stock assessment surveys during summer 2006–2009.

	BT surveys		AT surveys	
Year	Charter vessel (length)	Survey dates	NOAA vessel (length)	Survey dates
2006	*Arcturus* (40 m), *Northwest Explorer* (49 m)	30 May – 28 July	*Miller Freeman* (66 m)	3 June – 25 July
2007	*Arcturus*	4 June – 2 August	*Oscar Dyson* (63 m)	2 June – 30 July
2008	*Arcturus*, *Aldebaran* (40 m)	2 June – 26 July	*Oscar Dyson*	2 June – 31 July
2009	*Arcturus*, *Aldebaran*	28 May – 31 July	*Oscar Dyson*	9 June – 7 August

as walleye pollock, which would dramatically shorten the processing time needed to produce an index.

BT survey index and index–survey comparisons

Between 2006 and 2009, a BT survey index (I_{BT}) was computed in the same way as I_{AT} (eq. 1), except using BT survey acoustic data. Following AT survey procedures for assessing walleye pollock, we used only BT survey data that were collected during daylight hours and when the vessels were not trawling (defined as vessel speeds > 2.1 m·s⁻¹). The maximum depth limit for analysis was set at 200 m, roughly the outer Bering Sea shelf break. In each of those years, for reasons not connected to this study, annual summer AT surveys were conducted as opposed to the usual biennial schedule. This allowed us to compare the AT survey biomass with I_{BT} to validate the new abundance index. For the comparison, the AT survey biomass was normalized to mean 1999–2004 values, and the I_{BT} time series was normalized to the mean I_{AT} values from 1999–2004, as there were no BT survey data from those years. The trend in each time series was compared to assess whether I_{BT} tracked the AT survey biomass and could therefore be used to increase the number of walleye pollock stock abundance observations at a low additional cost.

Spatial statistics (Bez et al. 1997; Woillez et al. 2007, 2009) were computed to compare the distribution patterns and degree of overlap and coherence between walleye pollock backscatter from the AT survey and I_{BT}. The spatial indices included center of gravity (CG) and corresponding inertia, as well as global and local indices of spatial collocation (I_g and I_l; Bez and Rivoirard 2000; Petitgas et al. 2009). The global index of collocation is computed from CG and inertia and measures the large-scale overlap of two distributions with values ranging from 0 (no overlap) to 1 (complete overlap). The local index of collocation measures the fine-scale spatial coherence, with values ranging from 0 (no coherence) to 1 (complete coherence). Each data set was averaged into the same set of 37 km × 37 km BT survey cells (Fig. 1*a*) prior to computation of spatial statistics. Finally, the percentage of AT survey walleye pollock biomass in the index area each year was computed to gauge whether the index area developed in the retrospective analysis captured the spatial extent of most EBS walleye pollock.

Relative estimation errors associated with acoustic data sampling variability and spatial structure were derived for index and survey totals in each year using a one-dimensional geostatistical method (Petitgas 1993; Rivoirard et al. 2000; Walline 2007). North–south columns of BT grid cells were treated as transects for the purpose of the computations. Relative estimation error is defined as the ratio of the square root of the geostatistical estimation variance to the summed biomass or acoustic backscatter (Rivoirard et al. 2000). The relative estimation errors were multiplied by 1.96 to approximate 95% confidence intervals about each survey sum, assuming errors were normally distributed. This procedure is reasonable; Walline (2007) used conditional geostatistical simulations to show that biomass estimates from Bering Sea walleye pollock surveys were approximately normally distributed and furthermore that confidence intervals computed as twice the one-dimensional relative estimation error were very similar to 95% confidence intervals estimated from the probability distribution function of survey estimates derived from many simulations.

Results

Calibration and data quality

The acoustic system calibrations for all vessels in each year indicated that instrument performance was acceptable and that there were no large changes in sensitivity in the acoustic systems during the surveys (Fig. 2). This allowed for unbiased comparison in acoustic backscatter trends. The variability in S_v gain for BT survey vessels was generally similar to that for the AT survey vessels. The wider variation between calibrations for *Arcturus* in 2007 was likely due to poor conditions experienced during the calibrations when the vessel was in open water rather than being sheltered inside a bay as was more typical.

The centerboard-mounted transducers on the AT survey vessels were not noticeably affected by bubble sweepdown, but the hull-mounted transducers on the BT survey vessels were affected, particularly in rough sea conditions or high vessel speeds. Using the transmit pulse and bottom data filters on BT survey data sets removed, on average, about 7% of the 0.5 nmi (0.93 km) EDSUs (Table 2). The greatest percentage of interval removals occurred in 2007 (17.2%). This was likely because *Arcturus*' mean transit speed in 2007 was about 0.4 m·s⁻¹ higher than in other years, which potentially exacerbated bubble sweepdown effects. The increased speeds occurred because *Arcturus* covered extra trackline to sample index area cells that were surveyed by the second (non-38 kHz) vessel. Higher percent removals were also correlated with adverse weather conditions. In 2006, *Northwest Explorer* experienced some relatively rough sea states and bad weather conditions, while *Arcturus* surveyed elsewhere. In 2009, sea state conditions were generally worse throughout the summer than in the other years. As pings affected by bubble sweepdown have very low s_A, their presence negatively biased the water column backscatter data, decreasing the total measured s_A, and their removal resulted in a proportional increase in s_A for these data sets.

Table 2. Percent removal of 0.5 nmi (0.93 km) elementary distance sampling units (EDSUs) where ≥15% of pings failed the transmit pulse and bottom ping filters, by vessel and year.

	2006		2007	2008		2009		
	Arcturus	*Northwest Explorer*	*Arcturus*	*Arcturus*	*Aldebaran*	*Arcturus*	*Aldebaran*	2006–2009 mean
% intervals removed because of ≥15% pings failing filters	3.71	9.07	17.23	1.09	2.63	10.19	7.17	7.30
Mean vessel speed (m·s^{-1})	4.76	4.90	5.21	4.88	4.62	4.57	4.29	4.75
Total number of 0.5 nmi EDSUs	2968	4962	5822	2756	4140	4181	4127	4137

Note: Vessel speeds were >2.1 m·s^{-1}.

Fig. 2. Integration gain (i.e., S_v gain) measured in standard sphere calibrations normalized to the mean value for each vessel–year combination during the summer 2006–2009 eastern Bering Sea acoustic-trawl and bottom trawl surveys. System settings for data processing were as follows: frequency 38 kHz, sound speed 1470 m·s^{-1}, absorption 0.01 dB·m^{-1}, pulse length 1.024 ms, and power 2000 W. Two-way beam angle was −20.6 dB for *Aldebaran*, *Arcturus*, and *Northwest Explorer*. Two-way beam angle for *Miller Freeman* was −21.0 dB and for *Oscar Dyson*, −20.7 dB.

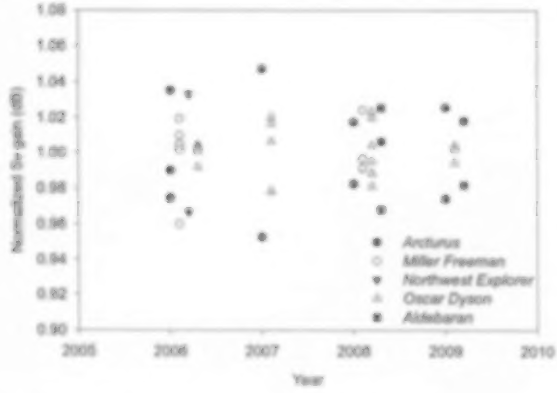

Fig. 3. Time series of acoustic-trawl (AT) survey biomass and I_{AT}, I_{UDB}, and I_{BT} indices. Each time series was divided by its average during the period 1999–2004. Error bars indicate 1D geostatistical 95% confidence intervals.

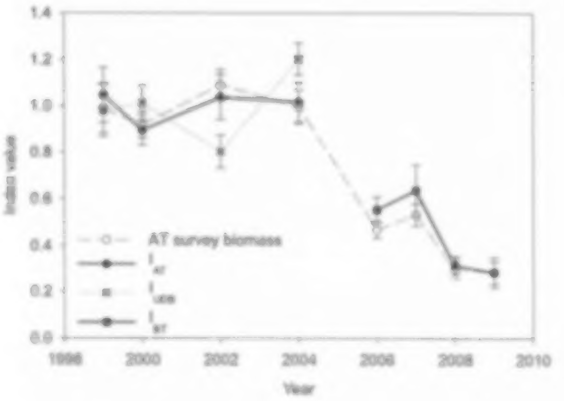

Retrospective analysis (1999–2004)

The I_{AT} closely tracked the temporal pattern in AT survey walleye pollock biomass, in terms of magnitude and direction of changes relative to 2004, across all 4 years ($r^2 = 0.58$; Fig. 3). The 1D geostatistical error bars about the values in each time series indicate that I_{AT} has a similar relative estimation error (0.04–0.06) to that of the AT survey (0.03–0.06; see table 7 in Honkalehto et al. 2010).

The simple procedures to evaluate the walleye pollock presence and predominance thresholds used to choose the cells of the index area indicated that using stricter criteria (e.g., requiring the minimum walleye pollock s_A to be more than 100 or the minimum total s_A attributed to walleye pollock to be more than 70% of total s_A) did not improve index performance, but simply reduced the size of the index area and resulted in more cells being identified for manual processing rather than autoprocessing. With substantially relaxed thresholds, the index no longer tracked the AT survey walleye pollock biomass. No matter what thresholds were used, autoprocessed backscatter data alone were not able to capture the pattern of variability in 1999–2004 AT survey walleye pollock biomass. Thus I_{UDB}, calculated using only autoprocessed data, was negatively correlated with the AT survey time series ($r^2 = 0.32$, Fig. 3), and relative estimation error bars did not overlap in 2 of 4 years.

BT survey index (I_{BT}, 2006–2009)

During 2006–2009, with data from both BT and AT surveys available, I_{BT} was compared within and between years with results of the full AT survey. In some years, for logistical reasons, not all criteria were met for all 138 index area cells to be included in the I_{BT} computation; for example, in a few instances all acoustic data were excluded from a cell because filters removed more than 15% of the pings from data files in that cell, or a cell was not transited by a vessel. The number of cells containing valid data was 136 in 2006, 121 in 2007, 137 in 2008, and 138 in 2009 (e.g., Figs. 1*b*, 1*c*, 1*d*). To ensure comparability among years, the I_{BT} value for each year was multiplied by a scaling factor consisting of the total number of index area cells divided by the number of index area cells containing valid BT survey data in that year. The results show that I_{BT} (2006–2009) closely tracked the temporal variation in midwater walleye pollock biomass as measured by the AT survey (2006–2009, $r^2 = 1.00$; Fig. 3).

Large-scale walleye pollock spatial patterns based on either the AT or BT survey acoustic data also agreed well with one another, showing similar walleye pollock distributions across the shelf during summer (Figs. 4*a*–4*h*). Although the index

Fig. 4. Backscatter classified as walleye pollock from the bottom trawl (BT) survey index area (panels *a*, *c*, *e*, *g*) and the acoustic-trawl (AT) survey (panels *b*, *d*, *f*, *h*) in summers 2006–2009. A solid blue line indicates the 200 m depth contour. The diagonal dashed line in the upper left corner of each plot indicates the boundary between the USA and the Russian Exclusive Economic Zone.

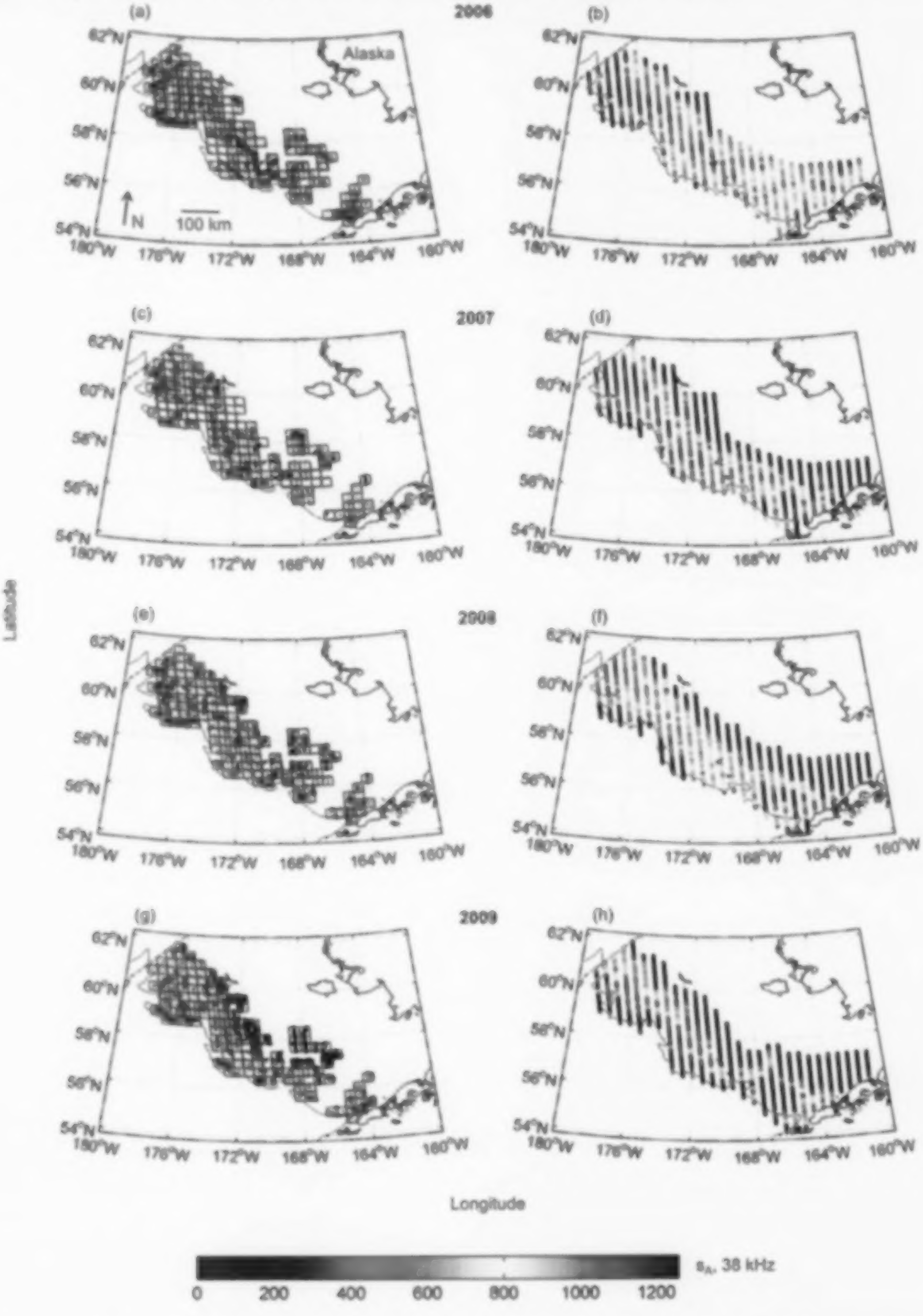
(a)
2006
(b)
Alaska
N
100 km
(c)
2007
(d)
(e)
2008
(f)
(g)
2009
(h)
62°N
60°N
58°N
56°N
54°N
180°W
176°W
172°W
168°W
164°W
160°W
Latitude
Longitude
0
200
400
600
800
1000
1200
s_A, 38 kHz

area covers only part of the AT survey, both data sets indicated that most midwater walleye pollock were located west of 170°W in 2006–2009. As in the retrospective analysis results, over 80% of the total AT survey midwater walleye pollock biomass occurred in the index area. These observations corroborate the retrospective analysis findings that the index area is a reasonable indicator of both the distribution and the abundance of the entire EBS midwater walleye pollock stock. The I_{AT} CG was close to and west of the CG of the AT survey in each year (Fig. 5). I_{AT} CG was within 46.0 km of the AT survey backscatter on average, ranging from 28.9 km in 1999 to 74.3 km in 2004. Likewise, the CG of I_{BT} (2006–2009) was close to the AT survey CG; it was to the west in 2006, 2008, and 2009, but it was to the east in 2007. The I_{BT} CG was within 38.6 km of the CG of the AT survey backscatter on average, ranging between 2.2 km in 2009 and 73.2 km in 2007 (Fig. 5). The global index of collocation (Fig. 6) for I_{AT} and AT survey indicated nearly complete overlap (I_g = 1.0), while the local index of collocation showed somewhat less fine-scale coherence (I_l = 0.9). On the large scale, I_g indicated that I_{BT} and the AT survey backscatter overlapped in all 4 years (>0.99). However, I_l indicated that on the fine scale there was much less spatial coherence (mean I_l = 0.5; Fig. 6).

Discussion

The new annual BT index (I_{BT}; 2006–2009) closely tracked the results of the AT survey and thus can provide information on midwater walleye pollock abundance at relatively little cost when the AT survey is not conducted. The retrospective index (I_{AT}; 1999–2004) demonstrated that analyzing a region smaller than the entire AT survey area to track walleye pollock abundance was feasible and allowed for use of an automated analysis procedure to save time and effort during data analysis.

Spatial analyses of I_{AT} and the AT survey backscatter provided context for subsequent comparison of the I_{BT} and AT survey backscatter. Both sets of comparisons showed broad overlap at a large scale. The I_{AT} and AT survey were expected to be very similar because they came from the same data set. The main differences between the two, namely the westward displacement of the I_{AT} CGs and fine-scale differences indicated by local collocation index values < 1, stem from using a subset of the AT survey data to compute I_{AT}. Proportionally more index area cells were in the western portion of the AT survey area, and the backscatter data were attributed to walleye pollock differently in I_{AT} than in the AT survey. The much lower fine-scale spatial coherence between I_{BT} and the AT survey than between I_{AT} and the AT survey is not surprising because the BT survey and the AT survey are different data sets; they sample the grid cells of the index region at different times while seasonal movement and migration of walleye pollock are occurring over the course of the summer (Kotwicki et al. 2005). In addition, while the AT survey progresses from east to west along the north–south survey transects, the order in which the BT survey vessel(s) move among the grid cells changes from year to year, which might lead to additional interannual sampling variability. Thus the weaker fine-scale coherence between I_{BT} and the AT survey may simply indicate localized fish movement within the surveyed area and increased sampling variability in the BT survey data.

The large-scale spatial agreement between the walleye pollock distributions estimated by the AT survey and the new I_{BT} suggests that the index provides a way of monitoring not only annual abundance, but also shelf-wide distribution of midwater walleye pollock. For example, the distribution of walleye pollock backscatter in the I_{BT} shows that most midwater walleye pollock were located west of 170°W in 2006–2009, an observation consistent with the results of AT surveys, BT survey trawl data, and reports from the commercial fishery during those years (Honkalehto et al. 2010; Lauth 2010; Ianelli et al. 2009). Knowledge of the large-scale spatial distribution of walleye pollock has both ecological and commercial importance. This information together with observations of physical oceanographic conditions, distribution of prey resources, and age structure of the stock can potentially be used to better understand the mechanisms that determine walleye pollock distribution patterns (Kotwicki et al. 2005; Mueter et al. 2006). These distribution patterns can be used in economic models to forecast economic impacts on the fishery (e.g., Haynie and Layton 2010). For example, fishing vessels traveled substantially greater distances from port during 2007 and 2008 and incurred greater transportation costs to find sufficient concentrations of walleye pollock (Ianelli et al. 2008).

The use of commercial vessels as platforms to collect acoustic data to assess commercial fish species is becoming more common (International Council for the Exploration of the Sea 2007), especially in lieu of using scientific vessels when competition for ship time is intense among programs and operational costs are high. As with dedicated AT surveys, acoustic data from commercial fishing vessel platforms should be from an unbiased sampling design using calibrated, scientific-quality echo sounders that are operated under favorable conditions (e.g., minimal noise interference). These data can then be used to reliably estimate fish distribution and abundance. In a number of these studies (e.g., Claytor and Allard 2001; Melvin et al. 2002), the commercial vessels collect acoustic data while conducting fishing operations and are unable (or do not attempt) to conduct comprehensive surveys or sample along regularly spaced transects, which are favored for the design of acoustic surveys of fish populations (Simmonds and MacLennan 2005). The present study took advantage of the regular sampling grid of the BT survey trawl stations. Despite design differences between the two surveys, the 2006–2009 I_{BT} showed similar temporal and spatial patterns of walleye pollock distribution, and similar sampling variance estimates, to the AT survey. The calibration variability among fishing vessel acoustics systems was not dramatically different than those of the research vessels. This was also the case in earlier work involving calibration comparisons between commercial and research vessels (Claytor and Allard 2001). Acoustic interference was eliminated in the present study by turning off or synchronizing other acoustic equipment on board the fishing vessels. Since the AT and BT surveys occur in summer months when the Bering Sea typically has fewer and smaller storms compared with winter conditions, weather-generated data collection problems such as bubble sweepdown (Ona and Traynor 1990) that might be severe with hull-mounted transducers were infrequent enough

Fig. 5. Center of gravity estimates for walleye pollock backscatter from the indices I_{AT} (1999–2004) and I_{BT} (2006–2009) (solid black lines), and the acoustic-trawl (AT) survey (dashed gray line) for 1999–2009. The 200 and 100 m isobaths are shown by solid gray lines.

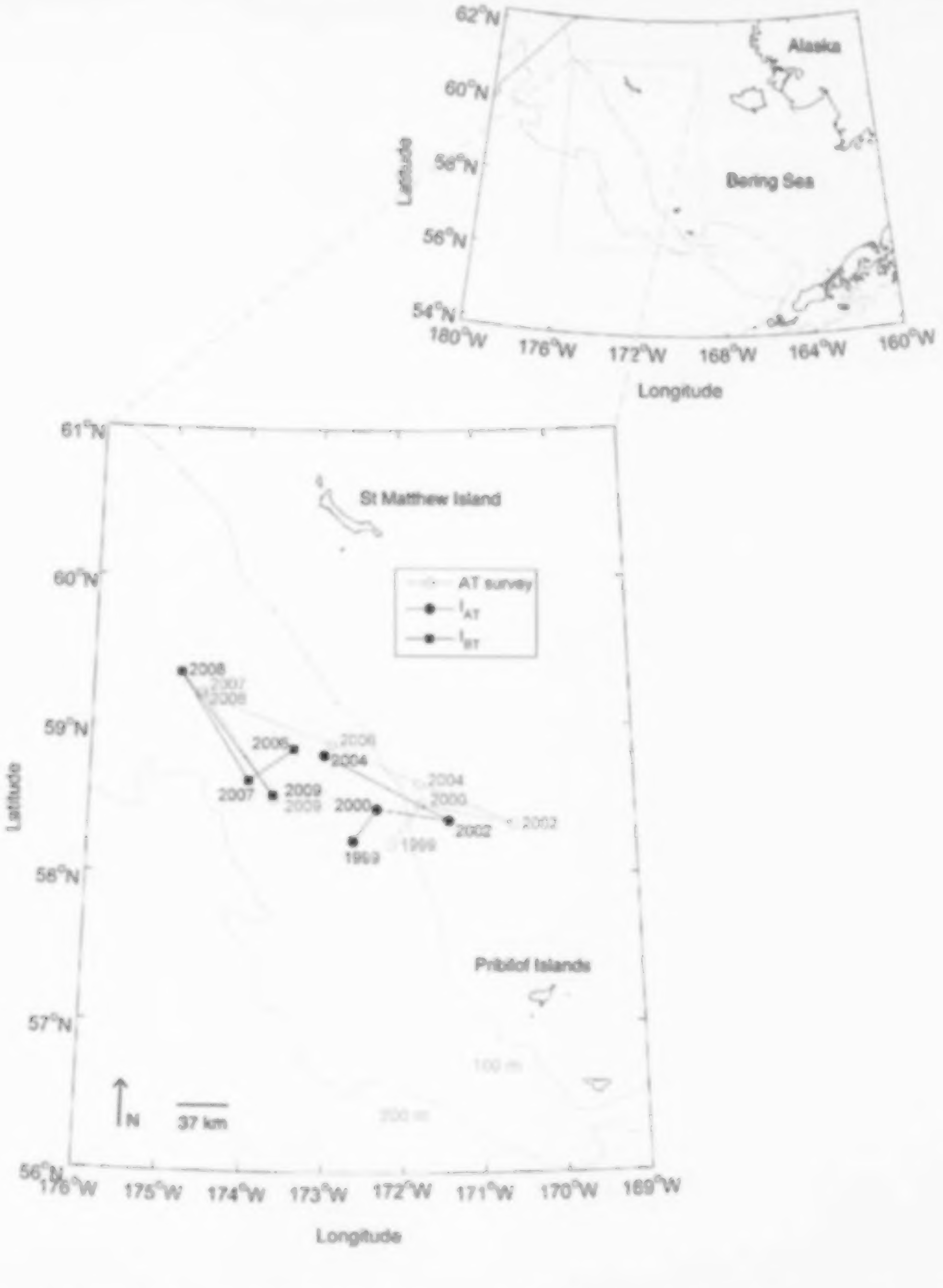
62°N
60°N
58°N
56°N
54°N
Latitude
Alaska
Bering Sea
180°W
176°W
172°W
168°W
164°W
160°W
Longitude
61°N
60°N
59°N
58°N
57°N
56°N
Latitude
St Matthew Island
AT survey
I_{AT}
I_{BT}
2008
2007
2006
2006
2006
2004
2004
2007
2009
2009
2000
2000
2002
2002
1999
1999
Pribilof Islands
100 m
200 m
N
37 km
176°W
175°W
174°W
173°W
172°W
171°W
170°W
169°W
Longitude

to be successfully detected and addressed during postprocessing. This study did not investigate or control for differences in fish density estimates caused by potential differences in fish reaction between vessels. Two vessel comparison of daytime acoustic measurements of Bering Sea walleye pollock density during the AT survey between a noise-reduced and a traditional research vessel found little difference in walleye pollock behavior that affected density estimates (De Robertis et al. 2008, 2010). Finally, although noise-reduced, special-purpose acoustic research vessels may be preferable for dedi-

Fig. 6. Global (I_g, open diamond with dot) and local (I_l, solid diamond) indices of collocation estimates between acoustic-trawl (AT) survey walleye pollock s_A and I_{AT} index s_A (1999–2004), and AT survey walleye pollock s_A and I_{BT} index s_A (2006–2009).

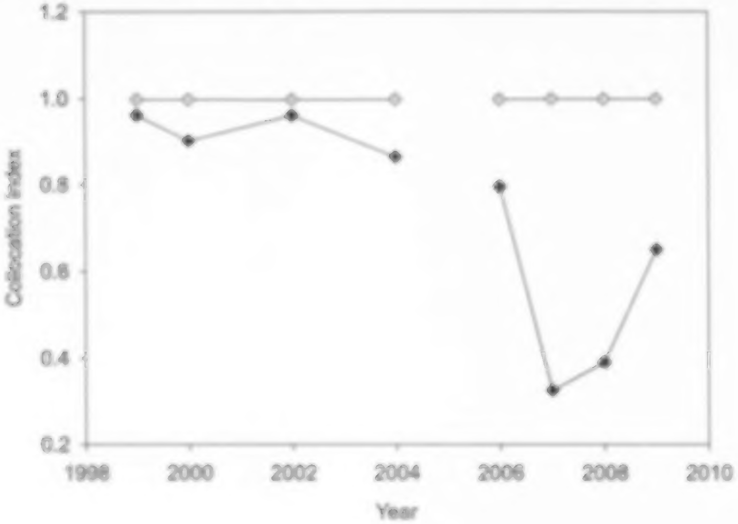

cated acoustic surveys of fish (International Council for the Exploration of the Sea 2007; De Robertis and Wilson 2010), the good spatial and temporal agreement demonstrated here between I_{BT} and the AT survey results suggests that data collected by these commercial fishing vessels were adequate for constructing a summer index of walleye pollock abundance and distribution.

A standard acoustic survey of fish abundance is assumed to detect all or some known fraction of the stock of interest; this fraction may be estimated by stock assessment models that use the survey results (Simmonds and MacLennan 2005; Ianelli et al. 2008). For a new index survey where only a portion of the stock of interest is detected, the trend in abundance for the index must accurately represent changes in the entire stock. Ressler et al. (2009) argued that a new index of widow rockfish (*Sebastes entomelas*) abundance based on acoustic data collected by fishing vessels would meet this standard based on the historical fish distribution inferred from commercial catches and habitat preferences of that species. The index for walleye pollock presented here, based on 4 years of BT survey data, was consistent with the trend in the abundance and spatial distribution of the midwater walleye pollock stock based on the dedicated AT survey. The study is unique because it not only provides an annual abundance index, but also allows evaluation of the index performance against an independent estimate of midwater walleye pollock abundance, namely the biennial AT survey results. Although some other studies involving collection of acoustic data from fishing vessels provide abundance indices (Stanley et al. 2000; Honkalehto and Ryan 2003; O'Driscoll and Macaulay 2005), none has built-in, research vessel survey comparisons for evaluation of index performance.

Acoustic-based estimates of abundance are critically important in fisheries management, as illustrated by their direct influence on quota recommendations (e.g., Ianelli et al. 2009). The costs of collecting, processing, and using results based on acoustic data from these fishing vessels are minor compared with the costs of conducting a dedicated AT survey. Although the precision of the acoustic data collected from the commercial vessels during the BT survey may be lower than that obtained with more costly dedicated efforts, the opportunity to collect and analyze these data to estimate the index presented here will undoubtedly provide better information for advice on critical near-term fisheries management actions.

Acknowledgements

The authors thank scientists from Resource Assessment and Conservation Engineering's (RACE) EBS groundfish program for assisting with acoustic data collections and calibrations amidst intense bottom trawl surveys. We thank the skippers and crews of the F/V *Aldebaran*, F/V *Arcturus*, and F/V *Northwest Explorer*, as well as vessel managers and port engineers from Trident Seafoods Corporation and the B & N Fisheries Company. We also thank the officers and crews of NOAA ships *Miller Freeman* and *Oscar Dyson*. Scott Furnish (AFSC Midwater Assessment Conservation and Engineering (MACE) Program), Gary McMurrin (AFSC RACE), Mike Hillers (Simrad), and Steve Branstiter (Furuno) all provided equipment consultation and electronic troubleshooting. Angie Greig (AFSC) provided helpful ArcGIS support. Paul Walline (AFSC MACE) provided valuable consultation on use and interpretation of geostatistical parameters. Finally, we are grateful to all of our acoustics colleagues in MACE and the International Council for the Exploration of the Sea Working Group on Fisheries Acoustics Science and Technology for helpful discussions during the project development and to Stan Kotwicki, Paul Walline, James Ianelli, and three anonymous reviewers for comments on previous drafts of this manuscript. Reference to trade names does not imply endorsement by the National Marine Fisheries Service, NOAA.

References

Barbeaux, S.J., Dorn, M., Ianelli, J., and Horne, J. 2005. Visualizing Alaska pollock (*Theragra chalcogramma*) aggregation dynamics. ICES CM U-01.

Bez, N., and Rivoirard, J. 2000. Indices of collocation between populations. *In* Report of a workshop on the use of continuous underway fish egg sampler (CUFES) for mapping spawning habitats of pelagic fish. *Edited by* D.M. Checkley, Jr., J.R. Hunter, L. Motos, and C.D. van der Lingen. GLOBEC Rep. 14. pp. 48–52.

Bez, N., Rivoirard, J., and Guiblin, P.H. 1997. Covariogram and related tools for structural analyses of fish survey data. *In* Geostatistics Wollongong '96, Vol. 2. *Edited by* E.Y. Baafi and N.A. Schofield. Kluwer Academic Publishers, Dordrecht, the Netherlands. pp. 1316–1327.

Claytor, R.R., and Allard, J. 2001. Properties of abundance indices obtained from acoustic data collected by inshore herring gillnet boats. Can. J. Fish. Aquat. Sci. **58**(12): 2502–2512. doi:10.1139/cjfas-58-12-2502.

Cox, M.J., MacKenzie, M.L., Watkins, J.L., and Brierley, A.S. 2006. The effect of missing acoustic observations (dropped pings) on mean area density estimates of Antarctic krill (*Euphausia superba*). ICES CM /I:16.

De Robertis, A., and Wilson, C.D. 2006. Walleye pollock respond to trawling vessels. ICES J. Mar. Sci. **63**(3): 514–522. doi:10.1016/j.icesjms.2005.08.014.

De Robertis, A., and Wilson, C.D. 2010. Silent ships sometimes do encounter more fish. 2. Concurrent echosounder observations from a freedrifting buoy and vessels. ICES J. Mar. Sci. **67**(5): 996–1003. doi:10.1093/icesjms/fsp301.

De Robertis, A., Hjellvik, V., Williamson, N.J., and Wilson, C.D. 2008. Silent ships do not always encounter more fish: comparison of acoustic backscatter recorded by a noise-reduced and a conventional research vessel. ICES J. Mar. Sci. **65**(4): 623–635. doi:10.1093/icesjms/fsn025.

De Robertis, A., Wilson, C.D., Williamson, N.J., Guttormsen, M.A., and Stienessen, S. 2010. Silent ships sometimes do encounter more fish. 1. Vessel comparisons during winter pollock surveys. ICES J. Mar. Sci. **67**(5): 985–995. doi:10.1093/icesjms/fsp299.

Food and Agriculture Organization of the United Nations. 2009. The state of world fisheries and aquaculture 2008, part 1. World review of fisheries and aquaculture. FAO Fisheries and Aquaculture Department, Rome, Italy. Available from http://www.fao.org/docrep/011/i0250e/i0250e00.htm.

Foote, K.G., Knudsen, H.P., Vestnes, G., MacLennan, D.N., and Simmonds, E.J. 1987. Calibration of acoustic instruments for fish density estimation: a practical guide. ICES Coop. Res. Rep. No. 144.

Haynie, A.C., and Layton, D.F. 2010. An expected profit model for monetizing fishing location choices. J. Environ. Econ. Manage. **59**(2): 165–176. doi:10.1016/j.jeem.2009.11.001.

Honkalehto, T., and Ryan, T.E. 2003. Analysis of industry acoustic observations of orange roughy (*Hoplostethus atlanticus*) spawning aggregations on the Cascade Plateau off southeastern Tasmania in June and July 2003. CSIRO report to the Deepwater Assessment Group, Hobart, Tasmania, Australia. Available from http://www.cmar.csiro.au/e-print/open/ryante_2003.pdf.

Honkalehto, T., Patton, W., de Blois, S., and Williamson, N. 2002. Echo integration-trawl survey results for walleye pollock (*Theragra chalcogramma*) on the Bering Sea shelf and slope during summer 1999. US Dept. Commer. NOAA Tech. Memo. NMFS-AFSC-125. Available from http://www.afsc.noaa.gov/Publications/AFSC-TM/NOAA-TM-AFSC-125.pdf.

Honkalehto, T., Williamson, N., Jones, D., McCarthy, A., and McKelvey, D. 2008. Results of the echo integration-trawl survey of walleye pollock (*Theragra chalcogramma*) on the U.S., and Russian Bering Sea shelf in June and July 2007. US Dep. Commer. NOAA Tech. Memo. NMFS-AFSC-190. Available from http://www.afsc.noaa.gov/Publications/AFSC-TM/NOAA-TM-AFSC-190.pdf.

Honkalehto, T., McCarthy, A., Ressler, P., Stienessen, S., and Jones, D. 2010. Results of the acoustic-trawl survey of walleye pollock (*Theragra chalcogramma*) on the U.S., and Russian Bering Sea shelf in June–August 2009 (DY0909). AFSC Processed Rep. 2010-03. Alaska Fish. Sci. Cent. NOAA, Natl. Mar. Fish. Serv. Available from http://www.afsc.noaa.gov/Publications/ProcRpt/PR2010-03.pdf.

Ianelli, J.N., Barbeaux, S., Honkalehto, T., Kotwicki, S., Aydin, K., and Williamson, N. 2008. Assessment of the walleye pollock stock in the Eastern Bering Sea. *In* Stock assessment and fishery evaluation report for the groundfish resources of the Bering Sea/Aleutian Islands regions. North Pacific Fishery Management Council, Anchorage, Alaska. Available from http://www.afsc.noaa.gov/refm/docs/2008/EBSpollock.pdf.

Ianelli, J.N., Barbeaux, S., Honkalehto, T., Kotwicki, S., Aydin, K., and Williamson, N. 2009. Assessment of the walleye pollock stock in the Eastern Bering Sea. *In* Stock assessment and fishery evaluation report for the groundfish resources of the Bering Sea/Aleutian Islands regions. North Pacific Fishery Management Council, Anchorage, Alaska. Available from http://www.afsc.noaa.gov/refm/docs/2009/EBSpollock.pdf.

International Council for the Exploration of the Sea. 2007. Collection of acoustic data from fishing vessels. ICES Coop. Res. Rep. No. 287.

Kotwicki, S., Buckley, T.W., Honkalehto, T., and Walters, G. 2005. Variation in the distribution of walleye pollock (*Theragra chalcogramma*) with temperature and implications for seasonal migration. Fish. Bull. **103**: 574–587.

Kotwicki, S., De Robertis, A., von Szalay, P., and Towler, R. 2009. The effect of light intensity on the availability of walleye pollock (*Theragra chalcogramma*) to bottom trawl and acoustic surveys. Can. J. Fish. Aquat. Sci. **66**(6): 983–994. doi:10.1139/F09-055.

Lauth, R.R. 2010. Results of the 2009 eastern Bering Sea continental shelf bottom trawl survey of groundfish and invertebrate resources. US Dept. Commer. NOAA Tech. Memo. NMFS-AFSC-204. Available from http://www.afsc.noaa.gov/Publications/AFSC-TM/NOAA-TM-AFSC-204.pdf.

Mackinson, S., and van der Kooij, J. 2006. Perceptions of fish distribution, abundance and behaviour: Observations revealed by alternative survey strategies made by scientific and fishing vessels. Fish. Res. **81**(2–3): 306–315. doi:10.1016/j.fishres.2006.06.023.

MacLennan, D.N., Fernandes, P.G., and Dalen, J. 2002. A consistent approach to definitions and symbols in fisheries acoustics. ICES J. Mar. Sci. **59**(2): 365–369. doi:10.1006/jmsc.2001.1158.

Melvin, G.D., Li, Y., Mayer, L.A., and Clay, A. 2002. Commercial fishing vessels, automatic acoustic logging systems and 3D data visualization. ICES J. Mar. Sci. **59**(1): 179–189. doi:10.1006/jmsc.2001.1124.

Mueter, F.J., Ladd, C., Palmer, M.C., and Norcross, B.L. 2006. Bottom-up and top-down controls of walleye pollock (*Theragra chalcogramma*) on the eastern Bering Sea shelf. Prog. Oceanogr. **68**: 152–183.

O'Driscoll, R.L., and Macaulay, G. 2005. Using fish processing time to carry out acoustic surveys from commercial vessels. ICES J. Mar. Sci. **62**(2): 295–305. doi:10.1016/j.icesjms.2004.11.013.

Ona, E., and Traynor, J.J. 1990. Hull-mounted, protruding transducer for improving echo integration in bad weather. ICES CM 1990/B: 31.

Pena, H. 2008. *In situ* target-strength measurements of Chilean jack mackerel (*Trachurus symmetricus murphyi*) collected with a scientific echosounder installed on a fishing vessel. ICES J. Mar. Sci. **65**(4): 594–604. doi:10.1093/icesjms/fsn043.

Petitgas, P. 1993. Geostatistics for fish stock assessments: a review and an acoustic application. ICES J. Mar. Sci. **50**(3): 285–298. doi:10.1006/jmsc.1993.1031.

Petitgas, P., Goarant, A., Masse, J., and Bourriau, P. 2009. Combining acoustic and CUFES data for the quality control of fish-stock survey estimates. ICES J. Mar. Sci. **66**(6): 1384–1390. doi:10.1093/icesjms/fsp007.

Ressler, P.H., Fleischer, G.W., Wespestad, V.G., and Harms, J. 2009. Developing a commercial-vessel-based stock assessment survey methodology for monitoring the U.S. west coast widow rockfish (*Sebastes entomelas*) stock. Fish. Res. **99**(2): 63–73. doi:10.1016/j.fishres.2009.04.008.

Rivoirard, J., Simmonds, J., Foote, K.G., Fernandez, P., and Bez, N. 2000. Geostatistics for estimating fish abundance. Blackwell Science, Ltd., Oxford, UK.

Shen, H., Dorn, M.W., Wespestad, V., and Quinn, T.J. 2009. Schooling pattern of eastern Bering Sea walleye pollock and its effect on fishing behavior. ICES J. Mar. Sci. **66**(6): 1284–1288. doi:10.1093/icesjms/fsp071.

Simmonds, J., and MacLennan, D. 2005. Fisheries acoustics: theory and practice. Blackwell Science, Ltd., Oxford, UK.

Stanley, R.D., Keiser, R., Cooke, K., Surrey, A.M., and Mose, B. 2000. Estimation of a widow rockfish (*Sebastes entomelas)* shoal off British Columbia, Canada, as a joint exercise between stock assessment staff and the fishing industry. ICES J. Mar. Sci. **57**(4): 1035–1049. doi:10.1006/jmsc.2000.0588.

Walline, P.D. 2007. Geostatistical simulations of eastern Bering Sea walleye pollock spatial distributions, to estimate sampling precision. ICES J. Mar. Sci. **64**(3): 559–569. doi:10.1093/icesjms/fsl045.

Woillez, M., Poulard, J.-C., Rivoirard, J., Petitgas, P., and Bez, N. 2007. Indices for capturing spatial patterns and their evolution in time, with application to European hake (*Merluccius merluccius*) in the Bay of Biscay. ICES J. Mar. Sci. **64**(3): 537–550. doi:10.1093/icesjms/fsm025.

Woillez, M., Rivoirard, J., and Petitgas, P. 2009. Notes on survey-based spatial indicators for monitoring fish populations. Aquat. Living Resour. **22**(2): 155–164. doi:10.1051/alr/2009017.

Wyeth, M.R., Stanley, R.D., Kieser, R., and Cooke, K. 2000. Use and calibration of a quantitative acoustic system on a commercial fishing vessel. Can. Tech. Rep. Fish. Aquat. Sci. 2324.

Assessment of stable isotopic signatures as a means to track the exchange of sea lice (*Lepeophtheirus salmonis*) between host fish populations

Susan Dean, Claudio DiBacco, and Robert Scott McKinley

Abstract: The viability of stable isotopic carbon ($\delta^{13}C$) and nitrogen ($\delta^{15}N$) signatures to track the exchange of sea lice, *Lepeophtheirus salmonis*, between hosts was tested. It was predicted that nonfeeding sea lice would experience lowered $\delta^{13}C$ signatures and enriched $\delta^{15}N$ signatures owing, at least in part, to moulting during development. It was also predicted that newly settled parasitic first generation sea lice (late stage copepodids) would retain isotopic signatures indistinguishable from their natal host fish population. During this laboratory study, $\delta^{13}C$ signatures of nonfeeding sea lice developmental stages declined over time, while the $\delta^{13}C$ signature of chalimus III sea lice was not significantly different from fin and gill signatures of their natal hosts, thus providing an isotopic link to their natal host fish population. In contrast, $\delta^{15}N$ analysis did not show promise as a tracer in this study, as host fish populations did not display distinct $\delta^{15}N$ signatures. These results suggest that $\delta^{13}C$ signatures may be applied to identify sources of sea lice epizootics and potentially quantify the exchange of sea lice between cultured and wild salmon populations.

Résumé : Nous évaluons l'utilisation des signatures d'isotopes stables de carbone ($\delta^{13}C$) et d'azote ($\delta^{15}N$) pour suivre les échanges de poux de mer, *Lepeophtheirus salmonis*, entre les hôtes. Nous prédisons que les poux de mer qui ne s'alimentent pas ont des signatures $\delta^{13}C$ réduites et des signatures $\delta^{15}N$ enrichies à cause, au moins en partie, de la mue durant le développement et que les poux de mer parasites de première génération récemment fixés (copépodites de derniers stades) retiennent des signatures isotopiques impossibles à distinguer de celles de leur population natale de poissons hôtes. Dans notre étude en laboratoire, les signatures $\delta^{13}C$ des stades de développement des poux de mer qui ne se nourrissent pas décroissent dans le temps, alors que les signatures $\delta^{13}C$ des poux de mer de stade chalimus III ne diffèrent pas significativement des signatures des nageoires et des branchies de leur hôte natal, ce qui fournit ainsi un lien isotopique avec leur population natale de poissons hôtes. En revanche, l'analyse des $\delta^{15}N$ ne s'avère pas prometteuse comme traceur dans notre étude puisque les populations de poissons hôtes ne possèdent pas de signatures $\delta^{15}N$ distinctes. Ces résultats font croire que les signatures $\delta^{13}C$ peuvent être utilisées pour identifier les sources d'épizooties à poux de mer et potentiellement pour mesurer les échanges de poux de mer entre les populations sauvages et cultivées de saumons.

[Traduit par la Rédaction]

Introduction

The sea louse, *Lepeophtheirus salmonis*, is an ectoparasitic, caligid copepod commonly found on both farmed and wild salmon in the Northern Hemisphere (Kabata 1988). The life history of this species includes a 6- to 12-day free-swimming (planktonic) phase consisting of nauplius I, nauplius II, and infectious copepodid stages. The copepodid stage represents a transitional phase where the sea louse matures from the planktonic phase into a parasitic phase. The copepodid stage is followed by four chalimus stages, two pre-adult stages, and one adult stage (Johnson and Albright 1991*a*). Development from egg to adult requires 40 days for males and 52 days for females at 10 °C (Johnson and Albright 1991*b*).

Sea lice do not feed during the planktonic phase and obtain energy for growth and development (e.g., moulting) from internal energy reserves acquired during embryogenesis

---

Received 9 October 2009. Accepted 17 March 2011. Published at www.nrcresearchpress.com/cjfas on 11 July 2011.
J21459

Paper handled by Associate Editor Marc Trudel.

S. Dean and R.S. McKinley. The University of British Columbia, Centre for Aquaculture and Environmental Research, 4160 Marine Drive, West Vancouver, BC V7V 1N6, Canada.
C. DiBacco. Ecosystem Research Division, Fisheries and Oceans Canada, Bedford Institute of Oceanography, Dartmouth, NS B2Y 4A2, Canada.

Corresponding author: Susan Dean (e-mail: dean11@interchange.ubc.ca).

Can. J. Fish. Aquat. Sci. **68**: 1243–1251 (2011) doi:10.1139/F2011-039 Published by NRC Research Press

(Kunz 1985; Tucker et al. 2000). Sea lice do consume host fish mucus, skin, and blood throughout the parasitic phase, at which time they can cause considerable stress and disease when abundant on host fish (Kabata 1988; Grimnes and Jakobsen 1996; Morton and Williams 2003). Epizootic densities that cause stress and disease are not unusual in salmon farming operations (Wooten et al. 1982), but few cases were noted on wild fish until relatively recently (Johnson and Albright 1992). High levels of infection on wild populations have now been recorded in almost all countries within North America that have established large-scale salmon aquaculture industries (Anonymous 1997). As a result, questions have arisen regarding the origins of sea lice parasitizing farmed stocks, whether farms act as amplification reservoirs for indigenous sea lice, and whether sea lice are transferred from farm operations to wild stocks at levels sufficient to cause disease and mortality.

Wild sea lice epidemics have been observed to occur about the same time as those on nearby farmed sites (MacKinnon 1997; Pike and Wadsworth 1999), and fish raised in experimental study sites exposed to farming operations have been found to display significantly higher loads of lice than those in areas with little farming activity (Bjorn et al. 2001). In addition, results from recent modeling studies have suggested that aquaculture operations can reduce the abundance and resilience of wild fish populations, as well as lead to their extirpation (Krkošek et al. 2007*a*). It is believed that sea lice are most commonly transferred between hosts through the release of free-swimming progeny (Jones et al. 2006; but see Connors et al. 2008, 2010). Documenting the transfer of lice between fish necessitates tracking the movement and transfer of individuals in the plankton through the nauplius I, nauplius II, and free-swimming copepodid stages. Determination of origin presents a considerable methodological challenge since planktonic sea lice stages are microscopic, can disperse considerable distances via tides and currents, and suffer high rates of mortality. In addition, sea lice originating from wild and cultured fish are morphologically indistinguishable.

Stable isotope analysis may present an effective and efficient approach to track sea lice transfer between hosts on appropriate temporal and spatial time scales. Detectable isotopic signatures may be imparted onto the parasites during consumption of host mucus, skin, and blood and can be likened to unique fingerprints that reflect each parasite's host fish population. Butterworth et al. (2004) found that adult sea lice collected from farmed and wild populations could be differentiated from one another using δ^{15}N signatures. The differing δ^{15}N signatures between sea lice were attributed to variations in diet between host fish populations. If these unique signatures are imparted to free-swimming offspring and these offspring then retain stable carbon isotope signatures indistinguishable from those inherited from their hosts, all sea lice progeny could be inherently marked with natal stable isotopic signatures and could in turn act as indicators of their source populations.

The identification of epizootic sea lice origins would help resolve whether sea lice found on wild salmon originate from natural populations or salmon aquaculture farms. In the latter case, these observations would provide some impetus for establishing sea lice management programs. Potential transfer of *L. salmonis* is considered a controversial topic (McVicar 1997). It is suggested that the parasites depress wild salmon populations and have the potential to induce local extinctions of salmon populations (Krkošek et al. 2007*b*). Although it is probable that there are instances where sea lice are transferred between farm operations and wild stocks, the extent of this has yet to be directly quantified (McVicar 1997). Existing correlative evidence can be interpreted in numerous ways, and instead of abating discussions regarding the role of aquaculture in wild sea lice epizootics, it has polarized opinions in both scientific and nonscientific communities (McVicar 1997; Krkošek et al. 2008). Stable isotopic signatures may provide direct evidence needed to settle this sea lice debate and help establish effective management programs that target sources of sea lice epizootics.

This laboratory-based study developed and assessed the applicability of stable isotope signatures as a tool to distinguish the origins of sea lice infestations in populations of cultured and wild salmon over short time periods (i.e., days). The objectives of this study were to determine (*i*) whether stable isotopic signatures of adult sea lice reflect host fish signatures, (*ii*) whether newly hatched nonfeeding and nonparasitic sea lice stages of development, namely planktonic eggs, nauplii, and copepodid stages of development, retain stable isotope signatures indistinguishable from those of sea lice parents and their host fish, (*iii*) whether the nonfeeding stages of sea lice, specifically the nauplii and free-swimming copepodid stages, experience lowered delta carbon (δ^{13}C) signatures and enriched delta nitrogen (δ^{15}N) signatures due, at least in part, to moulting during development (DeNiro and Epstein 1978), and (*iv*) which (if any) parasitizing stages of sea lice development, including parasitic copepodid, chalimus, pre-adult, and adult stages, retain stable isotope signatures that reflect those of sea lice parents and their original host fish. The last objective is designed to examine the longevity of natal isotope signatures in first generation sea lice after infecting a new host to test the applicability of signatures in distinguishing the origins of sea lice infestations in populations of cultured and wild salmon.

Materials and methods

Sample collection

In September 2005, seven wild adult pink salmon (*Oncorhynchus gorbuscha*) parasitized by sea lice (*L. salmonis*) were sampled in Fife Sound (50°46′59″N, 126°37′59″W; *N* = 1), Tribune Channel (50°43′00″N, 126°11′59″W; *N* = 1), Knight Inlet (50°46′59″N, 125°37′59″W; *N* = 2), Sutlej Channel (50°52′59″N, 126°43′59″W; *N* = 1), and the Strait of Georgia (49°30′00″N, 123°59′59″W; *N* = 2) off the coast of British Columbia, Canada.

Mucus, blood, skin, muscle, fin, and gills were sampled from each fish for stable carbon and nitrogen isotope analysis. A minimum of 5 mL of blood were drawn with a syringe posterior to the anus, and mucus was scraped from both sides of the body. Muscle and skin tissues were removed from near the anal fin. The dorsal, caudal, and pectoral fins, as well as the gills from the left side of the body, were removed for isotope analyses using scissors. Sixty-seven gravid female sea lice (i.e., each with two eggs strands) were removed from the seven host fish using forceps, and their locations on the host fish were noted. Positions on the host fish were separated into six areas, including the (*i*) tail located posterior of the anus and (*ii*) head located anterior of the pectoral fins. The rest of the body was divided into four equal quadrants when viewed laterally, including (*iii*) dorsal–anterior, (*iv*) dorsal–posterior, (*v*) ventral–anterior, and (*vi*) ventral–posterior quadrants. Isotopic signatures of host fish tissues remained stable over time (Supplemental Fig. S1[1]), thereby allowing first generation sea lice to be tracked back to their natal host fish population regardless of the time lag between their hatching and attachment to their new host fish.

The distal portions of egg strands from gravid sea lice were removed using scissors and placed in jars of seawater, leaving the proximate portions of the egg strands still attached to the adult lice. All host fish samples and adult sea lice were stored on ice for the duration of the 4-day trip and during transport back to the laboratory. Upon arrival at the laboratory, host fish tissues and adult lice samples, with partial egg strands still attached, were stored at –80 °C. The detached egg strands were separated into three groups and placed in baskets within individual aerated tanks through which filtered, ambient seawater could flow. One week was allotted for growth from hatching to the parasitic copepodid stage (i.e., first parasitic life stage following the free-swimming phase) to maximize the number of lice maturing to the parasitic copepodid stage while minimizing loss of infectivity of the copepodids as they aged (Tucker et al. 2000). The free-swimming lice were sampled daily for the first 2 days and every second day for the remaining 4 days to assess changes in the stable carbon and nitrogen isotope signatures of planktonic sea lice over time. Seawater dissolved oxygen content and temperature were monitored with an Oxyguard Handy Gamma Oxygen meter and salinity measured with a Vee Gee STX-3 refractometer (temperature ± standard error (SE), 12.6 ± 0.1 °C; dissolved oxygen ± SE, 8.5 ± 0.0 ppm; salinity ± SE, 31.0 ± 0.0 psu).

Approximately 7000 newly infective copepodids were introduced to 30 cultured juvenile Atlantic salmon, *Salmo salar*. The Atlantic salmon were from the same mating and had a mean mass (± SE) of 107.8 ± 1.7 g and a mean length (± SE) of 22.4 ± 0.3 cm. The sea lice were transferred between host fish to assess whether parasitic sea lice adopted the isotopic signatures of their new hosts and, if so, on what time scale (i.e., at what stage of development). The sea lice were transferred from wild pink salmon to pellet-fed Atlantic salmon to emulate the transfer of lice between farmed and wild fish in the field. The infection level was roughly 2 lice·g^{-1} of host fish (230 lice·L^{-1} or 10 lice·cm^{-1} length of host fish). The actual movement of sea lice was conducted by transferring baskets containing infective lice from aerated culture tanks to infection baths. Infection took place over 8 h in 30 L of seawater at (±SE) 12.2 ± 0.1 °C, 31.0 ± 0.0 psu, and 9.5 ± 1.0 ppm O_2. Pure oxygen was periodically bubbled into the seawater as it was previously observed that turbulence from a continuous flow of air inhibited settlement of copepodid sea lice. Oxygen levels were not allowed to fall below 7.0 ppm O_2 as a concentration of 6.0 ppm O_2 is regarded as the minimum for optimum health for salmon (Nash 2003). In addition, salmon and lice were held in static culture with no water exchanged during the infection phase to prevent the loss of parasitizing copepodids. Water temperatures were maintained by placing the infection bath tank within a larger tank of flowing, ambient seawater. All salmon were successfully infected with sea lice.

The newly infected Atlantic salmon were moved using a dipnet from the infection bath into one of three replicate holding tanks, each holding 10 fish, following the infection treatment. Sampling of host fish tissues and attached sea lice took place immediately following infection (T = 0 h) and subsequently at 12 and 36 h and 2, 3, 4, 6, 8, 10, and 12 days after infection. A total of three salmon, one from each holding tank, was removed using a dipnet, euthanized, and sampled during each fish sampling period. The blood, mucus, skin, muscle, fin, and gill tissues were sampled from cultured Atlantic salmon as described above for the wild pink salmon, with the exception that both sets of gills were removed for analysis. These gill samples were pooled for isotopic analysis because of their small size. Attached sea lice were removed using forceps, and their position on the body, gills, or fins was noted. All sampled lice were viewed at 4× magnification with a stereomicroscope to confirm that they were living at the time of sampling, thus ensuring they had the opportunity to consume host material until their removal. Movement of appendages or body contractions observed within a 2 min observation period were used to indicate live sea lice. Those failing to demonstrate movement were discarded. Sea lice from the gills, fins, and body were then refrigerated at 4 °C for a minimum of 6 h to allow for the digestion and excretion of any host material in the gut. Following refrigeration, the sea lice were frozen at –80 °C until preparation for stable isotope analysis.

In addition, samples of sea lice with full guts were collected from the gills of the Atlantic salmon. These samples were frozen immediately following their removal from host fish at –80 °C. Sea lice with empty and full guts were sampled from the gills of cultured host fish to examine the effect of gut content on the isotopic signatures of parasitic sea lice. In summary, parasitic sea lice were collected from a total of 30 fish during 10 sampling periods over 12 days. Holding tank water temperature (11.3 ± 0.0 °C), oxygen content (7.5 ± 0.0 ppm), and salinity (32.0 ± 0.0 psu) were monitored as described for planktonic sea lice rearing.

Sample preparation

Host fish muscle, gill, skin, and fin samples were rinsed with distilled water to remove host fish mucus and blood. In addition, skin and fin samples were rasped with a scalpel and scrubbed with a small plastic brush to remove scales. Fin tissues were then cut from attached cartilaginous material using a stereomicroscope and scalpel. All samples (i.e., host fish and sea lice tissue samples) were placed in individual scintillation vials and dried at 60 °C for 60 h (Power and Klein 2004). Dried muscle, gill, and blood samples were ground using a mortar and pestle. Fin and skin samples were crushed using the tip of a stainless steel probe owing to their small size. All tissues except mucus were then placed in 8 mm × 5 mm tin capsules for analysis. Mucus samples were rehydrated using distilled water as a means to remove scale fragments that remained attached to the scintillation vials during this process, thus allowing pure mucus to be isolated. The pure mucus was then pipetted into 8 mm × 5 mm tin capsules. Dry tissue masses from the wild pink salmon and cultured Atlantic salmon were recorded. Planktonic and first generation sea lice (i.e., sea lice progeny from the ovigerous adult sea lice collected from the wild pink salmon hosts) were rinsed in distilled water and staged with the aid of a stereomicroscope according to Johnson and Albright (1991*a*). The basal plates at the tips of sea lice frontal filaments were removed, as these structures are not replaced during growth and may mask changes in the isotopic signatures of sea lice over time (Gonzalez-Alanis et al. 2001). Sea lice were then placed in different tin capsules according to their stage, position on host fish, and gut content. Egg strand tissues and first generation parasitic sea lice sampled from the same host fish were treated as individual samples (i.e., sea lice were not grouped by host fish). Adult sea lice were grouped by host fish for all stable isotope analyses, since preliminary statistical analyses indicated an individual host effect on stable isotope signature (Supplemental Figs. S2*a*, S2*b*[1]). A minimum of 10 individuals for free-swimming and parasitic copepodid stages were pooled to provide a sufficient amount of material for stable isotope analysis. Sea lice in the chalimus stages were considerably larger than free-swimming or copepodid stages and only one to three individuals were required for isotope analysis. Gravid female lice, with proximate egg strands still attached, were rinsed in distilled water to remove host mucus. Remaining eggs were then detached using scissors, placed in tin capsules, and dried, resulting in a mean (± SE) dry mass of 0.5 ± 0.1 mg. Adult lice were placed in 20 mL scintillation vials and dried. Each adult louse was then ground individually using a mortar and pestle and placed in a tin capsule (average dry tissue mass 0.9 mg).

---

[1] Supplementary data are available with the article through the journal Web site (http://www.nrcresearchpress.com/cjfas).

Sample and statistical analyses

All host fish and lice samples were analysed at the University of California – Davis Stable Isotope Facility (Davis, California). Samples were combusted, separated, and detected using continuous flow isotope ratio mass spectrometry. Experimental precision was assessed through the analysis of two standards following every 10-sample run. The R_{standard} is Pee Dee Belemnite and atmospheric nitrogen for δ^{13}C and δ^{15}N, respectively.

δ^{13}C values were normalized for variations in lipid content using the correction factor for aquatic organisms according to Post et al. (2007). Statistical analyses were performed using SPSS (version 14.0, SPSS Inc., Chicago, Illinois). δ^{13}C and δ^{15}N values greater than two standard deviations of the mean were considered extreme and removed from both the δ^{13}C and δ^{15}N data sets (Langellotto et al. 2005). An $\alpha = 0.05$ was employed for all analyses, and data were inverse-transformed to meet normality and homogeneity of variance assumptions of parametric tests when possible. Nonparametric tests (i.e., Kruskal–Wallis, Mann–Whitney) were applied in lieu of parametric tests (i.e., analysis of variance (ANOVA), independent *t* tests) when normality and homogeneity of variance assumptions could not be met. Games–Howell's post hoc test was applied following significant ANOVA results in place of Tukey's post hoc test when sample sizes were uneven and variances were heterogeneous between sample groups (Field 2005).

Results

Stable isotope analyses of wild and cultured host fish tissues

Several differences were found among δ^{13}C signatures of wild adult pink salmon tissues (ANOVA, $p < 0.001$, $F_6 = 42.640$; Fig. 1*a*). Values for skin and fin tissues were different from all other groups. The isotopic signatures of mucus, blood, and muscle were indistinguishable (i.e., mucus and muscle, Tukey's, $p = 1.000$; mucus and blood, Tukey's, $p = 0.071$; muscle and blood, Tukey's, $p = 0.078$), as were the isotopic signatures of gill tissues with mucus (Tukey's, $p = 0.359$) and muscle tissues (Tukey's, $p = 0.337$). Overall, blood had the lowest δ^{13}C signature while skin had the highest. Differences were also observed in δ^{15}N signatures of wild adult pink salmon tissues (ANOVA, $p = 0.012$, $F_6 = 3.181$; Fig. 1*b*), as blood and muscle tissues were different from fin tissue (Tukey's, $p = 0.048$, $p = 0.004$, respectively).

Tissue δ^{13}C signatures of cultured Atlantic salmon differed significantly among tissue types (ANOVA, $p < 0.001$, $F_7 = 406.241$), with the following exceptions: blood and mucus (Games–Howell, $p = 0.968$) and muscle and mucus (Games–Howell, $p = 0.377$; Fig. 1*a*). As with the pink salmon, blood had the lowest mean δ^{13}C signature and skin had the highest. Confidence intervals were considerably smaller for cultured Atlantic salmon tissues compared with the wild pink salmon fish tissues, indicating greater within-tissue variability in the isotopic signatures of tissues in the wild host fish.

Unlike δ^{15}N results for wild fish in which only two significantly different tissue comparisons were observed, δ^{15}N signatures of cultured Atlantic salmon tissues varied considerably (ANOVA, $p < 0.001$, $F_7 = 96.811$; Fig. 1*b*). Out of 30 tissue comparisons among the tissues of the cultured Atlantic salmon, only four comparisons showed no difference among tissue δ^{15}N signatures (i.e., gills and blood, Games–Howell, $p = 1.000$; mucus and fins, Games–Howell, $p = 0.980$; fins and muscle, Games–Howell, $p = 0.108$; skin and muscle, Games–Howell, $p = 1.000$). Once again, confidence intervals for the cultured fish were noticeably smaller than those of the wild fish, supporting the finding that wild host fish display greater within-tissue isotopic signature variability than cultured host fish (Fig. 1*b*).

The δ^{13}C and δ^{15}N signatures of wild adult pink salmon and cultured juvenile Atlantic salmon tissues were compared to assess whether transfer of parasitic sea lice from wild to cultured hosts would provide newly settled lice with novel stable isotope signatures. Several differences were found between the δ^{13}C signatures of tissues within the two host fish populations (ANOVA, $p < 0.001$, $F_{13} = 458.026$; Fig. 1*a*). The δ^{13}C signatures of the wild host gills, blood, mucus, muscle, and fins differed from all tissues within the cultured Atlantic salmon (Games–Howell, $p < 0.042$). While the δ^{13}C signatures of skin tissues from the wild hosts were significantly different from the δ^{13}C signatures of skin, muscle, gill, and fin tissues from the cultured Atlantic salmon, they were indistinguishable from the δ^{13}C signatures of blood and mucus from the cultured Atlantic salmon (Games–Howell,

Fig. 1. (*a*) $\delta^{13}C$ and (*b*) $\delta^{15}N$ signatures of sea lice from the adult to the first generation chalimus III stage relative to wild pink salmon and cultured Atlantic salmon host fish tissues. Wild host fish tissues, sea lice influenced by wild host fish tissues, sea lice influenced by wild and farmed host fish tissues, and cultured host fish tissues are denoted by circles, triangles, squares, and diamonds, respectively. Error bars represent 95% confidence interval (CI). Error bars for the cultured Atlantic salmon are not visible, as the symbols are larger than the confidence intervals. On the *x* axes, "FS copepodid" represents free-swimming copepodids and "P copepodid" represents parasitic copepodids. Wild adult pink salmon $\delta^{13}C$ and $\delta^{15}N$ ratios were estimated from samples from $N = 7$ individuals for blood, mucus, skin, muscle, and fin tissues; and $N = 6$ individuals for gill tissues. Cultured juvenile Atlantic salmon $\delta^{13}C$ ratios were estimated from samples from $N = 28$ individuals for blood; $N = 30$ for mucus, skin, and muscle tissues; and $N = 29$ for gill and fin tissues. Sea lice $\delta^{13}C$ ratios were estimated from $N = 7$ for adult lice, $N = 16$ for egg strands, $N = 7$ for nauplii, $N = 7$ for free-swimming copepodids, $N = 6$ for parasitic copepodids, $N = 10$ for early chalimus, and $N = 17$ for chalimus III. Sea lice $\delta^{15}N$ ratios were estimated from $N = 43$ for adult lice, $N = 15$ for egg strands, $N = 8$ for nauplii, $N = 7$ for free-swimming copepodids, $N = 5$ for early chalimus, and $N = 12$ for chalimus III. $\delta^{13}C$ values were normalized for variations in lipid content using the correction factor for aquatic organisms according to Post et al. (2007).

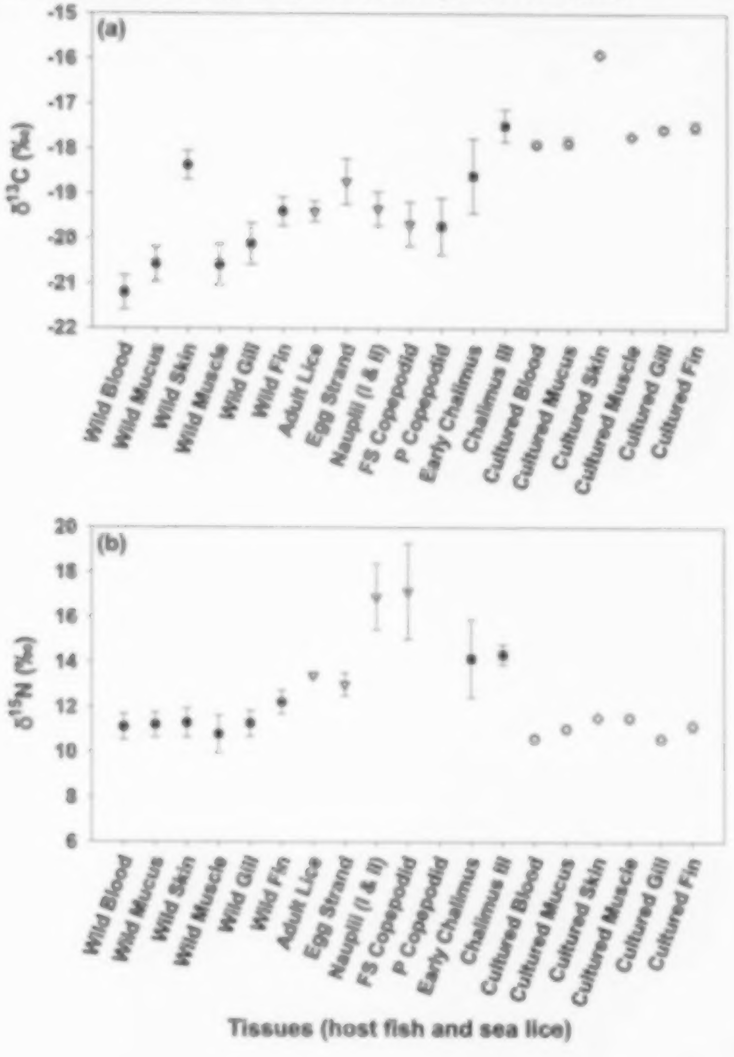

$p = 0.162$, $p = 0.113$, respectively). Unlike the $\delta^{13}C$ signatures, the $\delta^{15}N$ signatures of tissues within the host populations rarely differed from one another (ANOVA, $p < 0.001$, $F_{13} = 13.646$; Fig. 1*b*). The only differences observed among the $\delta^{15}N$ signatures of tissues from the host fish populations were between the wild pink salmon fins and the cultured Atlantic salmon blood, mucus, gill, and fin tissues (Games–Howell, cultured blood, $p = 0.002$; cultured mucus, $p = 0.019$; cultured gill, $p = 0.003$; cultured fin, $= 0.038$).

Stable isotope analyses of sea lice

Gut content had an effect on the $\delta^{13}C$ signatures of parasitic copepodids (t test, $p < 0.001$, $t_{30} = 4.362$) and early chalimus sea lice (Mann–Whitney, $p = 0.013$) but not on the $\delta^{13}C$ signatures of sea lice in the chalimus III stage (t test, $p = 0.152$, $t_{12} = 0.385$) collected from the gills of cultured host fish. With regard to $\delta^{15}N$ signature, gut content did not influence sea lice in the parasitic copepodid and early chalimus stages (t test, $p = 0.270$, $t_{16} = -1.142$; and $p = 0.068$, $t_{12} = 2.005$, respectively) but was found to impact the chalimus III stage (t test, $p = 0.039$, $t_{11} = 2.346$). The isotopic signature of sea lice did not vary significantly among recovery location, except in the case of $\delta^{15}N$ signature of chalimus III sea lice (Supplemental Fig. S3[1]).

Changes in the isotopic composition of adult sea lice through to the chalimus III stage of their offspring (i.e., fourth parasitic stage following the free-swimming phase) were observed relative to the host fish populations to assess the longevity of natal isotope signatures in sea lice progeny. All sea lice for this analysis were collected from the body and fins of cultured host fish. A steady decline in sea lice $\delta^{13}C$ signatures was observed from the egg through the nauplii I and II and, finally, the free-swimming copepodid stages (Fig. 1*a*). In contrast, $\delta^{13}C$ signatures became progressively less negative during maturation from the parasitic copepodid through the early chalimus and chalimus III stages. Adult to early chalimus sea lice were indistinguishable from wild pink salmon fin tissue (i.e., adult sea lice, Games–Howell, $p = 1.000$; egg strand, Games–Howell, $p = 0.619$; nauplius I and II, Games–Howell, $p = 1.000$; free-swimming copepodid, Games–Howell, $p = 0.998$; parasitic copepodid, Games–Howell, $p = 0.996$; early chalimus, Games–Howell, $p = 0.824$) and except for the egg strands, wild pink salmon gill tissue (i.e., adult sea lice, Games–Howell, $p = 0.210$; nauplius I and II, Games–Howell, $p = 0.249$; free-swimming copepodid, Games–Howell, $p = 0.995$; parasitic copepodid, Games–Howell, $p = 0.993$; early chalimus, Games–Howell, $p = 0.129$). The early chalimus life stage was the oldest stage to display an isotope signature indistinguishable from wild pink salmon tissues (i.e., skin, Games–Howell, $p = 1.000$; gill, Games–Howell, $p = 0.129$; fin, Games–Howell, $p = 0.824$) and the first stage to display an isotopic signature the same as the isotopic signatures of tissues from the parasitized, laboratory-cultured Atlantic salmon (i.e., blood, Games–Howell, $p = 0.868$; mucus, Games–Howell, $p = 0.822$; muscle, Games–Howell, $p = 0.642$; gill, Games–Howell, $p = 0.435$; fin, Games–Howell, $p = 0.375$). Chalimus III sea lice, which represent a later stage in the parasitizing phase of the sea lice life history, were indistinguishable from the same cultured Atlantic salmon tissues as the early chalimus sea lice (i.e., blood, Games–Howell, $p = 0.633$; mucus, Games–Howell, $p = 0.838$; muscle, Games–Howell, $p = 0.991$; gill, Games–Howell, $p = 1.000$; fin, Games–Howell, $p = 1.000$).

In contrast with $\delta^{13}C$ data, $\delta^{15}N$ signatures of adult lice, egg strands, and planktonic sea lice became progressively enriched over time (Fig. 1*b*). The signatures of the first generation parasitic sea lice became progressively depleted and only returned to approximately the same $\delta^{15}N$ value as the adult lice as opposed to surpassing it as in the $\delta^{13}C$ analysis. Furthermore, the only comparisons to show isotopic differences were between the egg strands and the fin tissues of the wild pink salmon (Games–Howell, $p = 0.624$) and the early chalimus stages and all of the wild and cultured salmon tissues.

Discussion

Early chalimus sea lice, *L. salmonis*, attached to laboratory-cultured Atlantic salmon retained stable carbon isotope signatures indistinguishable from those initially inherited from their wild pink salmon hosts. As such, stable carbon isotope ratios show potential in this study as a method to distinguish sea lice originating from wild or cultured salmon. This study exemplifies a viable technique that could provide direct evidence regarding sources of sea lice epizootics sampled in situ, including an ability to determine if sea lice found on wild fish originated from salmon aquaculture operations or wild sources.

Application of this technique is based on the assumption that all sea lice progeny are inherently tagged with natal host fish isotope signatures, as was the case in this study. These signatures are the product of the isotopic composition of host fish tissues consumed by maternal sea lice during egg strand synthesis. If host fish populations exhibit unique stable carbon isotope ratios, natal sea lice signatures can be likened to distinct “fingerprints” that provide innate links between the sea lice and their source host fish populations. The retention of these fingerprints over time allows identification of sea lice origins following the release of sea lice into the plankton and for a period of time following the attachment of sea lice to new host fish. As a result, stable carbon isotope signatures can potentially be used to identify and quantify the transfer of sea lice between farmed and wild salmon populations.

In contrast, $\delta^{15}N$ signatures were ineffective in identifying source populations of sea lice progeny, since the cultured and wild host fish populations used in the study were not isotopically distinct. This does not preclude that $\delta^{15}N$ may serve as an effective tracer in other sampling locations and for other fish species. Butterworth et al. (2004) demonstrated that $\delta^{15}N$ signatures could be used to differentiate between adult *L. salmonis* sea lice sampled from farmed salmonids and wild salmonids as well as among farmed salmonids of the same species from different farms. The Butterworth et al. (2004) study found no significant differences between the $\delta^{13}C$ signatures of these same sea lice (i.e., $\delta^{15}N$ and $\delta^{13}C$ analyses were run simultaneously). As with the $\delta^{15}N$ analysis in this study, it is likely that the host fish populations from which sea lice were sampled did not have sufficiently distinct $\delta^{13}C$ signatures.

Adult female sea lice displayed consumer-diet enrichment comparable to the typical $\delta^{13}C$ consumer-diet enrichment of 0‰–1‰ (DeNiro and Epstein 1978) relative to wild pink salmon mucus, skin, muscle, gill, and fin tissues. As the adult female sea lice had access to host fish blood, mucus, and skin, they were most likely consuming various combinations of these tissues, resulting in an average $\delta^{13}C$ signature reflective of not one tissue.

Factors that influence isotope signatures must be accounted for in any statistical analysis employed to determine lice origins. Several factors need be considered when sampling sea lice in the field, including sea lice stage, gut content, and attachment site on host fish. It was found that the

δ^{13}C signatures of sea lice egg strands, nauplii, free-swimming copepodids, parasitic copepodids, and early chalimus sea lice were indistinguishable from signatures of fin tissue of their natal host population and that sea lice from the nauplii to the early chalimus stage were indistinguishable from the gills. Thus, it is recommended that sea lice in no later than the early chalimus stage be sampled.

Gut content was found to influence the isotopic signature of sea lice. Relative to parasitic copepodid and early chalimus sea lice with empty guts, parasitic copepodid and early chalimus sea lice with full guts were, respectively, found to display stable carbon isotope signatures more similar to the signatures of their new host fish. Essentially, undigested host fish tissues within the guts of newly parasitic sea lice may shift the whole-body isotopic signature of sea lice towards that of their new host population, while individuals with empty guts have isotopic signatures that reflect trophic shifts associated with the assimilation of host fish tissues. To alleviate this effect, sampled sea lice should be held in filtered seawater for 1–2 h following collection to allow time for gut clearance.

Sea lice samples from the fins and body surface should not be grouped with sea lice sampled from the gills. Chalimus III sea lice parasitizing host fish gills were found to have significantly lower δ^{15}N signatures relative to chalimus III sea lice parasitizing the fins and body surface. This may have been due to the preferential consumption of blood by lice on the gills, which characteristically has a depleted δ^{15}N signature relative to other tissues, and the infrequent consumption of blood by lice sampled from the body surface and fins (Johnson and Albright 1992). Position on host fish was not found to have a significant effect on δ^{13}C signatures of newly settled sea lice. However, as a precaution to observed differences in δ^{15}N signatures, it is recommended that sea lice collected from fin and body surfaces not be grouped with those sampled from gills.

As predicted, egg strand and planktonic sea lice δ^{13}C signatures progressively declined over time. This is in contrast with the progressive enrichment in ^{13}C that is characteristic of nonfeeding animals (Hobson et al. 1993). The observed reduction in δ^{13}C signature is likely due to the process of ecdysis, in which the ^{13}C-rich chitinous exoskeletons of sea lice are shed during growth (DeNiro and Epstein 1978). During nonfeeding periods, ^{12}C levels are often reduced (i.e., δ^{13}C signatures are enriched) through the metabolism of ^{12}C-rich lipid stores as well as the preferential removal of ^{12}C through respiration and excretion (Cherel et al. 1988; Castellini and Rea 1992). In the case of sea lice, however, it appears ^{12}C loss is outweighed by the removal of ^{13}C during ecdysis, resulting in a lower δ^{13}C signature over time. This is supported by the finding that δ^{15}N signatures of planktonic sea lice followed typical enrichment patterns during the nonfeeding stages because chitinous exoskeletons are typically depleted in the heavier nitrogen isotope (DeNiro and Epstein 1981). Instead of opposing one another, the processes of ecdysis, respiration, and excretion act in concert to progressively raise the δ^{15}N signatures of planktonic sea lice over time. This is the first suggestion of the possible effect of ecdysis on the stable isotopic signatures of moulting animals during nonfeeding stages of development.

Wild fish tissues displayed greater isotopic variation between fish than did cultured fish tissues, and cultured fish tissues displayed greater isotopic variation in δ^{13}C signature of different tissue types than in δ^{15}N signature. The larger variation in wild fish tissues was most likely due to the controlled conditions the cultured fish were held under (Butterworth et al. 2004). The cultured fish were fed a homogeneous pellet diet; therefore, new tissues would have always been constructed with the same isotopic signature. In contrast, the process of isotopic routing, in which tissues synthesized at different times are made from materials with different isotope signatures, likely resulted in greater isotopic variation between the same tissues within individual wild fish (Schwarcz 1991). The larger variation in wild fish tissues may also have been influenced by the relatively large sampling area of the wild fish (i.e., wild salmon were sampled from a large spatial area that may have had variable prey with different isotopic signatures, translating into more variable wild host fish tissue signatures) and, to some extent, difference in sample size (i.e., seven wild fish were collected, while 30 cultured fish were sampled).

The most pressing topic for further study is the application of stable isotopes to identifying natal host populations of sea lice in the field. A number of factors that were controlled for in the laboratory during this study would require further consideration and assessment during a field study. For example, this study transferred a single population of sea lice of known origin (i.e., wild pink salmon) onto a second host population of known origin (i.e., cultured Atlantic salmon). The practical application of this technique will involve the sampling of sea lice of unknown origin with the goal of using their isotopic composition to identify their natal hosts from a range of possible fish populations. So as to create a clear link between sea lice progeny collected from wild fish and their natal host fish population, it is suggested that a single farmed fish population be selected as the target natal host fish population and that this target population be fed a feed with a distinctive isotopic signature. Sea lice from this target population would inherit the unique tag, thereby enhancing the ability of researchers to track the target sea lice following sea lice collection from wild host fish. Within such a field study, up to three infected fish would need to be sampled for every chalimus sea lice sample, as Krkošek et al. (2006) reported that juvenile salmon exhibited initial infection intensities of zero to five chalimus lice per fish.

The dispersal distances of free-swimming sea lice from their identified natal host fish population would need to be assessed for a field study. An understanding of sea lice dispersal ability would facilitate establishment of the size and location of the sampling area in which to recover sea lice; through modeling, Brooks (2005) inferred that sea lice are capable of infecting host fish tens of kilometres from their natal origins. The dispersal ability of sea lice would not hinder the use of stable isotope signatures in tracking sea lice between host fish. As shown in this study, parasitic copepodids retain stable carbon isotope signatures indistinguishable from those inherited from their wild pink salmon hosts and can be linked back to their natal host fish populations; hence, isotopic signatures would be stable regardless of the distance sea lice traveled across a specific set of life stages (i.e., the distances covered by sea lice would be limited because the time frame of a field study would be on the order of days, as opposed to weeks or months, as sea lice develop to the infective stages and remain capable of infecting new hosts over a time period of days).

This study supports the application of stable carbon isotopes to tracking the exchange of sea lice between host fish populations in situ. It puts forth a means to establish a direct link between host populations in the field, thus facilitating abatement of the controversy surrounding whether sea lice are transferred between wild and farmed populations. Should the transfer of sea lice between wild and farmed populations be established, stable isotopes also facilitate the assessment of the degree of parasite transfer as well as the development of effective sea lice management strategies.

Acknowledgements

The authors thank R. Sweeting and C. Cooper for sharing their ship, equipment, and insight in the field; J. Henry for sharing his vast knowledge of salmon; L. Skinner and N. Plantalech-Manel-la for their support in the laboratory; K. Hunter and C. Biagi for their counsel on fish health; K. Boxaspen for her advice on sea lice infection protocols; E. Kim and S. Johnson for their input on sea lice staging; J. Oakes and M. Rowshandeli for providing Atlantic salmon for the laboratory component of this study; B. Piercey and C. Payne for their guidance in isotope sample preparation; K. Gordon and D. Harris for their isotope analysis work; N. von Keyserlingk and T. Schulte for their input on experimental set-up and data analyses; and T. Kozak and J. Thomson for their advice on statistical analysis. Funding for this project was provided by grants from the BC Innovation Council to RSM and the BC Pacific Salmon Forum to CDB. SCD was supported by a postgraduate scholarship from the Natural Sciences and Engineering Research Council of Canada.

References

Anonymous. 1997. Report of the workshop on the interactions between salmon lice and salmonids. ICES, 1997/M:4 Ref:F.

Bjorn, P.A., Finstad, B., and Kristoffersen, R. 2001. Salmon lice infection of wild sea trout and Arctic char in marine and freshwaters: the effects of salmon farms. Aquacult. Res. **32**(12): 947–962. doi:10.1046/j.1365-2109.2001.00627.x.

Brooks, K.M. 2005. The effects of water temperature, salinity, and currents on the survival and distribution of the infective copepodid stage of sea lice (*Lepeophtheirus salmonis*) originating on Atlantic salmon farms in the Broughton Archipelago of British Columbia, Canada. Rev. Fish. Sci. **13**(3): 177–204. doi:10.1080/10641260500207109.

Butterworth, K., Weiming, L., and McKinley, S. 2004. Carbon and nitrogen stable isotopes: a tool to differentiate between *Lepeophtheirus salmonis* and different salmonid host species? Aquaculture, **241**: 529–538. doi:10.1016/j.aquaculture.2004.07.021.

Castellini, M.A., and Rea, L.D. 1992. The biochemistry of natural fasting at its limits. Experientia, **48**(6): 575–582. doi:10.1007/BF01920242. PMID:1612138.

Cherel, Y., Robin, J.-P., and Le Maho, Y. 1988. Physiology and biochemistry of long-term fasting in birds. Can. J. Zool. **66**(1): 159–166. doi:10.1139/z88-022.

Connors, B.M., Krkošek, M., and Dill, L.M. 2008. Sea lice esacpe predation on their host. Biol. Lett. **4**(5): 455–457. doi:10.1098/rsbl.2008.0276. PMID:18559311.

Connors, B.M., Hargreaves, N.B., Jones, S.R.M., and Dill, L.M. 2010. Predation intensifies parasite exposure in a salmonid food chain. J. Appl. Ecol. **47**(6): 1365–1371. doi:10.1111/j.1365-2664.2010.01887.x.

DeNiro, M.J., and Epstein, S. 1978. Influence of diet on the distribution of carbon isotopes in animals. Geochim. Cosmochim. Acta, **42**(5): 495–506. doi:10.1016/0016-7037(78)90199-0.

DeNiro, M.J., and Epstein, S. 1981. Influence of diet on the distribution of nitrogen isotopes in animals. Geochim. Cosmochim. Acta, **45**(3): 341–351. doi:10.1016/0016-7037(81)90244-1.

Field, A. 2005. Discovering statistics using SPSS, book 2. Sage Publications, London, UK.

Gonzalez-Alanis, P., Wright, G.M., Johnson, S.C., and Burka, J. 2001. Frontal filament morphogenesis in the salmon louse *Lepeophtheirus salmonis*. J. Parasitol. **87**(3): 561–574. PMID:11426719.

Grimnes, A., and Jakobsen, P.J. 1996. The physiological effects of salmon lice infection on post-smolt of Atlantic salmon. J. Fish Biol. **48**(6): 1179–1194. doi:10.1111/j.1095-8649.1996.tb01813.x.

Hobson, K.A., Alisauskas, R.T., and Clark, R.G. 1993. Stable-nitrogen isotope enrichment in avian tissues due to fasting and nutritional stress: implications for isotopic analysis of diet. Condor, **95**(2): 388–394. doi:10.2307/1369361.

Johnson, S.C., and Albright, L.J. 1991a. The developmental stages of *Lepeophtheirus salmonis* (Krøyer, 1837) (Copepoda: Caligidae). Can. J. Zool. **69**(4): 929–950. doi:10.1139/z91-138.

Johnson, S.C., and Albright, L.J. 1991b. Development, growth, and survival of *Lepeophtheirus salmonis* (Copepoda: Caligidae) under laboratory conditions. J. Mar. Biol. Assoc. UK. **71**(02): 425–436. doi:10.1017/S0025315400051687.

Johnson, S.C., and Albright, L.J. 1992. Comparative susceptibility and histopathology of the response of naïve Atlantic, chinook and coho salmon to experimental infection with *Lepeophtheirus salmonis* (Copepoda:Caligidae). Dis. Aquat. Organ. **14**: 179–193. doi:10.3354/dao014179.

Jones, S.R., Prosperi-Porta, G., Kim, E., Callow, P., and Hargreaves, N.B. 2006. The occurrence of *Lepeophtheirus salmonis* and *Caligus clemensi* (Copepdoda:Caligidae) on three-spine stickleback *Gasterosteus aculeatus* in coastal British Columbia. J. Parasitol. **92**(3): 473–480. doi:10.1645/GE-685R1.1. PMID:16883988.

Kabata, Z. 1988. Copepoda and branchiura. *In* Guide to the parasites of fishes of Canada, part II. Crustacea. *Edited by* L. Margolis and Z. Kabata. Can. Spec. Publ. Fish. Aquat. Sci. **101**: 3–127.

Krkošek, M., Lewis, M.A., Morton, A., Frazer, L.N., and Volpe, J.P. 2006. Epizootics of wild fish induced by farm fish. Proc. Natl. Acad. Sci. U.S.A. **103**(42): 15 506–15 510. doi:10.1073/pnas.0603525103. PMID:17021017.

Krkošek, M., Gottesfeld, A., Proctor, B., Rolston, D., Carr-Harris, C., and Lewis, M.A. 2007*a*. Effects of host migration, diversity and aquaculture on sea lice threats to Pacific salmon populations. Proc. Biol. Sci. **274**(1629): 3141–3149. doi:10.1098/rspb.2007.1122. PMID:17939989.

Krkošek, M., Ford, J., Morton, A., Lele, S., Myers, R.A., and Lewis, M. 2007*b*. Declining wild salmon populations in relation to parasites from farm salmon. Science (Washington, D.C.), **318**(5857): 1772–1775. doi:10.1126/science.1148744. PMID:18079401.

Krkošek, M., Ford, J.S., Morton, A., Lele, S., and Lewis, M.A. 2008. Sea lice and pink salmon declines: a response to Brooks and Jones (2008). Rev. Fish. Sci. **16**(4): 413–420. doi:10.1080/10641260802013692.

Kunz, E.W.M. 1985. Some aspects of the biology and population dynamics of *Lepeophtheirus salmonis* (Krøyer, 1838) and *Caligus elongates* (Nordmann, 1832) (Copepods, Caligidae), parasites of *Salmon salar* L. M.Sc. thesis, University of Stirling, Stirling, UK.

Langellotto, G.A., Rosenheim, J.A., and Williams, M.R. 2005. Enhanced carbon enrichment in parasitoids (Hymenoptera): a stable isotope study. Ann. Entomol. Soc. Am. **98**(2): 205–213. doi:10.1603/0013-8746(2005)098[0205:ECEIPH]2.0.CO;2.

MacKinnon, B.M. 1997. Sea lice: a review. World Aquacult. **28**: 5–10.

McVicar, A.H. 1997. Diseases and parasite implications of the coexistence of wild and cultured Atlantic salmon populations. ICES J. Mar. Sci. **54**(6): 1093–1103. doi:10.1016/S1054-3139(97)80014-8.

Minagawa, M., and Wada, E. 1984. Stepwise enrichment of ^{15}N along food chains: further evidence and the relation between δ^{15}N and animal age. Geochim. Cosmochim. Acta, **48**(5): 1135–1140. doi:10.1016/0016-7037(84)90204-7.

Morton, A.B., and Williams, R. 2003. First report of a sea louse, *Lepeophtheirus salmonis*, infestation on juvenile pink salmon, *Oncorhynchus gorbuscha*, in nearshore habitat. Can. Field Nat. **117**: 634–641.

Nash, C.E. 2003. Interactions of Atlantic salmon in the Pacific Northwest. VI. A synopsis of the risk and uncertainty. Fish. Res. **62**(3): 339–347. doi:10.1016/S0165-7836(03)00068-7.

Pike, A.W., and Wadsworth, S.L. 1999. Sea lice on salmonids: their biology and control. Adv. Parasitol. **44**: 233–337. doi:10.1016/S0065-308X(08)60233-X. PMID:10563397.

Post, D.M., Layman, C.A., Arrington, D.A., Takimoto, G., Quattrochi, J., and Montaña, C.G. 2007. Getting to the fat of the matter: models, methods and assumptions for dealing with lipids in stable isotope analyses. Oecologia, **152**(1): 179–189. doi:10.1007/s00442-006-0630-x. PMID:17225157.

Power, M., and Klein, G.M. 2004. Fish host – cestode parasite stable isotope enrichment patterns in marine, estuarine and freshwater fishes from Northern Canada. Isotopes Environ. Health Stud. **40**(4): 257–266. doi:10.1080/10256010410001678062. PMID:15621744.

Schwarcz, H.P. 1991. Some theoretical aspects of isotope paleodiet studies. J. Archaeol. Sci. **18**(3): 261–275. doi:10.1016/0305-4403(91)90065-W.

Tucker, C.S., Sommerville, C., and Wootten, R. 2000. An investigation into the larval energetics and settlement of the sea louse, *Lepeophtheirus salmonis*, an ectoparasitic copepodid of Atlantic salmon, *Salmo salar*. Fish Pathol. **35**: 137–143.

Wooten, R., Smith, J.W., and Needham, E.A. 1982. Aspects of biology of the parasitic copepodids *Lepeophtheirus salmonis* and *Caligus elongates* on farmed salmonids, and their treatment. Proc. R. Soc. Edinb. **81**: 185–197.

A hidden Markov model approach for determining vessel activity from vessel monitoring system data

David Peel and Norman M. Good

Abstract: Many fisheries worldwide have adopted vessel monitoring systems (VMS) for compliance purposes. An added benefit of these systems is that they collect a large amount of data on vessel locations at very fine spatial and temporal scales. This data can provide a wealth of information for stock assessment, research, and management. However, since most VMS implementations record vessel location at set time intervals with no regard to vessel activity, some methodology is required to determine which data records correspond to fishing activity. This paper describes a probabilistic approach, based on hidden Markov models (HMMs), to determine vessel activity. A HMM provides a natural framework for the problem and, by definition, models the intrinsic temporal correlation of the data. The paper describes the general approach that was developed and presents an example of this approach applied to the Queensland trawl fishery off the coast of eastern Australia. Finally, a simulation experiment is presented that compares the misallocation rates of the HMM approach with other approaches.

Résumé : Plusieurs pêches commerciales dans le monde ont adopté des systèmes de surveillance des navires (VMS) pour vérifier leur conformité. Un avantage additionnel de ces systèmes est la récolte d'une quantité importante de renseignements sur la position des navires à des échelles spatiales et temporelles très fines. Ces données peuvent constituer une mine d'information pour l'évaluation des stocks, la recherche et la gestion. Cependant, comme la plupart des versions de VMS enregistrent la position du navire à intervalles fixes sans égard à l'activité de ce navire, il faudrait une méthode pour déterminer quels enregistrements de données correspondent à des activités de pêche. Notre travail décrit une approche probabiliste, basée sur des modèles de Markov cachés (HMM), pour déterminer l'activité des navires. Un HMM fournit un cadre naturel pour ce problème et, par définition, il modélise la corrélation temporelle intrinsèque des données. Nous décrivons l'approche générale que nous avons mise au point et présentons un exemple de cette approche utilisée avec des données de la pêche commerciale au chalut du Queensland au large de la côte de l'Australie orientale. Enfin, nous présentons une expérience de simulation qui compare les taux d'attributions erronées de la méthodologie des HMM à ceux d'autres méthodes.

[Traduit par la Rédaction]

Introduction

Vessel monitoring systems (VMS) are being adopted as compliance tools in many fisheries, for example, to detect vessels encroaching into closures or protected areas or registering number of days at sea to enforce fishing effort quotas. A secondary outcome of this technology is large databases of fine-scale spatial and temporal information on vessel positions. This data can be invaluable for stock assessment, research, and management in a number of ways. Some examples of the uses of fine-scale spatial fisheries data include mapping of fishing intensity at fine temporal and spatial scales (Larcombe et al. 2001; Marrs et al. 2002; Harrington et al. 2007), measuring depletion (Deng et al. 2005), assessing trawling impacts (Rijnsdorp et al. 1998), and estimating spatial abundance (Vignaux et al. 1998; Bertrand et al. 2005; Good and Peel 2007).

A VMS collects positional data of vessels at regular–irregular time intervals (i.e., a poll), which is generally in the range of every 1 or 2 hours. This polling occurs irrespective of the vessel's activity (i.e., trawling, at anchor, or steaming). To use the VMS data beyond compliance, we require an indication of the vessel's activity. In general, we are mainly interested in trawling or fishing activity. However, it is foreseeable that in some instances the spatial distribution of steaming or the location of anchorages may be of interest. In some VMS implementations the vessel's activity may be known, such as when information from net winch sensors is

Received 30 July 2010. Accepted 26 March 2011. Published at www.nrcresearchpress.com/cjfas on 6 July 2011.
J21947

Paper handled by Associate Editor Terrance Quinn II.

D. Peel. Wealth from Oceans National Research Flagship and CSIRO Mathematics and Informatics and Statistics, Castray Esplanade, Hobart TAS 7001, Australia.
N.M. Good.[*] Department of Employment, Economic Development and Innovation (DEEDI), Agri-Science Queensland, Sustainable Fisheries, Northern Fisheries Centre, P.O. Box 5396 Cairns, 4870, Australia.

Corresponding author: D. Peel (e-mail: David.Peel@csiro.au).

[*] Present address: CSIRO Mathematics and Informatics and Statistics – Australian e-Health Research Centre, Level 7, UQ CCR Building 71/918 Royal Brisbane and Women's Hospital, Herston QLD 4029, Australia.

doi:10.1139/F2011-055

available to determine trawling activity (e.g., Mejias 1999). Generally this is not the case; however, such data would provide an excellent test data set to quantify the error of a classification method.

As there is a physical limitation on how fast a vessel can draw a trawl net through the water (which is considerably slower than a vessel's normal steaming speed), an obvious indicator of a vessel's activity is the vessel's speed. So, in theory, for a given vessel, there would be a trawling speed and a steaming speed. The reality is not as straightforward, as the trawling and steaming speeds at any given time are determined by a number of factors, for example, vessel engine power, currents and tides, weather, size of net, type of gear, target species, captain–crew preference, and frequency of tows. Also the VMS data does not directly provide average vessel speed over the poll period, but rather vessel speed is calculated from the direct distance from the previous poll divided by the polling time interval. Since vessels do not always travel in straight paths, this measure of speed will generally be biased downwards. However, we would generally expect a steaming vessel to take a straighter, more direct route than when trawling. Therfore, the bias will reduce trawling speeds and increase steaming speeds and so may actually help discriminate between the two activities. The calculated speed may also be effected by non-trawling activity within the polling period (e.g., bringing in – letting out – emptying nets, turning, sorting catch, etc.), during which time the vessel may slow. These activities are ignored and considered as unmodelled noise in our approach.

Another indicator of a vessel's activity is the time of day. In many fisheries, trawling generally occurs only during certain periods of the 24 h day, beause of regulation or target species behaviour (e.g., fishing occurs only during the night). At the simplest, all points occurring during the non-trawling period could be removed. However, after examining the data in our example and consulting with fishermen, it seems that there is some variation on when fishing occurs (particularly at the boundary between trawl periods).

The existing literature does not fully address the problem of determining vessel activity from VMS data. One reference that examined the problem specifically was Mills et al. (2007), which presents a speed and direction-based approach. So it must be assumed that generally, in practice, some rule based solely on speed is used to filter out vessels travelling too fast to be trawling. However, although a simple speed cutoff approach may often work in practice, this approach has several limitations. Firstly, it ignores the temporal correlation of the data, which is the probability that a vessel trawling at the next poll is not independent of the activity at the current poll. Secondly, an outright classification of the data into vessel activity does not provide any measure of the uncertainty of the classification (e.g., polls that correspond to speeds close to the boundary of plausible fishing speeds are less certain to be trawling). Also in some applications some further adjustments or extras steps are required for the method to perform well. For example, in practice often vessels slowing to enter or exit anchorages appear to be trawling, based on speed alone. Finally, it is difficult to incorporate other covariates into the "model" (i.e., we may wish to include other covariates, such as habitat or bottom type, to either inform the classification or to possibly examine the relationship between vessel activity and the covariate).

Initially, to determine vessel activity, we investigated an approach using finite mixture models fitted to individual vessel's historical speed and time of day data (Peel et al. 2007). While this approach did solve many of the issues, the temporal correlation of the data was not addressed. To model the temporal correlation, a natural avenue to pursue is hidden Markov models (HMMs), which can be thought of as a mixture model with autocorrelated hidden membership variables. The work in this paper extends and refines HMM for VMS, initially described in Peel and Good (2007). HMM are being used in many applications, including speech recognition, econometrics, biology, and image processing (see MacDonald and Zucchini 1997 or McLachlan and Peel 2000 for a more complete list of references). The most relevant to the application described in this paper is modelling animal movement from tagging data (e.g., Patterson et al. 2009).

This paper describes the HMM method and how it can be applied to VMS data to probabilistically classify vessel activity. The method is evaluated in a simulation experiment, and a real world application to a reasonably sized data set is presented.

Materials and methods

Description of model

A HMM is a statistical model of a system that switches over time between a finite number of states, or nodes, along predefined links. A HMM assumes that the system is a Markov process. That is, the conditional probability of the future states, given the present, is independent of past states. In the context of this paper, the states, or nodes, correspond to the vessel's activity. The process involves the activity of the vessel discretely stepping around this network, with each step corresponding to a polling event. Some transition links in the network loop back to the same state, allowing a possible step outcome to be that the vessel does not change state or activity.

The true state is hidden, as we do not observe it directly; rather a quantity whose distribution is dependent on the current node–state is observed. In this application, as discussed in the previous section, an obvious observable indicator of vessel activity or state is the vessel's calculated speed. Other possible indicators are general location, time of day, and direction.

A graphical representation of the model we used is provided (Fig. 1). The model includes the nodes corresponding to trawling, steaming, and at anchor (stationary). Also included are special "Entry" and "Exit" nodes. The purpose of the Entry and Exit nodes is to address an important issue in the data that we call false trawling. Because of the discrete nature of polling, when vessels approach or leave an anchorage at steaming speed a vessel will often be misclassified as trawling. To illustrate why this occurs, suppose a vessel is polled while returning to port at steaming speed, then arrives in port and is stationary until it is polled again. The calculated speed for this interval will be greater than zero as the vessel was steaming for the first portion of the poll interval, but will generally be less than the steaming speed (i.e., closer to trawling speed) because the vessel was stationary during

Fig. 1. Representation of a hidden Markov model (HMM) with the states–nodes (circles) and transition links (arrows) indicated. The states are the obvious anchored, trawling, and steaming, plus states exit and entry to avoid vessels entering port being falsely classified as trawling.

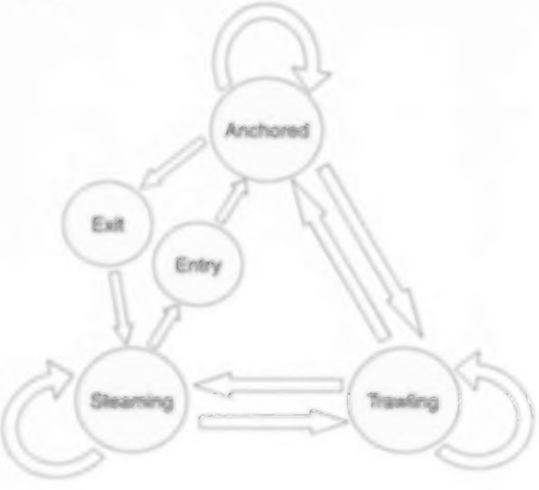

Fig. 2. Histogram of vessel monitoring systems (VMS) calculated speed (m·s^{-1}) for a selected vessel between January 2000 and March 2003. Obvious trawling and steaming modes are indicated. Notice also the almost bimodal nature of the trawling speeds. Polls with zero speed have been removed from the histograms for clarity.

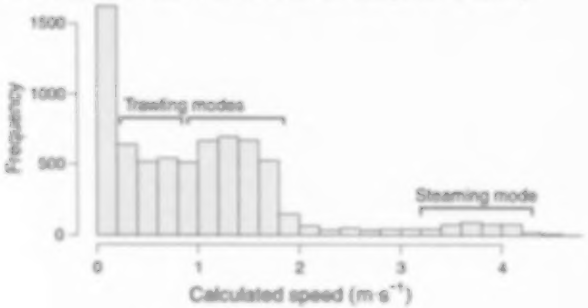

the second portion of the polling interval. The Entry–Exit nodes model this transition between anchorage and steaming. Similar nodes were not required between anchoring and trawling, because if trawling speed is biased downward upon entering a anchorage (trawling can occur when entering and exiting an anchorage, when the anchorage is very close to the trawl ground), it would most likely still be classified as trawling. However, the inclusion of such nodes may alleviate the observed non-normality of the trawling speeds that we discuss later in this section.

To describe the HMM more formally, consider a discrete Markov chain with s states and n time steps. The state of the process at time t is denoted by an indicator variable $z_{t,j}$, where $z_{t,j} = 1$ if the process is in state j at time t and 0 otherwise. The transition probability matrix **P** is defined such that

$$(1) \qquad P_{i,j} = \Pr\left[z_{t+1,j} = 1 \middle| z_{t,i} = 1\right]$$

for all times $t = 1, \ldots, n - 1$. The current state at any given time t is not observed directly, so z is a hidden variable. However the measurement of calculated speed (y_t) is observed and it is assumed to be distributed as

$$(2) \qquad f(y_t|z_t;\phi) = \prod_{j=1}^{s} f_j(y_t, \theta_j)^{z_{t,j}}$$

where for node j ($j = 1, \ldots, s$), f_j is a suitably chosen probability density function, θ_j denotes the parameters of the density, and $\phi = \{\theta_1, \theta_2, \ldots, \theta_s\}$.

The choice of f_j ($j = 1, \ldots, s$) in eq. 2 should be driven by the data (i.e., the choice of state distributions could be based on examination of the empirical distributions of VMS calculated speeds; for example, see Fig. 2).

The anchorage distribution was taken as a half normal (Johnson et al. 1994), with fixed mean of zero and a small variance, to encompass speeds very close to zero:

$$(3) \qquad f_1(y;\theta_1) \sim \mathrm{HalfN}(y;0, 0.01)$$

where HalfN(y; μ, σ^2) denotes the half-normal distribution with means μ and variances σ^2.

It was found that the distribution of trawling speeds was almost bimodal for some fisheries (as can be seen in Fig. 2). Upon further investigation, this seemed less prevalent when the polling frequency was increased. So the bimodal distribution is possibly due to non-trawling activities occurring during the polling period (e.g., sorting catch or turning around). To handle the non-normality of the data, a finite mixture model was used with unequal variances

$$(4) \qquad f_2(y;\theta_2) \sim \sum_{k=1}^{K} \pi_k N(y;\mu_{2k}, \sigma_{2k}^2)$$

where N(y; μ, σ^2) denotes the normal distribution with means μ and variances σ^2, and the mixing proportions are given by π_k.

The steaming distribution was taken to be a normal distribution

$$(5) \qquad f_5(y;\theta_5) \sim N(y;\mu_5, \sigma_5^2)$$

with mean μ_5 and variance σ_5.

The entry and exit distributions were assumed to be a uniform distribution with limits taken as the means of the anchorage and steaming distributions, i.e., for the entry state

$$(6) \qquad f_3(y;\theta_3) \sim U(y;0, \mu_5)$$

and for the exit state

$$(7) \qquad f_4(y;\theta_4) \sim U(y;0, \mu_5)$$

where U(y; a, b) denotes the uniform distribution with bounds a and b.

The trawling state parameters π_k, μ_{2k}, σ_{2k} ($k = 1, \ldots, K$) and the steaming state parameters μ_5, σ_5 are unknown parameters to be estimated.

To model the effect of the time of day, the transition matrix, **P** is taken to depend on time of day d, with each hour of the day having its own independent transition matrix. For example, in a particular fishery the probability of moving to the trawling state during the day may be very low, and moving to anchorage–steaming transition probabilities may be high, and vice versa during nighttime. It is assumed that the vessel's trawl and steaming speeds will be unrelated to time of day (i.e., the state distribution parameters ϕ do not depend on time of day).

The model was also extended to model the change in behaviour of vessels corresponding to the fisheries they are targeting at any given time, with each fishery treated independently with certain parameters chosen to be fishery-specific. Trawling behaviour can be quite different between fisheries (Fig. 3). To incorporate a fishery component in the model, each fishery c was allowed to have its own independent transition probabilities. For example, in some fisheries where very long trawls are common, the transition probability of remaining in the trawling state would be higher than a fishery where short, quick periods of trawling are the norm. In addition, since vessels may possibly trawl at different speeds when in different fisheries, the state distribution was taken to depend on fishery: $\phi_c = \{\theta_{1c}, \theta_{2c}, \ldots, \theta_{sc}\}$.

So the transition matrix $\mathbf{P}$ (from eq. 1) is now the probability of moving form state i to state j given time of day (d) and fishery (c) (i.e., for $t = 1, \ldots, n - 1$):

$$(8) \qquad P_{i,j}(d, c) = \Pr\left[z_{t+1,j} = 1 | \{z_{t,i} = 1\}, d, c\right]$$

In our application, the fishery c can be determined by the spatial location, the time of day, and caught species. It should be pointed out that even though we use the term "fishery", the aim is not necessarily to accurately identify true targeted species. Rather, we simply wish to provide a mechanism in the model to handle heterogeneity caused by differing trawl behaviour. So it is not critical to perfectly identify target species as long as fishing behaviour within our defined fishery is reasonably homogeneous for the vessel in question. However, it does seem that target species is a reasonable criterion on which to base the grouping strategy.

In our example application, information on catch species is available, and there exists a reasonable spatial separation of fisheries. Therefore, it is possible to use a simple function of most caught species to determine the fishery. In some fisheries, using the most caught species to determine the fishery would definitely not be appropriate, and a more complex approach would be required (for example, the model could also estimate the target species–fishery).

Fitting of model

The HMM is fitted to the data for each vessel independently to ascertain the parameters $\Omega = \{\phi, \mathbf{P}\}$ of the HMM and the transition matrix of the conditional probabilities

$$(9) \qquad w_{i,j,t} = \Pr\left[z_{t,i} = 1 \quad \text{and} \quad z_{t+1,j} = 1 | y_t, d_t, c_t\right]$$

Taking the row sums of $w_{i,j,t}$ provides the posterior probabilities of the vessel belonging to each state at each time point (i.e., $\Pr[z_{t,j} = 1 | y_t, d_t, c_t]$). These posterior probabilities then provide a probabilistic measure of being in any given state at time t.

The HMM can be fitted, obtaining estimates of $w_{i,j,t}$, using a brute force maximization of the likelihood

$$(10) \qquad L(y, \Omega) = \prod_{t=1}^{n} f(y_t | z_t; \phi) = \prod_{t=1}^{n} \prod_{j=1}^{s} f_j(y_t, \theta_j)^{z_{tj}}$$

However it is more efficient to maximize the likelihood via the Baum–Welch algorithm (Baum et al. 1970; see also Rabiner 1989), which can be described as a special case of the EM algorithm (Dempster et al. 1977). In essence the EM algorithm involves two steps: the E and M steps.

On the (k + 1)th iteration, given estimates of parameters $\Omega^{(k)}$, the E step estimates the transition matrix of posterior probabilities, $w_{i,j,t}^{(k+1)}$, of moving from node i to node j at time point t. This is done via a forward–backward algorithm (see Appendix A). Since the trawling state's speed distribution is a mixture model, we must also estimate the posterior probabilities of each of the normal mixture components $\tau_{t,k}^{(k+1)}$, at time $t = 1, \ldots, n$, and $k = 1, \ldots, g$ (see Appendix A).

The M step estimates the state parameters Ω, via maximum likelihood, given estimates of the transition probabilities $w_{i,j,t}^{(k+1)}$. So for example, in our application the parameters π_k, μ_{2k}, σ_{2k}, ($k = 1, \ldots, K$), μ_5, and σ_5 are the unknown parameters to be estimated (see Appendix A for further details).

This circular algorithm is repeated, refining the solution, until some form of convergence is achieved (e.g., when the log-likelihood changes by less than some predefined tolerance). In practice, it is possible that there may be a lack of historical data for some vessels (e.g., if a new vessel joins the fleet). In this case default model parameters Ω based on similar boats could be used. Another issue of data size may occur when a vessel switches to a different fishery for a very short time only. The easiest solution to this problem is to pool the relevant data together with another fishery for that vessel.

Simulation study

A simulation study was conducted to examine the performance and validate the HMM method, when time correlation assumptions are true. The only related work that could be found in the literature was part of the work to establish if VMS data could be used to estimate depletion by Deng et al. (2005). In Deng et al. (2005), a simulation study was presented to examine the effect of polling frequency on the statistical power of trawling classification.

A simulated data set was formed by mimicking vessel behaviour. Firstly, on any given day a realistic time was generated for when the vessel would begin and end fishing. The polls within this fishing time were then allocated a trawling speed. This trawling speed was generated by sampling random time segments from fishermen's actual on-board high frequency GPS data of trawling activity and by calculating a speed from the distance between the polls. Polls either side of the trawling period were then set to steaming and given a steaming speed (N(4,0.3)), and polls corresponding to entering an anchorage were given a biased steaming speed (i.e., false trawling, U(0,4)). The remaining polls were set to speed zero to indicate anchoring. A thousand sample data sets were generated, each consisting of a single vessel polling each hour over a single year. For comparison, a number of methods ranging in complexity were applied to the simulated data.

Firstly, two filters based on a speed rule with speed cutoffs of 2 m·s^{-1} as a naive "guess", based on general fishery information, and a second more informed classification using a

Fig. 3. Plots showing the difference in trawling behaviour between two of the fisheries considered in this paper; eastern king prawn (which generally consists of faster straighter trawling) and scallop (where slower, shorter trawling is the norm). Histograms of the calculated distance travelled between polls for (*a*) eastern king prawn (*Penaeus plebejus*) and (*b*) scallop (*Amusium* spp.). Corresponding plots of trawling positions for (*c*) eastern king prawn and (*d*) scallop (data corresponding to speeds greater than 2 m·s^{-1} have been removed to give a rough indication of trawling). Note that longitude and latitude are not shown because of confidentiality.

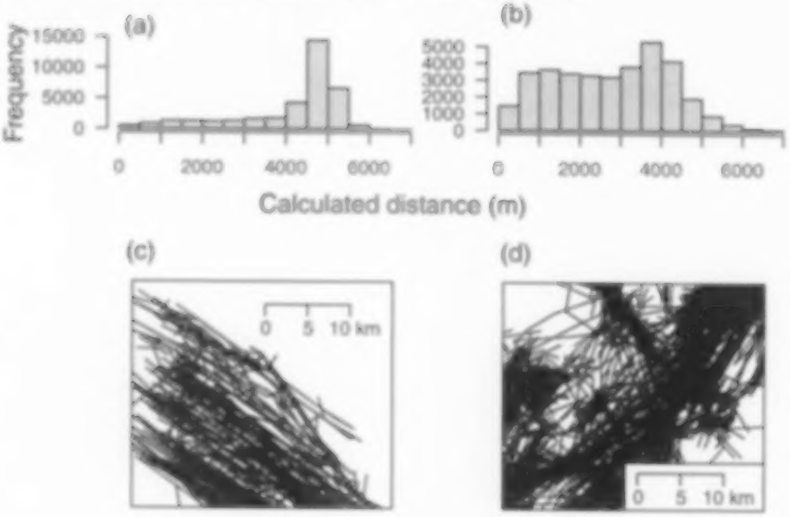

Table 1. Comparison of the misclassification rates for various methods, over a series of 1000 simulated data sets.

	Misclassification rate (%)					
Type of error	Filter: <2 m·s^{-1}	Filter: <1.7 m·s^{-1}	Filter+: <1.7 m·s^{-1}	2 group mixture	3 group mixture	HMM
Trawl as other	2.9	3.4	3.4	3.5	3.2	1.5
(90% CI)	(2.4, 3.3)	(2.9, 3.9)	(2.9, 4.0)	(2.8, 4.0)	(2.7, 3.7)	(0.8, 2.5)
Other as trawl	7.8	6.4	3.5	6.2	6.8	5.1
(90% CI)	(7.3, 8.2)	(6.0, 6.8)	(3.2, 3.9)	(5.6, 6.8)	(6.2, 7.5)	(4.0, 6.0)

Note: "Filter" corresponds to using a speed cutoff rule with the maximum trawling speed indicated; "Filter+" denotes a speed-based rule with a secondary postfixing of false trawling polls; the "2 and 3 group mixture" refer to the fitting of a standard univariate normal mixture to the data to classify between trawling and steaming; and "HMM" corresponds to the hidden Markov model approach. With regard to the types of error, "trawl as other" corresponds to the percentage of trawl polls that were misclassified as other activities (steaming, anchorage, or false trawling). Similarly, "other as trawl" corresponds to the percentage of predicted trawling activity that is actually other activities.

speed cutoff of 1.7 m·s^{-1} based on an empirical examination of the simulated data. For fairness, we also included an ad hoc classification to address the false trawling problem (i.e., we simply applied the filter speed cutoff rule and then forced any polls that were sandwiched between anchoring and steaming to be steaming).

Secondly, two univariate normal mixture models to classify trawling were examined, one with a two-component mixture (trawling and steaming) and one with a three-component mixture (two components for trawling and one for steaming).

Finally, a HMM was applied to the data, which, as we have discussed, can be thought of as a time-dependent mixture model. The results of the simulation are provided (Table 1), and it can be seen that the misallocation rate for the HMM was substantially lower than a traditional speed rule. However, it should be noted that modifying the simple speed cutoff using an ad hoc fixing of false trawling improves performance drastically. The HMM handles the simulated data very well and correctly identifies most of the polls (Fig. 4). Occasional discrepancies occur at the boundary between trawling and false trawling, as would be expected.

Example

To demonstrate the practical application of the HMM approach, we present an example from the coastal trawl fisheries of Queensland, Australia. VMS has been in operation in the fishery since 2000, covering a fleet of up to approximately 500 trawl vessels. The fishery covers a range of 2000 km of coastline from the New South Wales border to the tip of Cape York (Fig. 5). The fleet mainly targets eastern king prawn (*Penaeus plebejus*), tiger–endeavour prawn (*Penaeus esculentus*, *Penaeus semisulcatus*, and *Penaeus mono-*

Fig. 4. Examples of a typical fit to a section of time for a simulated vessel. (*a*) True states are shown: pink circles with T denote trawling, green diamonds with S correspond to steaming, blue squares with A show the anchored state, and brown triangles with F indicate the false trawling; (*b*) the corresponding HMM fit; and (*c*) the two-component mixture model fit. The polls in the fit plots have been allocated in an outright classification to states (based on maximum posterior probability) for clarity. The vertical dotted lines denote midnight each day, and the horizontal green line shows the 1.7 m·s^{-1} speed filter.

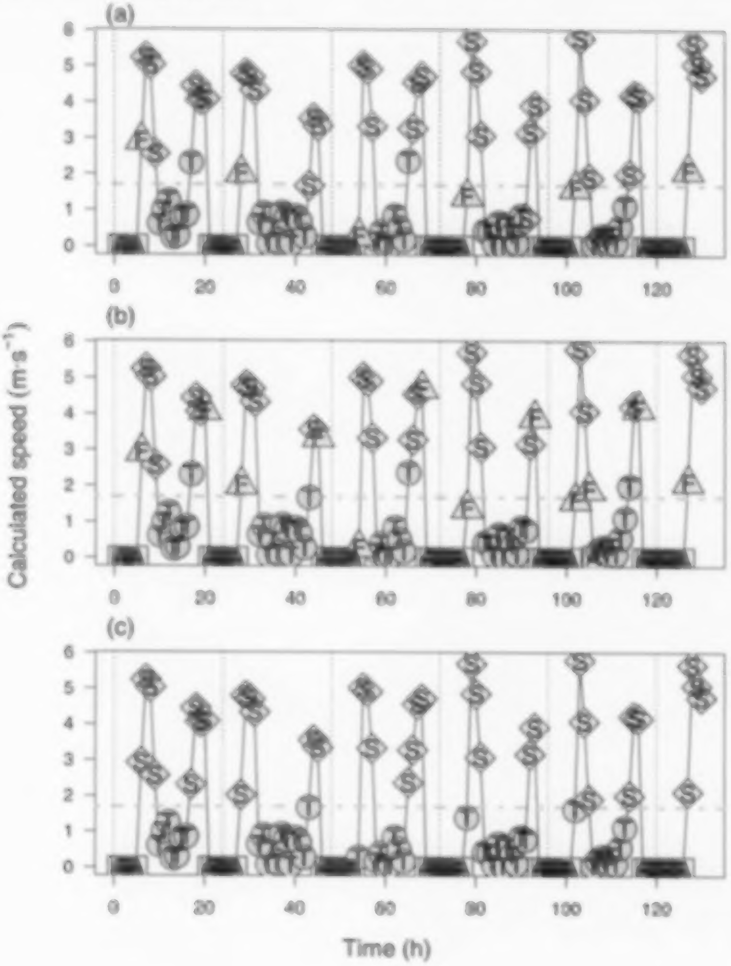

don – Metapenaeus endeavouri and *Metapenaeus ensis*), banana prawn (*Fenneropenaeus merguiensis*), and scallop (*Amusium japonicum* and *Amusium pleuronectes*).

This paper examines 3 years of VMS data recorded between January 2000 and March 2003 from 578 vessels, consisting of 2 791 901 polls, or positions. Extending the analysis to a longer time series of data should, if anything, improve the results, assuming numerical difficulties can be avoided and there is no unmodelled temporal change in vessel behaviour (for example, if the vessel's trawling speed changes over time because of net design changes). The fishery uses a fishermen logbook system to record catch amounts and species per day; this data is matched to the VMS data to provide a catch associated with each VMS data point. Further investigation has been done into using maximum entropy (Vignaux et al. 1998) to better combine logbook catches and VMS data (see Good and Peel 2007; Peel and Good 2007). Once a VMS record has a catch composition, the spatial separation of the fisheries allowed allocation to fisheries to be based on a simple maximum catch rule.

Because of the confidential nature of VMS data, we are unable to disclose the polling frequency, exact locations of individual vessels, or display fishing effort for areas where fewer than five boats were active. To work around this condition, in some of the figures spatial noise has been added, a transformation applied, no longitude–latitude indicated, and some data in sensitive areas hasve been removed.

A model consisting of five states was used (Fig. 1), and the choice of state distributions was based on examination of the empirical distributions of VMS calculated speeds. The

Fig. 5. Location and extent of Queensland trawl fishery. Light grey denotes land, and dark grey indicates general fishing extent.

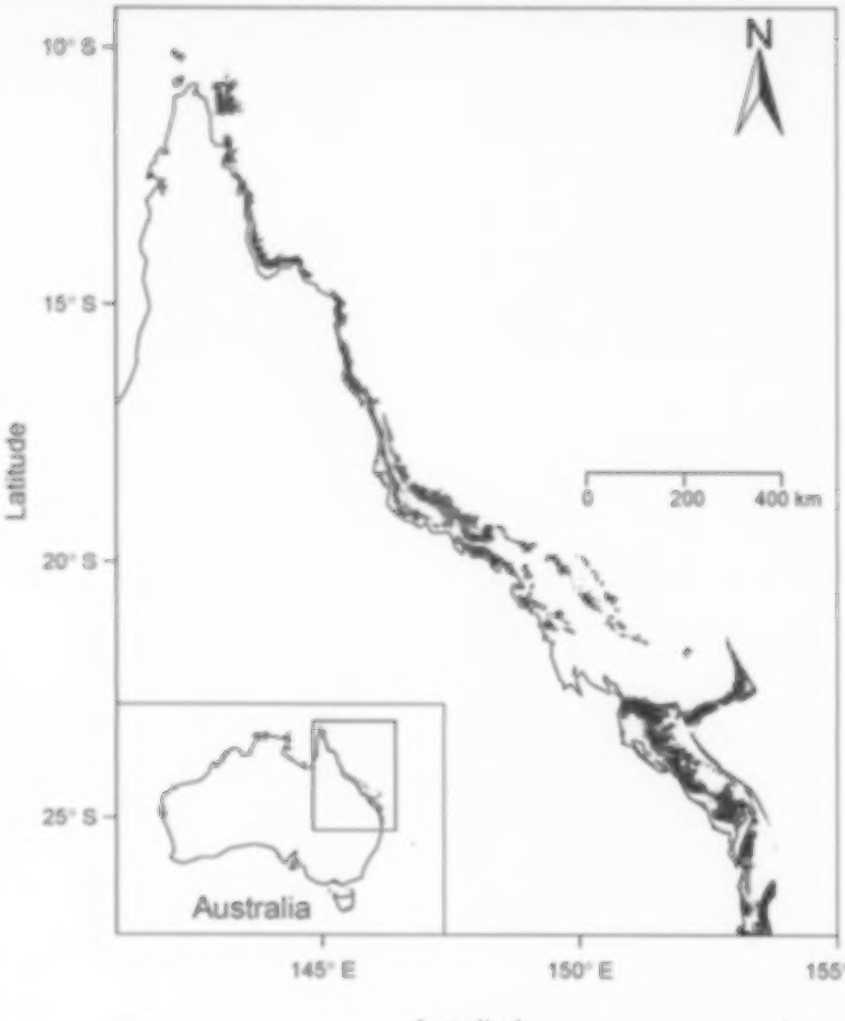

raw VMS data was matched to logbook records of catch to establish vessel fishery.

Results

The HMM was applied to the full fleet for the 3 years of data, with each vessel modelled independently by its own HMM. As expected, the model successfully determines the high speed polls to generally be steaming, the near stationary polls as anchorage, and the polls in the band between the two generally as trawling (for example, Fig. 6*a*). Also, the HMM has reasonably indicated several polls as false trawling (i.e., entry–exit from anchorage). The magnitude of the corresponding posterior probabilities (Fig. 6*b*) can also give an indication of the certainty of the allocation. For model diagnostics and outlier detection, pseudoresiduals (Patterson et al. 2009; Zucchini and MacDonald 2009) can also be examined (see Fig. 6*c*).

For some vessels there is evidence of a difference in trawl behaviour depending on targeted species (i.e., fishery), as can be seen in the histograms of calculated speed (Fig. 7). In the scallop fishery, generally there was a much greater number of lower trawling speeds because of shorter, less straight trawling behaviour (Fig. 7*a*). Whereas, for the eastern king prawn fishery there was a much more distinct mode corresponding to trawling because of longer, straight trawling behaviour (Fig. 7*b*). Interestingly, including a fishery component did not substantially change the final result for many of vessels examined. This is generally due to the vessels not changing between drastically different fisheries (e.g., the two extremes shown in Fig. 3).

The probabilistic allocation to the trawling state can be used to produce spatial and temporal maps of fishing effort for the whole fleet. At the simplest level, the fishery is divided into grid cells, and the total time trawled in each grid is calculated and plotted (Fig. 8). If spatial effort is examined

Fig. 6. Examination of a typical fit to a section of time for a single vessel. The polls have been allocated in an outright classification to states for clarity, based on maximum posterior probability (*a*). The pink circles with T denote trawling, green diamonds with S correspond to steaming, blue squares with A show the anchored state, and brown triangles with F indicate the false trawling. The *x* axis corresponds to time and the *y* axis shows the calculated speed (m·s^{-1}). The vertical dotted lines denote midnight each day. The corresponding maximum posterior probability are shown (*b*) to indicate the uncertainty of the allocations. The corresponding pseudoresiduals can be used for model diagnostics or outlier detection (*c*).

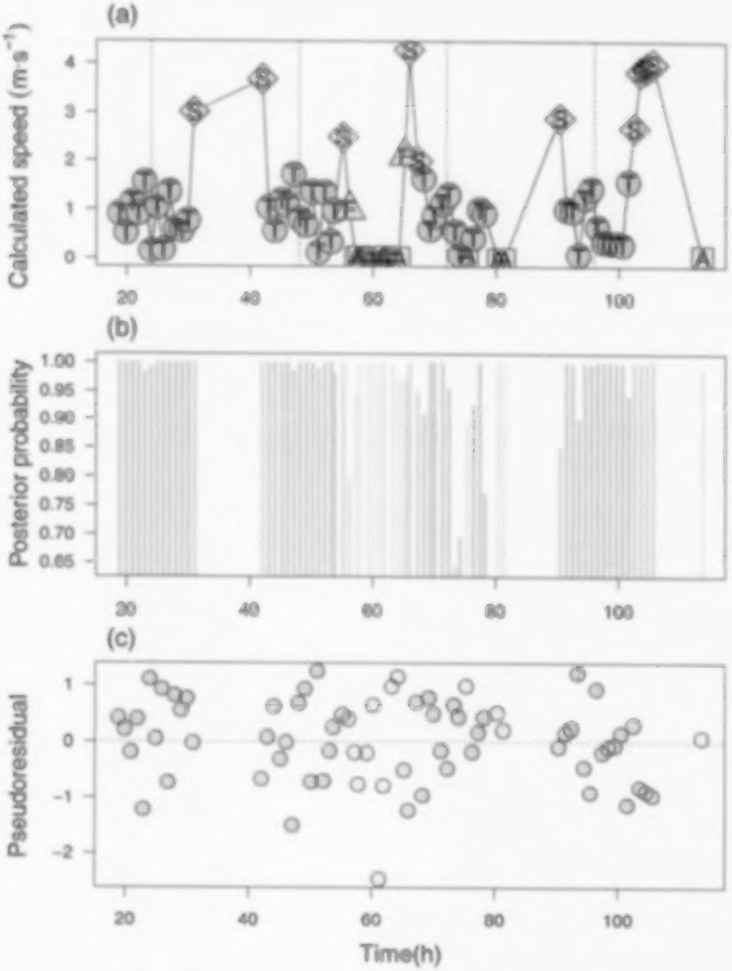

over long time periods, some form of standardization of effort would possibly be required because of changes in fishing technology and practices (O'Neill et al. 2003; Bishop et al. 2004; Maunder and Punt 2004). During this time period of the data in this paper, the Queensland fisheries logbook system recorded position at the degree level (and more recently to one tenth of a degree). Hence, the use of VMS data for effort mapping provides a substantial increase in spatial resolution over fishermen logbooks alone. It should also be noted that the VMS data provide a substantial increase in temporal resolution. Logbook entries correspond to a single point representing a full 24 h period of fishing, whereas the VMS system provides location information at a much higher frequency (for confidentiality we cannot disclose the actual polling frequency).

We can also plot the outright classifications of tracks on maps (Fig. 9). Closer examination of the allocations in this way does show some misclassified effort on the entrance and exit of an anchorage (Fig. 10*b*). However, the actual percentage of data misclassified around the anchorage is very small, especially when compared with a direct application of a speed rule (Fig. 10*a*).

The computation time to fit the model was quite reasonable; for example, a single vessel (10 548 polls over 3 years) took about 3 min to fit on a standard Intel i5 powered laptop (speed rule and mixture are both in the order of seconds). In practice, the fitting procedure should only have to be completed once and then the posterior probabilities stored to be used from then on to indicate vessel activity. As new data are collected, either a new fit to the complete time series

Fig. 7. Example of a fit for a single vessel of calculated speed corresponding to when the vessel is deemed to be in the scallop (*a*), tiger–endeavour prawn (*b*), and eastern king prawn (*c*) fisheries. The state distributions are denoted as a mixture and are overlaid on a histogram of calculated speed corresponding to the respective fishery. Polls with near zero speed have been removed from the histograms for clarity. It should be emphasized that the HMM used is not based on calculated speed alone, but also includes time of day and the underlying temporal correlated aspects of the data. Hence these plots of raw calculated speed and state distributions do not convey these important factors, but they are still useful to visualize the resulting fits. A larger section of plot corresponding to the dotted rectangle is inset in the final plot (*c*) to highlight the discontinuity due to uniform state–space distributions.

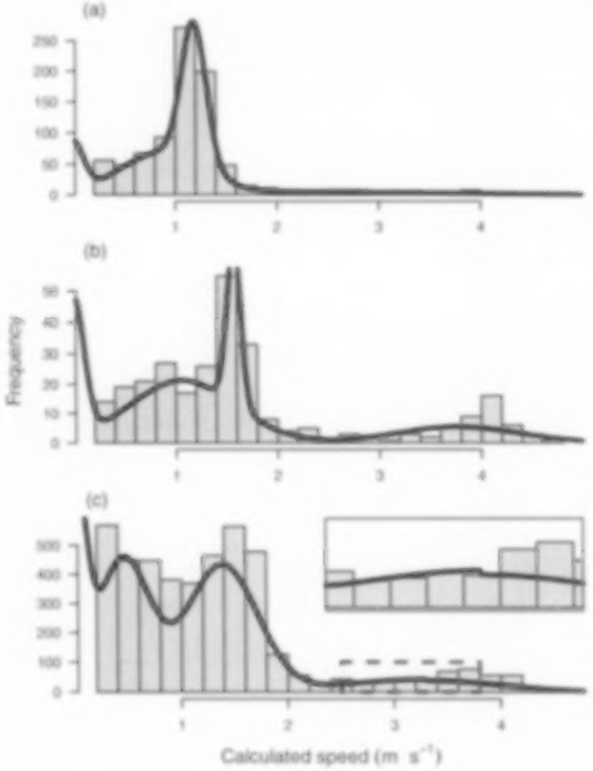

could be done, or if various conditions hold, the new data can be quickly assigned in a discriminant analysis context based on the existing HMM model parameters (i.e., simply implement a single E step).

Discussion

Hidden Markov models provide a flexible, automated method to determine vessel activity. The HMMs by their very nature model the inherent temporal correlation of the data. We have previously developed more complicated approaches combining several methods, or steps, plus ad hoc adjustments. However, the advantage of the HMM approach is that most of the issues with the data are addressed within a single, simple, statistical framework.

The flexibility of the HMM approach is a strength; however, this freedom also raises the question of model selection, for example, the choice of state distributions. The fact that the models are described within a statistical framework does provide some guidance through, for example, goodness-of-fit tests, criterion such as AIC–BIC, likelihood ratio hypothesis testing (in the case when models being considered are nested), and model diagnostics (such as pseudoresiduals). With regard to the assumed state distributions in our example, there is possibly a better choice for the entry–exit state distribution than the uniform distributions. The entry–exit state corresponds to a vessel that spends a proportion of the polling period stationary and the remaining portion at steaming speed. Hence, possibly a distribution consisting of the sum of randomly weighted steaming and anchorage speed distributions would be more appropriate. The effect of the blunt use of a uniform distribution can sometimes be seen by the non-smooth nature of the overall distribution at the upper limit of the entry–exit uniform.

Since the fitting of the HMM is reasonably automated, as seen by our example, it is feasible to use the approach on fleets consisting of a large number of vessels. However, compared with using a simpler approach, more care must be taken with the fitting procedure. In particular, it is important to avoid so-called spurious model fits, where the model fit converges to fit a random colinearity in the data (i.e., a mixture component fits small linear clumps randomly found in the data; see McLachlan and Peel (2000) for further details). To avoid spurious solutions, the use of a range of different starting values may be required. Alternatively, if spurious solutions are occurring, then constraining the covariance matrices of the normal mixture to be equal should avoid the issue. Therefore, it would be always be advisable to assess the individual vessel results to confirm that reasonable fits are being obtained.

We presented a real world example of the use of a HMM to demonstrate the practicality of the method. Specifically, the model was able to efficiently handle a large amount of VMS data (in the order of minutes per vessel) and provide sensible results. One possible drawback is that the HMM approach is much more complex to implement than a simple cutoff. Compared with the finite normal mixture approach, there is a small increase in complexity, with the added forward–backward steps required within the Baum–Welch algorithm and the computation of transition rates.

In our example, the need for a fishery component in the model, generally, did not seem to be as important as first thought. This was because the vessels seemed to generally stay in similar fisheries. This meant that much of the fishery heterogeneity in the data was modelled adequately by each vessel having its own independent HMM.

The use of VMS data provides a large increase in spatial precision over traditional logbook data. However, care should be taken not to overestimate the spatial accuracy of the resulting effort distributions. Since the VMS position is accurate (say, for example, to 50 m), it is tempting to examine the data at an extremely fine spatial scale. However, the spatial uncertainty of vessel positions between polls needs to also be considered. To better portray this uncertainty, a natural progression from the assumption that vessels travel in a straight line is to develop more realistic models (Horne et al.

Fig. 8. An example of mapping fishing effort intensity (hours) for a section of the Queensland fishery between January 2000 and March 2003 (for all fisheries). White indicates no effort, dark colours denote low intensity, and yellow shows high intensity (areas where a low numbers of vessels are active have been deleted for privacy). Gray colouring indicates land.

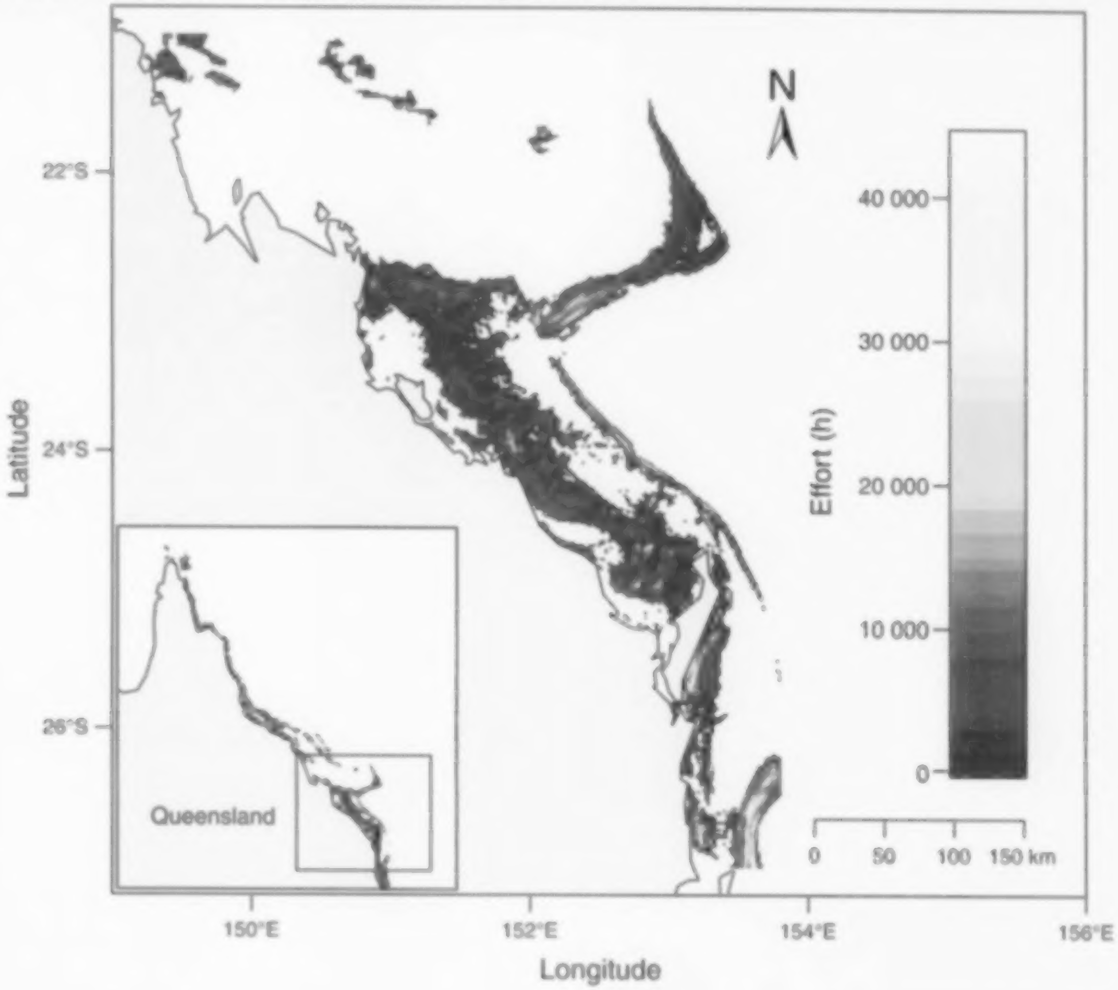

2007; Hintzen et al. 2010). In our example, we have high-frequency GPS logger data, that could be used to produce empirical distributions of models of vessel location between polls depending on spatial distance between polls.

Further work is required to develop greater ground truthing and validation. Collection of true activity for a sample of data would be one obvious way to accomplish this. Without further data on true vessel activity, it is impossible to truly validate the result but it would seem that the classifications are generally reasonable, with distinct steaming and trawling spatial locations visible. Furthermore, pseudoresiduals on the whole seem to be well behaved.

A simulation experiment compared the HMM with other approaches ranging from a simple speed cutoff rule to a mixture model approach. As expected, when temporally correlated data were analyzed, the HMM considerably outperformed a simple speed cutoff approach. Interestingly, with a postcorrection to force non-trawling on to entry–exit polls, the speed cut-off rule improved drastically. This improvement may be slightly artificial, since in the simulation all polls entering–exiting anchorage were simulated as false trawling, so obviously the ad hoc fix works extremely well and reduces the rules error. In reality, the proportion of such cases may be different and less clear cut. We could also argue that even if the modified non-HMM approach could be further refined, so that for a given situation it produced similar results to the HMM, the method would be less defendable and less robust to data changes.

The HMM approach lends itself easily to a more complex model if required. For example, the model could be adapted to estimate targeting as well as vessel activity. In the example presented in this paper, it was assumed that the most caught species and the spatial location on any given trawl indicated the target species. This is true to a large extent, although not perfect, and obviously the targeting behaviour of fishermen will be temporally correlated. The HMM method could also

Fig. 9. Plots of selected regions of VMS data for the scallop (*a*) and the eastern king prawn (*b*) fisheries over a single year. The HMM was fitted and transects with trawl probability < 0.5 are denoted by grey lines; trawl probability ≥ 0.5 are denoted by black lines.

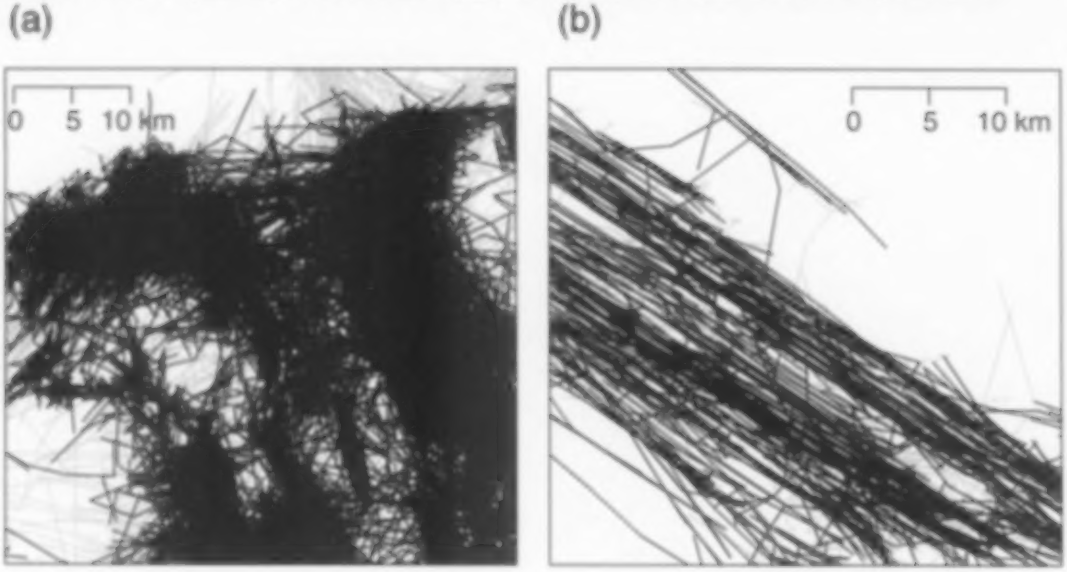

Fig. 10. Plot demonstrating some misclassification related to navigation into a port. Tracks of VMS data from a particular region: (*a*) trawling determined via a HMM and (*b*) trawling determined via speed cutoff rule (based on a mixture model). Transects with trawl probability < 0.5 are shown in grey, and trawl probability ≥ 0.5 are denoted by black lines.

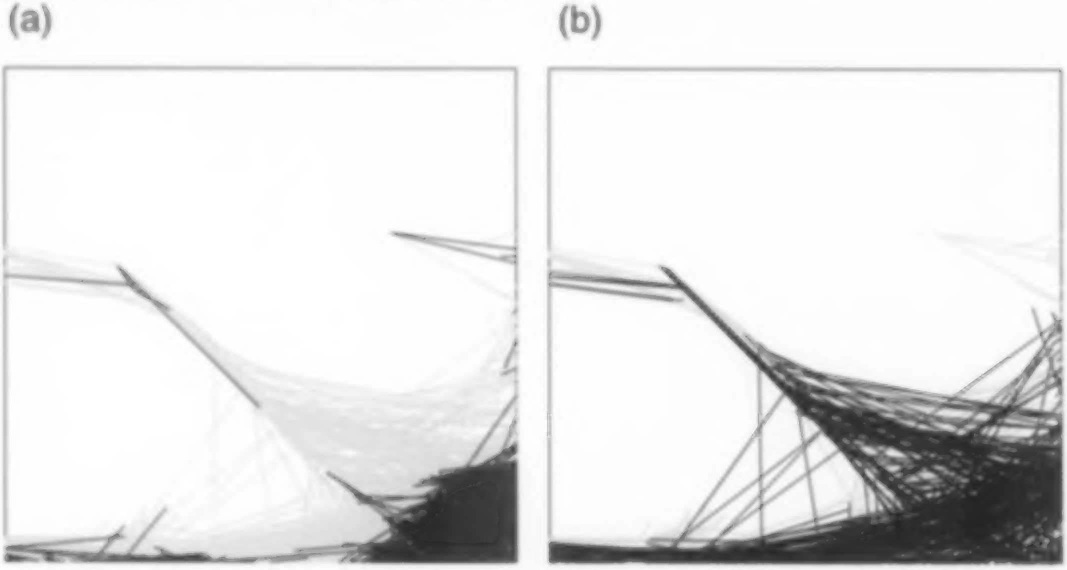

allow additional covariates (e.g., net type or size) to be included that help predict targeting behaviour and incorporate the temporal correlation. Assuming that the change over of fishing gear required to switch between fisheries only occurs when a vessel is anchored, then the model can be extended so that each fishery has its own corresponding branch of the Markov model, with the interchange node being a common anchorage node. Then the caught species could be included as an observation dependant on node–state. However, a reasonable amount of data would be required to allow the model to be extended in such a manner.

Another reasonably straightforward extension to the model would be to include other information or data that help predict vessel activity (e.g., weather, habitat–bottom type, or vessel direction) into the HMM model. This could be incorporated as a covariate on any of the parameters, as we saw with our inclusion of time of day in our example. Furthermore, in some cases the inclusion of covariates could actually be the motivation in itself, where we are trying to elicit relationships between the activity and the covariate (e.g., relating trawling to habitat type). Alternatively, extra data could be incorporated as another state-observed variable, for example, direction could be included by making the state distribution bivariate and, assuming speed and direction are independent, with the second variable corresponding to direction (i.e., modelled as an Von Mises distribution). Including this extra information may increase the acuracy of the method.

In some VMS implementations, polling frequency is not fixed and may vary. For example, when a vessel nears a closure or protected area, some systems increase polling frequency. In this case the model would have to be modified to accommodate different time steps; one approach could be to reframe the model as a continuous time Markov model.

In summary, we have found that using a HMM approach successfully addresses many of the issues in VMS data, such as temporal correlation and misclassification of entry–exit to anchorage as trawling. The HMM was shown to work within a practical implementation and generally was validated via simulation experiment. Overall HMMs provide a powerful, eloquent tool to extract vessel activity information from VMS data.

Acknowledgements

We thank Simon Hoyle and Neil Gribble for initiating the project. The project was funded by the Australian Fisheries Research and Development Corporation (FRDC). Thanks also go to Toby Patterson for the seminar that inspired the use of HMM in this work, Mark Bravington for his insightful statistical suggestions, and Tony Courtney for his advice on trawl fisheries and enthusiasm for the results VMS can provide. Thanks to the large amount of VMS data provided by Cameron Baker and the Queensland DPI&F VMS unit. Also thanks to the fishermen who provided GPS logger data and the anonymous referees for their valuable comments.

References

Baum, L.E., Petrie, T., Soules, G., and Weiss, N. 1970. A maximization technique occurring in the statistical analysis of probabilistic functions of Markov chains. Ann. Math. Stat. **41**(1): 164–171. doi:10.1214/aoms/1177697196.

Bertrand, S., Burgos, J.M., Gerlotto, F., and Atiquipa, J. 2005. Lévy trajectories of Peruvian purse-seiners as an indicator of the spatial distribution of anchovy (*Engraulis ringens*). ICES J. Mar. Sci. **62**(3): 477–482. doi:10.1016/j.icesjms.2004.12.002.

Bishop, J., Venables, W.N., and Wang, Y.G. 2004. Analysing commercial catch and effort data from a Penaeid trawl fishery: a comparison of linear models, mixed models, and generalised estimating equations approaches. Fish. Res. **70**(2–3): 179–193. doi:10.1016/j.fishres.2004.08.003.

Dempster, A.P., Laird, N.M., and Rubin, D.B. 1977. Maximum likelihood from incomplete data via the EM algorithm. J. R. Stat. Soc. B (Method.), **39**: 1–38.

Deng, R., Dichmont, C., Milton, D., Haywood, M., Vance, D., Hall, N., and Die, D. 2005. Can vessel monitoring system data also be used to study trawling intensity and population depletion? The example of Australia's northern prawn fishery. Can. J. Fish. Aquat. Sci. **62**(3): 611–622. doi:10.1139/f04-219.

Good, N., and Peel, D. 2007. An index of abundance for prawn stocks in Queensland using maximum entropy methods and VMS data. *In* GIS/spatial analyses in fishery and aquatic sciences. Vol. 3. *Edited by* T. Nishida, P.J. Kailola, and A. Caton. Fishery–Aquatic GIS Research Group, Saitama, Japan. pp. 161–180.

Harrington, J.J., Semmens, J.M., and Haddon, M. 2007. Spatial distribution of commercial dredge fishing effort: application to survey design and the spatial management of a patchily distributed benthic bivalve species. Mar. Freshw. Res. **58**(8): 756–764. doi:10.1071/MF06101.

Hintzen, N.T., Piet, G.J., and Brunel, T. 2010. Improved estimation of trawling tracks using cubic Hermite spline interpolation of position registration data. Fish. Res. **101**(1–2): 108–115. doi:10.1016/j.fishres.2009.09.014.

Horne, J.S., Garton, E.O., Krone, S.M., and Lewis, J.S. 2007. Analyzing animal movements using Brownian bridges. Ecology, **88**(9): 2354–2363. doi:10.1890/06-0957.1. PMID:17918412.

Johnson, N.L., Kotz, S., and Balakrishnan, N. 1994. Continuous univariate distributions, Vol. 1. John Wiley and Sons, New York.

Larcombe, J.W.P., McLoughlin, K.J., and Tilzey, D.J. 2001. Trawl operations in the South East Fishery, Australia: spatial distribution and intensity. Mar. Freshw. Res. **52**(4): 419–430. doi:10.1071/MF99169.

MacDonald, I.L., and Zucchini, W. 1997. Hidden Markov and other models for discrete-valued time series. Chapman & Hall, London.

Marrs, S.J., Tuck, I.D., Atkinson, R.J.A., Stevenson, T.D.I., and Hall, C. 2002. Position data loggers and logbooks as tools in fisheries research: results of a pilot study and some recommendations. Fish. Res. **58**(1): 109–117. doi:10.1016/S0165-7836(01)00362-9.

Maunder, M.N., and Punt, A.E. 2004. Standardizing catch and effort data: a review of recent approaches. Fish. Res. **70**(2-3): 141–159. doi:10.1016/j.fishres.2004.08.002.

McLachlan, G.J., and Peel, D. 2000. Finite mixture models. John Wiley and Sons, New York.

Mejias, A., Jr. 1999. Vessel monitoring system sensor applications in the Gulf of Mexico shrimp fishery. *In* Proceedings of the International Conference on Integrated Fisheries Monitoring, 1–5 February 1999, Sydney. *Edited by* C.P. Nolan. FAO, Rome. pp. 291–303.

Mills, C.M., Townsend, S.E., Jennings, S., Eastwood, P.D., and Houghton, C.A. 2007. Estimating high resolution trawl fishing effort from satellite-based vessel monitoring system data. ICES J. Mar. Sci. **64**(2): 248–255. doi:10.1093/icesjms/fsl026.

O'Neill, M.F., Courtney, A.J., Turnbull, C.T., Good, N.M., Yeomans, K.M., Staunton-Smith, J., and Shootingstar, C. 2003. Comparison of relative fishing power between different sectors of the Queensland trawl fishery, Australia. Fish. Res. **65**(1–3): 309–321. doi:10.1016/j.fishres.2003.09.022.

Patterson, T.A., Basson, M., Bravington, M.V., and Gunn, J.S. 2009. Classifying movement behaviour in relation to environmental conditions using hidden Markov models. J. Anim. Ecol. **78**(6): 1113–1123. doi:10.1111/j.1365-2656.2009.01583.x. PMID:19563470.

Peel, D., and Good, N. 2007. Refined trawl signature and trawl track definitions using a hidden Markov model approach. *In* Innovative stock assessment and effort mapping using VMS and electronic logbooks. *Edited by* N.A. Gribble, N. Good, D. Peel, M. Tanimoto, and R. Officer. Department of Primary Industries: Fisheries Research and Development Corporation, Brisbane, Australia. pp. 55–77.

Peel, D., Good, N., and Tanimoto, M. 2007. Mapping the spatial intensity of fishing effort using a speed filter method. *In* Innovative stock assessment and effort mapping using VMS and electronic logbooks. *Edited by* N.A. Gribble, N. Good, D. Peel, M. Tanimoto, and R. Officer. Department of Primary Industries: Fisheries Research and Development Corporation, Brisbane, Australia, pp. 20–54.

Rabiner, L.R. 1989. A tutorial on hidden Markov models and selected applications in speech recognition. Proc. IEEE, **77**(2): 257–286. doi:10.1109/5.18626.

Rijnsdorp, A.D., Buys, A.M., Storbeck, F., and Visser, E.G. 1998. Micro-scale distribution of beam trawl effort in the southern North Sea between 1993 and 1996 in relation to the trawling frequency of the sea bed and the impact on benthic organisms. ICES J. Mar. Sci. **55**(3): 403–419. doi:10.1006/jmsc.1997.0326.

Vignaux, M., Vignaux, G.A., Lizamore, S., and Gresham, D. 1998. Fine-scale mapping of fish distribution from commercial catch and effort data using maximum entropy tomography. Can. J. Fish. Aquat. Sci. **55**(5): 1220–1227. doi:10.1139/f97-297.

Zucchini, W., and MacDonald, I.L. 2009. Hidden Markov models for time series: an introduction using R. Chapman & Hall, New York.

Appendix A

This section contains a more detailed description of the fitting process using the Baum–Welch algorithm (Baum et al. 1970). Let s denote the number of states in the HMM, n the number of time intervals (polls). Then given the observed vessel speeds $\boldsymbol{y} = \{y_1, \ldots, y_n\}$, time of day $\boldsymbol{d} = \{d_1, \ldots, d_n\}$, and fishery $\boldsymbol{c} = \{c_1, \ldots, c_n\}$, the algorithm on the $(k + 1)$th iteration is given by

E step

Forward recursion The values $a_{i,t}^{(k)}$ ($i = 1, \ldots, s$; $t = 1, \ldots, n - 1$) corresponding to the forward probabilities (i.e., the probability of being in a state at time t, given the previous $1, \ldots, t - 1$ observations) are calculated as

Initialization $a_{i,1}^{(k+1)} = P_{0,i}^{(k+1)}(d_1, c_1) f_i^{(k+1)}(y_1, \theta_{i,c_1})$

Induction

$$a_{i,t+1}^{(k+1)} = \left[\sum_{h=1}^{s} a_{h,t}^{(k+1)} P_{h,i}^{(k+1)}(d_t, c_t)\right] f_i^{(k+1)}(y_{t+1}, \theta_{i,c_{t+1}})$$

where $P_{0,i}(d_1, c_1)$ are the initial probabilities of being in each state.

Backward recursion The values $b_{i,t}^{(k+1)}$ ($i = 1, 2, \ldots, s$; $t = n - 1, n - 2, \ldots, 1$) corresponding to the backward probabilities (i.e., the probability of being in a state at time t, given the future $t + 1, \ldots, n$ observations) are calculated as

Initialization $b_{i,n}^{(k+1)} = 1$

Induction

$$b_{i,t}^{(k+1)} = \sum_{h=1}^{s} P_{h,i}^{(k+1)}(d_t, c_t) f_i^{(k+1)}(y_{t+1}, \theta_{i,c_{t+1}}) b_{h,t+1}^{(k+1)}$$

Also within the E step we estimate the posterior probabilities $w_{i,j,t}^{(k)}$ of moving from node i to node j at time point t

$$w_{i,j,t}^{(k)} = \frac{a_{i,t}^{(k+1)} P_{h,i}^{(k+1)}(d_t, c_t) f_i^{(k+1)}(y_{t+1}, \theta_{i,c_{t+1}}) b_{j,t+1}^{(k+1)}}{\sum_{h=1}^{s}\sum_{i=1}^{s} a_{h,t}^{(k+1)} P_{h,i}^{(k+1)}(d_t, c_t) f_i^{(k+1)}(y_{t+1}, \theta_{i,c_{t+1}}) b_{i,t+1}^{(k+1)}}$$

Since the trawling state distribution is a mixture model, we must also estimate the posterior probabilities of each of the K normal mixture components, i.e., for observation at time $t = 1, \ldots, n$, and $m = 1, \ldots, K$

$$\tau_{t,m}^{(k+1)} = \frac{\pi_{m,c_t}^{(k)} N(y_t; \mu_{2,m,c_t}, \sigma_{2,m,c_t})}{\sum_{h=1}^{K} \pi_{h,c_t}^{(k)} N(y_t; \mu_{2,h,c_t}, \sigma_{2,h,c_t})}$$

M step

For example, for the state distributions and corresponding Ω, let $w_{\cdot,j,t}^{(k+1)}$ denote the probability of the vessel being in state j at time t, i.e., $w_{\cdot,j,t}^{(k+1)} = \sum_{i=1}^{s} w_{i,j,t}^{(k+1)}$ and ψ be the set of all times that the vessel was allocated to fishery C

$$\mu_{S,C}^{(k+1)} = \frac{\sum_{t \in \psi} w_{\cdot,j,t}^{(k+1)} y_t}{\sum_{t \in \psi} w_{\cdot,j,t}^{(k+1)}}$$

$$\sigma_{S,C}^{(k+1)} = \frac{\sum_{t \in \psi} w_{\cdot,j,t}^{(k+1)} (y_t - \mu_{S,C}^{(k+1)})^2}{\sum_{t \in \psi} w_{\cdot,j,t}^{(k+1)}}$$

where also since the trawling component is a mixture distribution we also have the K component mixture parameters to estimate

$$\pi_{m,C}^{(k+1)} = \sum_{t \in \psi} \tau_{t,m}^{(k+1)}$$

$$\mu_{2,m,C}^{(k+1)} = \frac{\sum_{t \in \psi} \tau_{t,k}^{(k+1)} w_{\cdot,j,t}^{(k+1)} y_t}{\sum_{t \in \psi} \tau_{t,m}^{(k+1)} w_{\cdot,j,t}^{(k+1)}}$$

$$\sigma_{2,m,C}^{(k+1)} = \frac{\sum_{t \in \psi} \tau_{t,k}^{(k+1)} w_{\cdot,j,t}^{(k+1)} (y_t - \mu_{2,m,C}^{(k+1)})^2}{\sum_{t \in \psi} \tau_{t,m}^{(k+1)} w_{\cdot,j,t}^{(k+1)}}$$

Reference

Baum, L.E., Petrie, T., Soules, G., and Weiss, N. 1970. A maximization technique occurring in the statistical analysis of probabilistic functions of Markov chains. Ann. Math. Stat. **41**(1): 164–171. doi:10.1214/aoms/1177697196.

Exploring the role of fish in a lake ecosystem (Lake Kinneret, Israel) by coupling an individual-based fish population model to a dynamic ecosystem model

Vardit Makler-Pick, Gideon Gal, James Shapiro, and Matthew R. Hipsey

Abstract: To explore the role that fish play in aquatic ecosystems, a hydrodynamic–ecological model (DYRESM–CAEDYM) was coupled to a novel fish population model. The coupled model (DYCD–FISH) combined two modelling approaches: a complex dynamic model and an individual-based model. The coupled model simulates fish growth population dynamics and predicts fish impacts on various ecosystem components, including nutrients and lower trophic levels. The model was employed to explore the role of the dominant fish in Lake Kinneret (Israel), *Acanthobrama terraesanctae* (Kinneret bleak, or in Hebrew, lavnun ha'kinneret; hereafter lavnun). Model results suggested that the lavnun has a significant impact ($p < 0.05$) on the magnitude of output variables including its prey food (the predatory and microzooplankton), major nutrients such as ammonium (NH_4) and phosphate (PO_4), and on several phytoplankton species, but not on the seasonality of any of the output variables. Since the model incorporates trophic levels from nutrients to fish, it revealed the nonlinear dynamic impacts of fish on different ecosystem components and in particular has led to quantitative insights into the relative influence of top-down control on water quality attributes. Besides being an ecosystem research tool, DYCD–FISH can also be employed as a fishery management tool, and in particular facilitate ecosystem-based fishery management.

Résumé : Afin d'examiner le rôle que jouent les poissons dans les écosystèmes aquatiques, nous avons couplé un modèle hydrodynamique–écologique (DYRESM–CAEDYM) à un nouveau modèle de dynamique de population de poissons. Ce modèle couplé (DYCD–FISH) combine deux approches de modélisation, un modèle dynamique complexe et un modèle basé sur l'individu. Le modèle couplé simule la croissance et la dynamique de population des poissons et prédit les impacts des poissons sur diverses composantes de l'écosystème, en particulier les nutriments et les niveaux trophiques inférieurs. Nous utilisons le modèle pour étudier le rôle du poisson dominant du lac de Kinnereth (Israël), *Acanthobrama terraesanctae* (« Kinneret bleak », ou en hébreu lavnun ha'kinneret; appelé ci-après lavnun). Les résultats du modèle indiquent que le lavnun a un impact significatif ($p < 0,05$) sur l'amplitude des variables de sortie, entre autres sur les proies dont il se nourrit (le zooplancton prédateur et le microzooplancton), sur les principaux nutriments tels que l'ammonium (NH_4) et le phosphate (PO_4), sur plusieurs espèces du phytoplancton, mais pas sur la saisonnalité d'aucune des variables de sortie. Puisque le modèle incorpore les niveaux trophiques, des nutriments aux poissons, il révèle les impacts à dynamique non linéaire des poissons sur les différentes composantes de l'écosystème et, en particulier, il apporte des perspectives quantitatives sur l'influence relative du contrôle descendant sur les attributs de la qualité de l'eau. En plus d'être un outil de recherche pour les écosystèmes, DYCD–FISH peut aussi servir d'outil de gestion des pêches, et en particulier faciliter la gestion des pêches basée sur l'écosystème.

[Traduit par la Rédaction]

Introduction

The impact of fish on lake ecosystem food webs has been extensively investigated and it is well established that fish can directly or indirectly affect biological and chemical components of lake ecosystems (Reissig et al. 2006; McIntyre et al. 2007; Gozlan et al. 2010). Most of these findings support the "trophic cascade hypothesis", which predicts that the top trophic level of an aquatic food web, regardless of whether it has piscivorous fishes or not, can have cascading affects

Received 4 August 2010. Accepted 25 March 2011. Published at www.nrcresearchpress.com/cjfas on 22 July 2011.
J21953

Paper handled by Associate Editor Cliff Kraft.

V. Makler-Pick. Faculty of Civil and Environmental Engineering, Technion-Israel Institute of Technology, Technion City, Haifa 32000, Israel.
G. Gal. Y. Allon Kinneret Limnological Laboratory, Israel Oceanographic & Limnological Research, P.O. Box 447, Migdal 14950, Israel.
J. Shapiro. Department of Fisheries, Ministry of Agriculture, Tiberias, Israel.
M.R. Hipsey. Centre for Water Research, University of Western Australia, 35 Stirling Highway, Crawley, Western Australia 6009, Australia; School of Earth & Environment, University of Western Australia, 35 Stirling Highway, Crawley, Western Australia 6009, Australia.

Corresponding author: Vardit Makler-Pick (e-mail: vardit@oranim.ac.il).

Can. J. Fish. Aquat. Sci. **68**: 1265–1284 (2011) doi:10.1139/F2011-051 Published by NRC Research Press

Fig. 1. Conceptual diagram of Computational Aquatic Ecosystem Dynamics Model (CAEDYM), including the new fish population model and related processes (dotted lines). For description of the state variables used in CAEDYM see Gal et al. (2009).

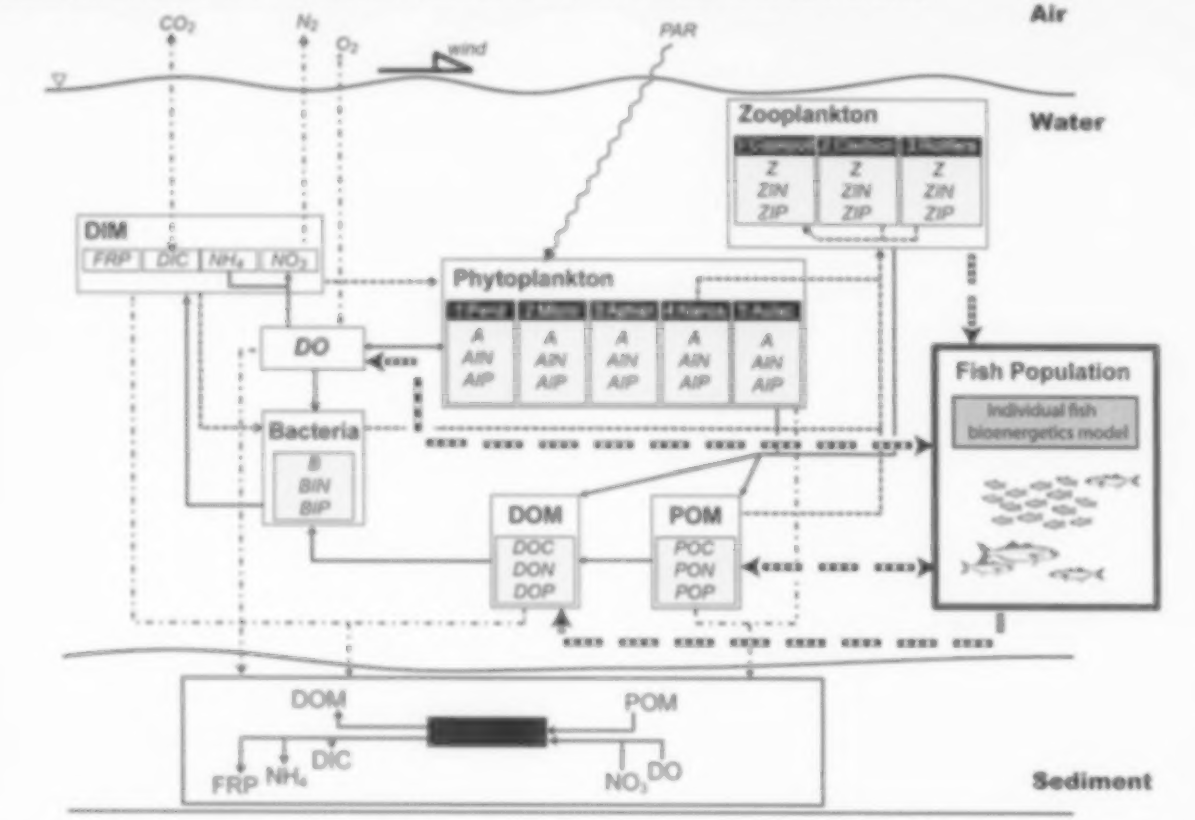

Fig. 2. Predicted average weight at age (*g*) for a single fish hatched in 1997 over 5 years of simulation.

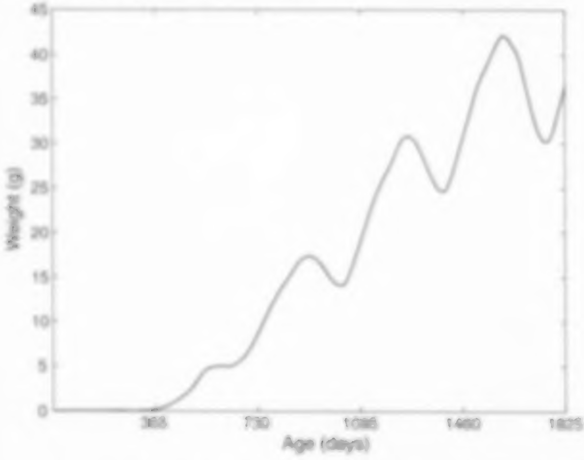

down trophic levels, ultimately impacting algal biomass (Carpenter et al. 1985; Carpenter and Kitchell 1988). Numerous experiments have been conducted to demonstrate the validity of the trophic cascade hypothesis, and they have explored a large number of variables, such as the duration of the experiment, the experimental system, the climatic zone, species composition, etc., (Lazzaro 1987; Northcote 1988; Brett and Goldman 1996). Meta-analyses of trophic cascade experiments have shown that a large number of studies confirm the top-down cascade in aquatic ecosystems (Brett and Goldman 1996). However, almost since its first appearance, the validity of the theory has been questioned and embroiled in controversy over whether "top-down" (i.e., consumer) or "bottom-up" (i.e., nutrient) forces determine the structure of aquatic food webs (McQueen et al. 1986; DeMelo et al. 1992; Elser et al. 1998). The arguments were based on whether or not the studies satisfactorily demonstrated a statistically significant impact of piscivorous or zooplanktivorous fish on the structure of freshwater food webs. For example, in some cases small decreases in zooplankton biomass corresponded to large increases in phytoplankton biomass, whereas in other cases large decreases in zooplankton biomass corresponded to only minor increases in the phytoplankton (Brett and Goldman 1996). In a literature survey by Drenner and Hambright (2002), only 7 out of 17 experimental studies provided evidence of trophic cascade from piscivores to phytoplankton.

A long-term (1994–2006) biomanipulation (culling) program was implemented in the widely studied Lake Kinneret (Israel) based on the trophic cascade hypothesis, with the aim of preventing or reducing the likelihood of deterioration in water quality. The unexpected results of the biomanipulation

Fig. 3. (*a*) Average consumption rate (solid line) at age for a fish hatched in 1997 over a 5-year simulation ($g_{prey} \cdot g_{fish}^{-1} \cdot day^{-1}$) and best-fitted logarithmic curve (dashed line). (*b*) Average respiration rate at age (solid line) for a fish hatched in 1997 over a 5-year simulation ($g_{prey} \cdot g_{fish}^{-1} \cdot day^{-1}$) and best-fitted logarithmic curve (dashed line).

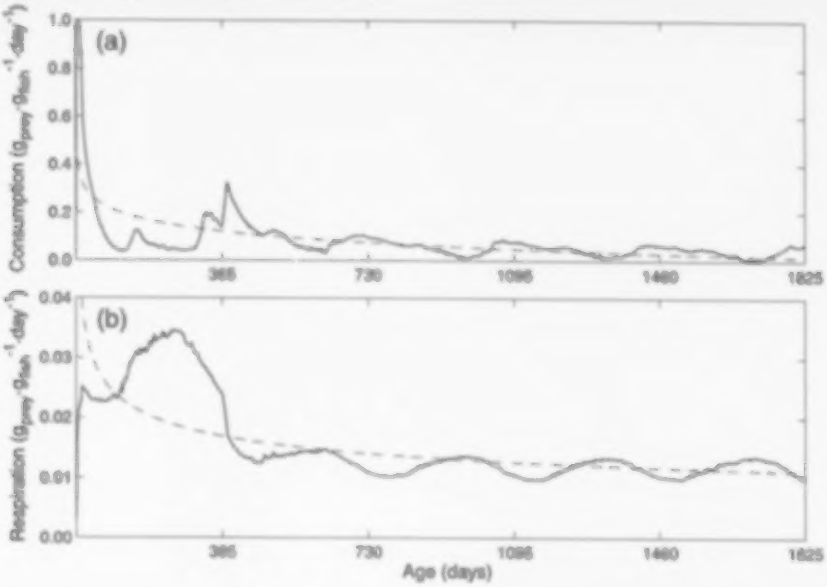

Fig. 4. Simulated weight–length relationship over the entire simulation period (dots) and observed weight at length data (pluses) with associated standard deviation (SD, ±) for year 2000 as reported by the fishery authority (Department of Fisheries, Israel).

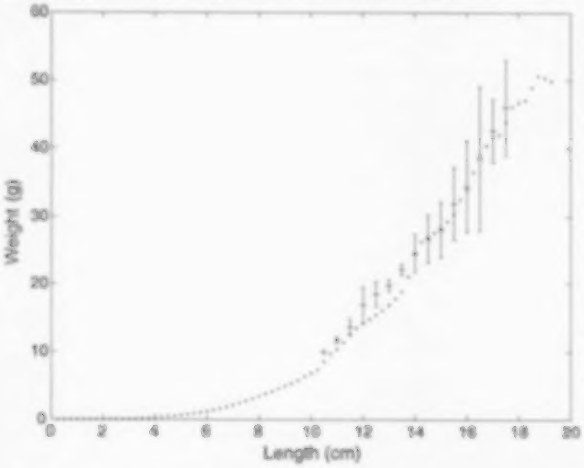

raised questions about the impact of the dominant fish in the lake, *Acanthobrama terraesanctae* (Steinitz 1952; Kinneret bleak, local name lavnun), on the food web and water quality in the lake (Zohary 2006). The motivation for this research was to gain insights into the ecosystem processes that shape the ultimate response of food web components to changes in the fishery, using Lake Kinneret as a case study.

Considering the time scale of changes and the complexity of measuring ecosystem dynamics in the field, a numerical approach that couples fish dynamics with ecosystem processes is attractive, since it can help us to quantify key ecosystem pathways and explore the direct and indirect feedbacks of fish on different ecosystem components. In addition, such models are useful tools for fishery managers to assess possible impacts of management actions on the lake ecosystem. Many examples (Hinckley et al. 1996; Werner et al. 1996; Hermann et al. 2001) have successfully integrated knowledge across several trophic levels of the ecosystem. Yet, only a limited number of them (e.g., Megrey et al. 2007) allow full feedbacks and interactions among the various components for the purpose of assessing the impacts of the fish. Fish growth is often simulated using bioenergetics models, and the results are used to explore feed requirements and the impact of different factors such as temperature or prey abundance on fish growth (Zhou et al. 2005; Lee and Johnson 2005). However, the feedbacks resulting from food consumption, excretion, waste production, and mortality on lower trophic level processes, (e.g., primary productivity and algal succession) are not dynamically incorporated. This limits possible insight from these models into the long-term effects of fish. Given the large variation within fish populations in terms of traits such as size and mass, an individual-based approach (DeAngelis and Mooij 2005) could be more appropriate for studying fish feedbacks such as those listed above.

In this study, a coupled hydrodynamic–ecological model (Dynamic Reservoir Simulation Model – Computational Aquatic Ecosystem Dynamics Model, or DYRESM–CAEDYM; DYCD hereafter), was employed as the base platform to which a new mass-conserving, individual-based model (IBM) for a fish population was coupled. By combining the two modelling approaches, it is hypothesized that we can numerically assess the role of fish population dynamics on key water quality processes in a large lake ecosystem. Specifically, the study applies the approach to Lake Kinneret by exploring the role of lavnun on water quality attributes such as

Table 1. Comparison between length and weight data based on literature and simulation results.

	Reference value		DYCD-FISH
Reference	Length (cm)	Weight (g)	Weight (g)
Steinitz (1959)	5–13	1.1–21.7	0.5–22.5
	14–16	23.3–46.3	17.7–46.3
	>16	35–75	28.8–57.7
Easton and Gophen (2003)	**July 1994**		**July 2002**
	8–10	20–25	4–7
	13–16	30–40	17–35
Gophen et al. (1999)	**June 1994–1996**		**June 2002**
	8.8–12.7	4.8–17.2	3.9–15.4

Fig. 5. Predicted length at age (circles) in comparison with Steinitz (1959); Yashouv and Berner (1960); Davidoff (1986); and Ostrovsky and Walline (1999). Model equivalent outputs for each year are taken from simulation days 365, 730, 1095, and 1460 for years 1, 2, 3, and 4 of a single cohort, respectively.

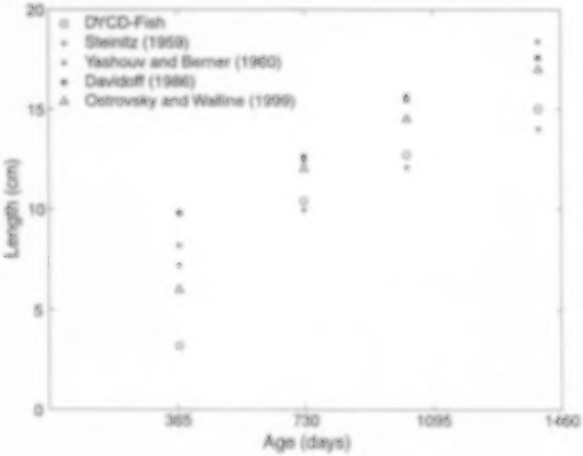

nutrients and phytoplankton. The aims of the paper are to (*i*) develop and validate a bioenergetics-based IBM for a fish population in two stages: an uncoupled stage (hereafter the "static model"), where feedbacks from the fish model to the ecological model are not engaged, and a coupled stage (hereafter the "dynamic model"), where those feedbacks were implemented; (*ii*) explore and quantify the fish growth and fish population dynamics using the dynamic model; and (*iii*) explore the impact of the fish on the lower ecosystem components by comparing the static and the dynamic model outputs.

Materials and methods

Site description and lavnun ecology

Lake Kinneret (Sea of Galilee) is a large monomictic lake located in the Syrian–African Rift Valley in northeastern Israel. It covers an area of 170 km^2, is 21 km long, 16 km wide, and has a maximum depth of 43 m. Lake Kinneret is of critical importance since it supplies about 30% of Israel's drinking water. For further information on the lake, the reader is referred to Serruya (1978) and Berman et al. (1995).

The lake has been monitored regularly for 40 years by the Kinneret Limnological Laboratory (KLL). The monitoring program includes weekly and biweekly collection of water samples from various locations in the lake and analyses of numerous physical, chemical, and biological variables (see Shlichter 2004; Gal et al. 2009). These lake-based data were used for model calibration and validation.

As the aim of this study is to explore the effect of the lavnun on the ecosystem, a brief description of lavnun biology and fishery is given here, though we focus on aspects relevant to the development of the model described below. The endemic cyprinid lavnun is a small, pelagic, lacustrine fish. The largest reported specimen had a total length (TL) of 25.3 cm, weighed 213 g, and was aged 7+ years. This was an exceptionally large example, and based on fishery data, most adult lavnun are 12–14 cm long (TL), weigh 15–38 g, and are 2–4 years old. The lavnun lives near the surface in large schools with occasional forays to deeper water (Steinitz 1959; Serruya 1978; Easton and Gophen 2003). Kalikhman et al. (1992) suggested that oxygen and temperature are the key parameters affecting fish vertical distribution.

The lavnun is a zooplanktivorous fish having a possible top-down effect, which was thought to indirectly contribute to an increase in nanoplankton (Gophen and Threlkeld 1989). Stomach content analyses have shown a consumption of mainly zooplankton, chiefly cladocera and copepoda (Komarovsky 1952). It was also noted that small rotifers and nauplii were rarely selected (though it is also possible that they are digested more rapidly than other zooplankton, making them difficult to detect). Phytoplankton was only a minor food component, and organic material such as detritus, higher plant debris, and sand was occasionally found in the guts. There were differences between the consumption of adults and young fish, with the guts of larger fish containing more copepods than those from smaller fish (Gophen and Scharf 1981). A stable isotope study of the Kinneret food web (Zohary et al. 1994) confirmed that zooplankton is the likely main food for the lavnun.

The spawning behavior of the pelagic lavnun is specifically adapted to the seasonal change in temperature and lake level. The lavnun spawns from November to May (Yaron et al. 1980) when temperature is at its annual minimum and lake level rises, inundating shallow shore areas. Lavnun spawning is limited to a narrow belt of up to 6 m from shore at a depth of no more than 0.5 m (usually between 0.1 and 0.2 m). The spawning is performed by attaching adhesive eggs to algae-free surfaces of newly inundated rocky areas and macrophytes (Landau et al. 1988; Gafny et al. 1992).

Fig. 6. Predicted size distribution of the fish population for year 2002 as simulated by the dynamic model.

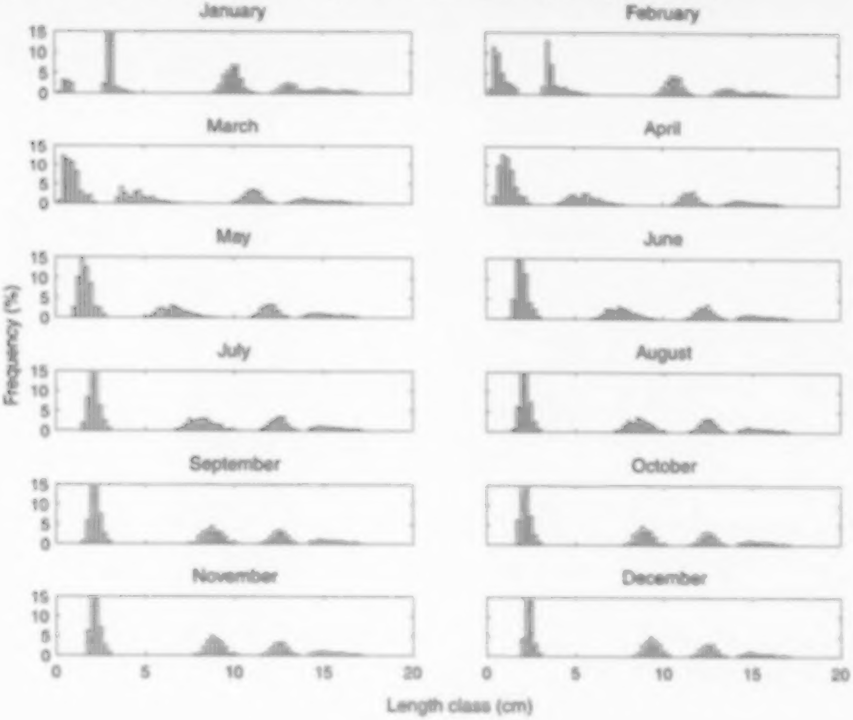

Fig. 7. Simulated total lavnun biomass (t) for the years 1997–2003.

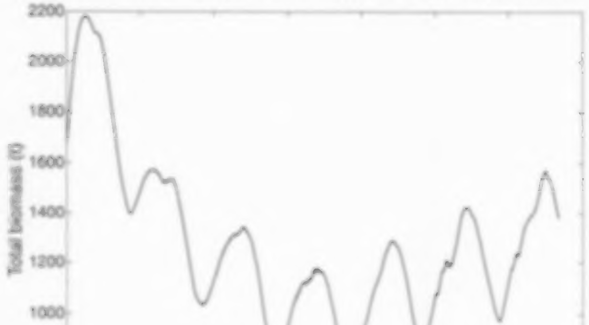

Fig. 8. Average daily depth-dependent fish consumption of zooplankton (% of zooplankton biomass) for predatory zooplankton (squares), herbivorous zooplankton (triangles), and microzooplankton (circles).

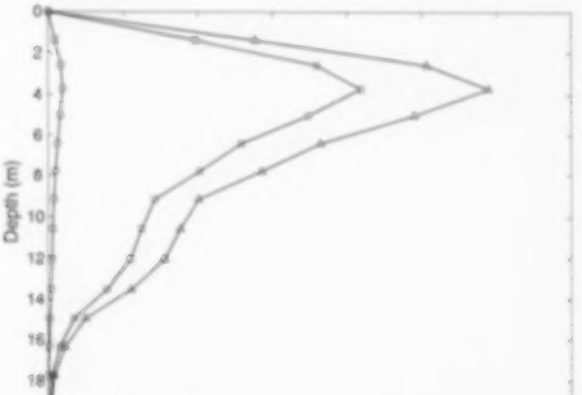

The lower depth limit of spawning is determined by the development of benthic diatoms on stones that do not allow the fish to attach their eggs to the surface (Gafny et al. 1992). Water level fluctuation increases the potential area of the spawning grounds and hence affects the size distribution of the fish population (Gasith and Gafny 1990).

There have been a number of attempts to estimate the lavnun biomass in the lake. Serruya et al. (1980) estimated that lavnun biomass ranged from 3000 to 6000 t during the period 1968–1978. In 1981, Gophen (1986) estimated the total fish biomass to be approximately 6000 t. Ostrovsky and Walline (1999) estimated a total of 2800 t of lavnun biomass during the period from the late 1980s to early 1990s. They approximated this to constitute 50%–70% of the total fish stock in the lake. The number of the pelagic fish in the lake (mostly lavnun) was assessed acoustically and estimated to range between 61 and 218 million based on annual surveys

Table 2. Mean concentration and standard deviation (SD) of chemical (mg·L^{-1}), phytoplankton (mg C·L^{-1}), and zooplankton (mg C·m^{-2}) state variables, *t* test value and *p* value for the comparison between the static and the dynamic models.

State variable	*N*	Static Mean	Static SD	Dynamic Mean	Dynamic SD	*t*	*p*
NH_4	23	0.0172915	0.0156205	0.0141804	0.0154932	2.442	0.023
NO_3	17	0.0117312	0.017831	0.0133739	0.0208324	–1.246	0.231
PO_4	33	7.574×10^{-5}	0.0001775	7.119×10^{-5}	0.000175	3.940	<0.001
DINOF	33	0.2383209	0.3251917	0.2076893	0.310107	6.255	<0.001
NODUL	33	0.0169523	0.0199344	0.0096676	0.0107524	4.442	<0.001
CYANO	17	0.031819	0.0316835	0.019452	0.0309962	4.815	<0.001
FDIAT	33	0.0526413	0.1105274	0.0466599	0.097522	2.143	0.040
CHLOR	33	0.1189125	0.0334868	0.1286861	0.0190814	–2.037	0.050
ZOOP1	33	0.505332	0.7565506	0.370123	0.6276148	3.698	0.001
ZOOP2	33	0.914405	0.6878677	0.835026	0.7804753	1.651	0.108
ZOOP3	33	0.2200049	0.3261964	0.1682788	0.2631467	2.997	0.005
BAC	33	0.1407864	0.0482172	0.1243452	0.0513844	10.543	<0.001

Note: DINOF, dinoflagellates (*Peridinium gatunense*); NODUL, cyanobacteria (*Aphanizomenon ovalisporum*); CYANO, cyanobacteria (*Microcystis*); FDIAT, diatom (*Aulacoseira granulata*); CHLOR, chlorophyll *a* concentration; ZOOP1, predator zooplankton; ZOOP2, large herbivores – macrozooplankton; ZOOP3, microzooplankton; BAC, bacteria.

Fig. 9. Size distribution for the months September, October, and December 2002 for fish larger than 10 cm as simulated by the dynamic model (*a*–*c*), the static model (*d*–*f*), and observed length–frequency distribution for fish taken in purse seine samples collected in September 2002 (*n* = 874), October 2002 (*n* = 436), and December 2002 (*n* = 160). Total length was measured to the nearest 0.5 cm (*g*–*i*).

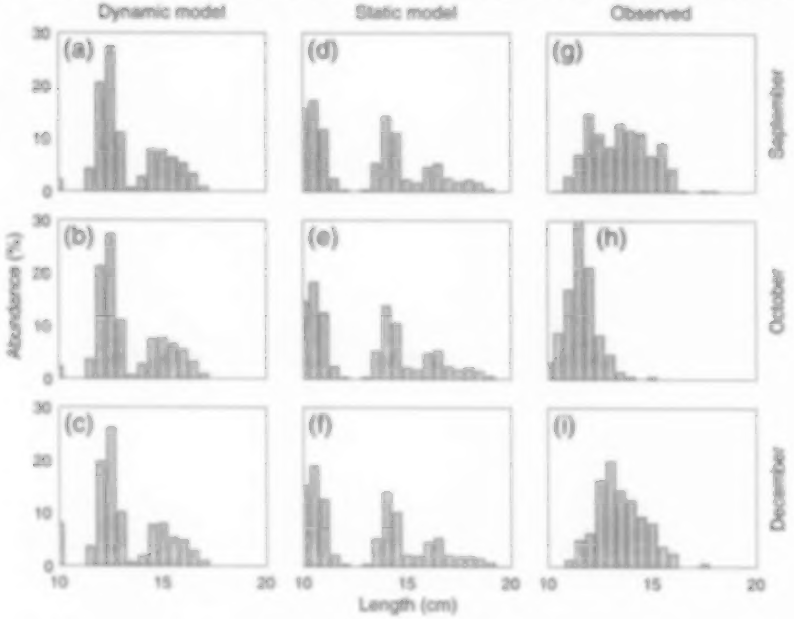

conducted during March–April over the period from 1987 to 1990 (Walline et al. 1992).

Piscivorous fish, and therefore predation on lavnun, is largely absent in Lake Kinneret (Serruya et al. 1980). According to Ostrovsky and Walline (1999), the number of lavnun fish older than 3 years decreases exponentially with age. Following the addition of large mesh bunts to the purse seine since 1982–1983, harvest pressure on older fish (3 and 4 years old) was intensified, and fish older than 5 years are rare. The total mortality (both natural and fishing mortality) rates of males and females for lavnun larger than 12 cm was estimated to be 78% per year. This estimate is similar to the 70% calculated using the Pauly (1980) formula (Ostrovsky and Walline 1999). For more than two decades (1970–1993) lavnun constituted the largest part of the commercial fishery with a fairly constant catch of 900–1000 t·year^{-1}. During 1993–1994, and again in 2004–2005, the lavnun fishery collapsed with less than 10% of the typical harvest being caught and most of the fish falling below the commercial size of 12 cm (Hambright and Shapiro 1997; J. Shapiro, unpublished

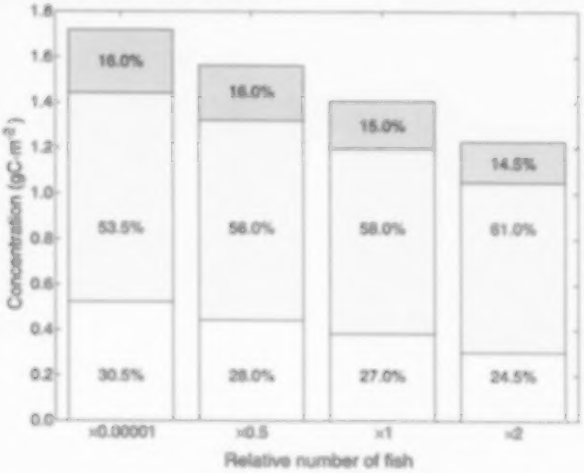

Fig. 10. Predatory zooplankton (open), herbivorous zooplankton (light gray), and microzooplankton (dark gray) average concentration (g C·m^{-2}) and the relative fractions of each zooplankton group at different levels of fish population size, where ×1 is equal to initial number of 100 million in the lake.

data). Using data from acoustic surveys, Ostrovsky and Walline (1999) estimated that the typical annual catch (~1000 t·year^{-1}) between the late 1980s to early 1990s represented approximately one third of the available lavnun standing stock. According to Ostrovsky and Walline (1999), this catch level allowed a stable population structure to be sustained. However, Hambright and Shapiro (1997) claimed that the fishery collapse in 1993–1994 is because of a long-term shift in harvested fish size and overharvest that led to depletion of the 2–3 year class. Recruitment of lavnun young-of-the-year following 1991–1992 was exceptionally high, which Hambright and Shapiro (1997) explained as resulting from lack of competition by previous year classes.

Model description and application

To simulate the interactions among the hydrodynamics, biogeochemistry, phytoplankton, zooplankton, and fish, DYCD, a coupled one-dimensional (1D) hydrodynamic–ecological model, was used as the model platform to which a newly developed fish population model was coupled, creating a new combined ecosystem–fish model, DYCD–FISH (Fig. 1). The fish were modelled using a generic bioenergetics formulation with lavnun-specific parameters and reproduction details. The bioenergetics equation simulated the growth and metabolism of a single fish and was applied to numerous "super" individuals (Scheffer et al. 1995), together representing the total fish population in the lake. The models can run statically (no feedbacks engaged), but when dynamically coupled, the mass of carbon and nutrients are tracked between the models, and the combined DYCD–FISH model accounts for the direct and indirect feedbacks between fish and the biogeochemical and planktonic components of the ecological model.

The hydrodynamic–ecological model (DYCD)

DYCD couples the 1D hydrodynamic model DYRESM and the aquatic ecological model CAEDYM. DYRESM is a laterally averaged Lagrangian code for predicting the vertical stratification and mixing dynamics in lakes and reservoirs (Imberger and Patterson 1981, 1989) and more recently includes pseudo-2D processes such as benthic boundary layer mixing (described in Yeates and Imberger 2003). Based on the inflows, withdrawals, and meteorological conditions, DYRESM calculates the changes to the water level and changes in water temperature and salinity (and hence density) over depth and time. These outputs are used as inputs to the ecological model CAEDYM. The mathematical equations in CAEDYM consist of a series of process-based, partial differential equations to simulate time-varying concentrations of biogeochemical variables accounting for processes such as primary production, secondary production, nutrient cycling, oxygen dynamics, and sediment–water interactions. A number of configurations of the model have previously been validated in various reservoirs and lakes (e.g., Romero et al. 2004; Trolle et al. 2008), and it has been previously applied to Lake Kinneret for simulating the biogeochemistry, five phytoplankton groups (*Peridinium gatunense*, *Aulacoseira granulate*, *Aphanizomenon* sp., *Microcystis* sp., and a general group, termed nanoplankton), three zooplankton groups (predatory zooplankton — adult stages of the predatory copepods and predatory rotifers; herbivorous zooplankton — cladocerans, copepodites, and microzooplankton), and heterotrophic microbial loop dynamics (Bruce et al. 2006; Hipsey et al. 2006; Gal et al. 2009). The reader is referred to these accounts for a detailed description of the configuration, differential equations, and parameterizations. In this paper, the Gal et al. (2009) version of the model is used as the base platform for development of the fish model. However, this study uses CAEDYM version 3.3 with several different parameters values adopted (see Appendix A for list of changes to parameters and values). The differences between the simulation results of Gal et al., (2009) and the CAEDYM version 3.3 employed in the current research were not significant. We therefore do not provide a graphical or statistical comparison.

Fish bioenergetics model

Bioenergetics models have been intensively used for freshwater and marine fish species (Hanson et al. 1997; Rose et al. 2007; Mateo 2007). The fish model developed here employs the "Wisconsin" bioenergetics equation (Ney 1993) with age-specific parameters to account for the metabolism and growth of different age groups. The bioenergetics equation simulates the daily changes in wet weight per unit of weight per day (g wet weight·g$_{\text{fish}}^{-1}$·day^{-1}) that occur through consumption, respiration, excretion, egestion, specific activity, and reproduction, assuming that the change in weight is equal to the difference between the consumption and loss of energy. The growth rate of an individual lavnun is calculated as weight increment per unit of weight per time and is defined by

$$(1)\qquad \frac{1}{W}\frac{\mathrm{d}W}{\mathrm{d}t} = [C - (R + S + F + E + P)]\left(\frac{\mathrm{CAL}_{\text{prey}}}{\mathrm{CAL}_{\text{fish}}}\right)$$

where C is consumption, R is respiration, S is specific dynamic activity, F is egestion, E is excretion, P is reproduction, W is wet weight of the fish (g), and $\mathrm{CAL}_{\text{prey}}/\mathrm{CAL}_{\text{fish}}$ is the caloric equivalence for converting caloric equivalence of food to caloric equivalence of fish. Consumption, respiration, specific dynamic activity, excretion, egestion, and reproduction are in units of $g_{prey} \cdot g_{fish}^{-1} \cdot day^{-1}$, which are converted to $g_{fish} \cdot g_{fish}^{-1} \cdot day^{-1}$ by the ratio of the prey to fish energy densities.

For computing the consumption term of the bioenergetics equation, the bioenergetics model accounts for the effects of important external regulators such as temperature and available food using species-specific, empirically derived parameters (Hansen et al. 1993). The diet composition in DYCD–FISH included predatory zooplankton, herbivorous zooplankton, microzooplankton, and particulate organic material. The terms for egestion, excretion, reproduction, and specific activity are dependent on the consumption term, while respiration is dependent on body weight, water temperature, and swimming activity. Energy costs associated with reproduction vary from 0%·day^{-1} (of consumed energy) in the first year of life to 25%·day^{-1} by maturation.

Based on eq. 1, the internal carbon, nitrogen, and phosphorus dynamics are also simulated assuming a typical constant C:N:P ratio for a cyprinid (46%, 9.7%, and 1.5% of dry weight, respectively, Sterner and George 2000).

Using two sets of parameters, we simulated two discrete age groups: fish younger than 1 year and fish 1 year of age or older (see Appendix B for list of parameters and values). For a detailed description of the bioenergetics model, the reader is also referred to Megrey et al. (2007).

IBM for a fish population

To simulate the fish population, we applied the bioenergetics equation (eq. 1) to numerous individual fish. The individuality of the fish was created through a behavioural submodel that reallocated each fish within the water column, dependent on criteria related to oxygen, temperature, light, and food. This serves to expose each fish to a unique history of biotic and abiotic environmental conditions. In addition, each fish was "genetically different" from the other fish, since it acquired individual random values, within a defined range (parameters *a* and *b* in Appendix B), of the parameters for the weight–length relationship. Other bioenergetics parameters were not individualized and were common for the population.

Data structure

As it was not practical to simulate the entire fish population as individual computational units, a set of "representative fish" were used to aggregate a number of similar fish into a single computational entity. The number of representative fish changed dynamically during the simulation according to simulated processes of recruitment and natural and fishing mortality.

The lake-wide fish population was initialized with 1000 representative fish, with each set to represent 100 000 fish in the lake, equating to 100 000 000 fish in total. Each representative fish has a record with fields such as age (day), wet weight (g), location (layer number and depth), length (cm), the parameters of the weight–length allometric equation (described below), total daily consumption ($g_{prey} \cdot g_{fish}^{-1} \cdot day^{-1}$), and the daily consumption of each of the various prey types (mg C·L^{-1}·day^{-1}).

Fish location in water column

Each representative fish had a different individual life history that was a result of daily relocation of each fish to one of several possible layers in the water column. These layers were selected and then ranked based on suitability of ambient conditions such as oxygen, light, temperature, and zooplankton biomass for the fish population. Only layers that had an oxygen concentration greater than 0 mg O·L^{-1} and light intensity greater than 10 μE·m^{-2}·s^{-1} (1 μE = 54 lx) were included. A location function (L_c) was developed to rank the layers and subsequently used to determine the number of fish in each layer. The ranking of a layer, *c*, was computed as a multiplication of three functions relating to temperature, *f*(*T*), light, *f*(*L*), and prey (zooplankton) availability, *f*(*Z*), each returning a value in the range (0–1):

$$(2) \qquad L_c = f(T) f(L) f(Z)$$

The temperature and light functions are similar to the temperature function for consumption described by Megrey et al. (2007), except that here we adopt parameters more suited to the lavnun. The food availability function is a linear function that assigns the value 0 to the layer with the lowest available food and a value of 1 to the layer with the highest available food. All other layers are assigned a value between 0 and 1 according to the food concentrations.

Based on the L_c value, the fraction of fish in each layer was calculated. A distribution function (D_c) assigned each layer a value computed by dividing the L_c value by the sum of those values over all allowable layers:

$$(3) \qquad D_c = \frac{L_c}{\sum_{c=1}^{N_{layers}} L_c}$$

where N_{layers} represent the number of allowable layers, and the distribution function over the whole range of allowable layers is enforced to obey $\sum_{c=1}^{N_{layers}} D_c = 1$. The D_c value is the percentage of fish (out of the total number of representative fish) to be allocated to that layer at the current time step. According to the distribution function, the fish were distributed randomly between the layers. The allocation of a certain fish to a certain layer was independent of its previous location. In essence, this procedure simulates vertical movement of fish on a daily time step. The vertical movement ensures exposure of the fish to different biotic and abiotic conditions, and as the movement of the fish is vertical it is not unreasonable to assume that the fish can move that distance over the give time period.

Mortality

Daily mortality (both natural and from fishing) was implemented by removing fish from the population. The model requires parameters that account for the daily percentage of population removal due to natural mortality (NM) and fishing mortality (FM) for both commercial (com, weight > 14 g) and noncommercial (ncom) sizes. The natural and fishing mortality functions are calculated as

$$(4) \qquad \mathrm{NM_{com}} = k_{\mathrm{Mcom}} N_{\mathrm{com}}$$

$$(5) \qquad \mathrm{NM_{ncom}} = k_{\mathrm{Mncom}} N_{\mathrm{ncom}}$$

$$(6) \qquad \mathrm{FM_{com}} = k_{\mathrm{Fcom}} N_{\mathrm{com}}$$

$$\text{(7)}\qquad \mathrm{FM}_{\mathrm{ncom}} = k_{\mathrm{Fncom}} N_{\mathrm{ncom}}$$

where $\mathrm{NM}_{\mathrm{com}}$, $\mathrm{NM}_{\mathrm{ncom}}$, $\mathrm{FM}_{\mathrm{com}}$, and $\mathrm{FM}_{\mathrm{ncom}}$ are the number of fish to be eliminated because of natural and fishing mortality (day^{-1}) of commercial and noncommercial size fish, respectively. N_{com} and N_{ncom} are the number of commercial and noncommercial sized fish, respectively, and k_{Mcom}, k_{Mncom}, k_{Fcom}, and k_{Fncom} are the daily fraction of natural and fisheries mortality of commercial and noncommercial size fish, respectively.

Natural and fishing mortality of commercial and noncommercial size groups was implemented by selecting a subset of fish from these size groups using a uniform random number generator and removing them from the population. Natural mortality for commercial sized fish was applied in two steps. First, fish over the age of 5 were eliminated and then a randomly selected group of the commercial fish was eliminated. Since only a whole number of representatives can be eliminated, daily mortality was calculated, and if the mortality was less than 1 (representative fish), then it was accumulated until it reached a number of representatives greater than 1.

Recruitment

The number of reproduced fish (N_{rec}) is a function of the number of mature fish (fish older than 18 months, N_{mat}), the time of the year, *f*(*d*), and water level fluctuation, *f*(WL). The recruitment is calculated as

$$\text{(8)}\qquad N_{\mathrm{rec}} = k_{\mathrm{rep}} N_{\mathrm{mat}} f(d) f(\mathrm{WL})$$

where k_{rep} is the fraction of reproducing (mature) fish. The *f*(*d*) function allows fish to reproduce from December to March, with maximum reproduction occurring in January and February, and is defined by

$$\text{(9)}\qquad f(d) = \begin{cases} X_1 d^2 + Y_1 d + Z_1 & \text{December} \\ X_2 d^2 + Y_2 d + Z_2 & \text{January} - \text{March} \\ 0 & \text{other} \end{cases}$$

where *d* is the day of the year starting 1 January of each year. The values of the coefficients X_1, Y_1, Z_1, X_2, Y_2, and Z_2 are described in Appendix B.

The dependence of the recruitment on water level is a function of the daily increment in water level (Gasith and Gafny 1990; Gafny et al. 1992). We define the recruitment dependence on water level, *f*(WL), based on a 14-day running average change in lake level. The period of 14 days is assumed to be the time required for the development of benthic diatoms on stones that prevents fish from attaching their eggs to the surface (Gafny et al. 1992). The water level function is parameterized as

$$\text{(10)}\qquad f(\mathrm{WL}) = A\log(x) + B \qquad \text{if } x > a$$

where *x* (cm) is the fortnightly average daily increment in the water level. The values of the coefficients *A* and *B* are given in Appendix B.

Total biomass

The total wet weight (W_{T}) was computed as

$$\text{(11)}\qquad W_{\mathrm{T}} = \sum_{i=1}^{N_{\mathrm{fish}}} w_i N_{\mathrm{rep}}$$

where N_{fish} is the number of the fish, w_i is the wet weight of the *i*th representative, and N_{rep} is the number of fish that are accounted for by each representative fish.

Size distribution

Fish length (cm) was computed based on the allometric weight–length (*W*–*L*) equation for wet weight of fish (g):

$$\text{(12)}\qquad L = (W/a)^{1/b}$$

Our computation is based on Ostrovsky and Walline (1999), where a = 0.00281 ± 0.000343 and b = 3.43 ± 0.0042. A random value selected from a uniform distribution within the standard deviation range of each parameter, *a* and *b*, was assigned to each fish when it was "born" (that is, added to the model) and introduced variation into the population characteristics based on variation observed in the natural population. Each fish gained and lost weight according to the bioenergetics equation. The fish weight, and hence length, was calculated based on the output of the bioenergetics model and the individual *a* and *b* values, except that fish length was forced to remain unchanged during the period of fish weight losses caused by starvation to avoid the artificial (unrealistic) shrinkage of fish body length.

Coupling the fish model to the ecological model

The user can either enable or disable the feedbacks from the fish submodel (e.g., consumption, egestion, excretion, and respiration) to the lower trophic levels. When the feedbacks are enabled (the dynamic model), mass balance between the submodels is conserved and all fluxes directly affect the concentrations of the zooplankton, the particulate and dissolved organic matter (POM and DOM, respectively), the oxygen, and the dissolved inorganic carbon in the grid cells in which the fish are located. The biomass of zooplankton and particulate organic material consumed by the fish are reduced from the respective pools. Fish respiration (mg C·day^{-1}) effects are added to the dissolved oxygen and dissolved inorganic carbon pools, respectively, using conversion factors given in Appendix B.

Egestion and natural mortality contribute to the particulate organic material pools. The former is calculated based on the composite C:N:P ratio of all the different food sources, and the later is based on the internal C:N:P ratio of the fish:

$$\text{(13)}\qquad \mathrm{POM}_{\mathrm{fb}} = \sum_{i=1}^{N_{\mathrm{fish}}} \sum_{j=1}^{N_{\mathrm{prey}}} C_{ij} \times \mathrm{eg}_i \times \mathrm{IR}_j + \sum_{k=1}^{N_{\mathrm{dead}}} W_k \times \mathrm{IR}_k$$

where $\mathrm{POM}_{\mathrm{fb}}$ is the fish feedback (fb) to the pool of particulate organic material (e.g., carbon, nitrogen, or phosphorus in units of mg C·L^{-1}, mg N·L^{-1}, and mg P·L^{-1}, respectively), N_{fish} and N_{prey} are the number of fish and the number of prey food, respectively, C_{ij} is the consumption of prey *j* by the *i*th fish, eg_i is the egestion coefficient (losses due to faeces), IR_j is the internal ratio of organic material to carbon in the *j*th prey food, N_{dead} is the number of dead fish, W_k is the dry weight of the *k*th dead fish, and IR_k is the internal ratio of carbon, nitrogen, and phosphorus to dry weight for the *k*th fish.

Excretion by fish (losses of excretory wastes) is also included and enters the dissolved organic material pool (DOM). Excretion is used to maintain the constant internal nutrient ratio within the fish. Therefore, each of the processes described above (consumption and loss terms) are performed first, and the resulting changes in the internal C, N, and P are accumulated. Then, based on the limiting element, any excessive C, N, or P is excreted and added to the DOM pools to maintain the constant C:N:P ratio of the fish. If required, a new weight is computed according to the loss.

Model setup and simulation description

As with Gal et al. (2009), model simulations were configured to run from January 1997 to September 2003, as these years contained the most complete record for both the ecological model inputs (forcing data) and in-lake data (validation data). The base model was run with a 1 h time step and daily output. A daily time step was used for the fish model to reduce simulation time.

Initialization, forcing, and input data

The model requires input data for initialization of simulated variables and meteorological, inflow and outflow, forcing data. The initialization file for the ecological model was prepared from field data collected on 5 January 1997 and included vertical profiles for each of the state variables simulated. Inflow data included the daily volume, temperature, salinity, and nutrient concentrations of each of the six simulated inflows. Phytoplankton and zooplankton concentrations are negligible in the inflows and were set to zero. The outflow data included the total daily outflows and pumping from the lake. Meteorological input data included hourly short-wave and long-wave radiation, air temperature, vapor pressure, wind speed, and precipitation collected from a meteorological station located at Tabha approximately 1 km from the northwest shore of the lake (see Gal et al. 2003). The fish model requires initialization for each one of the 1000 initial representative fish. The initialization includes weight, age, location, and random assignment values for the parameters *a* and *b* of the weight–length equation (eq. 12). Based on catch data from year 1997, which demonstrated, on average, a normal size distribution with a mean weight of 15.9 g and a total of 626 t (approximated to be one third of total lavnun biomass), the weight and age distribution of the initial population was set to be normally distributed with a mean weight of 16.5 g (standard deviation, SD = ±4 g) and total biomass of 1700 t wet weight over the whole lake. The initial location for all representative fish was set to depth of 15–20 m.

Simulations and validaion process

The calibration and validation of the lavnun model was based on data from different sources, mainly the routine monitoring of the catch and size analysis (weight and length) as measured by the Fisheries Department, Ministry of Agriculture, in addition to data from the literature and KLL reports. The parameters for the bioenergetics model (see Appendix B for list of parameters and values) were derived from published literature, other models, or from KLL reports. Where parameters were not available, a series of model runs were performed, maintaining parameter values within the bounds of literature values for similar cyprinid species, the parameter values showing the best fit to the field data was chosen. The calibration was implemented by adjusting parameters in such a way that there was good agreement between the predicted and observed data for growth: weight–length data, length at age, weight at age, total biomass, population size distribution, and estimated zooplankton consumption.

To determine the impact of the lavnun on water quality variables such as zooplankton biomass, chlorophyll *a* concentration, and inorganic nitrogen and phosphorus, we compared the results of the static and dynamic models visually and statistically using the Student's *t* test. Since the output time series data are autocorrelated, we conducted a preliminary autocorrelation test on all output variables to construct subsets of the output data for which autocorrelation levels would be <0.25. We found that for most variables, a randomly selected subset consisting of a third of the output data effectively reduced autocorrelation values below the required level (typically to <0.1), while a subset of one quarter of the output data achieved the required autocorrelation levels for NO_3, NH_4, and cyanobacteria. These subsets were then used in the paired-samples *t* test.

To study the impact of the fish population size, the model was run with different numbers of fish that each representative fish represented. The ×1 scenario was equal to an initial number of 100 million fish in the lake (e.g., each representative fish represented 100 000 fish in the lake); the ×2, ×0.5, and ×0.00001 scenarios were equal to initial numbers of fish of 200 million, 50 million, and 1000 fish in the lake, respectively.

Results

The validation results for the physical and biogeochemical aspects of the Lake Kinneret application of DYCD are explained in detail in Gal et al. (2009). Here we describe the growth dynamics of fish as simulated by the dynamic model and how they compare with observed data. The outputs of the static and dynamic models are compared to explore the impact of the fish on the other components of the ecosystem.

The bioenergetics-based fish population model

A single cohort analysis was calculated for the cohort that hatched in 1997 and ended in 2001. The average weight at age (Fig. 2) for this cohort demonstrates that the fish growth decreases in summer when food availability is relatively limited and then increases again towards the spawning period in winter. For example, in the third year of life the fish reached a maximum weight of 18 g in the winter. During the summer the weight decreased by 30% and rose again toward the winter of the next year. The average food consumption per unit of body weight and the respiration rate as simulated by the bioenergetics model decrease with age. In the second year of life, for example, the average consumption is 0.1 $g_{prey}\cdot g_{fish}^{-1}\cdot day^{-1}$, and in the fifth year it is 0.03 $g_{prey}\cdot g_{fish}^{-1}\cdot day^{-1}$ (Fig. 3). The weight–length relationship curve shows a typical relationship resulting from the metabolic activity and ambient conditions (Fig. 4). The predicted weight and length fall within the range of the data reported in the literature (Table 1; Fig. 5) and data collected by the fishery authorities during the years 1997–2003 (Fig. 4; J. Shapiro, unpublished data).

The population dynamics, as expressed in the form of size frequency distributions, reflect a population that spawn seasonally from December to March (Fig. 6). The model results indicate that during the first 2 years of life, the smallest dominant size groups are isolated clearly from larger size groups by distinct minima (~10 cm) on the frequency distribution curve. During the first 3 months (January to March) the number of the fish in the smallest size group increases as a result of annual recruitment reaching a total of 50% of the population. The rate at which the fish grow and move from one size group to the next is dependent on the ambient conditions and the parameters of the bioenergetics equation. At the end of the year, the second age group (age group 1+) reached a size of 10 cm and the third age group (age group 2+) reached a size of 13–14 cm. After the third year of life, when fish lengths are greater than 14 cm, it is more difficult to distinguish between the different age groups.

The predicted total biomass during the simulation period falls within the range of 800–2200 t and varies annually because of changes in ambient conditions resulting in fish growth variation, water level fluctuation affecting recruitment, and natural and fishing mortality (Fig. 7). The interannual variability in the total biomass in the first 4 years of the simulation is affected, at least in part, by the size distribution of the initial population. Afterwards, the biomass is entirely related to the fish population generated throughout the simulation.

Role of fish in the ecosystem

In this model, fish were distributed throughout the water column according to ambient conditions including temperature, light, oxygen, and food. The daily fish consumption of their prey food was therefore depth-dependent with maximum daily consumption values of 6%, 4%, and 0.2% of the herbivorous, predatory, and microzooplankton biomass, respectively, at depths ranging between 3.5 and 4 m (Fig. 8). This is a measure of the direct effect of the fish on their prey and reflects the vulnerability–preferences parameters defined in Appendix B.

The effect of the fish on the mean monthly concentration of several state variables and the difference between the static model and the dynamic model were evaluated. The results indicate a statistically significant impact ($p < 0.05$) of the fish on most simulated biological and chemical state variables including two of its prey types: the predatory and microzooplankton. Interestingly, the effect on the main diet source of the fish (the herbivorous zooplankton) was not significant (Table 2). The use of the dynamic model did not introduce any visible change in the seasonality of the different state variables when compared with the static model. The effects were mainly seen in the magnitude of the biomass of the biological variables, including the zooplankton. For example, in comparison with the static model, the dynamic model demonstrated 27% and 24% decreases in the average biomass of the predatory and microzooplankton, respectively, mainly during the annual peaks of the zooplankton. The timing of the peak, however, remained unchanged. The effect on the herbivorous zooplankton was demonstrated more notably throughout the year, since this group was not as seasonal in its nature. Though there was no statistical impact by the lavnun on the herbivorous zooplankton, the concentrations in the dynamic model were typically lower than that observed in the static model, except for during the periods of the annual peaks in which their concentrations were equal to or greater than the static model (data not shown). The dynamic model introduced a decrease greater than 20% in the mean concentration of phytoplankton such as *Aphanizomenon ovalisporum* and *Microcystis*. One of the reasons for the change in the phytoplankton can be related to the phosphorus and nitrogen limitation functions. For example, when comparing the phosphorus and nitrogen limitation functions of *Microcystis* at a depth of 3 m, an average decrease of 8% and 5%, respectively, was predicted, demonstrating that growth of *Microcystis* is limited by nutrients to a greater extent in the dynamic model.

The overall fish growth pattern simulated in the static and the dynamic models is similar. However, there is considerable variation in the size distribution between the two models. The impact is evident ($p < 0.05$) mainly for large fish (length > 15 cm) and small fish (10–13 cm). By the sixth year of the simulation (year 2002), the predicted maximum length and average length in the different age groups was lower in the dynamic model (Figs. 9*a*–9*c*) than in the static model (Figs. 9*d*–9*f*). The maximum predicted length in the static model was 19.5 cm in comparison with 17.5 cm in the dynamic model. The average size in the group of age 2 fish (group size 13–15.5 cm) was 14 cm in the static model and 12 cm in the dynamic model (group size 11–14 cm). However, the abundance of this age group in the dynamic model was higher. The reason for the difference is related to the lower fish growth rate simulated in the dynamic model. A lower growth rate resulted in lower exposure to the commercial fishery (as the fish reach commercial size at an older age) in comparison with the corresponding age group in the static model. The group of age 1 fish (group size 10–12 cm) is more abundant in the outputs of the static model and only moderately appears in the dynamic model. These results reveal the impact of fish inducing indirect feedbacks on the fish population itself.

Length–frequency distribution of fishery catch from the corresponding time period in year 2002 (September, October, and December 2002) shows maximum distribution at 11.5 and 13 cm in September and a unimodal distribution in October and December with peak distributions at 12 and 13 cm, respectively (Figs. 9*g*–9*i*). In October and December 2002, the predicted abundance of fish smaller than 15 cm is similar to the field data. However, the model also demonstrates larger fish (length > 15 cm) and age groups not detected in the field.

Discussion

The model presented here couples a complex ecological model with a novel fish-population IBM. The modelling approach has not been reported previously in this context and can be considered as a "hybrid" modelling approach (i.e., combining several types of models; Mooij et al. 2010). The advantage of this approach is that it merges some of the advantages and eliminates some disadvantages of existing models (Jørgensen 2008). Specifically, the new model integrates a coupled hydrodynamic–NPZ (nutrient–phytoplankton–zooplankton) model with a fish-population IBM built from the bioenergetics equation. The bioenergetics equation is commonly used to simulate fish growth (Chipps and Wahl 2008); however, in this study we constructed a fish IBM based on the bioenergetics equation nested within an ecosystem model to better simulate trophic interactions. This merging of approaches has allowed us to demonstrate the importance of linking the fish dynamics to lower trophic levels and other ecosystem components. The hybrid model, including the fish trophic level, is a more realistic presentation of the complexity of aquatic ecosystems than the basic NPZ model (Fulton et al. 2003). It is also different from most ecosystem models that typically concentrate on either end of the trophic chain (i.e., on fish or on nutrients and phytoplankton), but rarely on both (Fulton et al. 2004).

The approach adopted here is similar to that employed in the NEMURO.FISH model (Megrey et al. 2007), though we make a number of major advances. In the current study, DYCD–FISH couples the fish model to a 1D hydrodynamic model using real data collected for Lake Kinneret during the years 1997–2003 as model input. Furthermore, we take advantage of the IBM approach by modelling representative fish, each with unique weight–length characteristics. Additionally, DYCD–FISH includes a simple behavioural submodel that was introduced to allow for spatial (vertical) variability in the fish population to resolve the range of environmental conditions they experience. Therefore, each simulated fish experienced a unique history of ambient conditions throughout its life cycle. The difference in ambient conditions, along with the difference in the weight–length relationship, resulted in variation in development of the individuals in the population.

The simulation results are comparable with the available published data. The model predicted a total lavnun biomass of 800–2200 t for the 7-year simulation period based on an initial number of 100 million fish (which was equivalent to 1700 t). This initial number was estimated based on the average number of fish during the years 1987–1990 determined acoustically (Walline et al. 1992). From the late 1980s to early 1990s the total lavnun biomass was 2800 t (Ostrovsky and Walline 1999). Acoustic surveys estimated the total pelagic fish stock in Lake Kinneret to be around 4000–6000 t (61–218 million fish), from which the lavnun was considered to be approximately 50% (Walline et al. 1992). Our results are also supported by a total estimated annual production of 200×10^3 t of zooplankton that can maintain about 2900 t of planktivorous fish, based on the assumption that a unit of fish biomass requires about 70 units of wet weight of zooplankton per year to satisfy their metabolic expenses (i.e., $200 \times 10^3/70$; Ostrovsky and Walline 1999). While the differences between the reported and simulated biomass are not large, they are expected and can be attributed to several issues. These include the changes in the state of Lake Kinneret as a result of long-term fishing pressure over the past two decades, natural interannual variation in phytoplankton abundance, changes to the phytoplankton annual succession patterns that occurred during the 1990s (Zohary 2004; Roelke et al. 2007), and occurrence of a regime shift and associated changes in the zooplankton population (Gal and Anderson 2010; Hambright 2008). These differences can also be attributed to possible errors in the model formulation and uncertainty in field data. Nonetheless, the results are considered to be sufficiently accurate for the purposes of this study.

The model largely captured the reported pattern of size frequency distributions of the fish as well as the positions of the minima in the size distribution plot (Walline et al. 1992; Ostrovsky and Walline 1999), demonstrating that the smallest size groups consist of a specific age group. However, the comparison of the predictions to field data for fish larger than 10 cm demonstrated that while the model simulated distinct age groups, the field data illustrated a unimodal distribution and a smaller maximum length. One possible reason for the unimodal distribution and the lack of large fish (length > 15 cm) detected in the lake since 1993 is the long-term (1994–2006) "culling" program (Hambright and Shapiro 1997), not simulated in the current study. The culling program was meant to remove subcommercial and commercial size fish from the lake, and a possible outcome of this action is the loss of large fish from the population.

The differences between the static and the dynamic models demonstrate the effect of the fish through the various feedback mechanisms. For example, the differences in the size distribution and particularly the differences in the large size group (length > 15 cm) and in the small size group (10–12 cm) between the static and the dynamic models were significant and indicate that the direct and indirect feedbacks have an effect on the fish growth rate. The fish population simulated with the static model had a higher growth rate than the population simulated with the dynamic model.

The effects of the fish on the food web can be categorized as either direct or indirect; direct effects are due to the reduction of available prey by the fish and their subsequent excretion of nutrients. These have the potential to indirectly impact water quality dynamics (as measured, for example, by indirect feedbacks affecting the zooplankton concentration, chlorophyll *a* concentration, or the percentage of cyanobacteria) and subsequently to alter the food available for fish consumption, which in turn may affect the growth and the size distribution of the fish themselves. The fish feedbacks applied in the dynamic model accounted for the decrease in the biomass of the food sources and therefore the lower growth rate. The results demonstrate the impact of competition occurring within the specific species (i.e., intraspecies competition) on fish growth rate. The impact of intraspecies competition on fish growth rate is a key issue in fisheries science (Kozák et al. 2007). Our results are in agreement with other studies (Ward et al. 2006; Cuenco et al. 1985) showing that intraspecies competition leads to a decline in growth rate and lower productivity and yields. However, other possible implications of intraspecies competition such as adaptive behavioural strategies, feeding patterns, establishment of dominance hierarchies, feeding territories at the level of the individual fish, and long-term evolutional implications (Ward et al. 2006) are not modelled in the current model version.

Fish have the potential to directly and indirectly affect freshwater ecosystems through feeding (Reissig et al. 2006; Gozlan et al. 2010), storing, releasing of nutrients (via sediment disturbance), and excretion of waste products (McIntyre et al. 2007; Schindler et al. 1993; Vanni 2002). Reissig et al. (2006) demonstrated that in the presence of fish, the zooplankton size distribution tended to be narrower and the zooplankton composition varied. Fish introduction into Patagonian Lakes in Argentina, for example, resulted in a decrease of centropagid species richness and an increase in rotifers. Our analysis of the difference between the dynamic and static models showed a statistically significant impact of lavnun on the majority of simulated variables, with dynamic model values typically lower than the static model values. However, for two thirds of the output variables, the difference in average concentration was relatively moderate (less than 20% difference), and the impact of the fish was mainly on the amplitude of the variables but not on the temporal dynamics. Surprisingly, there were no significant differences in biomass of the main diet source of the fish, the herbivorous zooplankton. On the other hand, we found a significant decrease in water column nutrients that was caused by the storing of nutrients in fish tissues. These results are comparable to previous reports that most water column phosphorus, in the highly productive Lake Wingra (Wisconsin), is stored in fish biomass (Kitchell et al. 1975).

The differences between the static and the dynamic models are the outcome of the increased complexity simulated by the dynamic model. The results can be associated with the relevant species composition and nonlinear food web interactions, such as intraguild predation (Holt and Polis 1997; Hart 2002) existing among the fish, herbivorous zooplankton, and predatory zooplankton. The results, therefore, point to the need to further study the relationship among fish, predatory zooplankton and herbivorous zooplankton and also study the regime shift in the predatory zooplankton population evident in Lake Kinneret in recent years (Gal and Anderson 2010).

The current model suffers from a number of limitations. First, insufficient field data exist; the published literature includes few sporadic documents of fish biomass, mainly from the 1980s and early 1990s (Walline et al. 1992; Ostrovsky and Walline 1999; Landau 1991). Additionally, being a multispecies fishery, the fishery data does not include species-specific fishing effort and therefore does not allow the estimation of fish biomass based upon species-specific catch and effort data. Second, there are inconsistencies of the field data; Landau (1991) assessed the lavnun standing stock on the order of 15 000–20 000 t for the 1980s. These estimates exceed three to five times the total fish stock estimated acoustically by Walline et al. (1992). Total fish numbers were estimated by Walline et al. (1992) to be 61 million in 1987 and 218 million in 1988, with an average total biomass of 2785 t in 1988–1990. Furthermore, Landau (1991) estimated the maximum age of the fish at ~20 years based on inspection of opercular structure. This estimation is three to four times higher than that found by other authors (Davidoff 1986; Steinitz 1959). As the variation in field data is large, it is clear that more research is required. Third, only partial proof of recruitment and water level dependency exists and was demonstrated in the lake only twice, after heavy floods during the winter of 1991–1992 and the winter of 2002–2003. While circumstantial evidence links the two factors (Gafny et al. 1992; Gasith and Gafny 1990), no rigorous experimental evidence has been reported for Lake Kinneret. However, more research should be conducted to reveal these relationships. Fourth, the fish model simulates vertical movement of fish on a daily time step. Since fish constantly move vertically and horizontally in the water and continuously effect the different components of the ecosystem, this oversimplification can be a source of bias in model results. Fish also have a spatially heterogeneous distribution (Kalikhman et al. 1992; Yacobi et al. 1993; Mason et al. 2005); however, because of the lack of spatial information here, a 1D approach has been adopted. A 3D approach should, however, be addressed in the future as available fish data is improved.

A considerable change in the number of lavnun can occur in years in which the water level raises rapidly and extensively, allowing a high spawning rate and a boost in the number of the fish. A large change in planktivore fish density has the potential to affect the zooplankton population (Wu et al. 1997). Ostrovsky and Walline (1999) suggested that the large lavnun 1991–1992 winter year class upset the existing balance between the fish and their food (zooplankton), causing the disappearance of large fish and the subsequent fishery collapse in 1993. We used DYCD–FISH to explore the impacts of the number of fish on their prey by increasing the number of simulated fish and determining the effect on average zooplankton concentration (Fig. 10). Both the average zooplankton concentration and the relative contribution of the various groups to the total zooplankton concentration were affected by the number of fish in the lake. The results confirm the presence of a lower zooplankton biomass at higher abundances of zooplanktivorous fish; however, the decrease in zooplankton biomass was lower than expected. For example, a twofold increase in the number of the fish resulted in a decrease in the zooplankton biomass by only 13% in comparison with the base level (×1). Interestingly, the increase in the number of fish had an impact on the relative contributions of the different zooplankton groups in the zooplankton population. The ×2 scenario, for example, resulted in a decrease in the percentage of predatory zooplankton (from 27% to 24%), while the relative part of the herbivorous zooplankton increased from 56% to 61%. This outcome can be explained as the consequence of the decrease in predatory zooplankton biomass (in the presence of higher number of fish) and the subsequent lower predation pressure of predatory zooplankton on herbivorous zooplankton.

The model presented here is a generic dynamic model applicable to most stratified lake ecosystems. The model simulates a range of biological, chemical, and physical processes, from nutrients up to the trophic level of planktivorous fish, essentially expressing the variables that are commonly associated with lake water quality. The model can therefore serve as an experimental system to study links and effects between aquatic ecosystem components that cannot be otherwise explored. It allows exploring hypotheses, such as the trophic cascade hypothesis, the impact of climate change, or the impact of a fishery. To apply proper fishery management measures in lakes, it is important to assess a priori the inclusive outcome of such measures. The current model, as it also includes fishery-induced mortality, has the potential to be used as an ecosystem-based fishery management tool (Ecosystem Principles Advisory Panel 1999; Pikitch et al. 2004). To apply the model as a practical decision support tool, there is a need to extend the current approach to include other fish species, more life stages, age classes, and to be supported by continuous fishery data.

Acknowledgements

We thank Yohay Carmel for his helpful assistance in statistical analysis of the data and two anonymous reviewers for helpful comments. Support for V.M. was provided by the Yohay Ben-Nun Scholarship fund, the Australia–Israel Scientific Exchange Foundation, (AISEF) Postgraduate Fellowship Scholarship for 2007, and the Centre for Water Research, University of Western Australia.

References

Berman, T., Stone, L., Yacobi, Y.Z., Kaplan, B., Schlichter, M., Nishri, A., and Pollingher, U. 1995. Primary production and phytoplankton in Lake Kinneret: a long-term record (1972–1993). Limnol. Oceanogr. **40**(6): 1064–1076. doi:10.4319/lo.1995.40.6.1064.

Brett, M.T., and Goldman, C.R. 1996. A meta-analysis of the freshwater trophic cascade. Proc. Natl. Acad. Sci. U.S.A. **93**(15): 7723–7726. doi:10.1073/pnas.93.15.7723. PMID:11607694.

Bruce, L.C., Hamilton, D.P., Imberger, J., Gal, G., Gophen, M., Zohary, T., and Hambright, D. 2006. A numerical simulation of the role of zooplankton in C, N and P cycling in Lake Kinneret, Israel. Ecol. Model. **193**(3–4): 412–436. doi:10.1016/j.ecolmodel.2005.09.008.

Carpenter, S.R., and Kitchell, J.F. 1988. Consumer control of lake productivity. Bioscience, **38**(11): 764–769. doi:10.2307/1310785.

Carpenter, S.R., Kitchell, J.F., and Hodgson, J.R. 1985. Cascading trophic interactions and lake productivity. Bioscience, **35**(10): 634–639. doi:10.2307/1309989.

Chipps, S.R., and Wahl, D.H. 2008. Bioenergetics modeling in the 21st century: reviewing new insights and revisiting old constraints. Trans. Am. Fish. Soc. **137**(1): 298–313. doi:10.1577/T05-236.1.

Cuenco, M.L., Stickney, R.R., and Grant, W.E. 1985. Fish bioenergetics and growth in aquaculture ponds. III. Effects of intraspecific competition, stocking rate, stocking size and feeding rate on fish productivity. Ecol. Model. **28**(1–2): 73–95. doi:10.1016/0304-3800(85)90014-6.

Davidoff, E.B. 1986. Verification of the scale method for ageing the cyprinid *Mirogrex terraesanctae* (Steinitz, 1952) in Lake Kinneret, Israel. The Israeli Journal of Aquaculture – Bamidgeh, **38**: 108–125.

DeAngelis, D.L., and Mooij, W.M. 2005. Individual-based models of ecological and evolutionary processes. Annu. Rev. Ecol. Evol. Syst. **36**(1): 147–168. doi:10.1146/annurev.ecolsys.36.102003.152644.

DeMelo, R., France, R., and McQueen, D.J. 1992. Biomanipulation: hit or myth? Limnol. Oceanogr. **37**(1): 192–207. doi:10.4319/lo.1992.37.1.0192.

Drenner, R.W., and Hambright, K.D. 2002. Piscivores, trophic cascades, and lake management. ScientificWorldJOURNAL, **2**: 284–307. doi:10.1100/tsw.2002.138. PMID:12806017.

Easton, J., and Gophen, M. 2003. Diel variation in the vertical distribution of fish and plankton in Lake Kinneret: a 24-h study of ecological overlap. Hydrobiologia, **491**(1–3): 91–100. doi:10.1023/A:1024466600402.

Ecosystem Principles Advisory Panel. 1999. Ecosystem-based fishery management. NOAA National Marine Fisheries Service, Silver Spring, Md. Available from http://www.nmfs.noaa.gov/sfa/EPAPrpt.pdf.

Elser, J.J., Chrzanowski, T.H., Sterner, R.W., and Mills, K.H. 1998. Stoichiometric constraints on food-web dynamics: a whole-lake experiment on the Canadian Shield. Ecosystems, **1**(1): 120–136. doi:10.1007/s100219900009.

Fulton, E.A., Smith, A.D.M., and Johnson, C.R. 2003. Effect of complexity on marine ecosystem models. Mar. Ecol. Prog. Ser. **253**: 1–16. doi:10.3354/meps253001.

Fulton, E., Anthony, D.M.S., and Johnson, C.R. 2004. Biogeochemical marine ecosystem models I: IGBEM — a model of marine bay ecosystems. Ecol. Model. **174**(3): 267–307. doi:10.1016/j.ecolmodel.2003.09.027.

Gafny, S., Gasith, A., and Goren, M. 1992. Effect of water level fluctuations on shore spawning of *Mirogrex terraesanctae* (Steinitz), (Cyprinidae) in Lake Kinneret, Israel. J. Fish Biol. **41**(6): 863–871. doi:10.1111/j.1095-8649.1992.tb02715.x.

Gal, G., and Anderson, W. 2010. A novel approach to detecting a regime shift in a lake ecosystem. Methods in Ecology and Evolution, **1**(1): 45–52. doi:10.1111/j.2041-210X.2009.00006.x.

Gal, G., Imberger, J., Zohary, T., Antenucci, J., Ayal, A., and Rosenberg, T. 2003. Simulating the thermal dynamics of Lake Kinneret. Ecol. Model. **162**(1–2): 69–86. doi:10.1016/S0304-3800(02)00380-0.

Gal, G., Hipsey, M.R., Parparov, A., Wagner, U., Makler, V., and Zohary, T. 2009. Implementation of ecological modeling as an effective management and investigation tool: Lake Kinneret as a case study. Ecol. Model. **220**: 1697–1718. doi:10.1016/j.ecolmodel.2009.04.010.

Gasith, A., and Gafny, S. 1990. Effects of water level fluctuation on the structure and function of the littoral zone. *In* Large lakes, ecological structure and function. *Edited by* M.M. Tilzer and C. Serruya. Springer-Verlag, Berlin. pp. 156–171.

Gophen, M. 1986. Fisheries management in Lake Kinneret (Israel). *In* Lake and reservoir management. Vol. 2. *Edited by* G. Redfield, F. Taggart, and L.M. Moore. North American Lake Management Society, Washington, D.C. pp. 327–332.

Gophen, M., and Scharf, A. 1981. Food and feeding habits of *Mirogrex* fingerlings in Lake Kinneret (Israel). Hydrobiologia, **78**(1): 3–9. doi:10.1007/BF00011933.

Gophen, M., and Threlkeld, S. 1989. An experimental study of zooplankton consumption by the Lake Kinneret sardine. Arch. Hydrobiol. **115**: 91–95.

Gophen, M., Walline, P., Ostrovsky, I., Azoulay, B., and Easton, J. 1999. Water quality and fishery management in Lake Kinneret, Israel. *In* Theoretical reservoir ecology and its applications. *Edited by* J.G. Tundidsi and M. Straskraba. International Institute of Ecology, Brazilian Academy of Sciences; and Backhuys Publishers, Sao Carlos, Brazil. pp. 493–503.

Gozlan, R.E., Britton, J.R., Cowx, I., and Copp, G.H. 2010. Current knowledge on non-native freshwater fish introductions. J. Fish Biol. **76**(4): 751–786. doi:10.1111/j.1095-8649.2010.02566.x.

Hambright, K.D. 2008. Long-term zooplankton body size and species changes in a subtropical lake: implications for lake management. Fundamental and Applied Limnology, **173**(1): 1–13. doi:10.1127/1863-9135/2008/0173-0001.

Hambright, K.D., and Shapiro, J. 1997. The 1993 collapse of the Lake Kinneret bleak fishery. Fish. Manag. Ecol. **4**(4): 275–283. doi:10.1046/j.1365-2400.1997.00053.x.

Hansen, M.J., Boisclair, D., Brandt, S.B., Hewett, S.W., Kitchell, J.F., Lucas, M.C., and Ney, J.J. 1993. Applications of bioenergetics models to fish ecology and management: Where do we go from here? Trans. Am. Fish. Soc. **122**(5): 1019–1030. doi:10.1577/1548-8659(1993)122<1019:AOBMTF>2.3.CO;2.

Hanson, P.C., Johnson, T.B., Schindler, D.E., and Kitchell, J.F. 1997. Fish bioenergetics 3.0. University of Wisconsin, Sea Grant Institute, Madison, Wisc.

Hart, D.R. 2002. Intraguild predation, invertebrate predators, and trophic cascades in lake food webs. J. Theor. Biol. **218**(1): 111–128. doi:10.1006/jtbi.2002.3053. PMID:12297074.

Hermann, A.J., Hinckley, S., Megrey, B.A., and Napp, J.M. 2001. Applied and theoretical considerations for constructing spatially explicit individual-based models of marine larval fish that include multiple trophic levels. J. Mar. Sci. **58**: 1030–1041.

Hinckley, S., Hermann, A.J., and Megrey, B.A. 1996. Development of a spatially explicit, individual-based model of marine fish early life history. Mar. Ecol. Prog. Ser. **139**: 47–68. doi:10.3354/meps139047.

Hipsey, M.R., Gal, G., Antenucci, J.P., Zohary, T., Makler, V., and Imberger, J. 2006. Lake Kinneret water quality modelling system. *In* Proceedings of the Seventh International Conference on Hydroscience and Engineering, Philadelphia, Pa., 10–13 September 2006. Michael Piasecki and College of Engineering, Drexel University. Available from http://idea.library.drexel.edu/handle/1860/1449.

Holt, R.D., and Polis, G.A. 1997. A theoretical framework for intraguild predation. Am. Nat. **149**(4): 745–764. doi:10.1086/286018.

Imberger, J., and Patterson, J.C. 1981. A dynamic reservoir simulation model, DYRESM: 5. *In* Transport models for inland and coastal waters. *Edited by* H.B. Fischer. Academic Press, New York. pp. 310–361.

Imberger, J., and Patterson, J.C. 1989. Physical limnology. *In* Advanced applied mechanics. *Edited by* T. Wu. Academic Press, Boston, Mass. pp. 303–475.

Jørgensen, S.E. 2008. Overview of the model types available for development of ecological models. Ecol. Model. **215**(1–3): 3–9. doi:10.1016/j.ecolmodel.2008.02.041.

Kalikhman, I., Walline, P., and Gophen, M. 1992. Simultaneous patterns of temperature, oxygen, zooplankton and fish distribution in Lake Kinneret, Israel. Freshw. Biol. **28**(3): 337–347. doi:10.1111/j.1365-2427.1992.tb00592.x.

Kitchell, J.F., Koonce, J.F., and Tennis, P.S. 1975. Phosphorus flux through fishes. Verhandkungen sed Internationalen Verein Limnologie, **19**: 2478–2484.

Komarovsky, B. 1952. An analysis of the stomach contents of *Acanthobrama terraesanctae* from Lake Tiberius. Bulletin of Sea Fisheries Research Station, Caesaria, **4**: 1–8.

Kozák, P., Buřic, M., Policar, T., Hamáčková, J., and Lepičová, A. 2007. The effect of inter- and intra-specific competition on survival and growth rate of native juvenile noble crayfish *Astacus astacus* and alien spiny-cheek crayfish *Orconectes limosus*. Hydrobiologia, **590**(1): 85–94. doi:10.1007/s10750-007-0760-0.

Landau, R. 1991. *Mirogrex terraesanctae* (Cyprinidae) of Lake Kinneret: biomass changes in relation to inflow; growth rate in relation to fish zooplankton interaction. Hydrobiologia, **218**(1): 1–14. doi:10.1007/BF00006413.

Landau, R.M., Gophen, M., and Walline, P. 1988. Larval *Mirogrex terraesanctae* (Cyprinidae) of Lake Kinneret (Israel): growth rate, plankton selectivities, consumption rates and interaction with rotifers. Hydrobiologia, **169**(1): 91–106. doi:10.1007/BF00007937.

Lazzaro, X. 1987. A review of planktivorous fishes: their evolution, feeding behaviours, selectivities, and impacts. Hydrobiologia, **146**(2): 97–167. doi:10.1007/BF00008764.

Lee, V.A., and Johnson, T.B. 2005. Development of bioenergetics model for the round goby (*Neogobius melanostomus*). J. Great Lakes Res. **31**(2): 125–134. doi:10.1016/S0380-1330(05)70244-6.

Mason, D.M., Johnson, T.B., Harvey, C.S., Kitchell, J.F., Schram, S.T., Bronte, C.R., Hoff, M.H., Lozano, S.J., Trebitz, A.S., Schreiner, D.R., Lamon, E.C., and Hrabik, T.R. 2005. Hydroacoustic estimates of abundance and spatial distribution of pelagic fisheries in western Lake Superior. J. Great Lakes Res. **31**(4): 426–438. doi:10.1016/S0380-1330(05)70274-4.

Mateo, I. 2007. A bioenergetics based comparison of growth conversion efficiency of Atlantic cod on Georges Bank and in the Gulf of Maine. J. Northwest Atl. Fish. Sci. **38**: 23–35. doi:10.2960/J.v38.m590.

McIntyre, P.B., Jones, L.E., Flecker, S.A., and Vanni, M.J. 2007. Fish extinctions alter nutrient recycling in tropical freshwaters. Proc. Natl. Acad. Sci. U.S.A. **104**(11): 4461–4466. doi:10.1073/pnas.0608148104. PMID:17360546.

McQueen, D.J., Post, J.R., and Mills, E.L. 1986. Trophic relationships in freshwater pelagic ecosystems. Can. J. Fish. Aquat. Sci. **43**(8): 1571–1581. doi:10.1139/f86-195.

Megrey, B.A., Rose, K.A., Klumb, R.A., Hay, D.E., Werner, F.E., Eslinger, D.L., and Smith, S.L. 2007. A bioenergetics-based population dynamics model of Pacific herring (*Clupea harengus pallasi*) coupled to a lower trophic level nutrient–phytoplankton–zooplankton model: description, calibration and sensitivity analysis. Ecol. Model. **202**(1–2): 144–164. doi:10.1016/j.ecolmodel.2006.08.020.

Mooij, W.M., Trolle, D., Jeppesen, E., Arhonditsis, G., Belolipetsky, P.V., Chitamwebwa, D.B.R., Degermendzhy, A.G., DeAngelis, D.L., De Senerpont Domis, L.N., Downing, A.S., Elliott, J.A., Fragoso, C.R., Jr, Gaedke, U., Genova, S.N., Gulati, R.D., Håkanson, L., Hamilton, D.P., Hipsey, M.R., Hoen, J., Hülsmann, S., Los, F.H., Makler-Pick, V., Petzoldt, T., Prokopkin, I.G., Rinke, K., Schep, S.A., Tominaga, K., Van Dam, A.A., Van Nes, E.H., Wells, S.A., and Janse, J.H. 2010. Challenges and opportunities for integrating lake ecosystem modelling approaches. Aquat. Ecol. **44**(3): 633–667. doi:10.1007/s10452-010-9339-3.

Ney, J.J. 1993. Bioenergetics modeling today: growing pains on the cutting edge. Trans. Am. Fish. Soc. **122**(5): 736–748. doi:10.1577/1548-8659(1993)122<0736:BMTGPO>2.3.CO;2.

Northcote, T.G. 1988. Fish in the structure and function of freshwater ecosystems: a "top-down" view. Can. J. Fish. Aquat. Sci. **45**(2): 361–379. doi:10.1139/f88-044.

Ostrovsky, I., and Walline, P. 1999. Growth and production of the dominant pelagic fish, *Acanthobrama terraesanctae*, in subtropical Lake Kinneret, Israel. J. Fish Biol. **54**(1): 18–32. doi:10.1111/j.1095-8649.1999.tb00609.x.

Pauly, D. 1980. On the interrelationship between natural mortality, growth parameters and mean environmental temperature in 175 fish stocks. J. Cons. Cons. Int. Explor. Mer, **39**: 175–192.

Pikitch, E.K., Santora, C., Babcock, E.A., Bakun, A., Bonfil, R., Conover, D.O., Dayton, P., Doukakis, P., Fluharty, D., Heneman, B., Houde, E.D., Link, J., Livingston, P.A., Mangel, M., McAllister, M.K., Pope, J., and Sainsbury, K.J. 2004. Ecosystem based fishery management. Science (Washington, D.C.), **305** (5682): 346–347. doi:10.1126/science.1098222. PMID:15256658.

Reissig, M., Trochine, C., Queimalinos, C., Balseiro, E., and Modenutti, B. 2006. Impact of fish introduction on planktonic food webs in lakes of the Patagonian Plateau. Biol. Conserv. **132**(4): 437–447. doi:10.1016/j.biocon.2006.04.036.

Roelke, D.L., Zohary, T., Hambright, K.D., and Montoya, J.V. 2007. Alternative states in the phytoplankton of Lake Kinneret, Israel (Sea of Galilee). Freshw. Biol. **52**(3): 399–411. doi:10.1111/j.1365-2427.2006.01703.x.

Romero, J.R., Antenucci, J.P., and Imberger, J. 2004. One- and three-dimensional biogeochemical simulations of two differing reservoirs. Ecol. Model. **174**(1–2): 143–160. doi:10.1016/j.ecolmodel.2004.01.005.

Rose, K.A., Werner, F.E., Megrey, B.A., Aita, M.K., Yamanaka, Y., Hay, D.E., Schweigert, J.F., and Foster, M.B. 2007. Simulated herring growth responses in the Northeastern Pacific to historic temperature and zooplankton conditions generated by the 3-dimensional NEMURO nutrient–phytoplankton–zooplankton model. Ecol. Model. **202**(1–2): 184–195. doi:10.1016/j.ecolmodel.2006.06.020.

Scheffer, M., Baveco, J., Deangelis, D., Rose, K., and Van Nes, E. 1995. Super-individuals a simple solution for modelling large populations on an individual basis. Ecol. Model. **80**(2–3): 161–170. doi:10.1016/0304-3800(94)00055-M.

Schindler, D.E., Kitchell, J.F., He, X., Carpenter, S.R., Hodgson, J.R., and Cottingham, K.L. 1993. Food web structure and phosphorus cycling in lakes. Trans. Am. Fish. Soc. **122**(5): 756–772. doi:10.1577/1548-8659(1993)122<0756:FWSAPC>2.3.CO;2.

Serruya, C. 1978. Lake Kinneret. Dr. W. Junk, B.V. Publishers, The Hague, the Netherlands.

Serruya, C., Gophen, M., and Pollinger, U. 1980. Lake Kinneret: carbon flow patterns and ecosystem management. Arch. Hydrobiol. **88**: 265–302.

Shlichter, M. 2004. The database of the Yigal Alon Kinneret Limnological Laboratory. Israel Oceanographic and Limnological Research (IOLR) Report No. T25/2004, Yigal Alon Kinneret Limnological, Laboratory, IOLR, Tiberias, Israel. [In Hebrew.]

Steinitz, H. 1952. *Acanthobrama terrae-sanctae* n. sp. from Lake Tiberias, Israel. Ann. Mag. Nat. Hist. **12**: 293–298.

Steinitz, H. 1959. Dr. H. Lissner's study of the biology of *Acanthobrama terrae-sanctae* in Lake Tiberias. Bull. Res. Counc. Isr. **24**: 43–64.

Sterner, R.W., and George, N.B. 2000. Carbon, nitrogen and phosphorus stoichiometry of cyprinid fishes. Ecology, **81**(1): 127–140. doi:10.1890/0012-9658(2000)081[0127:CNAPSO]2.0.CO;2.

Trolle, D., Jorgensen, T.B., and Jeppesen, E. 2008. Predicting the effects of reduced external nitrogen loading on the nitrogen dynamics and ecological state of deep Lake Ravn, Denmark, using the DYRESM–CAEDYM model. Limnologica, **38**: 220–232.

Vanni, M.J. 2002. Nutrient cycling by animals in freshwater ecosystems. Annu. Rev. Ecol. Syst. **33**(1): 341–370. doi:10.1146/annurev.ecolsys.33.010802.150519.

Walline, P.D., Pisanty, S., and Lindem, T. 1992. Acoustic assessment of the number of pelagic fish in Lake Kinneret, Israel. Hydrobiologia, **231**(3): 153–163. doi:10.1007/BF00018199.

Ward, A.J., Webster, M.M., and Hart, P.J. 2006. Intraspecific food competition in fishes. Fish Fish. **7**: 231–261.

Werner, F.E., Perry, R.I., Lough, R.G., and Naimie, C.E. 1996. Trophodynamic and advective influences on Georges Bank larval cod and haddock. Deep Sea Res. Part II Top. Stud. Oceanogr. **43**(7–8): 1793–1822. doi:10.1016/S0967-0645(96)00042-2.

Wu, L., Xie, P., Dai, M., and Wang, J. 1997. Effects of silver carp density on zooplankton and water quality: implications for eutrophic lakes in China. J. Freshw. Ecol. **12**(3): 437–444. doi:10.1080/02705060.1997.9663554.

Yacobi, Y.Z., Kalikhman, I., Gophen, M., and Walline, P. 1993. The spatial distribution of temperature, oxygen, plankton and fish determined simultaneously in Lake Kinneret, Israel. J. Plankton Res. **15**(6): 589–601. doi:10.1093/plankt/15.6.589.

Yaron, Z., Cocos, M., and Salzer, H. 1980. Effects of temperature and photopheriod on ovarian recrudescence in the cyprinid fish *Mirogrex terrae-sanctae*. J. Fish Biol. **16**(4): 371–382. doi:10.1111/j.1095-8649.1980.tb03715.x.

Yashouv, A., and Berner, E. 1960. The growth rate of several unusually large specimens of *Acanthobrama terraesanctae* (Steinitz) in Lake Tiberias. Fish Bull. **3**: 20–22.

Yeates, P.S., and Imberger, J. 2003. Pseudo two-dimensional simulations of internal and boundary fluxes in stratified lakes and reservoirs. International Journal of River Basin Management, **1**(4): 297–319. doi:10.1080/15715124.2003.9635214.

Zhou, A., Xie, S., Lei, W., Zhu, X., and Yang, Y. 2005. A bioenergetic model to estimate feed requirement of gibel carp, *Carassius auratus gibelio*. Aquaculture, **248**(1–4): 287–297. doi:10.1016/j.aquaculture.2005.03.011.

Zohary, T. 2004. Changes to the phytoplankton assemblage of Lake Kinneret after decades of a predictable, repetitive pattern. Freshw. Biol. **49**(10): 1355–1371. doi:10.1111/j.1365-2427.2004.01271.x.

Zohary, T. 2006. Monitoring. Israel Oceanographic and Limnological Research (IOLR) Rep. T5/2006. Yigal Alon Kinneret Limnological Laboratory, IOLR, Tiberias, Israel. pp. V–VI.

Zohary, T., Erez, J., Gophen, M., Berman-Frank, I., and Stiller, M. 1994. Seasonality of stable carbon isotopes within Lake Kinneret food web. Limnol. Oceanogr. **39**: 1030–1043. doi:10.4319/lo.1994.39.5.1030.

Appendices A and B appear on the following pages.

Appendix A

Table A1. List of parameter changes in DYCD 3.3.

Parameter	Description	Unit	Previous value	Assigned value
μ_{MAX}	Maximum potential growth rate for FDIAT	day^{-1}	3.6	3
I_S	Light saturation for maximum production for FDIAT	$\mu E{\cdot}m^{-2}{\cdot}s^{-1}$	200	20
K_N	Half saturation constant for nitrogen uptake for FDIAT	$g\ N{\cdot}m^{-3}$	0.05	0.15
UN_{MAX}	Maximum rate of nitrogen uptake for FDIAT	$g\ N{\cdot}g\ C^{-1}{\cdot}day^{-1}$	0.15	0.1
Smp_{NH4}	Release rate of NH_4 from sediments at 20 °C	$g\ NH_4{\cdot}m^{-2}{\cdot}day^{-1}$	0.09	0.06
K_{DN2}	Denitrification rate coefficient	day^{-1}	0.04	0.03
K_{N2}	Half saturation constant for denitrification	$g\ N{\cdot}m^{-3}$	0.4	0.5
d_{POM}	Diameter of POM particles	m	$5.00{\times}10^{-6}$	$5.5{\times}10^{-6}$
μ_{DECPON}	Maximum rate of PON decomposition to DON at 20 °C	day^{-1}	0.005	0.01
μ_{DECPOP}	Maximum rate of POP decomposition to DOP at 20 °C	day^{-1}	0.03	0.1
S_{mpDONL}	Release rate of DONL	$g\ N{\cdot}m^{-2}{\cdot}day^{-1}$	0.001	−0.01
Z_{Dm}	Z3 Mortality rate coefficient	day^{-1}	0.07	0.15
Z_{Dr}	Z3 Respiration rate coefficient	day^{-1}	0.08	0.1
g_{MAX}	Z1 Grazing rate	$g\ C{\cdot}m^{-3}{\cdot}(g\ Z{\cdot}m^{-3})^{-1}{\cdot}day^{-1}$	2.032	3.032
K_{Dm}	Z1 Mortality rate coefficient	day^{-1}	0.02	0.04
g_{MAX}	Z3 Grazing rate	$g\ C{\cdot}m^{-3}{\cdot}(g\ Z{\cdot}m^{-3})^{-1}{\cdot}day^{-1}$	10	9
Min_{res}	Minimum grazing limit	$g\ C{\cdot}m^{-3}$	0.05	0.03

Note: FDIAT, diatom (*Aulacoseira granulata*); POM, particulate organic matter; PON, particulate organic nitrogen; DON, dissolved organic nitrogen; POP, particulate organic phosphorus; DOP, dissolved organic phosphorus; DONL, dissolved organic nitrogen concentration.

Appendix B

Table B1. Parameter values and initial conditions used in the lavnun bioenergetics-based fish population model.

	Description	Values for age group < 1 year	Values for age group ≥ 1 year
Parameter			
Consumption			
a_C	Intercept for C_{max} at (te1 + te3)/2	0.28	0.28[a]
b_C	coefficient for C_{max} vs. weight	–0.33	–0.33[b]
V_1	Vulnerability of predatory zooplankton (dimensionless)	0.05	0.4[c]
V_{12}	Vulnerability of herbivore zooplankton (dimensionless)	0.1	0.5[c]
V_{13}	Vulnerability of microzooplankton (dimensionless)	0.01	0.02[c]
V_{14}	Vulnerability of POM (dimensionless)	0.01	0.05
K_{11}	Half saturation constant for predatory zooplankton ($mg_{prey} \cdot L^{-1}$)	0.75	0.45
K_{12}	Half saturation constant for herbivorous zooplankton ($mg_{prey} \cdot L^{-1}$)	0.45	0.4
K_{13}	Half saturation constant for microzooplankton ($mg_{prey} \cdot L^{-1}$)	0.1	0.5
K_{14}	Half saturation constant for POM ($mg_{prey} \cdot L^{-1}$)	0.5	0.05
Temperature function for consumption [d]			
te1	Temperature for Xk1 (°C)	8[e]	
te2	Temperature for Xk2 (°C)	18[f]	
te3	Temperature for Xk3 (°C)	26[g]	
te4	Temperature for Xk4 (°C)	32[h]	
Xk1	Proportion of C_{max} at te1	0.5[g]	
Xk2	Proportion of C_{max} at te2	0.98[g]	
Xk3	Proportion of C_{max} at te3	0.98[g]	
Xk4	Proportion of C_{max} at te4	0.1[g]	
Respiration			
a_R	Intercept for R	0.024[i]	0.012[j]
b_R	Coefficient for R versus weight	–0.007[k]	–0.227[j]
c_R	Coefficient for R versus temperature	0.03	0.02[g]
d_R	Coefficient for R versus swimming speed	0[g]	0.026[g]
Swimming speed, U			
a_A	Intercept U ($cm \cdot s^{-1}$)	1[k]	12.3[g]
b_A	Coefficient U vs. weight	0[g]	0.27
c_A	Coefficient U vs. temperature	0[g]	0
Specific dynamic action			
S_{cal}	Coefficient for specific dynamic action	0.125	0.175[l]
Excretion and egestion			
a_f	Proportion of consumed food egested	0.1[m]	0.12[n]
a_e	Proportion of consumed food excreted	0.18	0.16[o]
Reproduction [d]			
a_{rep1}	Proportion of consumed food used for reproduction in age 0+	0	
a_{rep2}	Proportion of consumed food used for reproduction in age 1+	0.1	
a_{rep}	Proportion of consumed food used for reproduction for fish at age 1.5+	0.25[p]	
W–L relationship [d]			
a	Range for "a" parameters of the W–L equation	2.46×10^{-3} to 3.14×10^{-3}[q]	
b	Range for "b" parameters of the W–L equation	34.258×10^{-1} to 34.342×10^{-1}[q]	
Location function (L) [d]			
Temperature function for location			
L_{te1}	Temperature for L_{XK1} (°C)	12.00[r]	
L_{te2}	Temperature for L_{XK2} (°C)	20.0[g]	
L_{te3}	Temperature for L_{XK3} (°C)	25.00[g]	
L_{te4}	Temperature for L_{XK4} (°C)	31.00[g]	
L_{XK1}	Temperature function at L_{te1}	0.1[s]	
L_{XK2}	Temperature function at L_{te2}	0.98[s]	
L_{XK3}	Temperature function at L_{te3}	0.98[s]	
L_{XK4}	Temperature function at L_{te4}	0.01[s]	

Table B1 (*concluded*).

	Description	Values for age group < 1 year	Values for age group ≥ 1 year
Light function for location [d]			
L_{lte1}	Light for L_{CXA1} (µE)		15.00
L_{lte2}	Light for L_{CXA2} (µE)		120.0
L_{lte3}	Light for L_{CXA3} (µE)		1200.0
L_{lte4}	Light for L_{CXA4} (µE)		1400.0
L_{CXA1}	Value of light function at L_{lte1}		0.1
L_{CXA2}	Value of light function at L_{lte2}		0.98
L_{CXA3}	Value of light function at L_{lte3}		0.98
L_{CXA4}	Value of light function at L_{lte4}		0.1
Mortality [d]			
k_{Mcom}	Natural mortality for commercial fish (%·year^{-1})		0.5[q]
k_{Mncom}	Natural mortality for noncommercial fish (%·year^{-1})		0.5[q]
k_{Fcom}	Fishing mortality of commercial fish (%·year^{-1})		0.28[q]
k_{Fncom}	Fishing mortality of noncommercial fish (%·year^{-1})		0
k_{rep}	Ratio of reproducing (mature) fish		0.2
List of coefficients and initial conditions			
Dep_{max}	The maximum depth (m) of the lake of the last 14 days before the beginning of the simulation (15 Dec. 1996 to 1 Jan. 1997)[r]	40.91, 40.90, 40.90, 40.90, 40.90, 40.91, 40.92, 40.92, 40.92, 40.92, 40.92, 40.92, 40.92, 40.92	
W_{int}	Wet weight at the first day of simulation (g)		0.26×10^{-3}[q]
N_{rep}	Number of fish that each simulated fish represents		10^{5}[s]
COM_{size}	Wet weight at commercial size (g)		14[q]
$F_{C:N:P}$	C:N:P as percentage of dry weight for fish (%)		46%, 9.7%, 1.5%[t]
$CAL_{zoop}\cdot CAL_{fish}^{-1}$	Caloric equivalence of prey food to fish		0.333[q]
$DW\cdot WW_{zoop}^{-1}$	Wet weight to dry weight conversion factor for zooplankton		0.05[m]
$DW\cdot WW_{fish}^{-1}$	Wet weight to dry weight conversion factor for fish		0.15
$DW\cdot WW_{pom}^{-1}$	Wet weight to dry weight conversion factor for POM		1
O_{conv}	Converts g O_2·g $_{fish}^{-1}$·day^{-1} into g_{prey}·g $_{fish}^{-1}$·day^{-1}		0.59[j]
$C–O_{conv}$	Converts grams carbon into grams oxygen		2.6
X_1	Coefficient for recruitment function *f*(*d*)		2.91×10^{-4}[u]
Y_1	Coefficient for recruitment function *f*(*d*)		0.213[u]
Z_1	Coefficient for recruitment function *f*(*d*)		38.5[u]
X_2	Coefficient for recruitment function *f*(*d*)		-4.72×10^{-6}[u]
Y_2	Coefficient for recruitment function *f*(*d*)		0.0379[u]
Z_2	Coefficient for recruitment function *f*(*d*)		0.236 [v]
A	Coefficient for water level function *f*(WL)		0.097 [v]
B	Coefficient for water level function *f*(WL)		0.624[v]

[a] Walline et al. (2000): 0.36; Ito et al. (2004): 0.6.

[b] Ito et al. (2004): –0.34; Walline et al. (2000): –0.31.

[c] Komarovsky (1952).

[d] Values for all age groups.

[e] Ito et al. (2004): 5.

[f] Ito et al. (2004): 16–20.

[g] Ito et al. (2004).

[h] Ito et al. (2004): 30.

[i] Ito et al. (2004): 0.0033.

[j] Hölker and Haertel (2004): 0.0019.

[k] Megrey et al. (2007).

[l] Hölker and Haertel (2004): –0.25.

[m] Gophen and Threlkeld (1989).

[n] Ito et al. (2004): 0.16.

[o] Ito et al. (2004): 0.1.

[p] Megrey et al. (2007); Ito et al. (2004): 0.35.

[q] Ostrovsky and Walline (1999).

[r] Kinneret Limnological Laboratory database.

[s] Walline et al. (1992).

[t] Sterner and George (2000).

[u] Gal et al. (2009).

[v] Estimated according to Gafny et al. (1992) and Gasith and Gafny (1990).

References

Gafny, S., Gasith, A., and Goren, M. 1992. Effect of water level fluctuations on shore spawning of *Mirogrex terraesanctae* (Steinitz), (Cyprinidae) in Lake Kinneret, Israel. J. Fish Biol. **41**(6): 863–871. doi:10.1111/j.1095-8649.1992.tb02715.x.

Gal, G., Hipsey, M.R., Parparov, A., Wagner, U., Makler, V., and Zohary, T. 2009. Implementation of ecological modeling as an effective management and investigation tool: Lake Kinneret as a case study. Ecol. Model. **220**: 1697–1718. doi:10.1016/j.ecolmodel.2009.04.010.

Gasith, A., and Gafny, S. 1990. Effects of water level fluctuation on the structure and function of the littoral zone. *In* Large lakes, ecological structure and function. *Edited by* M.M. Tilzer and C. Serruya. Springer-Verlag, Berlin. pp. 156–171.

Gophen, M., and Threlkeld, S. 1989. An experimental study of zooplankton consumption by the Lake Kinneret sardine. Arch. Hydrobiol. **115**: 91–95.

Hölker, F., and Haertel, S.S. 2004. Application of a bioenergetics model to roach. J. Appl. Ichthyology, **20**(6): 548–550. doi:10.1111/j.1439-0426.2004.00586.x.

Ito, S., Kishi, M.J., Kurita, Y., Oozeki, Y., Yamanaka, Y., Megrey, B.A., and Werner, F.E. 2004. Initial design for a fish bioenergetics model of Pacific saury coupled to a lower trophic ecosystem model. Fish. Oceanogr. **13**(suppl. 1): 111–124. doi:10.1111/j.1365-2419.2004.00307.x.

Komarovsky, B. 1952. An analysis of the stomach contents of *Acanthobrama terraesanctae* from Lake Tiberius. Bulletin of Sea Fisheries Research Station, Caesaria, **4**: 1–8.

Megrey, B.A., Rose, K.A., Klumb, R.A., Hay, D.E., Werner, F.E., Eslinger, D.L., and Smith, S.L. 2007. A bioenergetics-based population dynamics model of Pacific herring (*Clupea harengus pallasii*) coupled to a lower trophic level nutrient–phytoplankton–zooplankton model: description, calibration and sensitivity analysis. Ecol. Model. **202**(1–2): 144–164. doi:10.1016/j.ecolmodel.2006.08.020.

Ostrovsky, I., and Walline, P. 1999. Growth and production of the dominant pelagic fish, *Acanthobrama terraesanctae*, in subtropical Lake Kinneret, Israel. J. Fish Biol. **54**(1): 18–32. doi:10.1111/j.1095-8649.1999.tb00609.x.

Sterner, R.W., and George, N.B. 2000. Carbon, nitrogen and phosphorus stoichiometry of cyprinid fishes. Ecology, **81**(1): 127–140. doi:10.1890/0012-9658(2000)081[0127:CNAPSO]2.0.CO;2.

Walline, P.D., Pisanty, S., and Lindem, T. 1992. Acoustic assessment of the number of pelagic fish in Lake Kinneret, Israel. Hydrobiologia, **231**(3): 153–163. doi:10.1007/BF00018199.

Walline, P.D., Tyler, J.A., Brandt, S.B., Ostrovsky, I., and Jech, J.M. 2000. Lavnun abundance: how changes may affect consumption of Lake Kinneret zooplankton. Archiv fur Hydrobiologie, **55**: 493–511.

A state–space multistage life cycle model to evaluate population impacts in the presence of density dependence: illustrated with application to delta smelt (*Hyposmesus transpacificus*)

Mark N. Maunder and Richard B. Deriso

Abstract: Multiple factors acting on different life stages influence population dynamics and complicate the assessment and management of populations. To provide appropriate management advice, the data should be used to determine which factors are important and what life stages they impact. It is also important to consider density dependence because it can modify the impact of some factors. We develop a state–space multistage life cycle model that allows for density dependence and environmental factors to impact different life stages. Models are ranked using a two-covariates-at-a-time stepwise procedure based on AIC$_c$ model averaging to reduce the possibility of excluding factors that are detectable in combination, but not alone. Impact analysis is used to evaluate the impact of factors on the population. The framework is illustrated by application to delta smelt (*Hyposmesus transpacificus*), a threatened species that is potentially impacted by multiple anthropogenic factors. Our results indicate that density dependence and a few key factors impact the delta smelt population. Temperature, prey, and predators dominated the factors supported by the data and operated on different life stages. The included factors explain the recent declines in delta smelt abundance and may provide insight into the cause of the pelagic species decline in the San Francisco Estuary.

Résumé : Les multiples facteurs qui agissent sur les différents stades du cycle biologique influencent la dynamique des populations et compliquent l'évaluation et la gestion des populations. Afin de fournir des avis de gestion appropriés, il faut utiliser les données pour déterminer quels facteurs sont importants et quels stades du cycle ils affectent. Il est aussi important de considérer la densité dépendance, car elle peut modifier l'impact de certains facteurs. Nous mettons au point un type de modèle état–espace à stades de vie multiples qui tient compte de l'impact de la densité dépendance et des facteurs du milieu sur les différents stades de vie. Les modèles sont placés par ordre à l'aide d'une procédure pas-à-pas de deux covariables à la fois basée sur l'établissement de la moyenne des modèles de type AIC$_c$ afin de réduire la possibilité d'exclure des facteurs décelables en combinaison, mais non isolément. Une analyse d'impacts sert à évaluer les effets des facteurs sur la population. Nous illustrons ce cadre d'analyse en l'appliquant à l'éperlan du delta (*Hyposmesus transpacificus*), une espèce menacée qui est potentiellement affectée par de multiples facteurs anthropiques. Nos résultats montrent que la densité dépendance et quelques facteurs clés affectent la population d'éperlans du delta. La température, les proies et les prédateurs dominent parmi les facteurs révélés par les données et ils agissent sur différents stades de vie. Les facteurs retenus expliquent les déclins récents de l'abondance de l'éperlan du delta et peuvent fournir une perspective sur la cause de la diminution des espèces pélagiques dans l'estuaire de San Francisco.

[Traduit par la Rédaction]

Introduction

Multiple factors acting on different life stages influence population dynamics and complicate the assessment and management of natural populations. To provide appropriate management advice, the available data should be used to determine which factors are important and what life stages they impact. It is also important to consider density-dependent processes because they can modify the impact of some factors, and the strength of density dependence can vary among life stages (Rose et al. 2001). Management can then better target limited resources to actions that are most effective. Unfortunately, the relationships among potential factors, the life stages that they influence, and density dependence are often difficult to piece together through standard correlation or linear regression analyses.

Received 11 April 2011. Accepted 28 April 2011. Published at www.nrcresearchpress.com/cjfas on 11 July 2011.
J2011-0122

Paper handled by Associate Editor Carl Waters.

M.N. Maunder. Quantitative Resource Assessment LLC, San Diego, CA 92129, USA; Inter-American Tropical Tuna Commission, 8604 La Jolla Shores Drive, La Jolla, CA 92037-1508, USA.
R.B. Deriso. Inter-American Tropical Tuna Commission, 8604 La Jolla Shores Drive, La Jolla, CA 92037-1508, USA.

Corresponding author: Mark N. Maunder (e-mail: mmaunder@iattc.org).

Can. J. Fish. Aquat. Sci. **68**: 1285–1306 (2011) doi:10.1139/F2011-071 Published by NRC Research Press

Life cycle models are an essential tool in evaluating factors influencing populations of management concern (Buckland et al. 2007). They can evaluate multiple factors that simultaneously influence different stages in the presence of density dependence. They also link the population dynamics from one time period to the next propagating the information and uncertainty. This link allows information relating to one life stage (i.e., abundance estimates) to inform processes influencing other life stages and is particularly important when data is not available for all life stages for all time periods. The life cycle model should be fit to the available data to estimate the model parameters, including parameters that represent density dependence, and determine the data-based evidence of the different factors that are thought to influence the population dynamics. Finally, the model should be used to direct research or provide management advice.

Deriso et al. (2008) present a framework for evaluating alternative factors influencing the dynamics of a population. It extends earlier work by Maunder and Watters (2003), Maunder and Deriso (2003), and Maunder (2004) and is similar to approaches taken by others (e.g., Besbeas et al. 2002; Clark and Bjornstad 2004; Newman et al. 2006). The Deriso et al. framework involves several components. First, the factors to be considered are identified. Second, the population dynamics model is developed to include these factors and then fitted to the data. Third, hypothesis tests are performed to determine which factors are important. Finally, to provide management advice, the impact of the factors on quantities of management interest, are assessed. They illustrate their framework using an age-structured fisheries stock assessment model fit to multiple data sets. Their application did not allow for density dependence in the population dynamics, except through the effect of density on the temporal variation in which ages are available to the fishery.

Inclusion of density dependence is important in evaluating the impacts on populations. Without density dependence, modeled populations can increase exponentially. This is unrealistic and can also cause computational or convergence problems in fitting population dynamics models to data. Density dependence can also moderate the effects of covariates. This is important because factors affecting density-independent survival may be much less influential in the presence of density dependence compared with factors that affect carrying capacity (e.g., habitat). It is also important to correctly identify the timing of when the factors influence the population with respect to the timing of density dependence processes and available data. The approach also provides a framework for amalgamating the two paradigms of investigating population regulation outlined by Krebs (2002): the density paradigm and the mechanistic paradigm.

Here we develop a life cycle model that allows for density dependence at multiple life stages and allows for factors to impact different life stages. We apply the framework of Deriso et al. (2008) where the first component also includes identifying the life stages that are impacted by each factor and where density dependence occurs. We illustrate the framework by applying it to delta smelt (*Hyposmesus transpacificus*). Delta smelt is an ideal candidate to illustrate the modeling approach because there are several long-term abundance time series for different life stages and a range of hypothesized factors influencing its survival for which covariate data is available. Life cycle models have been recommended to evaluate the factors effecting delta smelt (Bennett 2005; Mac Nally et al. 2010; Thomson et al. 2010).

Delta smelt is of particular management concern because of declines in abundance and the myriad of anthropogenic factors that could be causing the decline. Delta smelt is endemic to the San Francisco Estuary, which has multiple stressors, including habitat modification, sewage outflow, farm runoff, and water diversions, to name just a few. Delta smelt was listed as threatened under the US and California Endangered Species Acts in 1993. Several other pelagic species in the San Francisco Estuary have also experienced declines, but the factors causing the declines are still uncertain (Bennett 2005; Sommer et al. 2007). Recent studies have investigated the factors hypothesized to have caused the declines at both the species and ecosystem level, but the results were not conclusive (Mac Nally et al. 2010; Thomson et al. 2010).

Materials and methods

Model

The model is stage-based with consecutive stages being related through a function that incorporates density dependence. For simplicity and to be consistent with the predominant dynamics of delta smelt, we assume an annual life cycle. However, it is straightforward to extend the model to a multiple year life cycle or to stages that cover multiple years (i.e., adding age structure; e.g., Rivot et al. 2004; Newman and Lindley 2006). Within a year the number of individuals in each stage is a function of the numbers in the previous stage. The number of individuals in the first stage is a function of the numbers in the last stage in the previous year (i.e., the stock–recruitment relationship), except for the numbers in the first stage in the first year, which is estimated as a model parameter. The functions describing the transition from one stage to the next are modeled using covariates. A state–space model (Newman 1998; Buckland et al. 2004, 2007) is used to allow for annual variability in the equation describing the transition from one life stage to the next. Traditionally, state–space models describe demographic variability (e.g., using a binomial probability distribution to represent the number of individuals surviving based on a given survival rate; e.g., Dupont 1983; Besbeas et al. 2002); however, environmental variability generally overwhelms demographic variability (Buckland et al. 2007) so we model the process variability (e.g., Rivot et al. 2004; Newman and Lindley 2006) using a lognormal probability distribution (Maunder and Deriso 2003). Our approach differs from modeling the log abundance and assuming additive normal process variability (e.g., Quinn and Deriso 1999, page 103), and the population dynamics function models the expected value rather than the median. The difference in the expectation will simply be a scaling factor ($\exp(-0.5\sigma^2)$) unless the variance of the process variability changes with time.

$$(1) \qquad N_{t,s} \sim \mathrm{Lognormal}\left[f(N_{t,s-1}), \sigma^2_{s-1}\right]; \qquad s > 1$$

$$(2) \qquad N_{t,1} \sim \mathrm{Lognormal}\left[f(N_{t-1,\mathrm{nstages}}), \sigma^2_{\mathrm{nstages}}\right]$$

where t is time, s is stage, nstages is the number of stages in the model, and σ_s is the standard deviation of the variation not explained by the model (process variability) in the transition from stage s to the next stage.

The three-parameter Deriso–Schnute stock–recruitment model (Deriso 1980; Schnute 1985) is used to model the transition from one stage to the next. The Deriso–Schnute model is a flexible stock-recruitment curve in which the third parameter (γ) can be set to represent the Beverton–Holt ($\gamma = -1$) and Ricker ($\gamma \to 0$) stock–recruitment models (Quinn and Deriso 1999, page 95).

$$(3) \qquad f(N) = aN(1 - b\gamma N)^{\frac{1}{\gamma}}$$

where the parameter a can be interpreted as the number of recruits per spawner at low spawner abundance or the survival fraction at low abundance levels. In cases for which only the relative abundance at each stage can be modeled (as in the delta smelt example), a also contains a scaling factor from one survey to the next. The parameter b determines how the number of recruits per spawner or the survival rate decreases with abundance. Constraints can be applied to the parameters to keep the relationship realistic: $a \geq 0$, $b \geq 0$. The additional constraint $a \leq 1$ can be applied when the relationship is used to describe survival and the consecutive stages are modeled in the same units.

Covariates are implemented to influence the abundance either before density dependence ($g(N,x)$) or after density dependence ($h(x)$). Although, when no density dependence is present, the two methods are identical.

$$(4) \qquad f(N) = ag(N,x)[1 - b\gamma g(N,x)]^{\frac{1}{\gamma}}h(x)$$

$$(5) \qquad g(N,x) = N\exp\left(\sum \lambda x\right)$$

$$(6) \qquad h(x) = \exp\left(\sum \beta x\right)$$

where λ and β are the coefficients of the covariate (x) for before and after density dependence, respectively, and are estimated as model parameters.

For survival it might be important to keep the impact of the environmental factors within the range 0 to 1 and the logistic transformation can be used, e.g.,

$$(7) \qquad ag(N,x) = N\frac{\exp\left(a' + \sum \lambda x\right)}{1 + \exp\left(a' + \sum \lambda x\right)}$$

Where the parameter a' defines the base level of survival (i.e., $a = \frac{\exp(a')}{1+\exp(a')}$) and replaces a of the density dependence function.

If the covariate values are all positive, the negative exponential can be used, e.g.,

$$(8) \qquad g(N,x) = N\exp\left(-\sum \lambda x\right); \qquad \lambda \geq 0, \quad x \geq 0$$

A combination of the above three options may be appropriate depending on the application.

The importance of the placement of the covariates (i.e., before or after density dependence) relates to both the timing of density dependence and the timing of the surveys, which provide information on abundance. Covariates could be applied to the other model parameters. For example, covariates that are thought to be related to the carrying capacity (e.g., habitat) could be used to model b.

The model is fit to indices of abundance ($I_{t,s}$). The abundance indices are assumed to be normally distributed, but other sampling distributions could be assumed if appropriate. Typically, if the index of abundance is a relative index and not an estimate of the absolute abundance, the model is fit to the index by scaling the model's estimate of abundance using a proportionality constant (q, often called the catchability coefficient; Maunder and Starr 2003).

$$(9) \qquad I_{t,s} \sim \mathrm{Normal}(qN_{t,s}, v_{t,s}^2)$$

However, the scaling factor is completely confounded with the a parameter of the Deriso–Schnute model, and therefore the population is modeled in terms of relative abundance that is related to the scale of the abundance indices for each life stage and only makes sense in terms of total abundance if the abundance indices are also in terms of total abundance. Therefore, the proportionality constant (q) should be set to one. Other data could also be used in the analysis if appropriate (e.g., information on survival from mark–recapture studies; Besbeas et al. 2002; Maunder 2004).

Model parameters to estimate

The model parameters estimated include the initial abundance of the first stage $N_{1,1}$; the parameters of the stock–recruitment model for each stage $\boldsymbol{a}$, $\boldsymbol{b}$, $\boldsymbol{\gamma}$; the coefficients of the covariates $\boldsymbol{\lambda}$, $\boldsymbol{\beta}$; the standard deviation of the process variability for each stage $\boldsymbol{\sigma}$; and the standard deviation of the observation error (used in defining the likelihood function) for each index of abundance $\boldsymbol{v}$. The observation error standard deviation, $\boldsymbol{v}$, is often fixed based on the survey design or restricted so that there is not a parameter to estimate for each survey and time period (e.g., Maunder and Starr 2003). The state–space model can be implemented by treating the process variability as random effect parameters (de Valpine 2002). The likelihood function that is optimized is calculated by integrating over these parameters (Skaug 2002; Maunder and Deriso 2003). Therefore, they are not treated as parameters to estimate. However, realizations of the random effects can be estimated by using empirical Bayes methods (Skaug and Fournier 2006), so that the unexplained process variation can be visualized. The estimated parameters of the model are $N_{1,1}$, $\boldsymbol{a}$, $\boldsymbol{b}$, $\boldsymbol{\gamma}$, $\boldsymbol{\lambda}$, $\boldsymbol{\beta}$, $\boldsymbol{\sigma}$, and $\boldsymbol{v}$.

Implementation in AD Model Builder

Dynamic models like the multistage life cycle model described here can be computationally burdensome if they are carried out in a state–space modeling framework (i.e., integrating over the state–space or equivalently the process variability), and efficient parameter estimation is needed if multiple hypotheses are being tested. Implementation is facilitated by the use of Markov chain Monte Carlo and related methods (Newman et al. 2009), and their use has increased in recent years (Lunn et al. 2009). In particular, authors have found a Bayesian framework convenient for implementation (Punt and Hilborn 1997). An alternative approach is to use the Laplace approximation to implement the integration (Skaug 2002). AD Model Builder (ADMB; http://admb-project.org/) has an efficient implementation of the Laplace approximation using automatic differentiation (Skaug and Fournier 2006). The realizations of the random effects are estimated by using empirical Bayes methods adjusted for the uncertainty in the fixed effects (Skaug and Fournier 2006). ADMB was originally designed as a function minimizer, and therefore likelihoods are implemented in terms of negative log-likelihoods, and probability distributions are implemented in terms of negative log-probabilities. A more complete description of ADMB and its implementation of random effects can be found at http://admb-project.org/.

The population is modeled using random effects to implement the state–space model (de Valpine 2002):

$$(10)\qquad N_{i,s} = f(N_{i,s-1})\exp\left(\sigma_{s-1}\varepsilon_{i,s-1} - 0.5\sigma_{s-1}^2\right)$$

$$(11)\qquad N_{i,1} = f(N_{i-1,\text{nstages}}) \times \exp\left(\sigma_{\text{nstages}}\varepsilon_{i-1,\text{nstages}} - 0.5\sigma_{\text{nstages}}^2\right)$$

$$(12)\qquad \varepsilon_{i,s} \sim N(0, 1)$$

A penalty is added to the objective function to implement the random effects

$$(13)\qquad 0.5\sum_{i,s}\varepsilon_{i,s}^2$$

The negative log-likelihood function for the abundance indices ignoring constants is

$$(14)\qquad -\ln(L) = \sum_{i,s}\ln(v_{i,s}) + \frac{(I_{i,s} - qN_{i,s})^2}{2v_{i,s}^2}$$

Model selection

Model selection (Hilborn and Mangel 1997) can be used to determine if the data supports density dependence for a particular stage or the factors that impact the population dynamics. In our analysis different models are represented by different values of the model parameters. The relationship between one stage and the next is density independent if $b = 0$. Therefore, a test for density dependence tests whether $b = 0$. When $b = 0$, γ has no influence on the results, and unless a hypothesis about γ is made (i.e., Beverton–Holt, $\gamma = -1$; or Ricker, $\gamma \rightarrow 0$), testing between density independence and density dependence requires the estimation of two additional parameters (b, γ). A factor has no influence on the model when its coefficient (λ, β) is fixed at zero. Therefore, testing a factor requires estimating one parameter for each factor tested. There are a variety of methods available for model selection and hypothesis testing, each with their own set of issues (e.g., Burnham and Anderson 1998; Hobbs and Hilborn 2006). Given these issues, we rely on Akaike information criterion adjusted for sample size (AIC$_c$) and AIC$_c$ weights to rank models and provide an idea of the strength of evidence in the data about an a priori set of alternative hypotheses (factors), but they are not used as strict hypothesis tests (Anderson et al. 2000; Hobbs and Hilborn 2006).

The AIC$_c$ is useful for ranking alternative hypotheses when multiple covariates and density dependence assumptions are being considered. The AIC$_c$ (Burnham and Anderson 2002) is given by

$$(15)\qquad \text{AIC}_c = -2\ln L + 2K + \frac{2K(K+1)}{n-K-1}$$

where L is the likelihood function evaluated at its maximum, K is the number of parameters, and n is the number of observations. A better model fit is one with a smaller AIC$_c$ score.

AIC$_c$ weights are often used to provide a measure of the relative support for a model and to conduct model averaging (Hobbs and Hilborn 2006). AIC$_c$ weights are essentially the rescaled likelihood penalized by the number of parameters, which is considered the likelihood for the model (Anderson et al. 2000).

$$(16)\qquad w_i = \frac{\exp(-0.5\Delta_i)}{\sum_j \exp(-0.5\Delta_j)}$$

where Δ is the difference in the AIC$_c$ score from the minimum AIC$_c$ score.

The correct modeling of observation and process variability (error) is important for hypothesis testing. If process variability is not modeled, likelihood ratio and AIC-based tests are biased towards incorrectly accepting covariates (Maunder and Watters 2003). Other tests, such as randomization tests, should be used if it is not possible to model the additional process variability (e.g., Deriso et al. 2008). Incorrect sampling distribution assumptions (e.g., assumed values for the variance) can influence the covariate selection process, and the weighting given to each data set can change which covariates are chosen (Deriso et al. 2007). If data-based estimates of the variance are not available, estimating the variances as model parameters or using concentrated likelihoods is appropriate (Deriso et al. 2007). Missing covariate data need to be dealt with appropriately, such as by using the methods described in Gimenez et al. (2009) and Maunder and Deriso (2010).

Parameter estimation of population dynamics models generally requires iterative methods, which take longer than calculations based on algebraic solutions, and therefore limit the number of models that can be tested (Maunder et al. 2009). This is problematic when testing hypotheses because, arguably, all possible combinations of the covariates and density-dependent possibilities should be evaluated. All possible combinations should be used because a covariate by itself may not significantly explain process variation, but in combination they do (Deriso et al. 2008), and some covariates may only be significant if density dependence is taken into consideration. However, modeling of process variability, as we suggest, may minimize this possibility. In many cases, time and computational resource limitations may prevent testing all possible combinations, and therefore we suggest the strategy described in Table 1.

We stop evaluating covariates when the lowest AIC$_c$ model in the current iteration is at least four AIC$_c$ units higher than the model with the lowest overall AIC$_c$ (step 2e). The approach is based on a compromise between eliminating models for which there is definite, strong, or very strong evidence that the model is not the Kullback–Leibler (K–L) best model ($4 \leq \Delta$) and the fact that there is a maximum Δ when adding

Table 1. Algorithm for evaluating covariates for the delta smelt (*Hypomesus transpacificus*) application.

1	Evaluate density dependence.
(a)	Calculate all combinations of density-dependent processes without the inclusion of factors. Combinations include (*i*) density independent; (*ii*) Beverton–Holt; (*iii*) Ricker; and (*iv*) estimate both *b* and γ. These can be at any of the three stages.
(b)	Choose the density dependence combination that has the lowest AIC_c, or if there are several that have similar support, choose multiple combinations.
2	Evaluate covariates.
(a)	For each density dependence scenario chosen in 1b, run all possible one- and two-covariate combinations.
(b)	For each combination, set the AIC_c weight to zero if the sign is wrong for either of the coefficients in the combination or if the *b* parameter of a density dependence function is unrealistically high.
(c)	Sum AIC_c weights for a given covariate across all models that include that covariate.
(d)	Select the two covariates with the highest summed AIC_c weights to retain for the next iteration.
(e)	Iterate *a*–*d* until the AIC_c value of the best model in the current iteration is more than four units higher than the lowest AIC_c model.
3	Double check all included covariates.
(a)	Check confidence intervals of the estimated coefficients for all included covariates to see if they contain zero.
(b)	For all coefficients that contain zero, remove the associated covariate and see if the AIC_c is degraded. If the AIC_c is not degraded, exclude that covariate from the model.

covariates to the lowest AIC_c model. We have chosen to carry out the selection process by using the sum of the AIC_c weights over all models that include the corresponding factor (step 2d). This selection process chooses factors that have high support in general, work in combination with other factors, and are therefore less likely to preclude additional factors in subsequent steps. This approach embraces the multiple hypothesis weight of evidence framework and is somewhat consistent with model averaging. We also remove models for which any of the estimated covariate coefficients are the incorrect sign as assumed a priori (step 2b). Modification of this procedure may be needed depending on the available computational resources, the number of covariates and model stages, and the relative difference in the weight of evidence among models.

Burnham and Anderson (2002) note that in general, there are situations where choosing to make inferences using a model other than the lowest AIC_c model can be justified (their page 330) based on professional judgment, but only after the results of formal selection methods have been presented (their page 334). For example, model parameterizations that do not make sense biologically might be eliminated from consideration. Burnham and Anderson (2002) give an example (their page 197) where a quadratic model is rejected because it could not produce the monotonic increasing dose response that was desired. Sometimes AIC_c will select a model that fits to quirks or noise in the data but does not provide a useful model. The selected best model is a type of estimate, and so like a parameter estimate it can sometimes be a poor estimate (Ken Burnham, Colorado State University, Colorado Cooperative Fish and Wildlife Research Unit, Fort Collins, Colorado, personal communication, 2010).

Parameter estimates from stock–recruitment models in integrated assessments are often biased towards extremely strong density-dependent survival (recruitment is independent of stock size) (Conn et al. 2010), and this is unrealistic for stocks that have obtained very low population sizes. We therefore identify values of the Deriso–Shnute stock–recruitment relationship (for the Beverton–Holt and Ricker special cases) *b* parameter that are realistic (see Appendix A). We assume that recruitment (or the individuals surviving) cannot be greater than 80% of that expected from the average population size when the population is at 5% of the average population size seen in the surveys during the period studied. Models with unrealistic density dependence are given zero weight in that step of the model selection prodecure (step 2b).

Impact analysis

To determine the impact of the different factors on the stock, we conducted analyses using values of the covariates modified to represent a desired (e.g., null) effect. Following Deriso et al. (2008), these analyses were conducted simultaneously within the code of the original analyses so that the impact assessments shared all parameter values with the original analyses. This allowed estimation of uncertainty in the difference between the models with the covariate included and with the desired values of the covariate. The results are then compared for the quantities of interest, which may be a derived quantity other than the covariate's coefficients. For example, if a covariate is related to some form of mortality, the coefficient is set to zero to determine what the abundance would have been in the absence of that mortality (e.g., Wang et al. 2009).

Application to delta smelt

The multistage life cycle model is applied to delta smelt to illustrate the application of the model, covariate selection procedure, and impact analysis. Delta smelt effectively live for 1 year and one spawning season. Some adults do survive to spawn a second year, but the proportion is low (Bennett 2005) and we ignore them in this illustration of the modeling approach. The delta smelt life cycle is broken into three stages (Fig. 1). The model stages are associated with the timing of the three main surveys, (*i*) 20 mm trawl (20 mm), (*ii*) summer tow net (STN), and (*iii*) fall midwater tow (FMWT), and roughly correspond to the life stages larvae, juveniles, and adults, respectively. The reason for associating the model stages with the surveys is because the surveys are the only data used in the model, and therefore information is only available on processes operating between the surveys. The population is modeled from 1972 to 2006 because these are the years for which data for most of the factors are available. The STN abundance index is available for the whole

Fig. 1. Life cycle diagram of delta smelt (*Hypomesus transpacificus*) with survey, entrainment, and density dependence timing.

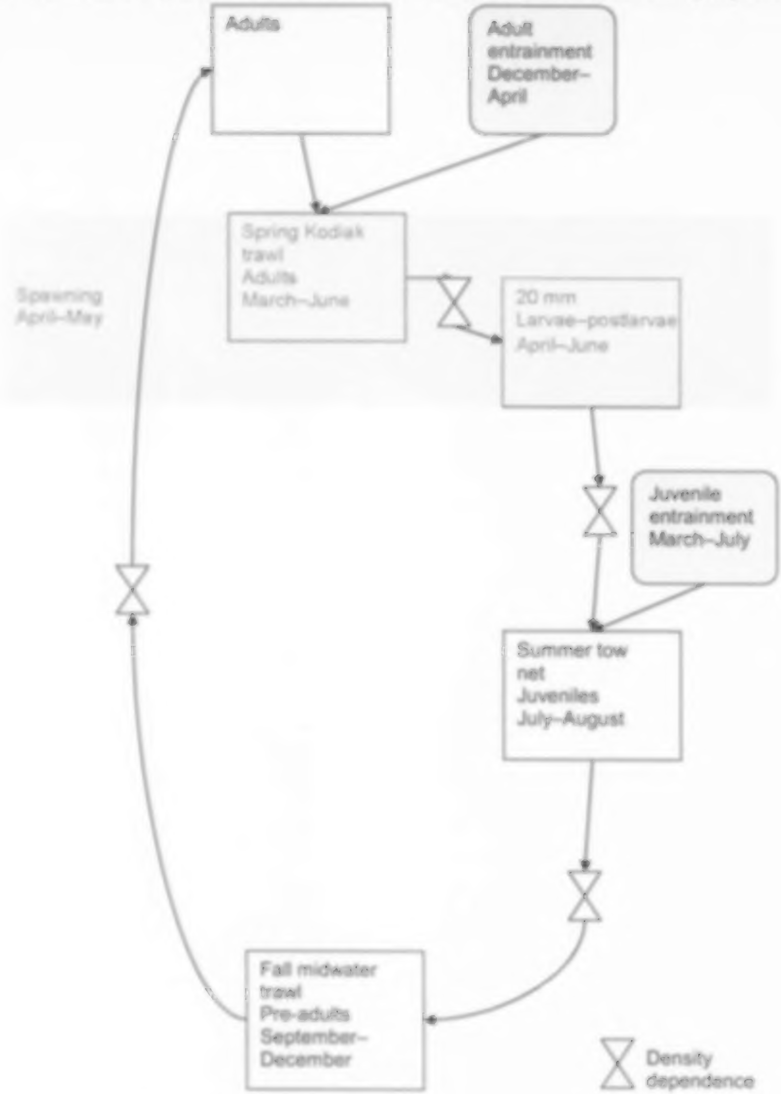
Adults
Adult entrainment December–April
Spring Kodiak trawl Adults March–June
Spawning April–May
20 mm Larvae–postlarvae April–June
Juvenile entrainment March–July
Summer tow net Juveniles July–August
Fall midwater trawl Pre-adults September–December
Density dependence

time period. The FMWT abundance index is available for the whole time period except for 1974 and 1979. The 20 mm abundance index is only available starting in 1995. Other survey data are available (e.g., the spring Kodiak trawl survey), but they are not used in this analysis.

The FMWT and STN survey indices of abundance are the estimates taken from Manly (2010*b*, tables 2.1 and 2.2). The standard errors were calculated by bootstrap procedures (Manly 2010*a*). The 20 mm survey index was taken from Nations (2007). The index values and standard errors are given in the supplementary material[1]. The results of the bootstrap analysis suggest that the abundance indices are normally distributed (Manly 2010*a*).

Two types of factors are used in the model (Table 2). The first are standard factors relating to environmental conditions. The second are mortality rates based on estimates of entrainment at the water pumps. The mortality rates are converted to the appropriate scale to use in the model. Let u represent the mortality fraction such that the survival fraction is $1 - \mu = \exp(\beta x)$, and x will be used as a covariate in the model. Setting $\beta = 1$ gives $x = \ln(1 - \mu)$.

Several factors were chosen for inclusion in the model (Table 3). These factors are used for illustrative purposes only, and they may differ in a more rigorous investigation of the factors influencing delta smelt. The environmental factors are taken as those proposed by Manly (2010*b*). The entrainment mortality rates are calculated based on Kimmerer (2008); the rates were obtained by fitting a piecewise linear

---

[1] Supplementary data are available with the article through the journal Web site (http://www.nrcresearchpress.com/cjfas).

Table 2. The variables used as candidates to account for the changes in delta smelt abundance.

Factor	Name	Covariate	Stage	Before–After	Sign	Description	Data scaling	Justification
1	SpDys	1	A	Before	+	Days where temperature is in the range 11–20 °C	Norm	This measures the number of days of spawning — the longer the spawning season, presumably the better chance of survival
2	TpAJ	2	L	Before	– or +	Average water temperature in delta smelt habitat for April–June	Norm	Temperature affects growth rate and survival of early life stages
3	TpAJ	2	A	After	– or +			
4	TpJul	3	L	After	–	Average water temperature in delta smelt habitat for July	Norm	Higher water temperatures can be lethal; could also include August temperature
5	EPAJ	4	L	Before	+	Minimum eurytemora and pseudadiaptomus density for April–June	Norm	Measures height of food "gap" in spring, as eurytemora falls from spring maximum and pseudodiaptomus rises from ~0
6	EPAJ	4	A	After	+			
7	EPJul	5	L	After	+	Average eurytemora and pseudodiaptomus density for July	Norm	Measures food availability in summer until summer tow net survey, identified as problem by Bennett (2005) based on smelt condition
8	Pred1	6	J	After	–	September–December abundance of other predators	Mean	Predation is a source of direct mortality, measured as the product of relative density from beach seine data with the square of average Secchi depth
9	Pred1	6	A	Before	–			
10	Pred1	6	A	After	–			
11	StBass	7	J	After	–	September–December abundance of striped bass	Mean	A major predator, whose abundance is measured as actual number of adults
12	StBass	7	A	Before	–			
13	StBass	7	A	After	–			
14	DSLth	8	L	After	+	Delta smelt average length	Norm	See Bennett (2005) for length vs. fecundity relationship, linear for 1-year-olds
15	DSLth	8	J	After	+			
16	DSLth	8	A	After	+			
17	TpJS	9	J	After	–	Maximum 2-week average temperature for July–September	Norm	Measure of whether lethal temperature is reached in hot months
18	EPJA	10	J	After	+	Average eurytemora and pseudodiaptomus density for July–August	Norm	Measures food availability in summer between STN and FMWT surveys, identified as problem by Bennett (2005) based on smelt condition
19	Secchi	11	A	Before	–	January–February weighted Secchi depth	Norm	Protection from predators
20	Secchi	11	A	After	–			
21	Jent	12	L	After	+[a]	Juvenile entrainment	Raw	Entrained in by water pumps
22	Aent	13	A	Before	+[a]	Adult entrainment	Raw	Entrained in by water pumps
23	Pred2	14	L	Before	–	April–June abundance of other predators	Mean	Predation is a source of direct mortality, measured as the product of relative density from beach seine data with the square of average Secchi depth
24	Pred2	14	A	After	–			

Note: A = occurs between adult and larval stages; L = occurs between larval and juvenile stages; J = occurs between juvenile and adult stages; Norm = subtract mean and divide by standard deviation; Mean = divide by mean; Raw = not scaled. The covariate is attributed to after density dependence unless it is known to occur before density dependence. This is because density dependence generally reduces the influence of the covariate.

[a] The effect of entrainment on survival is negative, but the covariate is formulated so setting the coefficient to 1 implies the assumption that entrainment is known without error, so the coefficient should be positive.

Table 3. AIC$_c$ weights for all possible density dependence models without covariates.

		J–No	J–BH	J–R	J–DD	Sum
L–No	A–No	0.000	0.079	0.062	0.027	0.168
	A–BH	0.000	0.075	0.067	0.026	0.168
	A–R	0.000	0.059	0.052	0.020	0.131
	A–DD	0.000	0.069	0.064	0.023	0.156
	Sum	0.000	0.281	0.245	0.096	0.622
L–BH	A–No	0.000	0.022	0.017	0.007	0.047
	A–BH	0.000	0.020	0.018	0.007	0.045
	A–R	0.000	0.016	0.014	0.005	0.035
	A–DD	0.000	0.018	0.017	0.006	0.040
	Sum	0.000	0.076	0.066	0.025	0.167
L–R	A–No	0.000	0.022	0.017	0.007	0.047
	A–BH	0.000	0.020	0.018	0.007	0.045
	A–R	0.000	0.016	0.014	0.005	0.035
	A–DD	0.000	0.018	0.017	0.006	0.040
	Sum	0.000	0.076	0.066	0.025	0.167
L–DD	A–No	0.000	0.006	0.005	0.002	0.013
	A–BH	0.000	0.005	0.005	0.002	0.012
	A–R	0.000	0.004	0.004	0.001	0.009
	A–DD	0.000	0.004	0.004	0.001	0.010
	Sum	0.000	0.020	0.017	0.006	0.043

Note: L = survival from larvae to juveniles; J = survival from juveniles to larvae; A = the stock–recruitment relationship from adults to larvae; No = no density dependence; BH = Beverton–Holt density dependence; R = Ricker density dependence; DD = Deriso–Schnute density dependence (i.e., estimate γ).

regression model of winter Old Middle River flow to his adult entrainment estimates and his larval–juvenile entrainment estimates were fitted to a multiple linear regression model with spring Old Middle River flow and spring low salinity zone (as measured by X). The values from Kimmerer (2008) were used for years in which they are available, and the linear regression predictions were used for the remaining years. Manly (2010*b*) provided several variables as candidates to account for the changes in delta smelt abundance from fall to summer and summer to fall. The fall to summer covariates could influence the adult and larvae stages, while the summer to fall covariates could influence the juvenile stage. The factors proposed by Manly (2010*b*) are those that are considered to act directly on delta smelt. There are many other proposed factors that act indirectly through these factors. We also include Secchi disc depth as a covariate for water turbidity–clarity, since it was identified as a factor by Thomson et al. (2010). Exports were also identified as an important factor and were assumed to be related to entrainment. However, we chose to use direct measures of entrainment. Interactions among the factors were not considered in the application. However, some of the covariates implicitly include interactions in their definition and construction.

Some manipulation of the data was carried out before use in the model (the untransformed covariate values used in the model are given in the supplementary material[1]). Delta smelt average length was missing for 1972–1974, 1976, and 1979 and was set to the mean based on Maunder and Deriso (2010). The factors were normalized (mean subtracted and divided by standard deviation) to improve model performance, except for the covariates relating to predator abundance, which were just divided by the mean, and the entrainment mortality rates, which were not transformed. These exceptions are factors that are hypothesized to have a unidirectional impact, and setting their coefficients to zero is needed for impact analysis. Setting the coefficient for the entrainment mortality rate covariates to one can be used to determine the impact if the entrainment estimates are assumed to be correct.

The standard approach outlined above and in Table 1 is applied to the delta smelt application. The Ricker model was approximated by setting $\gamma = -\exp(-10)$. We also constrained $\gamma < 0$ to avoid computational errors. It is difficult to scale the survey data to absolute abundance, so they are all treated as relative abundance and are not on the same scale. The scaling parameter a is not limited to $a \leq 1$, and the exponential model is used for all covariates. To illustrate the impact analysis, we implement three scenarios. In the first scenario, the covariates are all set to zero. This means that environmental conditions are average, predation is zero, and entrainment is zero. We implement the second scenario if one or both of the entrainment covariates are selected for inclusion in the model. In this case, only the entrainment coefficients are set to zero. In the third scenario, we take the final set of covariates and add the entrainment covariates (or substitute them if they were already included in the model) with their coefficients set to one and rerun the model. In this case, only the entrainment coefficients are set to zero in the impact analysis.

Results

AIC$_c$ values and weights were calculated for all possible combinations of density dependence that included no density dependence (No), a Beverton–Holt model (BH), a Ricker model (R), and estimation of both b and γ (DD) (Table 3). Density dependence was clearly preferred for survival from juveniles to adults (J), but it is not clear if the density dependence is Beverton–Holt, Ricker, or somewhere in between. The Beverton–Holt and Ricker models for juvenile survival appear to be influenced by three consecutive data points (years 1976–1978) of high juvenile abundance with corresponding average adult abundance (Figs. 2 and 3). The evidence for and against density dependence is about the same for the stock–recruitment relationship from adults to larvae (A), with slightly more evidence for no density dependence if survival from juveniles to adults is Beverton–Holt and slightly more evidence for Beverton–Holt density dependence if the survival from juveniles to adults is Ricker. The evidence for no density dependence in survival from larvae to juveniles (L) is moderately (three to four times) higher than that for density dependence. Therefore, we proceed with four density dependence scenarios: (*i*) Beverton–Holt density dependence in survival from juveniles to adults (JBH); (*ii*) Beverton–Holt density dependence in survival from juveniles to adults and a Beverton–Holt stock–recruitment relationship from adults to larvae (JBHABH); (*iii*) Ricker density dependence in survival from juveniles to adults (JR); and (*iv*) Ricker density dependence in survival from juveniles to adults and a Beverton–Holt stock–recruitment relationship from adults to larvae (JRABH).

The number and the type of factors supported by the data

Fig. 2. Relationship among stages in the model for the lowest AIC$_c$ model that has Ricker survival from juveniles to adults and a Beverton–Holt stock–recruitment relationship. Points are the model estimates of abundance, lines are the estimates from the stock–recruitment models without covariates or process variation, crosses are the estimates without covariates.

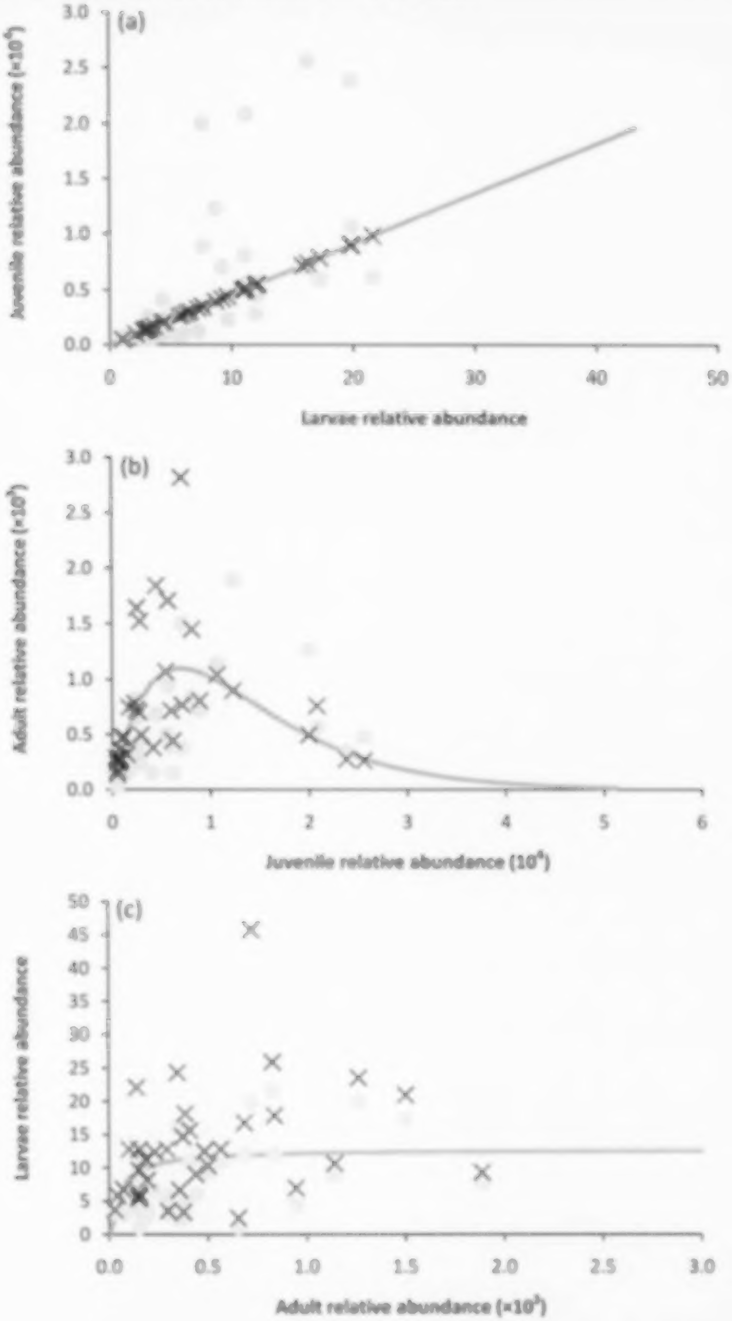

depended on the assumptions made about density dependence (Tables 4 and 5). The models with density dependence for both survival from juveniles to adults and a stock–recruitment relationship for adults to larvae included more covariates in the lowest AIC$_c$ models (eight and nine covariates for Beverton–Holt and Ricker density dependence in survival from juveniles to adults, respectively) than the models that included only density dependence for survival from juveniles to adults (five covariates each). Several temperature, prey, and predator covariates (TpAJ, EPAJ, EPJA, TpJul,

Fig. 3. Relationship among stages in the alternative model (the model that has the fewest covariates and the AIC is less than two AIC units greater than the lowest AIC model). Points are the model estimates of abundance, lines are the estimates from the stock–recruitment models without covariates or process variation, crosses are the estimates without covariates.

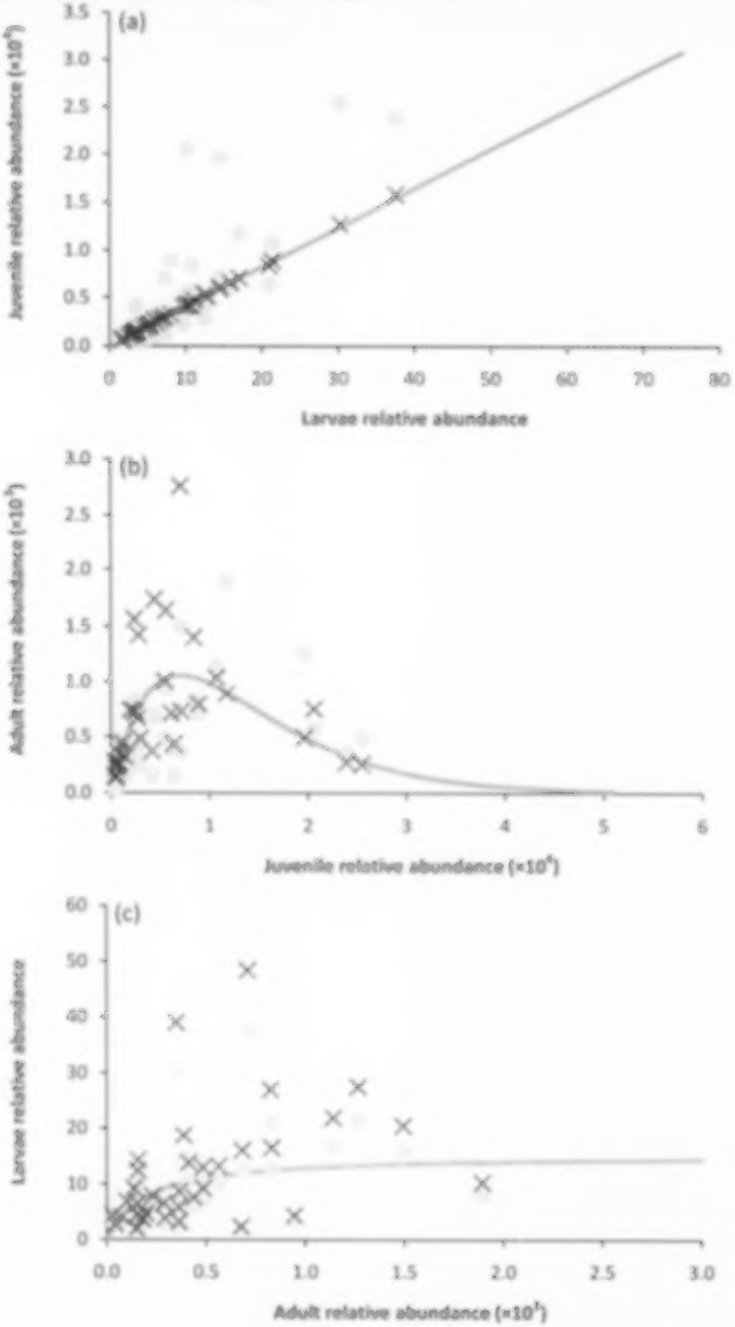

Pred1) were selected in the first few steps and were included in all models. The April–June abundance of predators (Pred2) was selected in the first few steps in one model, but not selected at all in the others.

Overall, the model with Ricker density dependence in survival from juveniles to adults and a Beverton–Holt stock–recruitment relationship from adults to larvae had better AIC_c scores than the other models (Table 5). This differs from the similarity in scores obtained when no covariates were included in the models (Table 3). For all density-

Table 4. Order of inclusion of factors into the analysis.

Factor	Name	Stage	Before–After	JBH	JBHABH	JR	JRABH
2	TpAJ	L	Before	1	1	2	2
4	TpJul	L	After	2	2	2	3
5	EPAJ	L	Before	1	1	1	1
7	EPJul	L	After	—	4	—	5
8	Pred1	J	After	2	2	3	3
18	EPJA	J	After	3	3	1	2
19	Secchi	A	Before	—	3	—	4
22	Aent	A	Before	—	4	—	4
23	Pred2	L	Before	—	—	—	1[*]

Note: JBH = Beverton–Holt density dependence from the juvenile (J) to adult (A) stage; JBHABH = Beverton–Holt density dependence from the juvenile to adult stage and Beverton–Holt density dependence from the adult to larvae (L) stage (the stock–recruitment relationship); JR = Ricker density dependence from the juvenile to adult stage; JRBH = Ricker density dependence from the juvenile to adult stage and Beverton–Holt density dependence from the adult to larvae stage (the stock–recruitment relationship). See Tables 2 and 3 for definitions.

[*] This covariate was excluded from the final model because the confidence interval of its coefficient included zero and including the covariate degraded the AIC_c.

dependent assumptions, there were alternatives with more (or less) covariates than the lowest AIC_c model (within the models for that density dependence assumption), for which there was not definite, strong, or very strong evidence that the model is not the K–L best model ($4 \leq \Delta$), suggesting that these factors should also be considered as possible factors that influence the population dynamics of delta smelt (Table 5). However, the asymmetrical nature of the AIC_c scores for nested models should be kept in mind.

The magnitude and the sign of the covariate coefficients are generally consistent across models (Table 6). The covariates were standardized so that the size of the coefficients are generally comparable across covariates. The coefficients are similar magnitudes for most covariates except those for water clarity (Secchi) and, particularly, adult entrainment (Aent), which had much larger effects. These both occurred before the stock–recruitment relationship from adults to larvae, which had a very strong density dependence effect. Pred2 had a small effect. The confidence intervals on the coefficients support inclusion of the covariates in the lowest AIC_c models except for Pred2 (Table 6). The effects for Secchi and Aent appear to be unrealistically large, and their coefficients have a moderately high negative correlation. This appears to be a consequence of the unrealistically strong density dependence estimated in the stock–recruitment relationship from adults to larvae for those models (see Supplemental Table S6 online[1]).

The five lowest AIC_c models in iteration 6 of the two factors at a time procedure had a *b* parameter of the Beverton–Holt stock–recruitment relationship from adult to larvae that was substantially greater than the critical value used to define realistic values of the parameter. The sixth model had an AIC of 812.53, which is worse than the lowest AIC_c model of iteration 5. The lowest AIC_c model with Beverton–Holt survival from juveniles to adults and Beverton–Holt stock–recruitment relationship from adult to larvae also had an unrealistic *b* parameter, and the next lowest AIC_c model had an AIC of 812.33. Therefore, the lowest AIC_c model after accounting for realistic parameter values is the lowest AIC_c model from iteration 5 with Ricker survival from juveniles to adults and Beverton–Holt stock–recruitment relationship from adult to larvae with one additional covariate (Table 5, $AIC_c = 808.47$). The confidence intervals for the Pred2 covariate for this model contained zero and removing the Pred2 covariate essentially had no effect on the likelihood. Therefore, we chose this model without the Pred2 covariate as the lowest AIC_c model ($AIC_c = 806.63$). Several models had an AIC_c score within two units of this model; according to the Burnham and Anderson (1998, p. 128) guidelines, "there is no credible evidence that the model should be ruled out". Therefore, to illustrate the sensitivity of results to the model choice, we also provide results for the model with the fewest parameters that was within two AIC_c units of the lowest AIC_c model. This alternative model is that selected with two additional parameters in iteration 3 of the selection procedure (Table 5, $AIC_c = 810.20$). Removing the Pred2 covariate improved the AIC_c score (808.63), so we also eliminated the Pred2 covariate from this model.

The models fit the survey data well (Figs. 4 and 5), in fact better than expected from the survey standard errors, indicating that most of the variation in abundance was modeled by the covariates or unexplained process variability. The unexplained process variability differed among the stages (Fig. 6; Table 7). Essentially all the variability in survival between larvae and juveniles was explained by the covariates. The amount of variability explained in the survival from juveniles to adults was higher than that in the stock–recruitment relationship, but they show similar patterns (Fig. 6; Table 7).

There was substantial correlation among estimated parameters (see supplementary material[1]). The lowest AIC model has moderate and high correlation between the covariate coefficients and several model parameters and also among the covariate coefficients themselves (Supplemental Table S6[1]). The alternative model has fewer parameter correlations (Supplemental Table S7[1]). The parameters of the density dependence function were highly positively correlated. The relative number of larvae in the first year is negatively correlated with parameters influencing larval survival, including the survival fraction at low abundance (*a*), the standard deviation of the process variability, and the prey covariate coefficients. The coefficients for the prey and temperature covariates influencing larval survival are correlated. This is partly related

Table 5. AIC_c values for each step in the model selection process.

	Step 1		Step 2		Step 3		Step 4		Step 5		Step 6		Step 7	
	Covar1	Covar2	Covar1	Covar2	Covar1	Covar2	Covar1	Covar2	Covar1	Covar2	Covar1	Covar2	Covar1	Covar2
JBH	841.06	833.44	827.58	824.00	823.01	823.30	824.61	825.95	828.28	831.08	—	—	—	—
JBHABH	832.46	824.68	818.25	815.18	813.92	814.32	814.17	811.85	812.33	814.75	—	—	—	—
JR	841.80	833.67	826.25	821.40	820.00	821.10	822.58	823.71	826.26	828.86	—	—	—	—
JRBH	833.16	824.93	817.96	814.72	811.60	810.20	810.72	810.38	808.47	809.23	810.86	813.39	817.03	820.83

Note: Shaded values are the lowest AIC_c for that density dependence configuration. See Table 4 for definitions.

to the fact that some of these covariates are also correlated (Supplemental Table S5[1]). The coefficients for water clarity (Secchi) and adult entrainment (Aent) in the lowest AIC model were highly negatively correlated and were correlated with the parameters of the density dependence survival function that relates adults and larvae. The coefficient for Aent is also unrealistically large. The coefficient for Pred1 is correlated with the parameters of the density dependence relationship for juvenile survival and is also highly positively correlated with year. The coefficient for EPJA is positively correlated with the parameter that controls density dependence for juvenile survival. The coefficient for EPJul in the lowest AIC model is correlated with several parameters.

The impact analysis of the selected covariates shows that the adult abundance under average conditions, with no predators and entrainment mortality set to zero, differs moderately from that estimated in the original model (Fig. 7). In particular, the recent decline is not as substantial under average conditions, indicating that the covariates describe some of the decline, although there is still substantial unexplained variation and a large amount of uncertainty in the recent abundance estimates. Entrainment is estimated to have only a small impact on the adult abundance in either the lowest AIC_c model, which uses the estimated adult entrainment coefficient and the juvenile entrainment coefficient is zero, or the alternative model, in which both the juvenile and adult entrainment coefficients are set to one (Fig. 8). The lowest AIC_c model with the two entrainment coefficients set at one did not converge, and results are not shown for that analysis, although the results are expected to be similar.

Discussion

We developed a state–space multistage life cycle model to evaluate population impacts in the presence of density dependence. Application to delta smelt detected strong evidence for a few key factors and density dependence operating on the population. Both environmental factors (e.g., Deriso et al. 2008) and density dependence (e.g., Brook and Bradshaw 2006) have been detected in a multitude of studies either independently or in combination (e.g., Sæther 1997; Ciannelli et al. 2004). Brook and Bradshaw (2006) used long-term abundance data for 1198 species to show that density dependence was a pervasive feature of population dynamics that holds across a range of taxa. However, the data they used did not allow them to identify what life stages the density dependence operates on. Ciannelli et al. (2004) found density dependence in different stages of walleye pollock (*Theragra chalcogramma*). In our application, we found evidence against density-dependent survival from larvae to juveniles, strong evidence for density dependence in survival from juveniles to adults, and weak evidence for density dependence in the stock–recruitment relationship from adults to larvae, which includes egg and early larval survival. Other studies have suggested that density dependence is more predominant at earlier life stages (e.g., Fowler 1987; Gaillard et al. 1998), although the life history of these species differs substantially from delta smelt. The density dependence in survival from juveniles to adults found in our study was probably heavily influenced by three consecutive years of data. Unfortunately, this is a common occurrence in which

Table 6. Estimates of coefficients (and 95% confidence intervals) from the lowest AIC$_c$ models for each density dependence assumption.

Factor	Name	Stage	B–A	JBH	JBHABH	JR	JRABH	JRABH, no Pred2	Alternative
2	TpAJ	L	B	–0.32 (–0.46, –0.18)	–0.21 (–0.36, –0.07)	–0.32 (–0.45, –0.19)	–0.20 (–0.34, –0.06)	–0.22 (–0.36, –0.09)	–0.31 (–0.44, –0.18)
4	TpJul	L	A	–0.29 (–0.50, –0.08)	–0.30 (–0.49, –0.12)	–0.28 (–0.49, –0.07)	–0.28 (–0.47, –0.09)	–0.32 (–0.50, –0.13)	–0.30 (–0.50, –0.11)
5	EPAJ	L	B	0.39 (0.15, 0.63)	0.40 (0.18, 0.62)	0.37 (0.13, 0.61)	0.32 (0.09, 0.55)	0.36 (0.14, 0.58)	0.47 (0.23, 0.71)
7	EPJul	L	A		0.32 (0.07, 0.58)		0.31 (0.05, 0.56)	0.33 (0.07, 0.59)	
8	Pred1	J	A	–0.45 (–0.84, –0.06)	–0.49 (–0.90, –0.08)	–0.37 (–0.71, –0.03)	–0.42 (–0.77, –0.07)	–0.44 (–0.78, –0.09)	–0.40 (–0.75, –0.05)
18	EPJA	J	A	0.21 (0.00, 0.42)	0.22 (0.00, 0.45)	0.44 (0.21, 0.66)	0.46 (0.22, 0.69)	0.46 (0.22, 0.69)	0.46 (0.23, 0.69)
19	Secchi	A	B		–1.08 (–1.97, –0.19)		–1.24 (–2.27, –0.22)	–1.15 (–2.11, –0.20)	
22	Acnt	A	B		9.50 (0.62, 18.38)		10.97 (0.93, 21.01)	10.32 (0.99, 19.65)	
23	Pred2	L	B				–0.19 (–0.52, 0.13)		
	a	L		396 (334, 458)	451 (373, 529)	396 (337, 456)	593 (307, 879)	454 (376, 532)	410 (340, 481)
	a	J		0.74 (0.01, 1.48)	0.77 (–0.02, 1.56)	0.39 (0.18, 0.6)	0.42 (0.19, 0.65)	0.43 (0.2, 0.66)	0.41 (0.19, 0.63)
	a	A		0.03 (0.02, 0.04)	0.2 (–0.13, 0.53)	0.03 (0.02, 0.04)	0.27 (–0.24, 0.78)	0.25 (–0.18, 0.67)	0.08 (0, 0.16)
	b	L		0	0	0	0	0	0
	b (×10^{-4})	J		8.38 (–0.19, 16.95)	7.95 (–0.57, 16.48)	1.43 (1.01, 1.84)	1.42 (1.01, 1.84)	1.44 (1.02, 1.85)	1.43 (1.01, 1.84)
	b (×10^{-2})	A		0	1.48 (–1.41, 4.38)	0	2.35 (–2.77, 7.47)	1.93 (–1.96, 5.81)	0.52 (–0.34, 1.39)
	γ	L							
	γ	J		–1	–1	0	0	0	0
	γ	A			–1		–1	–1	–1
	σ	L		0.07 (–0.32, 0.45)	0 (–0.35, 0.35)	0.04 (–0.5, 0.59)	0 (–0.35, 0.35)	0 (–0.26, 0.26)	0.1 (–0.2, 0.39)
	σ	J		0.52 (0.36, 0.67)	0.55 (0.39, 0.71)	0.46 (0.31, 0.6)	0.48 (0.32, 0.63)	0.48 (0.32, 0.63)	0.47 (0.32, 0.62)
	σ	A		0.79 (0.57, 1.01)	0.61 (0.45, 0.77)	0.82 (0.59, 1.04)	0.61 (0.45, 0.77)	0.62 (0.46, 0.78)	0.71 (0.52, 0.9)
	h_{min}	L		1	1	1	1	1	1
	h_{min}	J		0.24 (0.09, 0.4)	0.24 (0.08, 0.4)	0.11 (0.09, 0.14)	0.11 (0.09, 0.14)	0.12 (0.09, 0.14)	0.11 (0.09, 0.14)
	h_{min}	A		1	0.29 (–0.06, 0.64)	1	0.38 (–0.09, 0.85)	0.34 (–0.07, 0.75)	0.15 (0, 0.3)

Note: Definitions of abbreviations and a description of the covariates can be found in Table 2 and the density dependence configurations in Table 4; B–A, before–after. The alternative model is the model that has the fewest covariates and the AIC$_c$ is less than two AIC$_c$ units greater than the lowest AIC$_c$ model.

Fig. 4. Fit (line) to the survey abundance data (circles) for the lowest AIC$_c$ model that includes Ricker survival between juveniles and adults and a Beverton–Holt stock–recruitment relationship. Confidence intervals are the survey observations plus and minus two standard deviations as estimated from bootstrap analysis.

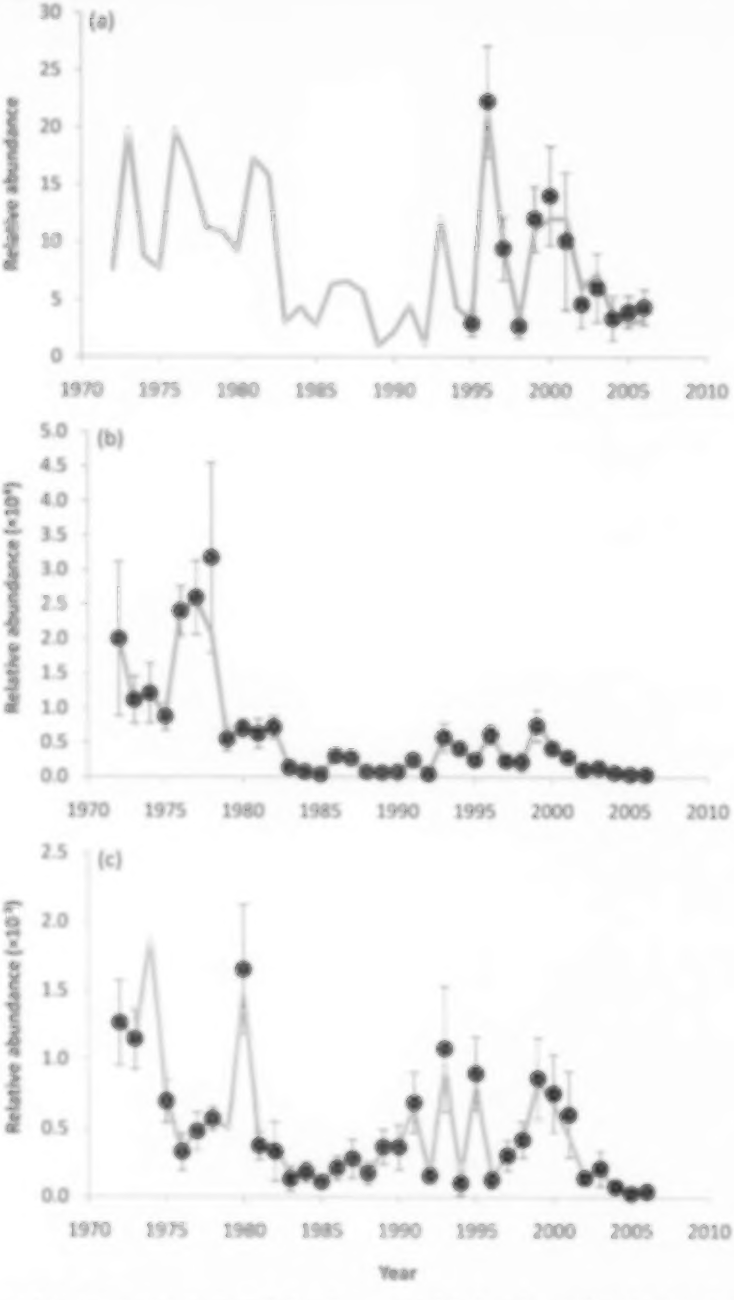

autocorrelated environmental factors cause autocorrelation in abundance within a stage, and this likely influences other studies as well. We only allowed factors to influence density-independent survival, either before or after density dependence; however, the factors could also influence the strength or form of the density dependence (Walters 1987). For example, Ciannelli et al. (2004) found that high wind speed induced negative density dependence in the survival of walleye pollock eggs. Our analysis is one of the few, but expanding, applications investigating both density-dependent and density-independent factors in a rigorous statistical framework that integrates multiple data sets within a life cycle model. The framework amalgamates the density and the mechanistic paradigms of investigating population regula-

Fig. 5. Fit (line) to the survey abundance data (circles) for the alternative model (the model that has the fewest covariates and the AIC is less than two AIC units greater than the lowest AIC model) that includes Ricker survival from juveniles to adults and a Beverton–Holt stock–recruitment relationship. Confidence intervals are the survey observations plus and minus two standard deviations as estimated from bootstrap analysis.

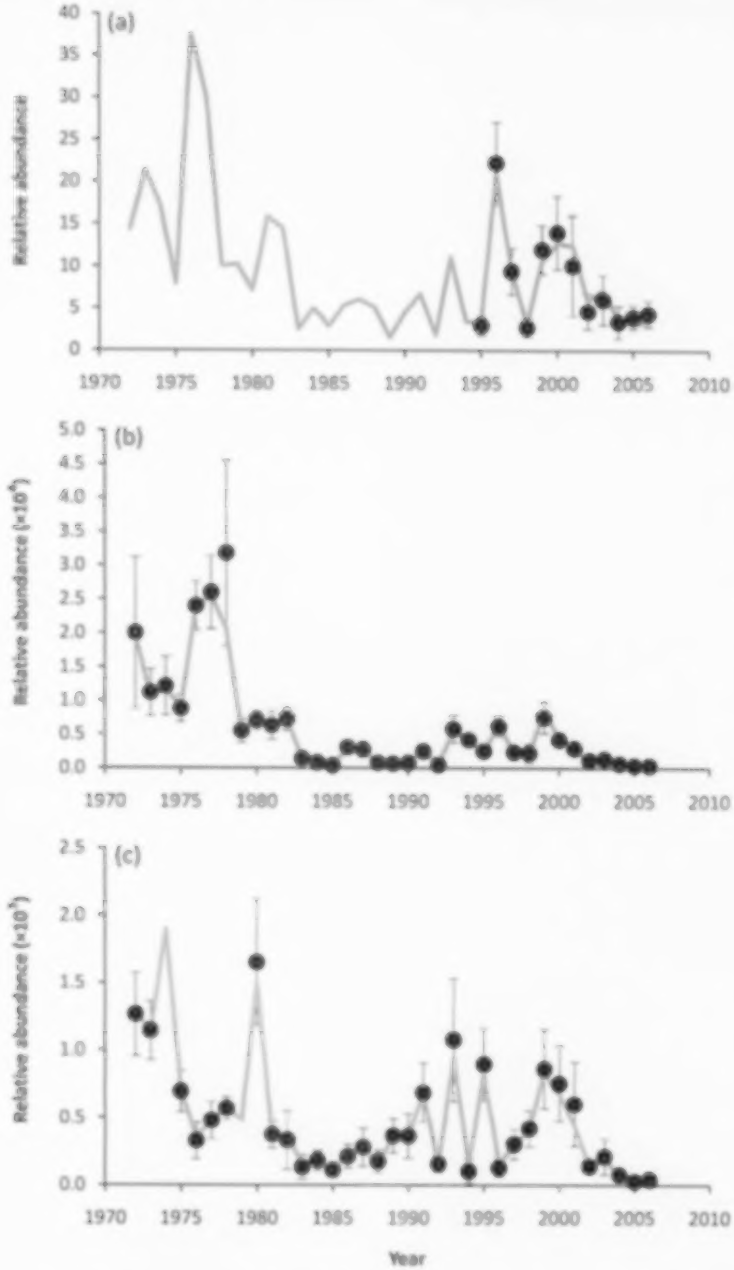

tion outlined by Krebs (2002) while accommodating the fact that most available data is observational rather than experimental. More detailed mechanistic processes could be included in the model if the appropriate observational or experimental data are available.

One factor is often erroneously singled out as the only major cause of population decline (e.g., overfishing; Sibert et al. 2006). However, there is a substantial accumulation of evidence that multiple factors interact to cause population declines. Our analysis found support for a variety of factors that influence delta smelt population dynamics. We also showed that together these factors explain the decline in the

Fig. 6. Estimates of the realizations of the process variation random effects ($\exp(\sigma_s \varepsilon_{s,t} - 0.5\sigma_s^2)$) for the lowest AIC$_c$ model that includes Ricker survival between juveniles and adults and a Beverton–Holt stock–recruitment relationship (*a*) and the alternative model (the model that has the fewest covariates and the AIC is less than two AIC units greater than the lowest AIC model) (*b*).

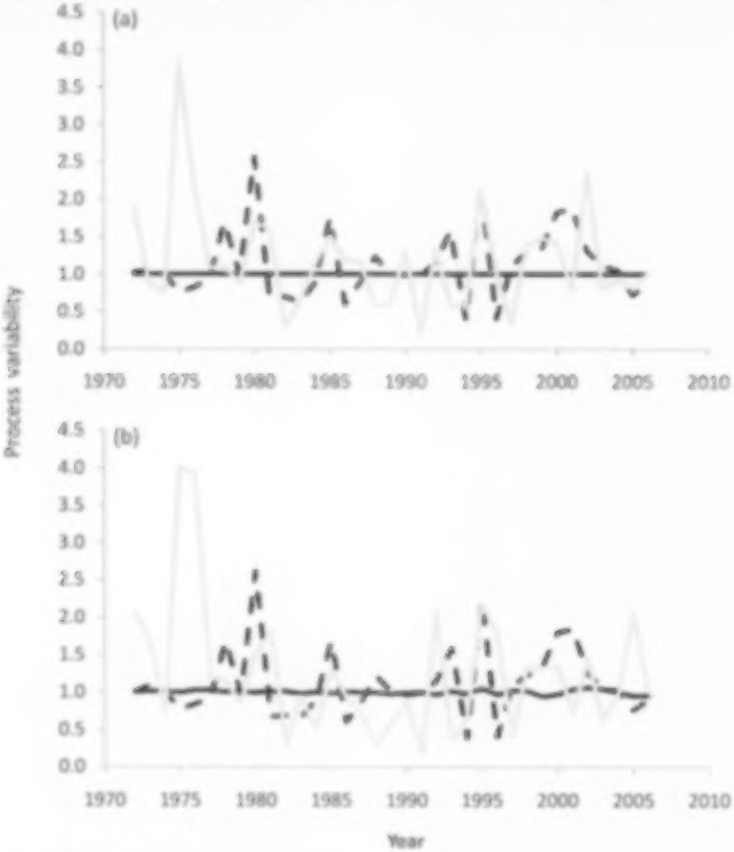

Table 7. Estimates of standard deviation of the process variation and the percentage of the process variation explained by the covariates for the lowest AIC$_c$ model.

	Standard deviation		
	Without covariates	With covariates	% variation explained
Larvae	0.72	0.00	100
Juvenile	0.63	0.48	43
Adult	0.71	0.62	24

delta smelt population. Deriso et al. (2008) also found support that multiple factors influenced the decline and suppression of the Prince William Sound herring (*Clupea pallasii*) population, including one or more unidentified factors related to a particular year.

Three of the first four factors included in the delta smelt application acted on the survival between larvae and juveniles. This is also the period where no density dependence in survival occurred. The final model estimates that the factors explain all the variability in survival from larvae to juveniles. The 20 mm trawl survey, which provides information on juvenile abundance, only starts in 1995 so there is less data to explain, and this may be partly why the unexplained process variability variance goes to zero. The process variability for the other stages may partly absorb the variability in survival from larvae to juveniles.

Deriso et al. (2008) showed that multiple factors influence populations and that analysis of factors in isolation can be misleading. We also found that multiple factors influence the dynamics of delta smelt and that evaluating factors in isolation can produce different results than evaluating them in combination. The type of density dependence assumed also impacted what factors were selected. Specifically, one predator covariate (Pred2) would be the first selected covariate based simply on AIC$_c$ for two of the density-dependent assumptions, but was not selected by the two-factor stepwise procedure (see supplementary material[1]). However, this covariate was selected in the first step of the two-factor stepwise procedure for another density-dependent assumption, which happened to be the final model with the lowest AIC$_c$. In the final model the confidence intervals on the coefficient indicate that this factor should not be included in the model. Exploratory analysis showed that this covariate had about a 0.6 correlation with a temperature (TpAJ) and a prey (EPAJ) covariate that were consistently selected in the first or seconds steps, which operated on the same stage (larvae), when these

Fig. 7. Estimates of abundance with and without covariates (coefficients of the covariates set to zero) (top panels) and ratio of the two with 95% confidence intervals (bottom panels, y axis limited to show details) from the lowest AIC$_c$ (left panels) model that has Ricker survival from juveniles to adults and a Beverton–Holt stock–recruitment relationship and the alternative model (the model that has the fewest covariates and the AIC is less than two AIC units greater than the lowest AIC model) (right panels).

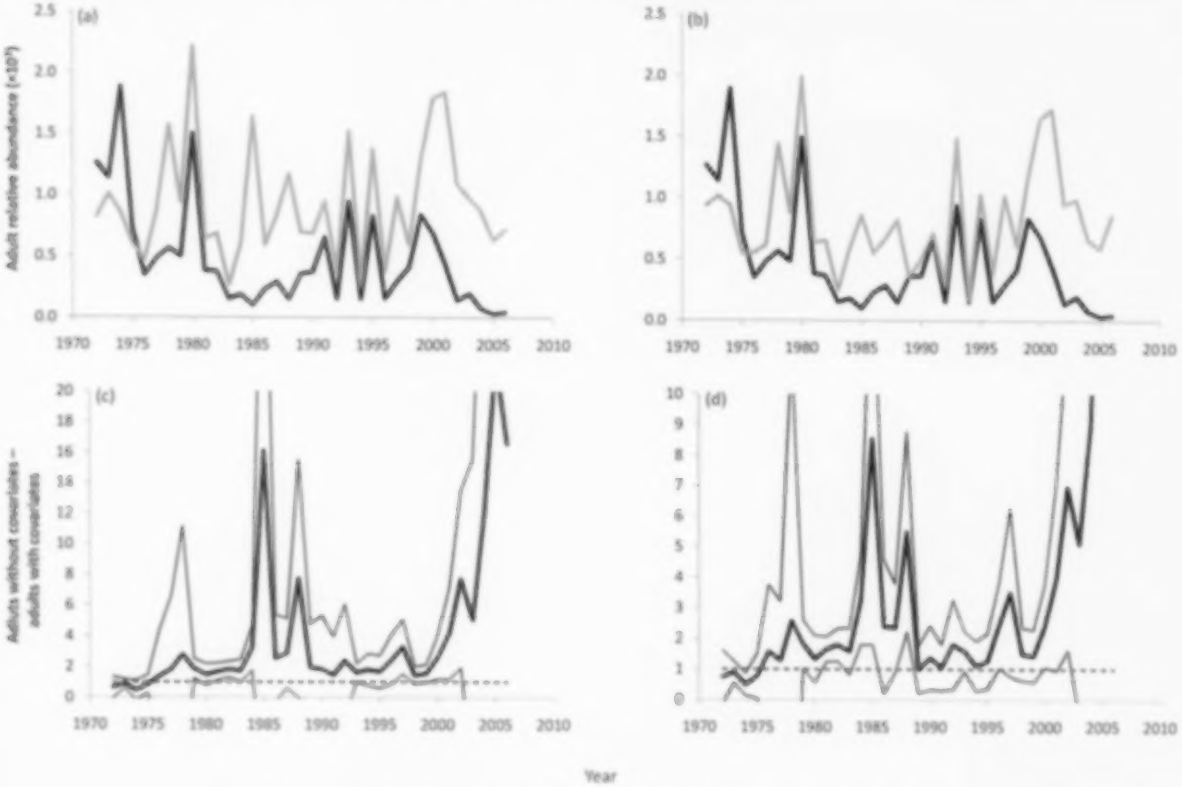

covariates were combined together. The covariate was also highly correlated with time (see supplementary material[1]). We did find, to some extent, which other covariates were included in the model, and the order in which they were included changed depending on the density dependence assumptions. However, apart from the one predator covariate, the four density dependence assumptions tended to select the same factors in the first few steps of the model selection procedure, although the order of selection differed.

Several of the model parameters show moderate to strong correlations. The three covariates included in the lowest AIC model, but not in the alternative model (EPJul, Secchi, and Aent), are highly correlated with other model parameters. The only coefficients that show strong correlation with each other in the alternative model are EPAJ and TPJul. These covariates have a moderate negative correlation, while the coefficients have a positive correlation and therefore offset each other. High correlation may indicate that the data do not provide enough information to separate the effects represented by the two parameters. However, hypothesis tests and the confidence intervals of the coefficients are used to judge if a particular hypothesis (covariate) is supported by the data. If there is not enough information in the data to separate two hypotheses, the hypothesis tests will fail to include one of the covariates or the confidence interval of the covariate's coefficient will contain zero. The parameters of the density dependence function were highly positively correlated as previously observed for stock–recruitment relationships (Quinn and Deriso 1999), and reparameterization might improve the estimation algorithm. The inclusion of several covariates (TpAJ, EPAJ, EPJA, TpJul, Pred1) were robust to the form of density dependence and only showed low to moderate correlation among their coefficients. The predator covariate coefficient was highly correlated with the juvenile survival density dependence parameters, making the inclusion of this covariate less convincing. The predator covariate was also positively correlated with year. The coefficients for water clarity and adult entrainment, which were included in the lowest AIC model but excluded from the alternative model, were highly confounded with density dependence and required constraining the density dependence to reasonable parameter space. This may indicate that the effect of adult entrainment only shows up when abundance is very low. A model within two AIC units of the lowest AIC model did not contain either adult entrainment or water clarity, but did include all the robust factors. The coefficient for adult entrainment is also unrealistically large, suggesting that the model including water clarity and adult entrainment is unreliable.

The covariates were included in the model as simple log-

Fig. 8. Estimates of the adult abundance with and without adult entrainment (top panels) and the ratio of adult abundance without adult entrainment to that with adult entrainment (bottom panels, *y* axis limited to show details) from the lowest AIC$_c$ model (left panels) with Ricker survival from juveniles to adults and a Beverton–Holt stock–recruitment relationship and the alterative model (the model that has the fewest covariates and the AIC is less than two AIC units greater than the lowest AIC model) (right panels).

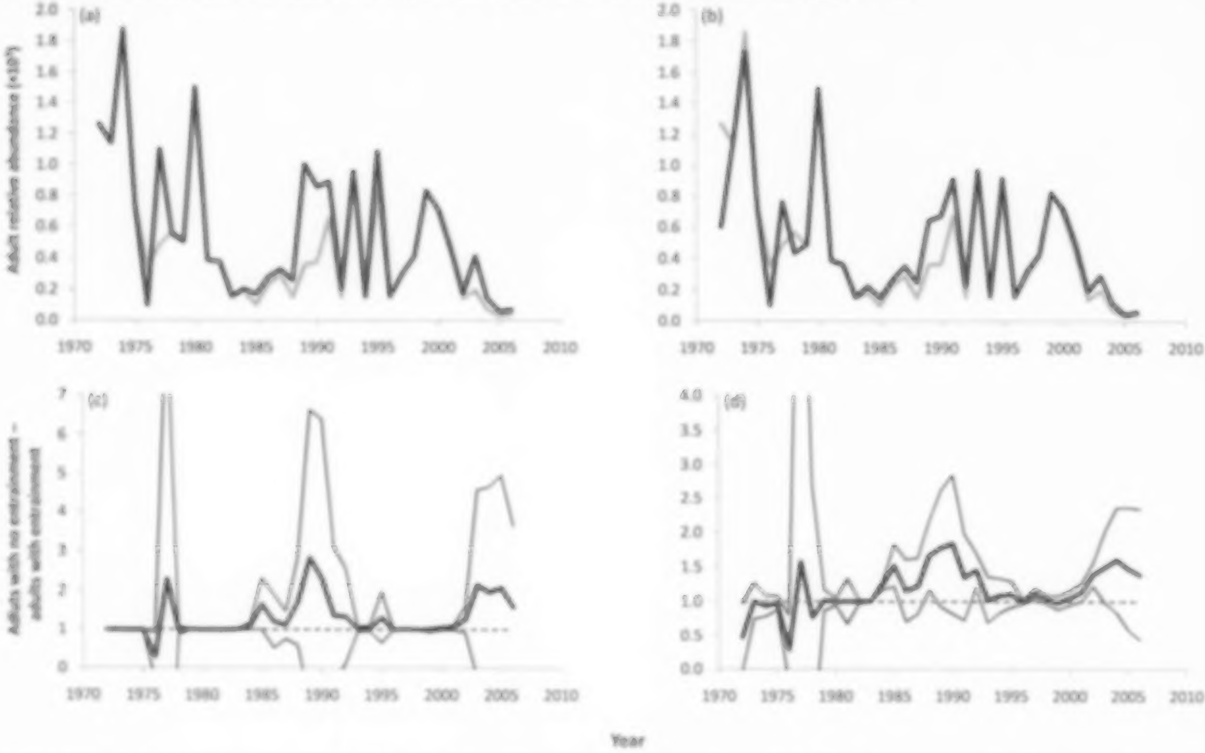

linear terms. There may be more appropriate relationships between survival and the covariates. For example, good survival may be limited to a range of covariate values, so a polynomial that describes a dome-shaped curve may be more appropriate. There may also be interactions among the covariates. Neither of these was considered in the delta smelt application, although some of the covariates were developed based on combining different factors such as water clarity and predator abundance. Some of the covariates were highly correlated (see supplementary material[1]), but those with the highest correlations were either for different stages or not selected in the final models.

Density dependence and environmental factors could influence other population processes (e.g., growth rates) or the ability (catchability) of the survey to catch delta smelt. Modeling of catchability has been extensively researched for indices of abundance based on commercial catch data (Maunder and Punt 2004), and results have shown that the relationship between catch per unit effort and abundance can be nonlinear (Harley et al. 2001; Walters 2003). Rigorous statistical methods have been developed to account for habitat quality in the development of indices of abundance from catch and effort data (Maunder et al. 2006). Methods have been developed to integrate the modeling of catchability within population dynamics models as a random walk (Fournier et al. 1998) or as a function of covariates (Maunder 2001; Maunder and Langley 2004). Surveys are less likely to be effected by systematic changes in catchability because sampling effort and survey design tend to be more consistent over time than effort conducted by commercial fishing fleets. Most fisheries stock assessments assume that there are no systematic changes in survey catchability unless there is an obvious change (e.g., change in survey vessel). Previous studies using the data in this study have also assumed that catchability is constant over time (Mac Nally et al. 2010; Thomson et al. 2010). However, catchability may change because of factors such as changes in the spatial distribution of the species or population density. Similar methods as used for survival can be used to model catchability as a function of density or environmental factors. The standard deviations used in the likelihood functions are based on bootstrap analysis that takes the within-year sampling variability into consideration, but does not account for between-year variation in catchability. Random influences on catchability beyond those caused by simple random sampling can be accommodated by estimating the standard deviation of the likelihood function used to fit the model to the survey data (Maunder and Starr 2003). However, the fit to the delta smelt data appears better than expected from the bootstrap confidence intervals, suggesting that the observation error is smaller than estimated by the bootstrap procedure. Systematic and additional random variation in catchability could bias the evaluation of strength and statistical significance of density dependence and environmental factors (Deriso et al. 2007).

The estimates of the b parameter of the Beverton–Holt stock–recruitment relationship between adults and larvae produced density dependence that was unrealistically strong in a few models. Consequently, this caused estimates of some coefficients that were also unrealistic (e.g., the coefficient for adult entrainment was nearly two orders of magnitude higher than expected). Even when a model was selected for which the b parameter was considered reasonable, the coefficient for adult entrainment was still an order of magnitude greater than expected. This illustrates that naively following AIC$_c$ model selection without use of professional judgment is not recommended. We could have included all models in the sum of the AIC$_c$ weights by bounding the b parameter in the parameter estimation process (the parameter would probably be at the bound), but we considered inference based on models with a parameter at the bound inappropriate. An alternative approach would be to use an informative prior for b (Punt and Hilborn 1997) to pull it away from unrealistic values, but we did not have any prior information that was considered appropriate.

Anderson et al. (2000) warn against data dredging as a method to test factors that influence population dynamics. In their definition of data dredging, they include the testing of all possible models, unless, perhaps, if model averaging is used. This provides somewhat of a dilemma when using a multistage life cycle model because there are often multiple candidate factors for each life stage and they may only be detectable if included in the model together. For this reason, we use an approximation to all possible models and rely on AIC$_c$ and AIC$_c$ weights to rank models and provide an idea of the strength of evidence in the data about the models and do not apply strict hypothesis tests. Some form of model averaging using AIC$_c$ weights might be applicable to the impact analysis, although the estimates of uncertainty would have to include both model and parameter uncertainty. The estimates of uncertainty in our impact analysis underestimate uncertainty because they do not include model selection uncertainty, and use of model averaging might provide better estimates of uncertainty (Burnham and Anderson 2002). In addition, we use symmetric confidence intervals and approaches that provide asymmetric confidence intervals may be more appropriate (e.g., based on profile likelihood or Bayesian posterior distribution).

Our results suggest that of all the factors that we tested, food abundance, temperature, predator abundance, and density dependence are the most important factors controlling the population dynamics of delta smelt. Survival is positively related to food abundance and negatively related to temperature and predator abundance. There was also some support for a negative relationship with water clarity and adult entrainment and a positive relationship with the number of days where the water temperature was appropriate for spawning. The first variables to be included in the model were those related to survival from larvae to juveniles, followed by survival from juveniles to adults, and finally the stock–recruitment relationship. Mac Nally et al. (2010) also found that high summer water temperatures had an inverse relationship with delta smelt abundance. Thomson et al. (2010) found exports and water clarity as important factors. We did not include exports, but included explicit estimates of entrainment. We found some support for adult entrainment, but it was not one of the main factors, and the coefficient was unrealistically high and highly correlated with the coefficient for water clarity. Mac Nally et al. (2010) and Thomson et al. (2010) only used the FMWT data and did not look at the different life stages, which probably explains why the factors supported by their analyses differ from what we found.

We found strong evidence for density dependence in survival from juveniles to adults, some evidence for density dependence for the stock–recruitment relationship from adults to larvae, and evidence against density dependence in survival from larvae to juveniles. This might be surprising since the population is of conservation concern owing to low abundance levels. However, the available data covers years, particularly in the 1970s, where the abundance was high, and data for these years provide information on the form and strength of the density dependence. At the recent levels of abundance, density dependence is probably not having a substantial impact on the population, and survival is impacted mainly by density-independent factors. Previous studies only found weak evidence for a stock–recruitment relationship and suggested that density-independent factors regulate the delta smelt population (e.g., Moyle et al. 1992). Bennett (2005) found that the strongest evidence for density dependence was between juveniles and pre-adults. Mac Nally et al. (2010) found strong support for density dependence, but Thomson et al. (2010) did not.

Several pelagic species in the San Francisco Estuary have also experienced declines, but the factors causing the declines are still uncertain (Bennett 2005; Sommer et al. 2007). Thomson et al. (2010) used Bayesian change point analysis to determine when the declines occurred and included covariates to investigate what caused the declines. They were unable to fully explain the decline, and unexplained declines were still apparent in the early 2000s. The impact analysis we applied to delta smelt suggests that the factors included in the model explain the low levels of delta smelt from 2002 to 2006. However, there is still substantial annual variation in the delta smelt abundance and uncertainty in the estimates of abundance for these years.

The theory for state–space stage-structured life cycle models is well developed (Newman 1998; de Valpine 2002; Maunder 2004), they have been promoted (Thomson et al. 2010; Mac Nally et al. 2010), they facilitate the use of multiple data sets (Maunder 2003), they provide more detailed information about how factors impact a population, they encompass all the statistical modeling advances advocated by Rose et al. 2001, and we have shown that they can be implemented. Therefore, we recommend that they are an essential tool for evaluating factors impacting species of concern such as delta smelt.

Acknowledgements

Brian Manly provided the survey data. Brian Manly and B.J. Miller provided the covariate data. Richard Deriso was funded by Metropolitan Water District of Southern California. Mark Maunder was funded by San Luis & Delta-Mendota Water Authority. Ray Hilborn provided advice on the modeling. Ken Burnham provided comments on a previous version of the paper. Members of a working group convened at the National Center for Ecological Analysis and Synthesis contributed to the work through discussions with

Mark Maunder. Members of the working group included Ralph Mac Nally, James R. Thomson, Wim J. Kimmerer, Frederick Feyrer, Ken B. Newman, Andy Sih, William A. Bennett, Larry Brown, Erica Fleishman, Steven D. Culberson, Gonzalo Castillo, Howard Townsend, Dennis D. Murphy, John M. Melack, and Marissa Bauer. Comments by two anonymous reviewers improved the manuscript.

References

Anderson, D.R., Burnham, K.P., and Thompson, W.L. 2000. Null hypothesis testing: problems, prevalence, and an alternative. J. Wildl. Manage. **64**(4): 912–923. doi:10.2307/3803199.

Bennett, W.A. 2005. Critical assessment of the delta smelt population in the San Francisco estuary, California. San Francisco Estuary and Watershed Science, **3**(2): 1–71.

Besbeas, P., Freeman, S.N., Morgan, B.J.T., and Catchpole, E.A. 2002. Integrating mark–recapture–recovery and census data to estimate animal abundance and demographic parameters. Biometrics, **58**(3): 540–547. doi:10.1111/j.0006-341X.2002.00540.x. PMID:12229988.

Brook, B.W., and Bradshaw, C.J.A. 2006. Strength of evidence for density dependence in abundance time series of 1198 species. Ecology, **87**(6): 1445–1451. doi:10.1890/0012-9658(2006)87[1445:SOEFDD]2.0.CO;2. PMID:16869419.

Buckland, S.T., Newman, K.B., Thomas, L., and Koesters, N.B. 2004. State–space models for the dynamics of wild animal populations. Ecol. Model. **171**(1–2): 157–175. doi:10.1016/j.ecolmodel.2003.08.002.

Buckland, S.T., Newman, K.B., Fernandez, C., Thomas, L., and Harwood, J. 2007. Embedding population dynamics models in inference. Stat. Sci. **22**(1): 44–58. doi:10.1214/088342306000000673.

Burnham, K.P., and Anderson, D.R. 1998. Model selection and multimodel inference: a practical information-theoretic approach. 1st ed. Springer, New York.

Burnham, K.P., and Anderson, D.R. 2002. Model selection and multimodel inference: a practical information-theoretic approach. 2nd ed. Springer, New York.

Ciannelli, L., Chan, K.-S., Bailey, K.M., and Stenseth, N.C. 2004. Nonadditive effects of the environment on the survival of a large marine fish population. Ecology, **85**(12): 3418–3427. doi:10.1890/03-0755.

Clark, J.S., and Bjornstad, O.N. 2004. Population time series: process variability, observation errors, missing variables, lags, and hidden states. Ecology, **85**(11): 3140–3150. doi:10.1890/03-0520.

Conn, P.B., Williams, E.H., and Shertzer, K.W. 2010. When can we reliably estimate the productivity of fish stocks? Can. J. Fish. Aquat. Sci. **67**(3): 511–523. doi:10.1139/F09-194.

de Valpine, P. 2002. Review of methods for fitting time-series models with process and observation error and likelihood calculations for nonlinear, non-Gaussian state–space models. Bull. Mar. Sci. **70**: 455–471.

Deriso, R.B. 1980. Harvesting strategies and parameter estimation for an age-structured model. Can. J. Fish. Aquat. Sci. **37**(2): 268–282. doi:10.1139/f80-034.

Deriso, R.B., Maunder, M.N., and Skalski, J.R. 2007. Variance estimation in integrated assessment models and its importance for hypothesis testing. Can. J. Fish. Aquat. Sci. **64**(2): 187–197. doi:10.1139/f06-178.

Deriso, R.B., Maunder, M.N., and Pearson, W.H. 2008. Incorporating covariates into fisheries stock assessment models with application to Pacific herring. Ecol. Appl. **18**(5): 1270–1286. doi:10.1890/07-0708.1. PMID:18686586.

Dupont, W.D. 1983. A stochastic catch–effort method for estimating animal abundance. Biometrics, **39**(4): 1021–1033. doi:10.2307/2531336. PMID:6689474.

Fournier, D.A., Hampton, J., and Sibert, J.R. 1998. MULTIFAN-CL: a length-based, age-structured model for fisheries stock assessment, with application to South Pacific albacore, *Thunnus alalunga*. Can. J. Fish. Aquat. Sci. **55**(9): 2105–2116. doi:10.1139/f98-100.

Fowler, C.W. 1987. A review of density dependence in populations of large mammals. *In* Current mammalogy. *Edited by* H.H. Genoways. Plenum Press, New York. pp. 401–441.

Gaillard, J.-M., Festa-Bianchet, M., and Yoccoz, N.G. 1998. Population dynamics of large herbivores: variable recruitment with constant adult survival. Trends Ecol. Evol. **13**(2): 58–63. doi:10.1016/S0169-5347(97)01237-8. PMID:21238201.

Gimenez, O., Bonner, S., King, R., Parker, R.A., Brooks, S., Jamieson, L.E., Grosbois, V., Morgan, B.J.T., and Thomas, L. 2009. WinBUGS for population ecologists: Bayesian modeling using Markov chain Monte Carlo methods. *In* Modeling demographic processes in marked populations. *Edited by* D.L. Thomson, E.G. Cooch, and M.J. Conroy. Environ. Ecol. Stat. 3: 883–916.

Harley, S.J., Myers, R.A., and Dunn, A. 2001. Is catch-per-unit effort proportional to abundance? Can. J. Fish. Aquat. Sci. **58**(9): 1760–1772. doi:10.1139/f01-112.

Hilborn, R., and Mangel, M. 1997. The ecological detective: confronting models with data. Princeton University Press, Princeton, N.J.

Hobbs, N.T., and Hilborn, R. 2006. Alternatives to statistical hypothesis testing in ecology: a guide to self teaching. Ecol. Appl. **16**(1): 5–19. doi:10.1890/04-0645. PMID:16705957.

Kimmerer, W.J. 2008. Losses of Sacramento River Chinook salmon and delta smelt to entrainment in water diversions in the Sacramento – San Joaquin Delta. San Francisco Estuary Watershed Science, **6**(2): 1–27.

Krebs, C.J. 2002. Two complementary paradigms for analysing population dynamics. Philos. Trans. R. Soc. Lond. B Biol Sci. **357**(1425): 1211–1219. doi:10.1098/rstb.2002.1122. PMID:12396513.

Lunn, D., Spiegelhalter, D., Thomas, A., and Best, N. 2009. The BUGS project: evolution, critique and future directions. Stat. Med. **28**(25): 3049–3067. doi:10.1002/sim.3680. PMID:19630097.

Mac Nally, R., Thomson, J.R., Kimmerer, W., Feyrer, F., Newman, K.B., Sih, A., Bennett, W., Brown, L., Fleishman, E., Culberson, S.D., and Castillo, G. 2010. Analysis of pelagic species decline in the upper San Francisco Estuary using multivariate autoregressive modeling (MAR). Ecol. Appl. **20**(5): 1417–1430. doi:10.1890/09-1724.1. PMID:20666258.

Manly, B.F.J. 2010*a*. Bootstrapping the July summer townet trawl data. Report available from Western EcoSystems Technology, Inc., Cheyenne, Wyo.

Manly, B.F.J. 2010*b*. Initial analyses of delta smelt abundance changes from fall to summer, summer to fall, and fall to fall. Report available from Western EcoSystems Technology, Inc., Cheyenne, Wyo.

Maunder, M.N. 2001. A general framework for integrating the standardization of catch per unit of effort into stock assessment models. Can. J. Fish. Aquat. Sci. **58**(4): 795–803. doi:10.1139/f01-029.

Maunder, M.N. 2003. Paradigm shifts in fisheries stock assessment: from integrated analysis to Bayesian analysis and back again. Nat. Resour. Model. **16**(4): 465–475. doi:10.1111/j.1939-7445.2003.tb00123.x.

Maunder, M.N. 2004. Population viability analysis based on combining Bayesian, integrated, and hierarchical analyses. Acta Oecol. **26**(2): 85–94. doi:10.1016/j.actao.2003.11.008.

Maunder, M.N., and Deriso, R.B. 2003. Estimation of recruitment in catch-at-age models. Can. J. Fish. Aquat. Sci. **60**(10): 1204–1216. doi:10.1139/f03-104.

Maunder, M.N., and Deriso, R.B. 2010. Dealing with missing covariate data in fishery stock assessment models. Fish. Res. **101**(1–2): 80–86. doi:10.1016/j.fishres.2009.09.009.

Maunder, M.N., and Langley, A.D. 2004. Integrating the standardization of catch-per-unit-of-effort into stock assessment models: testing a population dynamics model and using multiple data types. Fish. Res. **70**(2–3): 389–395. doi:10.1016/j.fishres.2004.08.015.

Maunder, M.N., and Punt, A.E. 2004. Standardizing catch and effort data: a review of recent approaches. Fish. Res. **70**(2–3): 141–159. doi:10.1016/j.fishres.2004.08.002.

Maunder, M.N., and Starr, P.J. 2003. Fitting fisheries models to standardised CPUE abundance indices. Fish. Res. **63**: 43–50.

Maunder, M.N., and Watters, G.M. 2003. A general framework for integrating environmental time series into stock assessment models: model description, simulation testing, and example. Fish. Bull. **101**: 89–99.

Maunder, M.N., Hinton, M.G., Bigelow, K.A., and Langley, A.D. 2006. Developing indices of abundance using habitat data in a statistical framework. Bull. Mar. Sci. **79**: 545–559.

Maunder, M.N., Schnute, J.T., and Ianelli, J. 2009. Computers in fisheries population dynamics. *In* Computers in fisheries research. 2nd ed. *Edited by* B.A. Megrey and E. Moksness. Springer Science +Business Media B.V. pp. 337–372.

Moyle, P.B., Herbold, B., Stevens, D.E., and Miller, L.W. 1992. Life history and status of delta smelt in the Sacramento – San Joaquin estuary, California. Trans. Am. Fish. Soc. **121**(1): 67–77. doi:10.1577/1548-8659(1992)121<0067:LHASOD>2.3.CO;2.

Nations, C. 2007. Variance in abundance of delta smelt from 20 mm surveys. Report available from Western EcoSystems Technology, Inc., Cheyenne, Wyo.

Newman, K.B. 1998. State–space modeling of animal movement and mortality with application to salmon. Biometrics, **54**(4): 1290–1314. doi:10.2307/2533659.

Newman, K.B., and Lindley, S.T. 2006. Accounting for demographic and environmental stochasticity, observation error and parameter uncertainty in fish population dynamics models. N. Am. J. Fish. Manage. **26**(3): 685–701. doi:10.1577/M05-009.1.

Newman, K.B., Buckland, S.T., Lindley, S.T., Thomas, L., and Fernandez, C. 2006. Hidden process models for aninmal population dynamics. Ecol. Appl. **16**(1): 74–86. doi:10.1890/04-0592. PMID:16705962.

Newman, K.B., Fernandez, C., Thomas, L., and Buckland, S.T. 2009. Monte Carlo inference for state–space models of wild animal populations. Biometrics, **65**(2): 572–583. doi:10.1111/j.1541-0420.2008.01073.x. PMID:18565166.

Punt, A.E., and Hilborn, R. 1997. Fisheries stock assessment and decision analysis: the Bayesian approach. Rev. Fish Biol. Fish. **7**(1): 35–63. doi:10.1023/A:1018419207494.

Quinn, T.J., II, and Deriso, R.B. 1999. Quantitative fish dynamics. Oxford University Press, New York.

Rivot, E., Prevost, E., Parent, E., and Bagliniere, J.L. 2004. A Bayesian state–space modelling framework for fitting a salmon stage-structured population dynamic model to multiple time series of field data. Ecol. Model. **179**(4): 463–485. doi:10.1016/j.ecolmodel.2004.05.011.

Rose, K.A., Cowan, J.H., Jr, Winemiller, K.O., Myers, R.A., and Hilborn, R. 2001. Compensatory density dependence in fish populations: importance, controversy, understanding and prognosis. Fish Fish. **2**: 293–327. doi:10.1046/j.1467-2960.2001.00056.x.

Sæther, B.E. 1997. Environmental stochasticity and population dynamics of large herbivores: a search for mechanisms. Trends Ecol. Evol. **12**(4): 143–149. doi:10.1016/S0169-5347(96)10068-9. PMID:21238011.

Schnute, J. 1985. A general theory for the analysis of catch and effort data. Can. J. Fish. Aquat. Sci. **42**(3): 414–429. doi:10.1139/f85-057.

Sibert, J., Hampton, J., Kleiber, P., and Maunder, M.N. 2006. Biomass, size, and trophic status of top predators in the Pacific Ocean. Science (Washington, D.C.), **314**(5806): 1773–1776. doi:10.1126/science.1135347. PMID:17170304.

Skaug, H.J. 2002. Automatic differentiation to facilitate maximum likelihood estimation in nonlinear random effects models. J. Comput. Graph. Statist. **11**(2): 458–470. doi:10.1198/106186002760180617.

Skaug, H., and Fournier, D. 2006. Automatic approximation of the marginal likelihood in non-Gaussian hierarchical models. Comput. Stat. Data Anal. **51**(2): 699–709. doi:10.1016/j.csda.2006.03.005.

Sommer, T., Armor, C., Baxter, R., Breuer, R., Brown, L., Chotkowski, M., Culberson, S., Feyrer, F., Gingras, M., Herbold, B., Kimmerer, W., Mueller-Solger, A., Nobriga, M., and Souz, K. 2007. The collapse of pelagic fishes in the upper San Francisco Estuary: El colapso de los peces pelagicos en la cabecera del Estuario San Francisco. Fisheries, **32**: 270–277.

Thomson, J.R., Kimmerer, W.J., Brown, L.R., Newman, K.B., Mac Nally, R., Bennett, W.A., Feyrer, F., and Fleishman, E. 2010. Bayesian change point analysis of abundance trends for pelagic fishes in the upper San Francisco Estuary. Ecol. Appl. **20**(5): 1431–1448. doi:10.1890/09-0998.1. PMID:20666259.

Walters, C. 1987. Nonstationarity of production relationships in exploited populations. Can. J. Fish. Aquat. Sci. **44**(Suppl. 2): 156–165. doi:10.1139/f87-319.

Walters, C.J. 2003. Folly and fantasy in the analysis of spatial catch rate data. Can. J. Fish. Aquat. Sci. **60**(12): 1433–1436. doi:10.1139/f03-152.

Wang, S.-P., Maunder, M.N., Aires-da-Silva, A., and Bayliff, W.H. 2009. Evaluating fishery impacts: application to bigeye tuna (*Thunnus obesus*) in the eastern Pacific Ocean. Fish. Res. **99**(2): 106–111. doi:10.1016/j.fishres.2009.05.010.

Appendix A. Calculating realistic values for the *b* parameter of the Beverton–Holt and Ricker versions of the Deriso–Schnute stock–recruitment model

The third parameter (γ) of the Deriso–Schnute stock–recruitment model (Deriso 1980; Schnute 1985)

$$f(N) = aN(1 - b\gamma N)^{\frac{1}{\gamma}}$$

can be set to represent the Beverton–Holt ($\gamma = -1$) and Ricker ($\gamma \to 0$) models (Quinn and Deriso 1999, page 95), which correspond to

$$f(N) = \frac{aN}{1 + bN} \quad \text{and} \quad f(N) = aN\exp(-bN)$$

The recruitment at a given reference abundance level (e.g., the carrying capacity N_0) can be calculated as

$$R_0 = \frac{aN_0}{1 + bN_0} \quad \text{and} \quad R_0 = aN_0\exp(-bN_0)$$

The recruitment when the abundance is at a certain fraction (p) of this reference level can be calculated as

$$R_p = \frac{apN_0}{1 + bpN_0} \quad \text{and} \quad R_p = aN_0\exp(-bpN_0)$$

A standard reference in fisheries is the recruitment as a fraction of the recruitment in the absence of fishing (the carrying capacity) that is achieved when the abundance is 20% of the abundance in the absence of fishing (steepness).

$$h = \frac{R_{0.2}}{R_0} = \frac{\frac{1}{N_0} + b}{\frac{5}{N_0} + b} \quad \text{and} \quad h = \frac{R_{0.2}}{R_0} = 0.2\exp(0.8bN_0)$$

To set b for a given steepness

$$b = \frac{5h - 1}{N_0 - hN_0} \quad \text{and} \quad b = \frac{\ln(5h)}{0.8N_0}$$

The 20% reference level was probably chosen because the objective of fisheries management has traditionally been to maximize yield, and it is generally considered that when a population falls below 20% of its unexploited level, the stock cannot sustain that level of yield. In the delta smelt application, the concern is about low levels of population abundance and we do not estimate the unexploited population size. Therefore, a more appropriate reference level might be 5% of the average level observed in the surveys.

$$h_{0.05} = \frac{R_{0.05}}{R_{avg}} = \frac{\frac{1}{N_{avg}} + b}{\frac{20}{N_{avg}} + b} \quad \text{and} \quad h_{0.05} = \frac{R_{0.05}}{R_{avg}} = 0.05\exp(0.95bN_{avg})$$

$$b = \frac{20h_{0.05} - 1}{N_{avg} - h_{0.05}N_{avg}} \quad \text{and} \quad b = \frac{\ln(20h_{0.05})}{0.95N_{0.05}}$$

This specification is also more appropriate when considering both the Beverton–Holt and Ricker models because the Ricker model reduces at high abundance levels, and the recruitment at an abundance level that is 20% of the carrying capacity could be higher than the recruitment at carrying capacity. We restrict the models to those that have b estimates such that the expected recruitment when the population is at 5% of its average level (over the survey period) is equal to or less than 80% of the recruitment expected when the population is at its average level (Table A1). This is equivalent to a Beverton–Holt $h_{0.2} = 0.95$ based on the abundance reference level being the average abundance from the surveys, which is probably conservative in the sense of not rejecting high values of b.

Table A1. Maximum values of the parameter b for inclusion of models in the model selection process.

	Average abundance	Maximum b	
		Beverton–Holt	Ricker
20 mm (larvae)	7.99	9.3867	0.3653
STN (juveniles)	6140	0.0122	0.0005
FMWT (adults)	459	0.1634	0.0064

Note: STN, summer tow net; FMWT, fall midwater tow.

References

Deriso, R.B. 1980. Harvesting strategies and parameter estimation for an age-structured model. Can. J. Fish. Aquat. Sci. **37**(2): 268–282. doi:10.1139/f80-034.

Quinn, T.J., II, and Deriso, R.B. 1999. Quantitative fish dynamics. Oxford University Press, New York.

Schnute, J. 1985. A general theory for the analysis of catch and effort data. Can. J. Fish. Aquat. Sci. **42**(3): 414–429. doi:10.1139/f85-057.

Contents (concluded) / Table des matières (suite et fin)

Taina Honkalehto, Patrick H. Ressler, Richard H. Towler, and Christopher D. Wilson	**1231–1242**	Using acoustic data from fishing vessels to estimate walleye pollock (*Theragra chalcogramma*) abundance in the eastern Bering Sea
Susan Dean, Claudio DiBacco, and Robert Scott McKinley	**1243–1251**	Assessment of stable isotopic signatures as a means to track the exchange of sea lice (*Lepeophtheirus salmonis*) between host fish populations
David Peel and Norman M. Good	**1252–1264**	A hidden Markov model approach for determining vessel activity from vessel monitoring system data
Vardit Makler-Pick, Gideon Gal, James Shapiro, and Matthew R. Hipsey	**1265–1284**	Exploring the role of fish in a lake ecosystem (Lake Kinneret, Israel) by coupling an individual-based fish population model to a dynamic ecosystem model
Mark N. Maunder and Richard B. Deriso	**1285–1306**	A state–space multistage life cycle model to evaluate population impacts in the presence of density dependence: illustrated with application to delta smelt (*Hyposmesus transpacificus*)

Postage paid at Ottawa | Port payé à Ottawa
Publications mail | Poste-publication
Registration No. 40110225 | Enregistrement n° 40110225

USPS periodical postage paid at Plattsburgh, NY 12901, USA

Canadian Journal of Fisheries and Aquatic Sciences

Volume 68, Number 7, July 2011

Journal canadien des sciences halieutiques et aquatiques

Volume 68, numéro 7, juillet 2011

RAPID COMMUNICATION | COMMUNICATION RAPIDE

C. Michael Wagner, Eric M. Stroud, and Trevor D. Meckley 1157–1160 A deathly odor suggests a new sustainable tool for controlling a costly invasive species

ARTICLES | ARTICLES

Jonathan W. Moore, Sean A. Hayes, Walter Duffy, Sean Gallagher, Cyril J. Michel, and David Wright 1161–1170 Nutrient fluxes and the recent collapse of coastal California salmon populations

Shijie Zhou, André E. Punt, Roy Deng, and Janet Bishop 1171–1181 Estimating multifleet catchability coefficients and natural mortality from fishery catch and effort data: comparison of Bayesian state–space and observation error models

Ming Feng, Nick Caputi, James Penn, Dirk Slawinski, Simon de Lestang, Evan Weller, and Alan Pearce 1182–1196 Ocean circulation, Stokes drift, and connectivity of western rock lobster (*Panulirus cygnus*) population

Even Moland, Esben Moland Olsen, Kristian Andvord, Jan Atle Knutsen, and Nils Chr. Stenseth 1197–1210 Home range of European lobster (*Homarus gammarus*) in a marine reserve: implications for future reserve design

Sergiusz J. Czesny, Jacques Rinchard, S. Dale Hanson, John M. Dettmers, and Konrad Dabrowski 1211–1230 Fatty acid signatures of Lake Michigan prey fish and invertebrates: among-species differences and spatiotemporal variability

Continued on inside back cover / Suite au verso

Front cover: Ihoko Saito/Toshiyuki Tajima/Dex Image/Getty Images.

Page couverture : Ihoko Saito/Toshiyuki Tajima/Dex Image/Getty Images.

NRC Research Press

CANADIAN SCIENCE PUBLISHING | ÉDITIONS SCIENCES CANADA

Printed in Canada by | Imprimé au Canada par
NRC Reprographic Services | Service de reprographie CNRC

Page production by | Mise en page par
NRC Research Press | NRC Research Press

0706-652X(201107)68:7;1-0